

Flood level prediction for regulated rain-fed rivers

Flood level prediction for regulated rain-fed rivers

Joop Gerretsen

Joop Gerretsen

UITNODIGING

voor de verdediging
van mijn proefschrift

**'Flood level prediction
for regulated rain-fed rivers'**

op vrijdag 9 januari 2009
om 13:00 uur
in Collegezaal 2
van gebouw 'de Spiegel'

Universiteit Twente
Drienerlolaan 5 te Enschede

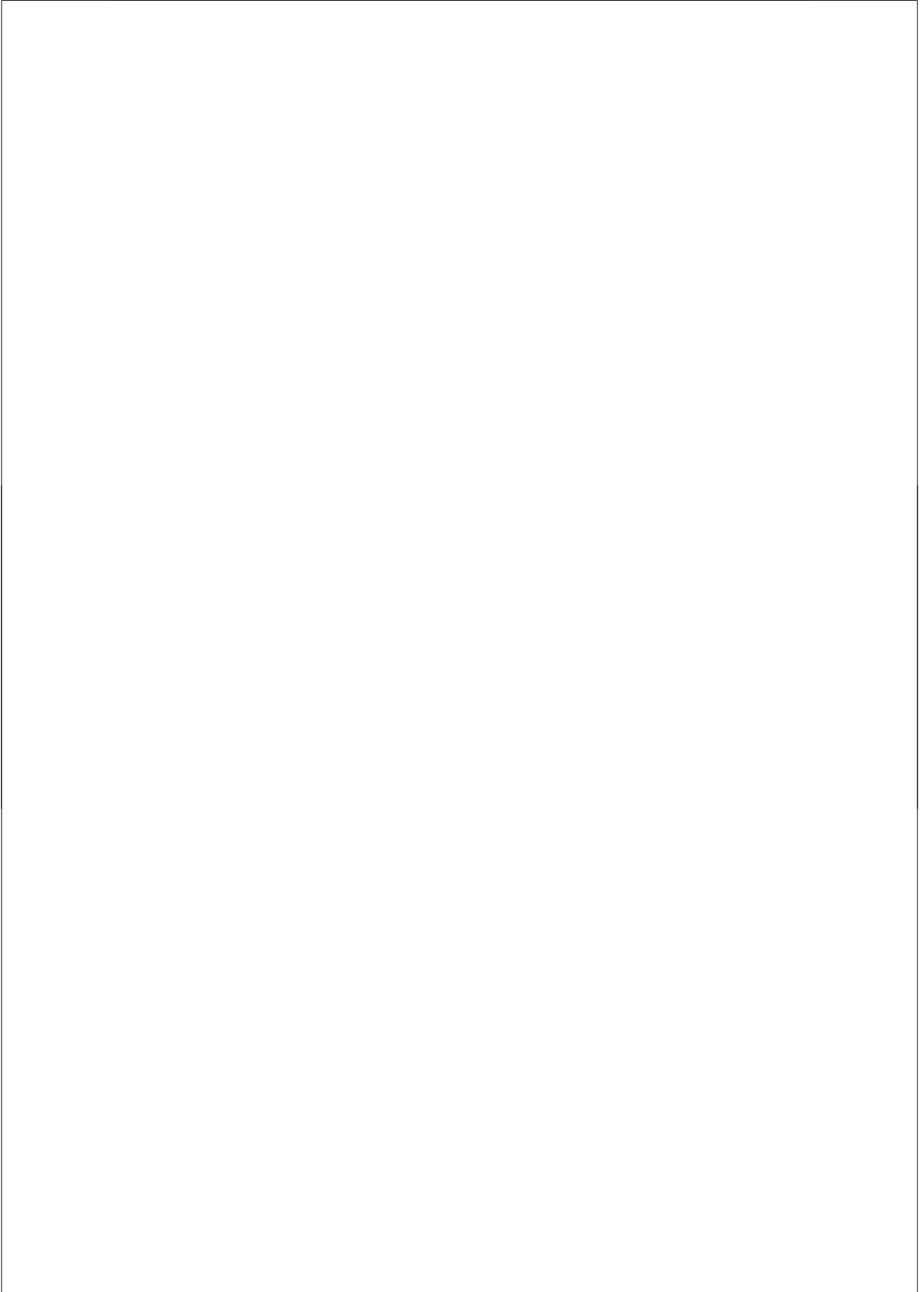
gevolgd door een receptie
in de kantine van gebouw
'de Spiegel'

J.H. Gerretsen

Prof. P. Willemsstraat 54
Maastricht
(043) 3625236
j.h.gerretsen@planet.nl

Flood level prediction for
regulated rain-fed rivers

Joop Gerretsen



FLOOD LEVEL PREDICTION FOR
REGULATED RAIN-FED RIVERS

AN INVESTIGATION INTO THE MEUSE RIVER FLOODS AND
GENERALIZATION OF THE FINDINGS TO SIMILAR RIVERS

Samenstelling promotiecommissie:

prof. dr. F. Eising	Universiteit Twente, voorzitter / secretaris
prof. dr. ir. H.J. de Vriend	Universiteit Twente, promotor
prof. dr. S.J.M.H. Hulscher	Universiteit Twente
prof. dr. ir. A.Y. Hoekstra	Universiteit Twente
prof. dr. ir. H.H.G. Savenije	Technische Universiteit Delft
dr. ir. H.E.J. Berger	Rijkswaterstaat
prof. dr. ir. C.B. Vreugdenhil	Universiteit Twente
prof. dr. ir. H.G. Wind	Universiteit Twente

Copyright © 2009 by Joop Gerretsen
Printed by Print Partners Ipskamp, Enschede, the Netherlands

ISBN 978-90-365-2764-4

FLOOD LEVEL PREDICTION FOR REGULATED RAIN-FED RIVERS

PROEFSCHRIFT

ter verkrijging van de graad van doctor
aan de Universiteit Twente, op gezag van
de rector magnificus, prof. dr. H. Brinksma,
volgens besluit van het College voor Promoties
in het openbaar te verdedigen op
vrijdag 9 januari 2009 om 13:15 uur

door

Johannes Hendrikus Gerretsen
ingenieur civiele technologie
geboren op 14 november 1933
te Elst (Gld.)

Dit proefschrift is goedgekeurd door de promotor:

prof. dr. ir. H. J. de Vriend

CONTENTS

SUMMARY	3
SAMENVATTING	9
CHAPTER 1	15
INTRODUCTION	15
1.1 Flood level prediction	15
1.2 Research objectives and research questions	19
1.3 Literature overview from other investigations	20
1.4 Research methodology	24
1.5 Expected results and practical relevance of the study	26
CHAPTER 2	27
PROBABILITY ANALYSIS OF FLOODS IN THE DUTCH MEUSE RIVER AT BORGHAREN	27
2.1 Frequency of occurrence of recorded and documented floods	27
2.2 Hydrological background	36
2.3 Sensitivity of the probability of exceedance at Borgharen to variable historical peak discharges	37
2.4 Comparison of the results of the DWL 2001 principle with those of the present study	39
2.5 Generalization of the findings for the Dutch Meuse River to other rivers ..	42
CHAPTER 3	43
FLOOD WAVE CHARACTERISTICS AT BORGHAREN DETERMINING THE RIVER STAGES	43
3.1 Introduction	43
3.2 Observed flood waves at Borgharen	44
3.3 Flood wave parameters at Borgharen	44
3.4 Which flood wave parameters at Borgharen are important for the downstream water levels	47
3.5 A first-order estimate of the influence of significant flood wave properties on the downstream water levels	50
3.6 Generalization of the findings for the Dutch Meuse River to other rivers ..	52
3.7 Discussion and conclusions	57
CHAPTER 4	59
DOWNSTREAM WATER LEVELS VERSUS CHARACTERISTIC FLOOD WAVE PROPERTIES AT BORGHAREN	59
4.1 Introduction	59
4.2 Mutual correlation between the relevant flood wave variables	60
4.3 Synthesization of a flood wave with given relevant parameters	60
4.4 Background of the Sobek water motion model	65
4.5 Relative frequency distribution of the water levels.....	67

4.6	Adaptation of probability distribution functions to the relative frequency distributions	71
4.7	Water level differences between the computations and the adapted probability distribution functions	80
4.8	The reliability of the local water levels related to the peak discharges at Borgharen	81
4.9	Water levels at Venlo and Mook: the results of the present study compared with the Design Water Levels 2001.....	86
4.10	Generalization of the findings for the Dutch Meuse River to other rivers ..	88
4.11	Discussion and conclusions	89
	CHAPTER 5	92
	FLOOD PREDICTION	92
5.1	Introduction	92
5.2	Development of an algorithm for provisional discharge-peak predictions at Borgharen	92
5.3	The 1-day Unit Hydrograph method	93
5.4	The forecasting-algorithm for future use	96
5.5	Application of the forecasting-algorithm	100
5.6	Generalization to other rivers	104
5.7	Discussion and conclusions	106
	CHAPTER 6	108
	DISCUSSION WITH REGARD TO THE RESEARCH QUESTIONS	108
6.1	Summary of the research questions	108
6.2	Change of the design discharges at Borgharen	108
6.3	Significant local water level differences between the results of the present study and the DWL 2001	109
6.4	The reliability of water level predictions with an easy-to-use warning algorithm	112
6.5	Learning from the Dutch Meuse River case for other rivers of this type ...	112
	CHAPTER 7	114
	CONCLUSIONS	114
	CHAPTER 8	116
	RECOMMENDATIONS	116
	APPENDICES	117
	REFERENCES	167
	ACKNOWLEDGEMENTS	171
	ABOUT THE AUTHOR	172

SUMMARY

Chapter 1

The way to deal with the investigation into the '*Flood level prediction for regulated rain-fed rivers*' is considered. It consists of a strategic and an operational part. The objectives, research questions, methodology, expected results and practical relevance of the study are clarified.

The strategic part deals with the problem of durable flood protection measures and the operational part deals with a timely first-order prediction of the water levels, if a flood can be expected.

To estimate the probability of occurrence of river floods, required to design river-engineering works, other estimation methods, data series and data processing are used than so far. As society makes stringent requirements to the acceptable risk of flooding, the investigation is aimed at reducing uncertainties in the estimation of the probability of occurrence of floods.

Operational flood level prediction requires a quick response to imminent flood events, so as to enable local managers and public services to take timely emergency measures. Therefore an algorithm is developed that yields a provisional first-order estimate of the peak discharge at Borgharen, in our case. On the basis of this information, the water levels at downstream locations are estimated using a numerical computer model, given the estimated flood wave shape at Borgharen.

The results of the strategic investigation of the present study are compared with the Design Water Levels 2001, and the necessity to change the DWL 2001 is discussed.

The operational results of the easy-to-use forecasting-algorithm are compared with the eight highest floods in the period 1980-2000 and corrected if necessary. Then, some recent flood events are validated.

The research questions are investigated for the Dutch Meuse River and the findings are generalized to similar rivers.

Chapter 2

The results of a new *probability analysis of the peak discharges at Borgharen*, based on other principles than used so far, may have consequences for the design of flood protection measures. Starting point of the analysis are the annual maximum discharges at Borgharen between 1911 and 2000. This data set was extended with estimated data from a number of documented disastrous floods in history.

The cumulative probability distribution of the annual maximum discharges at Borgharen shows irregularities, due to, among other things, the difference between the set-up and free-runoff river situation upstream of Borgharen. A discharge threshold is introduced to separate these two situations and to reduce irregularities in the total discharge distribution. Discrepant peak discharge distributions above and below the discharge threshold would be found if only the Weibull formula would be used for

each subset. To avoid this, the 'Exceedance formulae' are used to determine the relation between the probability of exceedance and the peak discharges at Borgharen, on the basis of a statistically acceptable and consistent probability distribution.

Comparison with another method (Dalrymple) shows that the resulting probabilities of exceedance do not differ significantly from each other. The 'Exceedance formulae' are used in the remainder of the study.

The best estimates of consistent plot positions of data, points in the 'probability of exceedance-peak discharge' relationship at Borgharen, is obtained if the discharge threshold is chosen at $2750 \text{ m}^3\text{s}^{-1}$. The best estimate of the peak discharges with probability of exceedance at 0.02, 0.004 and 0.0008 per annum (design standards) turns out to be 2808, 3089 and $3370 \text{ m}^3\text{s}^{-1}$, respectively. The 95% confidence limits of the regression line range from plus or minus 2.5% to plus or minus 3 %.

There is no reason to assume that changes in hydrological conditions, such as de- or reforestation, land use, land cover, or rainfall, have changed the very extreme discharge peaks. Such very extreme events only come about in situations where these conditions make little difference (saturated or frozen basin). For the moderate flood events however, a 5% increase of the discharge peak over the last forty years seems plausible.

Concerning the sensitivity of the design discharge, we see that 5% or more incorrect estimation of the highest documented peak discharge is significant, as it alters the probability distribution such that it exceeds the 95% reliability band of the preferred relation between probability of exceedance and peak discharge.

Not documented or forgotten peak discharges for floods just above the threshold at $2750 \text{ m}^3\text{s}^{-1}$ hardly influence the probability of exceedance.

Only if a peak discharge equal to the highest documented one would be missing, the design discharges would be influenced somewhat.

If the probability of exceedance curve of the peak discharge at Borgharen resulting from the present study is compared with the one underlying the Design Water Levels 2001, we see that the difference is significant for discharge peaks over $3000 \text{ m}^3\text{s}^{-1}$. Translated into water levels, it means that the corresponding water levels at Borgharen from the present study are significantly lower (i.e. 0.10 m or more difference) for p.o.e.'s equal or smaller than 0.0054 per annum.

Starting from the requirement that *in general for similar rivers* the probability of failure of flood protection structures may not exceed a few percents in a human lifetime, one would generally need an uninterrupted annual peak discharge series of several hundreds of years for a proper flood probability analysis. Such series are not available. Therefore, we use a complex series of as much as possible uninterrupted systematically recorded annual peak discharges, extended with documented peaks of major historic floods. The existence of significant river perceptions, e.g. the change from set-up to free flow river situation or the beginning of the overflow of a levee, give cause for the introduction of a discharge threshold for those situations.

Attention has to be paid to the homogeneity of the data series that is used, to changing hydrological conditions, and moreover to the sensitivity of the probability of

exceedance of the peak discharges because of incorrect estimates of historic flood peaks.

Chapter 3

In order to identify which *flood wave characteristics* at Borgharen are important to the water levels further downstream, the relative discharge hydrographs, for which the absolute peaks are over $1850 \text{ m}^3\text{s}^{-1}$ in the period 1930-2000, have been investigated. Starting point are the daily 08:00 a.m. discharge data at Borgharen.

To that end, single and composite flood wave shapes are defined. If the time span between two peaks is eight days or more, we speak of two single flood waves, otherwise of one composite flood wave with a number of peaks. Furthermore, weir operations upstream of Borgharen may bring about serious discharge fluctuations. In order to compensate for those effects, corrections of the discharges have been made for some floods.

Besides the given peak and base discharges, five flood wave characteristics at Borgharen, viz. the moments 0 through 4 of the relative discharge hydrographs, have been calculated. Because of large river works in earlier times in the Walloon region, each of the series of these parameter values for the floods above $1850 \text{ m}^3\text{s}^{-1}$ was split up into two sets, before and after 1980, the year in which the weir at Lixhe (B) near the Dutch border was put into operation. A trend analysis of the series showed that each of the two sets can be considered to belong to the same homogeneous series.

Besides the peak and base discharges, it turned out from correlation analysis that the moments 0, 3 and 4 can be considered as mutually independent. Independency is required, since random samples of parameter combinations have to be taken to produce synthetic floods, given the peak discharge. These are needed because the number of measured local floods is insufficient to determine the p.o.e. of the local downstream water levels.

As the skewness (third moment) of the relative discharge hydrograph at Borgharen on the local water levels turns out to be negligible in our case, random samples of combinations of peak discharge, base discharge, flood wave volume (zero moment) and wave crest curvature (fourth moment), are taken to synthesize flood waves at Borgharen. Subsequently, the water levels downstream of Borgharen are computed with a 1-D Sobek model, as will be shown in Chapter 4.

In general, for similar rivers it is obvious that parameters such as peak discharge, base discharge and flood wave volume influence the downstream water levels. The influence of the crest curvature, however, may be considerable, too.

Concerning the crest curvature, it turns out that the storage width at the water level influences the attenuation of the flood wave while passing through the river, and thus the downstream water levels.

For rivers stretches with a steep bottom slope (0.5 m/km or more) this influence is negligible.

The ratio between the total water depth and that at bank-full discharge also plays a role in the flood wave attenuation.

The skewness of the relative discharge hydrograph may be an indicator for attenuation. The difference between the steep gradient before and the gentle slope after the crest -so the skewness of the relative discharge hydrograph- is a reason for attenuation, for in that case the supply of water can not be discharged in it's totality and a part disappears into the storage, so the peak comes down.

Chapter 4

To compute downstream water levels from characteristic wave parameters of a flood at Borgharen, one thousand random samples have been taken from combinations of four independent characteristic parameter values. From those samples one thousand flood waves have been synthesized.

If the five measured major floods at Borgharen that have occurred in the last twenty years of the previous century are compared with the flood waves, synthesized on the basis of the four characteristic parameters (peak discharge, base discharge, wave volume, and crest curvature), then 1-D Sobek computations show that at Venlo and Mook the water level difference between the synthetic and real flood peaks is 0.03 m to 0.05 m and that difference is not significant in view of the accuracy (0.1 m) with which the Design Water Levels are published. So, it turns out that the method of synthesization of flood waves is satisfactory.

The Pearson type III distribution function is, according to the Kolmogorov-Smirnov test, the best approximation of a stable frequency distribution of the computed water levels. On the basis of this distribution function the probability of exceedance of the water levels at Venlo and Mook is determined. The differences between the computed and the approximated values are negligible for the smaller p.o.e. and for the rest (the lower floods) less than 0.1 m.

The influence of the characteristic flood wave parameters on the downstream water levels is larger for more extreme flood peaks at the measuring-station and also increases with the distance to this measuring-station.

The Design Water Levels 2001 at Venlo and Mook exceed the expected water levels according to the present study. At Venlo these are 0.3 and 0.5 m higher for p.o.e. 0.004 and 0.02, respectively. At Mook this is 0.6 and 0.8 m, respectively. This means that the DWL 2001 should have to be adapted. Anyway, the reliability band is not determined for DWL 2001.

The measured five major floods at Borgharen from the period 1980-2000 do not cause significantly higher peak water levels at Venlo and Mook than the Design Water Levels 2001. The peculiar flood of January 1995 has at Venlo a p.o.e. of once in 60 years according to DWL 2001, and once in 160 years according to the present study, whereas at Borgharen this is once in 40 years and once in 30 years, respectively.

In general, for similar rivers a procedure can be formulated to develop synthetic flood waves from combinations of values of independent characteristic flood wave parameters, measured at a certain location. From that, water levels can be computed for any downstream location with the help of a hydrodynamic model.

The number of random samples of those combinations depends on the degree to which a stable probability density distribution of computed water levels is obtained. The variance of the water levels obtained in that way can be considerable, related to a given discharge peak at the measuring-point, due to the various compositions of the synthetic flood waves.

Chapter 5

In operational flood management there is an urgent need for timely information, preferably some days ahead, about the nature of an imminent flood. For that reason, an *algorithm for a provisional prediction* of the peak discharge and corresponding peak water level at Borgharen (km 16) is developed.

Furthermore, it is the intention to make the broad public aware of the possibilities and limitations of water level predictions on the basis of observed rainfall, weather forecast and a computer model of the river flow.

On the basis of the daily discharge data of eight flood events at Borgharen, in the period 1980-2000, the average 1-day Unit Hydrograph is determined. This indicates the daily average direct catchment runoff ($\text{m}^3\text{s}^{-1} \text{mm}^{-1}$) that passes through the river at Borgharen, the so-called effective rainfall. The effective rainfall (mm) is calculated from the ratio of flood wave volume (m^3) and catchment area (m^2). Average 1-day Unit Hydrograph and effective rainfall are the tools to predict relative peak discharges (Q'_{peak}).

When applying the algorithm, the regression function 'operational rainfall – effective rainfall' has been used to determine the adjusted effective rainfall. By adding the base discharge value, i.e. the beginning of the rising stage of the flood wave, to the so obtained Q'_{peak} we get Q_{peak} and corresponding water level.

When comparing the predictions with the measured data, there are differences in the water levels, due to uncertainties in the rainfall data and the use of an average 1-day UH, for instance. This is practical reality by which the reliability of the prediction is influenced. Therefore we also determined, besides the expected discharges and corresponding water levels, the 95% and 50% upper limits of the effective rainfall from the confidence bands of the aforementioned regression function.

It turns out that a first-order prediction of the water level peaks at Borgharen on basis of rainfall is feasible, taking into account that, because of uncertainties, we assigned reasonable limits to the expected water levels, as aforementioned, for maximum possible water levels at highest (95% limit) and medium high floods (50% limit).

In general, for similar rivers, the process of water level prediction from rainfall is analogous to that for our case study. To improve future water level predictions, it is necessary to pay much attention to the reliability of the rainfall data, weather forecast and the confirmation of the relationship between operational rainfall and effective rainfall.

Careful maintenance of the algorithm for the prediction of peak discharges and peak water levels is necessary, because autonomous developments or human interventions

in the river(1) may make the 'discharge-stage' curve unstable and (2) may alter the average Time Unit Hydrograph.

Investigation into the influence of the variability of the TUH's on the predictions is advisable.

For first-order predictions of peak water levels at other locations than the measuring-station the flood wave, which was estimated from the rainfall prediction, can be input into a water-motion model for the benefit of computations for local water levels along the river, starting from that measuring-station.

SAMENVATTING

Hoofdstuk 1

Het plan van aanpak van het onderzoek naar de *'Hoogwaterstandvoorspelling voor gereguleerde regenrivieren'* wordt besproken. Het bestaat uit een strategisch en een operationeel gedeelte. Het doel, onderzoeksvragen, te volgen methode, verwachte resultaten en praktische betekenis van het onderzoek worden toegelicht.

Het strategische deel behandelt het probleem van duurzame beschermende maatregelen en het operationele deel betreft een tijdige eerste waterstandvoorspelling, wanneer een hoogwater kan worden verwacht.

Om de kans van optreden van hoogwaters te schatten, hetgeen vereist is om riviertechnische werken te ontwerpen, worden andere schattingsmethoden, gegevensreeksen en gegevensbewerkingen gebruikt dan tot nog toe. Daar er maatschappelijk strenge eisen worden gesteld aan het aanvaardbare risico van overstroming, heeft het onderzoek als doel om onzekerheden in de schatting van de kans van optreden van een hoogwater te reduceren.

Operationele hoogwaterstandvoorspelling vereist een snelle reactie op dreigende hoogwatergebeurtenissen, zodat in dat geval lokale beheerders en publieke diensten in staat zijn om tijdige noodmaatregelen te treffen. Daartoe wordt een rekenmethode ontwikkeld die een eerste voorlopige inschatting van de piekafvoer, in ons geval, te Borgharen oplevert. Op grond hiervan worden waterstanden benedenstrooms geschat door gebruik te maken van een numeriek computermodel, gegeven de geschatte hoogwater golfvorm te Borgharen.

De resultaten van het strategische onderzoek worden vergeleken met de 'Ontwerp Waterstanden 2001' en de noodzaak om de 'Ontwerp Waterstanden 2001' te wijziging wordt besproken.

De operationele resultaten van de gemakkelijk te hanteren rekenmethode voor voorspellingen worden vergeleken met de acht hoogste hoogwaters in de periode 1980-2000 en zonodig gecorrigeerd. Vervolgens worden enkele recente hoogwaters gevalideerd.

De onderzoeksvragen worden behandeld voor de Nederlandse Maas en de bevindingen worden veralgemeend voor vergelijkbare rivieren.

Hoofdstuk 2

De resultaten van een nieuwe *waarschijnlijkheidsanalyse van de piek afvoeren te Borgharen*, gebaseerd op andere principes dan tot dusver gebruikelijk, kunnen gevolgen hebben voor het ontwerp van hoogwaterbeschermende maatregelen.

Uitgangspunt van de analyse zijn de jaarlijkse maximale afvoeren te Borgharen (1911-2000). Deze gegevensreeks werd uitgebreid met geschatte gegevens uit een aantal gedocumenteerde catastrofale hoogwaters van vroeger.

De cumulatieve kansverdeling van de jaarlijkse maximale afvoeren te Borgharen vertoont onregelmatigheden, o.a. vanwege het verschil tussen de gestuwde en ongestuwde riviersituatie bovenstrooms van Borgharen.

Een afvoerdrempel is geïntroduceerd om beide situaties van elkaar te scheiden en om onregelmatigheden in de algehele afvoerverdeling te verminderen. Er zou verschil in aansluiting tussen de piekafvoer verdeling boven en beneden de afvoerdrempel worden gevonden als slechts de Weibull formule zou worden gebruikt voor iedere deelreeks boven en beneden de drempel. Om dit te vermijden zijn de 'Exceedance formules' gebruikt ter bepaling van de relatie tussen de overschrijdingskans en de afvoerpieken te Borgharen, op basis van een statistisch acceptabele en samenhangende kansverdeling.

Vergelijking met een andere methode (Dalrymple) toont aan dat de overschrijdingskansen niet significant van elkaar verschillen. In het vervolg van de studie zijn de Exceedance formules gebruikt.

De beste schattingen van samenhangende plot posities van gegevens, leidend tot de 'overschrijdingskans – piekafvoer' relatie te Borgharen, wordt verkregen indien de afvoerdrempel op $2750 \text{ m}^3\text{s}^{-1}$ wordt gekozen. De beste schatting van de piekafvoeren met overschrijdingskans 0.02, 0.004 en 0.0008 per jaar (ontwerpnormen) blijkt respectievelijk 2808, 3089 en $3370 \text{ m}^3\text{s}^{-1}$ te zijn. De 95% betrouwbaarheidsgrenzen van de regressielijn variëren van plus of min 2.5% tot plus of min 3%.

Er is geen reden om te veronderstellen, dat wijzigingen in hydrologische omstandigheden, zoals ontbossing en bebossing, landgebruik, bodemverharding of regenvalhoeveelheden, veranderingen hebben teweeg gebracht in de zeer hoge piekafvoeren. Zulke zeer extreme gebeurtenissen komen slechts voor tijdens situaties waarin deze omstandigheden er weinig toe doen, vanwege een reeds met water verzadigde of bevroren bodem. Echter voor gematigde hoogwaters lijkt een 5% toename van de afvoerpiek in de loop van de laatste 40 jaren aannemelijk.

Ten aanzien van de gevoeligheid van de ontwerpafvoer zien we dat 5% of meer verkeerd ingeschatte hoogst gedocumenteerde piekafvoer significant is, daar dit de kansverdeling zodanig verandert dat het de 95% betrouwbaarheidsband van de voorkeur hebbende relatie tussen 'overschrijdingskans en piekafvoer' te buiten gaat. De invloed op de overschrijdingskans vanwege niet gedocumenteerde of vergeten piekafvoeren, juist boven de afvoerdrempel van $2750 \text{ m}^3\text{s}^{-1}$, is te verwaarlozen. Slechts als een piekafvoer gelijk aan de hoogst gedocumenteerde verloren zou zijn gegaan, dan veranderen de ontwerpafvoeren enigszins.

Indien de overschrijdingskans kromme van de piekafvoer te Borgharen uit de huidige studie wordt vergeleken met die waaraan de 'Ontwerp Waterstanden 2001' ten grondslag liggen, dan zien we dat het verschil significant is voor afvoerpieken boven $3000 \text{ m}^3\text{s}^{-1}$. Vertaald naar waterstanden betekent het, dat de corresponderende waterstanden te Borgharen volgend uit de huidige studie significant lager zijn (d.i. 0.1 m of meer verschillen) voor overschrijdingskansen gelijk aan of minder dan 0.0054 per jaar.

Uitgaande van de eis dat *in algemene zin voor vergelijkbare rivieren* de faalkans van hoogwaterbeschermende constructies tijdens een mensenleven niet meer dan enkele

procenten mag zijn, dan zou er ruwweg een ononderbroken reeks van vele honderden jaren jaarlijkse afvoerpieken nodig zijn voor een correcte hoogwater kansanalyse en zulke reeksen zijn niet beschikbaar. Daarom gebruiken we een samengestelde reeks van zoveel mogelijk ononderbroken systematisch geregistreerde jaarlijkse piekafvoeren, aangevuld met gedocumenteerde afvoerpieken van indrukwekkende historische hoogwaters. De aanwezigheid van belangrijke rivier stroombeelden zoals de overgang van een gestuwde rivier naar een vrij afvoerende rivier of het begin van het overstromen van een waterkerende kade, is een reden om voor die situaties een afvoerdrempel te introduceren.

Aandacht moet worden geschonken aan de homogeniteit van de te gebruiken gegevensreeks, aan veranderende hydrologische omstandigheden en bovendien aan de gevoeligheid van de overschrijdingskans van de afvoerpieken door een foute inschatting van historische hoogwatertoppen.

Hoofdstuk 3

Om vast te stellen welke *eigenschappen van een hoogwatergolf* te Borgharen belangrijk zijn voor de waterstanden benedenstrooms, zijn de relatieve afvoerhydrografen van Borgharen onderzocht, waarvoor de absolute toppen vanaf $1850 \text{ m}^3\text{s}^{-1}$ zijn gebruikt uit de periode 1930-2000. Uitgangspunt zijn de dagelijkse 08:00 uur afvoergegevens te Borgharen.

Voor dat doel worden definities afgesproken ten aanzien van enkelvoudige en samengestelde golfvormen. Indien het tijdsinterval tussen twee afvoerpieken 8 dagen of meer bedraagt spreken we van twee enkelvoudige golven en anders van een samengestelde golf met meerdere toppen. Verder kan het stuwbeheer bovenstrooms van Borgharen ernstige afvoerfluctuaties voortbrengen. Om deze effecten te compenseren zijn correcties toegepast voor enkele hoogwaters.

Behalve de gegeven piek- en basisafvoeren, zijn vijf golfkarakteristieken, te weten de momenten 0 t/m 4 van de relatieve afvoerhydrografen te Borgharen berekend. Vanwege vroegere op grote schaal uitgevoerde rivierwerken in Wallonië werd ieder van de reeksen met deze parameterwaarden van de hoogwaters boven $1850 \text{ m}^3\text{s}^{-1}$ gesplitst in twee subreeksen van vóór en ná 1980, het jaar waarin de stuw van Lixhe (B) nabij de Nederlandse grens in bedrijf werd genomen. Uit trend analyse bleek, dat ieder van de twee subreeksen kan worden beschouwd tot dezelfde homogene reeks te behoren.

Buiten de piek en basisafvoeren bleek uit correlatie analyse, dat de momenten 0, 3 en 4 als onderling onafhankelijk kunnen worden beschouwd. Onderlinge onafhankelijkheid is noodzakelijk, omdat willekeurige steekproeven van parametercombinaties moeten worden genomen om synthetische golven samen te stellen, voor gegeven piekafvoeren. Deze synthetische golven zijn nodig omdat het aantal gemeten lokale hoogwaters onvoldoende is om daaruit overschrijdingskansen van lokale benedenstroomse waterstanden te bepalen.

Omdat de scheefheid (derde moment) van de relatieve afvoerhydrograaf te Borgharen voor de lokale waterstanden in ons geval verwaarloosbaar blijkt te zijn, worden willekeurige steekproeven genomen van combinaties van piekafvoer, basisafvoer,

golfvolume (nulde moment) en topkromming (vierde moment) om hoogwatergolven samen te stellen te Borgharen. Vervolgens worden de waterstanden benedenstrooms van Borgharen berekend met behulp van een 1-D waterbewegingmodel (Sobek), zoals zal worden getoond in hoofdstuk 4.

In het algemeen is het voor vergelijkbare rivieren evident dat parameters, zoals piek en basisafvoer en golfvolume invloed hebben op de waterstanden benedenstrooms. De invloed van de topkromming kan echter ook aanzienlijk zijn.

Wat betreft de topvervlakking blijkt het dat de bergende breedte, op de waterlijn gemeten, de inzakking van de hoogwatergolf beïnvloedt tijdens het doorlopen van de rivier en bij gevolg van invloed is op de waterstanden benedenstrooms.

Voor delen van de rivier met een steile bodemgradiënt (0.5 m/km of meer) is deze invloed verwaarloosbaar.

De verhouding tussen de totale water diepte en die voor de volle zomerbedafvoer speelt ook een rol in de topvervlakking.

De rol van de scheefheid (derde moment) van de relatieve afvoerhydrograaf kan een aanwijzing zijn voor topvervlakking. Het verschil tussen de steile gradiënt vóór en de flauwe helling ná de top -dus de scheefheid van de relatieve afvoerhydrograaf- is een reden voor afvlakking, want in dat geval kan de toevoer van water niet geheel worden afgevoerd en vloeit een deel af naar de berging, dus de top zakt in.

Hoofdstuk 4

Om waterstanden benedenstrooms te berekenen uit karakteristieke golfparameters van een hoogwater te Borgharen zijn duizend willekeurige steekproeven genomen uit combinaties van vier onafhankelijke karakteristieke parameterwaarden. Uit die steekproeven zijn duizend synthetische hoogwatergolven samengesteld.

Als de vijf gemeten hoogste hoogwaters te Borgharen van de laatste twintig jaar van de vorige eeuw worden vergeleken met de hoogwaters, samengesteld uit de vier karakteristieke parameters (piekafvoer, basisafvoer, golfvolume en topkromming), dan tonen 1-D Sobek berekeningen aan, dat het waterstandverschil tussen de samengestelde en de werkelijk opgetreden golven te Venlo en Mook 0.03 m tot 0.05 m bedraagt en dat verschil is niet significant, gezien de nauwkeurigheid (0.1 m) waarmee de Ontwerp Waterhoogten worden gepubliceerd. Het blijkt dus dat de methode van samenstelling van hoogwatergolven redelijk is.

De beste benadering van de stabiele frequentieverdeling van berekende waterstanden is, volgens de Kolmogoroff-Smirnov toets, de Pearson III verdelingsfunctie. Op basis van deze verdelingsfunctie is de overschrijdingskans van de waterstanden te Venlo en Mook bepaald. De verschillen tussen de berekende en benaderde waarden zijn verwaarloosbaar voor de kleinere overschrijdingskansen en voorts minder dan 0.1 m voor de lagere hoogwaters.

De invloed van de karakteristieke hoogwatergolf parameters op de waterstanden benedenstrooms is groter naarmate de toppen bij het meetstation hoger worden en neemt eveneens toe met de afstand tot dit meetstation.

De Ontwerp Waterstanden 2001 te Venlo en Mook overschrijden de verwachte standen volgens de huidige studie. Te Venlo zijn deze respectievelijk 0.3 en 0.5 m

hoger voor overschrijdingskansen van respectievelijk 0.004 en 0.02 per jaar. Te Mook is dit respectievelijk 0.6 en 0.8 m. Het betekent, dat de Ontwerp Waterstanden 2001 zouden moeten worden aangepast. Overigens is voor de Ontwerp Waterstanden de betrouwbaarheidsband niet bekend.

De gemeten vijf hoogste hoogwaters te Borgharen uit de periode 1980-2000 veroorzaken te Venlo en Mook geen significant hogere waterstanden dan de Ontwerp Waterstanden 2001. Het bijzondere hoogwater van januari 1995 heeft volgens de Ontwerp Waterstanden 2001 te Venlo een overschrijdingskans van eens per 60 jaar en volgens de huidige studie van eens per 160 jaar, terwijl dit te Borgharen eens per 40 jaar respectievelijk eens per 30 jaar is.

In het algemeen kan voor vergelijkbare rivieren een procedure worden opgesteld om synthetische golven te ontwikkelen uit combinaties van waarden van onafhankelijke karakteristieke golfparameters, gemeten op een zekere locatie. Daaruit kunnen, met behulp van een hydrodynamisch model, waterstanden worden berekend voor iedere locatie benedenstrooms. Het aantal willekeurige steekproeven van die combinaties hangt af van de mate waarin een stabiele kans dichtheidsverdeling van berekende waterstanden wordt verkregen.

De spreiding in de aldus verkregen waterstanden kan, ten opzichte van een gegeven afvoertop bij de meetlocatie, aanzienlijk zijn vanwege de verschillende samenstellingen van de synthetische golven.

Hoofdstuk 5

In het operationele hoogwaterbeheer is er dringend behoefte aan tijdige informatie, bij voorkeur enkele dagen tevoren, over het karakter van een naderend hoogwater. Daarom is er *een rekenschema ontwikkeld voor een eerste voorlopige voorspelling* van de topafvoer en corresponderende topstand te Borgharen (km 16).

Voorts is het de bedoeling de burgers bewust te maken van de mogelijkheden en beperkingen van waterstandvoorspellingen op basis van gemeten regenval, weersverwachting en computergebruik voor rivierafvoeren.

Op basis van de dagelijkse afvoergegevens van acht hoogwaters te Borgharen in de periode 1980-2000 is de gemiddelde 1-dag Eenheidshydrograaf voor Borgharen bepaald. Deze geeft de gemiddelde dagelijkse directe afvoer uit het afstromingsgebied weer ($\text{m}^3\text{s}^{-1}\text{mm}^{-1}$), die bij Borgharen door de rivier wordt afgevoerd ten gevolge van de zogenoemde effectieve regenval. De effectieve regenval (mm) wordt berekend uit de verhouding van hoogwatergolf volume (m^3) en oppervlakte van het afstromingsgebied (m^2). Gemiddelde 1-dag Eenheidshydrograaf en effectieve regenval zijn dé instrumenten om relatieve afvoerpieken (Q^{piek}) te voorspellen.

Bij toepassing van het rekenschema is de regressiefunctie ‘operationele regenval–effectieve regenval’ gebruikt om de bijgestelde effectieve regenval te bepalen. Door de basisafvoer, d.i. het begin van het stijgende stadium van de hoogwatergolf, toe te voegen aan de aldus verkregen Q^{piek} ontstaat de topafvoer (Q_{piek}) en corresponderende waterhoogte.

Bij vergelijking van deze voorspellingen met die van riviermetingen zijn er verschillen in de waterstanden vanwege onzekerheid in de regenvalgegevens en het gebruik van een gemiddelde 1-dag Eenheidshydrograaf, bijvoorbeeld. Dit is de praktische realiteit waardoor de betrouwbaarheid van de voorspelling wordt beïnvloed. Daarom bepaalden we, behalve de verwachte afvoeren en corresponderende waterstanden, ook de 95% en 50% bovengrenzen van de effectieve regenval uit de betrouwbaarheidsgebieden van genoemde regressiefunctie.

Het blijkt, dat een eerste voorspelling van de topwaterstanden te Borgharen op basis van regenval haalbaar is, er rekening mee houdend dat, vanwege onzekerheden, we redelijke begrenzingen aan de verwachte waterstanden hebben toegekend, zoals bovenvermeld, voor maximaal mogelijke waterstanden bij hoge afvoeren (95% grens) en middelhoge afvoeren (50% grens).

In het algemeen is voor soortgelijke rivieren de werkwijze voor waterstand voorspelling uit regenval analoog aan die voor onze casus. Om toekomstige waterstandvoorspellingen te verbeteren is het noodzakelijk om veel aandacht te schenken aan de betrouwbaarheid van de regenval cijfers, weersvoorspelling en het staven van de relatie tussen operationele regenval en effectieve regenval.

Zorgvuldig onderhoud van het rekenschema voor de voorspelling van topafvoeren en topwaterstanden is noodzakelijk, omdat autonome ontwikkelingen of menselijke ingrepen in de rivier (1) de relatie tussen afvoer en waterstand instabiel kunnen maken en (2) de gemiddelde Tijd Eenheidshydrograaf kunnen wijzigen. Onderzoek naar de invloed van de variabiliteit van de Tijd Eenheidshydrografen op de voorspellingen is aan te bevelen.

Voor eerste voorspellingen van piekwaterstanden op andere locaties dan het meetstation kan vanaf dit station de hoogwatergolf, die uit de regenvalvoorspelling werd ingeschat, worden ingevoerd in een waterbewegingmodel ten behoeve van computerberekeningen voor locale waterstanden langs de rivier.

CHAPTER 1

INTRODUCTION

1.1 Flood level prediction

From time immemorial, investigations have been made into the probability of occurrence of river floods. Based on that knowledge, river-engineering works have been designed and flood protection measures have been taken. Yet, the data available are insufficient to draw firm conclusions on future effectiveness of these interventions. The more reliable the discharge data from the past, the smaller the risk of failure of the design conditions for flood protection measures. The estimation of the probability of exceedance of floods is open to improvement. To that end, other estimation-methods will be used, the data series will be extended and different methods of data processing will be used.

Society puts stringent demands on the acceptable risk of flooding, but it is difficult to determine reliable design dike heights. Over-dimensioning needs to be avoided, because of third-party interests and costs. The present study is partly aimed at reducing uncertainties in the probability of occurrence estimates of extreme floods.

As rivers, which are surrounded by steep rocks in the upper course, may respond within one day to heavy rainfall, flood risk management in the less protected hinterland of the lower course requires early forecasting tools. To be more responsive to flood events, it is essential for local managers, fire brigades and emergency services to be able to take timely protective measures. This requires an easy-to-use model, as developed in this study, to yield a satisfactory first estimate of the discharge and corresponding water level at a certain point along the river starting from rainfall forecasts.

The present study therefore addresses the following issues:

- (1) strategic flood level prediction, in relation to the design of river dikes, levees and other water-control structures, and
- (2) operational flood level prediction, especially early forecasting, to enhance operational decision making. As the flood event proceeds, the availability of more elaborate data and the use of more sophisticated flood forecasting models may enable more accurate predictions.

Because of the author's extensive experience with the Meuse River, his involvement with Meuse River studies and knowledge about the availability and origin of data, the strategic part will be approached by a specific case, viz. the Limburg Meuse River, of which the hinterland is not protected by primary dikes. The hinterland is in use for horticulture, agriculture, industry, living and recreation.

Because of the government's interest to improve design water levels and their accuracy, it is investigated which flood wave properties at Borgharen (the most upstream gauging station in the Netherlands) determine the water levels further downstream and what that means to the local design water levels. The results of the investigation will be tested against observed flood levels at the river locations Venlo and Mook. Their probability of exceedance will be compared with the Design Water Levels 2001, which are based on other principles than those of the present study. The

method developed for the Meuse River will be generalised to other rivers of the same type.

The operational part, viz. timely forecasting of extreme water levels, is developed for the same case. The methodology is shown to be applicable to similar rain-fed rivers, in general.

The Meuse River rises in the northeast of France (Pouilly) not far from Dijon at a height of 450 m above sea level and flows through France (Verdun, Stenay, Chooz), Belgium (Namur, Liège) and the Netherlands (Borgharen, Venlo, Lith) to the North Sea (Haringvliet), Fig.1.

The total length of the river is about 900 km, of which about 400 km in France, 200 km in Belgium and 300 km in The Netherlands. The hydraulic gradients are, on average, 0.7 m/km, 0.35 m/km and 0.15 m/km, respectively.

The basin area in France is 10^4 km^2 , in Belgium $1.1 \cdot 10^4 \text{ km}^2$ (i.e. $0.3 \cdot 10^4 \text{ km}^2$ for the Sambre basin and $0.8 \cdot 10^4 \text{ km}^2$ for the Ardennes basin) in Germany $0.3 \cdot 10^4 \text{ km}^2$ and in The Netherlands $0.6 \cdot 10^4 \text{ km}^2$.

More than 50% of the Meuse River in the Netherlands has no primary dikes.

Not far from the Dutch-Belgian border, the important measuring-station Borgharen (km 16) is situated.

The discharge of the Meuse River mainly depends on the capricious rainfall in its $3 \cdot 10^4 \text{ km}^2$ basin and for a small part on snowmelt. After a period of heavy rainfall, the discharge at Borgharen responds rapidly, mainly because of the steep and rocky character of the Belgian Ardennes basin. The travel time of a flood wave from Liège (tributary l'Ourthe) to Borgharen is about 7 hours and from the French border (Chooz) about 16 hours.

In general the period of high precipitation is from December through March. The floods at Borgharen may vary then from around $1250 \text{ m}^3 \text{ s}^{-1}$ to more than $3000 \text{ m}^3 \text{ s}^{-1}$. Then the weir elements in the Dutch Meuse River are completely hoisted and there is a free runoff. Every year this situation may last one to three weeks at Borgharen, depending on the discharge. The Belgian weirs near the Dutch border, at Monsin and Lixhe (formerly Visé) are in operation up to much higher discharges than the Dutch weirs.

The upstream part of the Dutch Meuse River is a more or less natural river without weirs, with a rather steep hydraulic gradient (0.5 m/km and more) and a coarse gravel bed (the Gravel Meuse) that has partly been excavated in former years. During most of the year the water depth in this river reach is too small for commercial navigation. Therefore a parallel shipping way, the 50 km long Juliana Canal, has been built in the nineteen-twenties. Downstream of the Juliana Canal, in the transition zone between the steeper foothills and the more or less flat lowlands, much gravel and sand has been excavated from the former floodplains. The resulting lakes in this 20 km river stretch Maasbracht – Roermond (Lakes Meuse) can store much water during floods.

Still further downstream, the hydraulic gradient of the Meuse River is small (0.1 m/km), and its bed predominantly consists of sand. This part, with a length of about 120 km to the tidal Meuse at Lith, is called the Sand Meuse (Gerretsen 1996 and 1997).



Gravel Meuse, Meers, km 32



Sand Meuse, Belfeld / Venlo, km 103



Lakes Meuse, Linne, km 70



Tidal Meuse, Lith, km 202

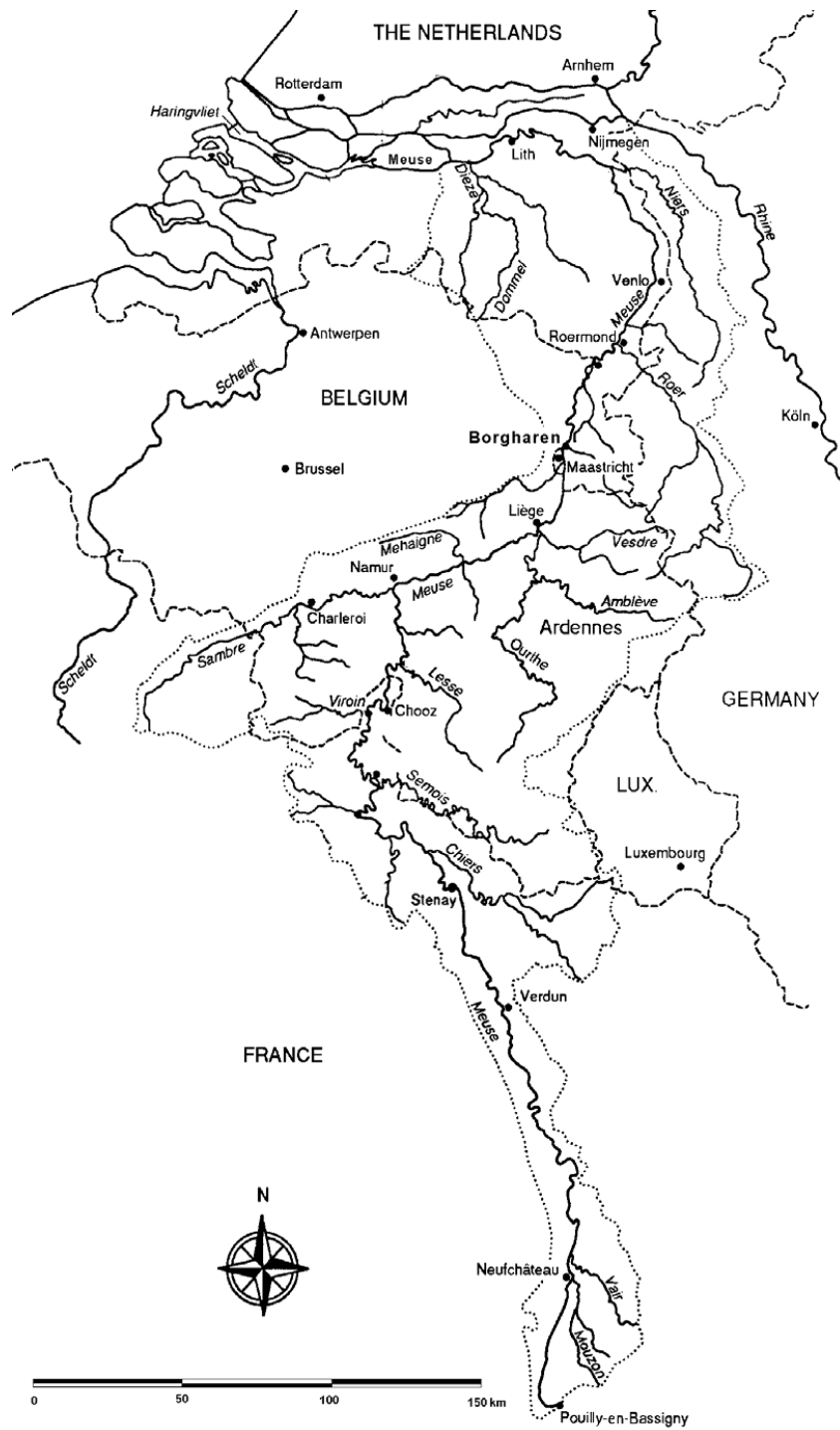


Fig.1 Meuse River basin

1.2 Research objectives and research questions

1.2.1 Objectives

The objectives of the project are:

- An improved estimation method for the probability of exceedance of annual flood peak discharges at Borgharen. As a consequence, design discharges¹ corresponding with the defined probabilities of exceedance (0.02, 0.004, 0.0008 per annum) may change.
- Improved accuracy (a narrower confidence interval) of the probability of exceedance estimates of flood peaks at Borgharen as a result of this determination. This is important for the safety margin of the dike and levee heights.
- Identification of the flood wave properties at Borgharen that determine the water levels further downstream.
- A method to determine these downstream water levels, their probability of exceedance and accuracy.
- Comparing of the DWL 2001 (Design Water Levels 2001) with those of the present study
- Development of an easy-to-use early operational prediction model.
- Generalisation of the findings for the Dutch Meuse River to similar rivers.

1.2.2 Research questions

The corresponding research questions are:

- Do the results of the first part of the study give cause for changing the design discharges? In other words, does the probability of exceedance of the peak discharges at Borgharen change to the extent, that the corresponding water levels differ significantly?
- Are the downstream water levels, e.g. at Venlo and Mook, resulting from the present study and based on local water levels statistics, significantly different from those according to the Design Water Levels 2001?
- To what extent can the discharge peaks and corresponding water levels at Borgharen and the uncertainties therein be estimated with an easy-to-use early warning algorithm? How do the results comply with recently measured flood peaks?
- What can we learn from the Dutch Meuse River case for other rivers of a similar type?

¹ In 1977, the River Dikes Committee (Committee-Becht), assisted by e.g. Delft/Hydraulics (WL) and Centre for Investigation of Water-Control Structures (COW), advised the Government about the design strength of the flood defence system for the inland upper river areas. This has led to legislation stating that these inland river dikes should be able to withstand a flood-peak with a probability of exceedance of 0.0008 per annum. (Ministry of Transport, Public Works and Water Management 1977). The corresponding water levels along the river are *the design water levels (DWL)*.

It should be noticed that in areas without primary dikes, such as the Limburg part of the Dutch Meuse River, a more differentiated approach may be taken. The Provincial Executive of Limburg ruled (1995) that the heights of the levees in the Meuse valley should be brought at a height that they should be able to withstand a water level with a probability of exceedance of 0.02 per annum, whereas after the completion of the "Maaswerken" this should be 0.004 per annum. From Mook and further downstream, where the hinterland is protected by primary dikes, the design water level has a probability of exceedance of 0.0008 per annum.

1.3 Literature overview from other investigations

The main problem in analysing Meuse floods is that the time series is not homogeneous. Non-homogeneity is clearly the result of the weir operation regime, but can also be the result of human interferences in the catchment, climatological trends and the dominant rainfall bringing mechanisms that generate the floods. The following papers deal with such non-homogeneous time series and some of them provide tools to deal with them, particularly the Mixed Distribution and the Multi-Component Distribution. The papers are briefly discussed below.

Adamowski (2000) considers the currently used parametric analysis of ‘annual maximum’ flood series. They reveal unimodal and multi modal probability density functions for floods in two Canadian Provinces Ontario and Quebec. Based on density function shapes and timing of floods both Provinces have been divided into nine homogeneous sub-regions, linked to similar flood-generating mechanisms. A similar analysis of ‘peak over threshold’ (or partial duration) data revealed results like those for the ‘annual maximums’ but there were deficiencies in currently used parametric approaches.

Nonparametric frequency analysis has been introduced as an alternative method. This method also revealed unimodal and multimodal ‘annual maximum’ and ‘peak over threshold’ flood probability density function shapes in both Provinces. A monthly partitioning of both flood series, as an indicator of mechanisms, showed that the stations with an unimodal density were subject to a single mechanism, while the multimodal densities were subject to two or more mechanisms.

L- moment analysis of annual maximum series supported the homogeneous delineation obtained by nonparametric methods (L-moments are defined as linear combinations of probability weighted moments and the first four moments are expressed in the Paper published in Journal of Hydrology No.229 [2000], page 221). However, the peak over threshold series was generated by a mixture of mechanisms and could not be adequately described by any parametric distribution nor did its regional data pass L-moment homogeneity tests.

Alila and Mtiraoui (2002) mention that floods are often generated by heterogeneous distributions composed of a mixture of two or more populations, due to a number of factors such as seasonal variations, changes in weather patterns resulting from low-frequency climate shifts or oscillations, changing channel routing or floodplain flow, and basin variability resulting from changes in antecedent soil moisture. Not recognizing these processes is the main reason that many frequency distributions do not provide an acceptable fit to flood data.

The authors use long-term hydro-climatic records from the Gila River basin (Arizona, USA) to explore the extent and significance of mixed populations. They discuss (1) the causes of heterogeneity, (2) investigate the implications of using various popular predicting distributions, (3) demonstrate how alternative frequency models, that account for floods generated by a mixture of several populations, are more appropriate and (4) illustrate the different results between (2) and (3).

Conventional flood-frequency analysis assumes that floods are drawn from a single population. None of the commonly used homogeneous distributions provide a satisfactory fit to the observed floods, particular at the upper tail of the empirical distribution, even not for the five-parameter Wakeby distribution, which is the most flexible of the homogeneous distributions concerned.

A heterogeneous distribution that accounts explicitly for the fact that floods are generated by more than one hydrological distinct mechanism produced a superior fit. Two challenging decisions need to be made (i) one must determine how many component distributions should be used. Hydro-climatic data often can be used to decide on the number of flood populations. One remedy for this problem is to use a regional approach for fitting the heterogeneous distribution. Such a technique has been justified in the studies of Fiorentino *et al.* (1985) and Gabriele & Arnell (1991). (ii) One must select an appropriate parent distribution for each component and that is rather subjective. More research on the selection of distributions using the physical nature of hydrological processes is desperately needed.

Bakker and Luxemburg (2005) consider the problem of heterogeneous distributions of floods, as research in the area of frequency analysis has been rather limited on this item, although several investigators confess that the assumption of homogeneity of flood distributions may not be valid. Therefore, the estimates of probabilities of exceedance are often very unreliable. The heterogeneity of the series of annual maximum runoffs can be explained by the fact that different extreme floods are caused by different mechanisms (ice-melt, rains, cyclones, etc.). The study focuses on promising methods to deal with heterogeneity and concerns methods to involve the physical nature of floods on the basis of several small catchments in east Russia. If the mechanism can realistically explain the heterogeneity, then the 'Mixed Distribution' gives much better probability estimates for the extreme high floods than the conventional method on basis of homogeneity.

A Mixed Distribution is a weighted sum of a couple of homogeneous probability distributions. The set of full annual maximums has to be split into subsets (the partial annual maximums) according to the flood-causing mechanisms. For these subsets the cumulative distribution functions have to be determined. Before summing the separate cumulative distribution functions they have to be multiplied by the probability of occurrence of the specific mechanism in the full annual maximums series. The sum of these probabilities of occurrence equals one.

Keim and Faiers (1996) explored heavy rainfall distributions by season and the associated differences in seasonal quantile estimates for selected recurrence intervals in Louisiana, as a result of the findings of other investigators. Known methods are implemented, but with additional synoptic analysis to acquire a better understanding of the dynamics behind differences in storm magnitudes between seasons. The results may be relevant to seasonal activities such as agricultural growing, short time construction projects, recreational activities, etc.

Four first-order gauging sites in Louisiana were selected for analysis because of their hourly rainfall records 1948-1991 during the four seasons. It was concluded by the test of Kruskal-Wallis and Mann-Whitney that the distribution of heavy rainfall events differs significantly between particular seasons at the three sites near the Gulf Coast. To get further insight into what may cause the storm events, the weather type mechanisms Frontal, Golf Tropical Disturbance and Airmass (convection) are confronted with the rainfall depths (minimum, mean, standard deviation). It turned out that seasonal frequency curves varied dramatically at the four mentioned sites. Quantile estimates are largest in spring, while winter estimates are smallest. The mechanisms that produced the events were found to change seasonally. The rainfall in winter and spring were primary generated by the Frontal type and summer and autumn rainfall by Golf Tropical Disturbance and Airmass.

The used method can serve as a guide for additional research.

Klemes (2000) critiques the common frequency analysis techniques for hydrological extremes, in particular the claims that their increasingly refined mathematical structures have increased the accuracy and credibility of the extrapolated upper tails of fitted distribution models. He argues that the increased mathematization of hydrological frequency analysis over the past 50 years has not increased the validity of estimates of the frequencies of high extremes, thus has not improved our ability to assess the safety of structures whose design characteristics are based on them. The Paper compares the common-sense engineering origins of frequency analysis with its present ostensibly 'rigorous theory'. Some myths advanced under the banner of the latter are analysed in greater detail. In the meantime, guesses must be made. In the interest of fair practice, simple extrapolation procedures, commensurate with the current lack of credible scientific basis for extrapolation of upper tails of distributions, should be adopted by professional consensus and, at the same time, serious work should continue on understanding the hydrological 'dice', being aware that it is the physical regime that determines the shape of the extrapolated upper tail of the fitted distribution model.

Luxemburg, W.M.J. et al. (2002) analysis the statistical properties of flood runoff of North Asian rivers under conditions of climate change. In the field of flood frequency distributions the estimates of the probability of exceedance are often very unreliable since the heterogeneity of the annual maximum series is not recognised or neglected. This heterogeneity of the annual maximum series can be explained by the fact that the different extreme floods are caused by different mechanisms, such as precipitation, basin conditions, human activities, etc., and belong to different statistical populations. The study compared theoretically and in practice two existing methods to deal with heterogeneous annual maximum series: The **Multi-Component Distribution** and the **Mixed Distribution**. The comparison is done on the basis of a case study on 26 catchments in Primorye and Amur basin in the Far East of Russia. With the help of the Kolmogorov-Smirnov test on the estimated probabilities and reduced variables, both methods are compared to each other and to conventional methods. In the case of heterogeneity, the annual maximum series have to be split according to their flood-causing mechanisms. After estimating the **Cumulative Distribution Functions** of the sub-series (components) they have to be combined. Such a combination is called a **Heterogeneous Distribution**. The **Cumulative Distribution Functions** to fit the components within the **Multi-Component Distribution** are estimated from the full annual series of the extreme floods caused by the relevant mechanisms. The independently estimated **Cumulative Distribution Functions** have to be multiplied to obtain the **Multi-Component Distribution**. The **Mixed Distribution** is a weighted sum of a couple of homogeneous probability distributions. These **Cumulative Distribution Functions** are estimated from **Partial Annual Maximum** series. A **Partial Annual Maximum** series contains all absolute annual extremes that are caused by one and the same flood-causing mechanism. So, the **Cumulative Distribution Function** estimates a conditional probability. This condition is that the extreme flood caused by the relevant mechanism exceeds all other floods in the same year. The weight of the **Mixed Distribution** estimates the probability that this condition is true. Recognition of the different character of the **Partial Annual Maximum** series is necessary in the research on suitable **Cumulative Distribution Functions** to fit the **Partial Annual Maximum** series. Besides it is needed

to show that the **Mixed Distribution** and the **Multi-Component Distribution** estimate the same relation.

Final conclusion: The **Multi-Component Distribution** gave better results than the **Mixed Distribution** and both **Heterogeneous Distributions** gave better results than conventional homogeneous distributions.

Mantje, et al. (2007) try to identify the different homogeneous subsets in a heterogeneous distribution (although the latter is often regarded as homogeneous in flood frequency analysis). Then, they try to identify the mechanics behind the heterogeneity. For the identification of the different subsets an analytical method based on the maximum likelihood criterion has been used and applied to runoff maximums from floods in Europe and Russia. This method determines the transition point between heterogeneity and homogeneity. What is the advantage of using this method compared with that of the homogeneity approach? Is it better to connect heterogeneity with seasonality or influence of cyclones?

By splitting of the dataset into the lowest and highest discharge extremes the distinctive form of heterogeneity is seen in the distribution as a threshold behaviour.

In conclusion: There was no hard reason to connect heterogeneity with one of the climatic or weather mechanisms or catchment conditions, although this differs from region to region. In the southern of Russia it was observed that heterogeneity is probably caused by the influence of weakened typhoons.

The research of Min Tu (2006) was based upon a combination of statistical trend analysis and hydrological modelling of the Meuse River discharges 1911-2000 at Borgharen. She concluded that the winter discharge has significantly increased since 1984 just like its frequency, while the influence of land use changes upstream of Borgharen could not justify this increase. It is remarkable that the European atmospheric circulation patterns illustrate a change since 1980 by bringing stronger westerly surface winds across the North Atlantic to Europe and can broadly be ascribed to climate variability that causes more precipitation.

Rossi et al. (1984) describe the theoretical considerations to obtain a parent flood distribution that closely represents the real flood experience, existing of 39 annual flood series of Italian river basins. The choice of a good parent flood distribution has been based mainly on its ability to reproduce the statistical characteristics of a great number of annual flood series. As the sample skew is a statistic that is particularly sensitive to the behaviour of the right-hand tail of the distribution the analysis of the skew of the observed annual flood series is useful. The property of skew is often connected with the presence of outliers. To overcome this deficiency, in the present Paper preference was given to two-component (basic and outliers) models based on the compound Poisson process. Within this class of models, the one apt to reproduce the upper tails of Italian annual flood series is that of the maximum of a Poissonian number of a mixture of two exponential random variables. The two-component extreme value distributions, ensuing from this approach, emerges as a generalization of the Gumbel distribution. The more general two-component extreme value distribution assumes individual floods to arise from a mixture of two exponential components. Its parameters can be estimated by the maximum likelihood method. It was shown that a regionalized two-component extreme value distribution, with parameters representative of a set of 39 Italian annual flood series, closely reproduce the observed distribution of skew and that of the largest order statistics.

Vogel and Wilson (1996) document that since the introduction of L-moments* (Hoskin 1990) many investigators have recommended them to assess the goodness-of-fit of probability distributions to samples of stream flow and precipitation. Others (Chow and Watt 1994) claim that it requires quite a few measuring-stations to provide a definitive assessment of goodness of fit.

This study construct L-moments (also see Adamowski 2000, aforementioned) for annual maximum floods at more than 1450 river basins in the United States. Goodness-of-fit comparisons turn out that (1) the general extreme value, (2) the three parameter lognormal and (3) the log Pearson type III distributions provide acceptable approximations to the distribution of annual maximum flood flows in the continental USA, whereas other three parameter alternatives are not acceptable. These results are consistent with previous L-moment studies in south western USA and Australia. L-moments applied in other parts of the world have all recommended the use of the general extreme value distribution for modelling annual maximum flood flows.

We will never know, with certainty, the true population from which observed stream flows arise, yet studies such as this can provide some guidance for a reasonable approximation.

* An L-moment diagram compares sample estimates of the L-moment ratios, viz.

L-volume, L-skew, and L-kurtosis with their population counterparts for a range of assumed distributions. An advantage of L-moment diagrams over other goodness-of-fit procedures is that one can compare the fit of several distributions to many samples of data using a single graphical instrument.

This ‘literature overview’ proves the context to a renewed approach of the problem to estimate the discharge peak at Borgharen, and corresponding water level, for a given probability of occurrence. The innovation consists of the application of a heterogeneous distribution to the given data base of annual peak discharges at Borgharen.

1.4 Research methodology

1.4.1 Determination of the probability of exceedance of the annual discharge peaks

In order to find a method to improve the accuracy of the design discharge estimates, the annual peak-discharge records at Borgharen from the period 1911-2000 are used. They are extended with information from some documented extreme flood events in previous centuries. The latter have been documented at that time, because of the damage and misery they caused.

In order to have a homogeneous data series, peak discharges from the early 20th century are translated into contemporary ones, taking account of the effects of large river works. The same goes for the documented peaks from previous centuries until 1571.

To establish the plotting positions in the ‘exceedance–discharge’ relationship, the formulae of the Weibull-Benson type combined with the introduced discharge threshold, as described by Hirsch and Stedinger (1987), are used. For comparison, Dalrymple’s method (1960) is also used, and the probability of exceedance of the flood peaks is determined. A probability distribution function is fitted to the plotted data and its 95% confidence interval is determined.

1.4.2 *Flood wave properties*

To the author's knowledge, the influence of the shape of the flood wave at Borgharen on the water levels further downstream has never been explored explicitly, so far. In order to identify the flood wave properties that may determine the downstream water levels, the daily observations at 08:00 a.m. of the Borgharen discharge in the period 1930 – 2000 are used. Peak discharge, base discharge, flood wave volume, centre of gravity, width, skewness and crest curvature are determined for the measured floods.

In order to account for the influence of the large river works upstream of Borgharen on the shape of the discharge hydrographs, the shape parameters are split into two sets, namely those before and after 1980, the year in which the latest major intervention was accomplished. Both sets of parameter series are tested on the presence of trends with the Spearman-test, and the equivalence of averages with the F-test (McClave 1997). Whenever there are significant differences between the corresponding series of both sets, they are homogenized to the present-day situation.

Different flood maxima at Borgharen may yield the same water level further downstream, if one or more other flood wave parameters are different. It is known that the rate of attenuation of a flood wave, propagating through a river, is associated with the crest curvature of the discharge hydrograph.

1.4.3 *Transformation of flood wave properties at Borgharen to downstream water levels*

To transform a combination of characteristic wave parameter values of a flood at Borgharen to a downstream water level at Venlo and Mook, for instance, a Monte Carlo simulation procedure is adopted, which consists of the following steps:

- Assess the correlation of the characteristic flood wave parameters and check their mutual independence, a necessary condition for random sampling.
- Randomly sample sets of the independent parameter values.
- Synthesize a flood wave at Borgharen from each set.
- Compute with a numerical model the water level peak at e.g. Venlo and Mook that is caused by this synthesized flood wave at Borgharen.
- Repeat the foregoing two steps for other sets of parameter value combinations and continue this procedure until the probability density function (pdf) of the water levels at Venlo and Mook has converged to a stable shape.
- The probability of exceedance of the local water levels at Venlo and Mook can be determined from this converged pdf.

1.4.4 *An easy-to-use forecasting-model*

An easy-to-use early forecasting model for the peak discharge at Borgharen is needed to enable local authorities to take timely protective measures when a flood is expected. Rainfall forecasts in the river catchments are supposed to be provided a few days ahead by the Meteorological Services. Other useful data from abroad, such as the discharges from the Belgian and French tributaries of the Meuse River and the Meuse River itself, are not to be expected at short notice, due to hectic situations at the

Belgian and French Services de la Meuse, as experience has shown. As a consequence, the model will be mainly based on rainfall forecasts, so the accuracy of the peak discharge prediction strongly depends on the accuracy of these forecasts.

In literature, various methods are used to relate precipitation to river runoff (Shaw 2002). In this study the method of the average 1-day Unit Hydrograph, applied to the effective rainfall, is chosen. To assess its reliability, predictions based on operational rainfall depths are tested against measured river discharge peaks at Borgharen from the period 1980 – 2000 and validated for some more recent floods.

1.4.5 *Models*

The translation of the synthesized discharge flood waves at Borgharen into water levels further downstream will be made using a 1-D Sobek computer model, which has been structured, calibrated and verified for the Dutch Meuse River by Rijkswaterstaat, RIZA (2002). Backgrounds of that model are described.

1.5 **Expected results and practical relevance of the study**

1.5.1 *Expected results*

The expected results of the study are:

- New design discharges and corresponding water levels at Borgharen.
- Identification of the properties of the flood wave hydrograph at Borgharen that have a significant influence on the water levels further downstream.
- Guidelines how to determine the probability of exceedance of local water levels from random samples of combinations of characteristic flood wave parameter values at Borgharen.
- Results of applying these guidelines to the locations Venlo and Mook, for instance, and comparing these water levels to those of floods that have occurred, and to the DWL 2001. Possibly, adaptation of the DWL 2001
- A simple peak discharge forecasting-algorithm for Borgharen from rainfall data in the Meuse River catchment abroad.
- Translation to more generic results, applicable to similar rivers.

1.5.2 *Practical relevance*

The relevance of the study to strategic flood level prediction is, that the results will be applicable to:

- the design of levees, dikes and other flood protection measures along the river;
- the design of river restoration schemes;
- policy development within the scope of the prevailing legislation.

The relevance of the study to operational flood risk management practice is:

- to have an easy-to-use model for an early assessment of the expected peak discharge at Borgharen and corresponding water level;
- to enable the prediction of downstream water levels, using a numerical computer model and estimating the relevant flood wave shape at Borgharen.

CHAPTER 2

PROBABILITY ANALYSIS OF FLOODS IN THE DUTCH MEUSE RIVER AT BORGHAREN

2.1 Frequency of occurrence of recorded and documented floods

As mentioned in the footnote to Section 1.2, at that time the River Dikes Committee (1977) had to investigate the efforts needed to attain the desired safety against inundation. Aspects such as costs, nature, landscape, culture and history were important. A design frequency of occurrence of 0.0008 per annum was adopted and laid down in law for dikes as a primary flood defence. In areas without dikes, such as the Limburg part of the Dutch Meuse River, a more differentiated approach of the design level was considered, because of the use of a part of the floodplains for housing, industry and horticulture.

The number of systematically recorded annual discharge peaks is modest (89), given the fact that we also have to predict the discharge peak that will occur once in 1250 and 250 years on average. Besides, there are many irregularities in the discharge probability distribution (Fig.2.1.1 and Appendix 2.1.1). This is why the free flow situation is separated from the remainder of the peak discharges.

In spite of the relatively small number of data, the aim of this part of the study is to improve the accuracy of estimated design discharges at Borgharen.

So far, the discharge probability distribution has been determined while neglecting the river situation upstream of Borgharen. In the present study improvements are expected (1) by adding documented discharge data of peaks from the period 1571 – 1910 (as far as approximately known) to the continuously recorded data series from the twentieth century (1911-2000), (2) by applying new methods to determine the probability of exceedance of the individual floods, and (3) by separating the free-runoff situation upstream of Borgharen from the set-up situation, so as to achieve more consistency in the exceedance plot of the peak discharges. The homogeneity of the annual peak discharge data is considered below.

Irregularities in the discharge probability distribution are not only caused by irregular hoisting of the weirs in Belgium, but also by not tuning with the Borgharen weir. The Borgharen weir is out of operation from about $1200 \text{ m}^3\text{s}^{-1}$, whilst the weirs in the Liège reaches are still operating incoherently, which causes scatter in the discharge probability distribution at Borgharen. From 1500 to $2000 \text{ m}^3\text{s}^{-1}$ at Borgharen, the weirs in the Liège areas are still in use and the water levels are lowered in the Belgian headwater reaches by about 0.6 m to create storage capacity in anticipation of the approaching top of the flood. Over $2500 \text{ m}^3\text{s}^{-1}$ it is difficult to maintain the backwater level there, and over about $2700 \text{ m}^3\text{s}^{-1}$ it is impossible to keep the weirs in operation.

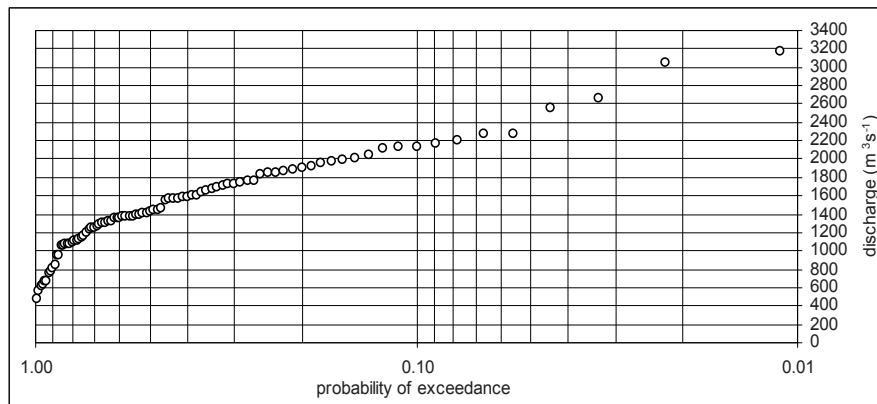


Fig.2.1.1 Probability of exceedance of the annual peak discharges at Borgharen 1911-2000, according to Weibull

In the Liège region it is important to keep the weirs in operation as long as possible, in order (1) to generate water-power energy for the town of Liège and (2) to maintain the water level in the upstream reach of the Albert Canal, the shipping route to Antwerp. Even during the flood of December 1993 (peak discharge $3040 \text{ m}^3\text{s}^{-1}$ at Borgharen), the weir of Lixhe, near the Dutch border just downstream of Visé, has been out of operation only during part of the peak-day (WL | Delft Hydraulics, 1994, Report 4, Chapter 9, page 18).

Before 1800, the Meuse River did not belong to the European River Communication Network. In Belgium the river was navigable to a depth of 1.2 m. All historical information (WL | Delft Hydraulics, 1994, Report 4, Chapter 5) points to the fact that this has been maintained since the fifteenth century and that after a period of neglect at the beginning of the nineteenth century, the river depth was restored to 1.2 m again from 1840 onwards.

Small-scale local works have been carried out to protect cities against flooding and, furthermore, moderate-size weirs have been constructed in the second part of the nineteenth century. It may be agreed that these small-scale works, which did not systematically improve the river in its entirety, did not influence the height and the shape of the flood waves at Borgharen. The much larger-scale modernisations of the Belgian Meuse River, which started end nineteenth beginning twentieth century, did have a significant influence: they caused floods to reach the Dutch border sooner and sometimes with higher maximum discharges. The large works were finished around 1980. In order to have comparable discharge values, data from the past have been converted to the present situation, using a hydrodynamic simulation model applied to historical as well as recent bottom data of the Walloon Meuse River, and discharges of recent floods (WL | Delft Hydraulics, 1994, Report 4, Chapter 7.1.5). Also the consequences of the change of discharge measuring equipment through time, from float gauging to Ott-meter, to integrated and to acoustic technique, were taken into consideration. The increased extractions of water from the Meuse River for shipping, agriculture and domestic use, are not significant in this context.

It turned out that some of the present annual peak discharges at Borgharen would have been a few percents less, from 2% for low floods to 5% for extraordinary high floods, if the former situation would still have existed.

The propagation of the discharge peak from the French border to Borgharen would have taken 3 hours (for $1500 \text{ m}^3\text{s}^{-1}$) to 10 hours (for $3000 \text{ m}^3\text{s}^{-1}$) longer than nowadays (WL | Delft Hydraulics, 1994, Table 7.1). The stage–discharge curves, resulting from the measurements at Borgharen in the period 1911–2000 are essential for the determination of the annual peak discharges. Unfortunately they have been adapted many times during that period. Consequently the peak discharges had to be corrected afterwards, which may have introduced extra errors.

The annual peak-values are available in the ‘Yearbooks of Water levels, Discharges and Temperatures’ (RIZA), and in Reports on remarkable floods (Directorate Limburg & RIZA). In Appendix 2.1.7 the recorded annual peak discharges at Borgharen are mentioned.

Fig.2.1.2 shows that there is no significant long-term trend in the peak discharges, although very dry and very wet periods, e.g. the seventies and the nineties, differ significantly.

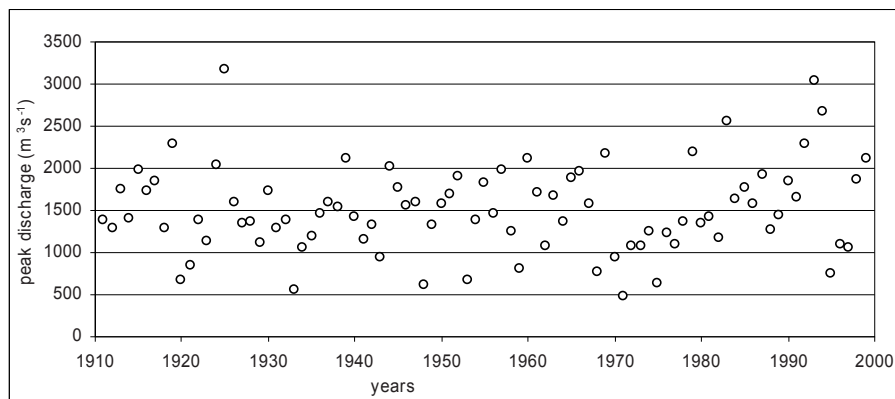


Fig.2.1.2 Annual peak discharge at Borgharen in the period 1911–2000. Free-flow over $1200 \text{ m}^3\text{s}^{-1}$

In previous centuries, at many locations along the Belgian Meuse River, particularly in the Liège region, the water levels were noted during the largest floods, so that for those floods one can derive hydraulic gradients. The hydraulic gradients could be interpreted later and converted into discharges on the basis of advanced discharge measurements, carried out since about 1880 at Visé, downstream of Liège, near the Dutch border. Furthermore, historic peak discharges can be derived from the data published in ‘Investigation Flooding Meuse River’ (WL | Delft Hydraulics, 1994, Report 4, pp.2.25–2.28), obtained from an analysis of the Royal Dutch Meteorological Institute (KNMI).

From 1571 until 1910 there have been four very extreme floods, not headed up by ice jams, namely in 1643, 1740, 1850 and 1880, with estimated peak discharges of 3075 , 3020 , 2850 and $2950 \text{ m}^3\text{s}^{-1}$, respectively. These values include the 5% correction, because of the effect of large river works as mentioned before. Only the largest floods that caused much damage and misery have been documented (Lorenz, 1997). As the less extreme floods were roughly estimated within class intervals of $500 \text{ m}^3\text{s}^{-1}$ and uncertainties about ice jams played a role on top of that, these less extreme discharges are not taken into account in the present study.

The series of discharges used in this investigation consists of 93 annual maximum discharges i.e. 89 systematically recorded floods from the period 1911-2000 and four documented floods from the period 1571-1910 (see Appendix 2.1.8 for the definition ‘flow year’). During the period 1571-2000, the hydrological situation did not change significantly, as explained in the next section.

Here the focus is on the special case when, in addition to the systematically recorded discharges over an uninterrupted period, one also knows the time and the estimated peak discharges of some floods in the preceding period (here called the historical floods). Hirsch and Stedinger (1987) have analyzed various proposals to determine the plotting positions in a p.o.e.-plot of recorded floods combined with documented historical floods. This led to (1) the Weibull-Benson development of the Exceedance formulae for the plotting position estimator, and to (2) the Dalrymple method, for comparison.

The E formulae for exceedance:

In our case, the complete flood series (Appendix 2.1.9) consists of $g=93$ observed floods during an observation period of $n=429$ years (1571-2000).

For such cases Benson et al. (1950) proposed to introduce a discharge threshold of perception (Y_0). The perception may consist of remarkable things as flooding houses, disastrous events, changing river dynamics (e.g. set-up situation into free flow), exceeding a particular stage, etc. If one only applies the Weibull formula for plotting-positions to each subset above and below a certain discharge threshold separately, the possibility of a discontinuity in the probability of exceedance (p.o.e.) assigned to the subset above and below the threshold was recognized by Benson. In order to arrive at consistent results, we have to obtain a series of peak discharges, properly representative of the total discharge distribution.

Hirsch and Stedinger (1987) developed a model that serves as the basis of statistically reasonable and consistent p.o.e.-plot positions.

Let s be the number of systematically recorded flood peaks in the period of 429 years ($s=89$), then $s \leq g < n$. Among these floods there is a subset consisting of the floods $Y(1)$ through $Y(k)$, which are known to have ranks 1 through k in the observation period of n years. These k floods (in our case $k=6$) may be referred to as ‘extraordinary floods’ as they exceed a certain discharge threshold of perception, namely a change of the river dynamics: the set-up situation changes into the free-flow situation in the Liège Meuse River branch and therewith in the whole Meuse River.

Some (or all) flood peaks may have occurred during the systematically recorded period. Let e be the number of ‘extraordinary floods’ from the systematic record ($e \leq k$), then $g=s+k-e$. In this case $e=2$. Also see Appendix 2.1.9.

Because of the aforementioned discontinuity, we do not only apply the usual Weibull formula for the probability of exceedance:

$$p_i = i/n+1, \quad (\dots 2.1.1)$$

for which i the ranking number of the flood in descending order, but we use the alternative plotting position formula (Weibull-Benson) which recognizes that there is some probability of exceedance p_e of the threshold Y_0 . The actual number of exceedances of Y_0 in n years, k , is a binomial random variable with parameter p_e .

The true expectation of the probability of exceedance of Y_0 , namely p_i , given p_e and values of k and e is:

$$E_{p_{oe}} \{p_i | p_e, k, e\} = (i/k+1) \cdot p_e, \text{ with } i = 1, \dots, k \quad \text{and } 0 < p_i < p_e \quad \dots(2.1.2)$$

for which:

Y_0 the discharge threshold (m^3s^{-1}),

p_i the true probability of exceedance of Y_0 ,

k the actual number of floods in the subset above the discharge threshold,

e the number of systematically recorded floods of the subset above the discharge threshold,

p_e the parameter of a binomial random variable

i the ranking number of the discharge peak in descending order

The true expectation of the probability of *not* exceedance of Y_0 , namely q_i , given p_e and values of k and e is:

$$E_{p_{one}} \{q_i | p_e, k, e\} = p_e + (1 - p_e) \cdot (i - k / s - e + 1), \quad \text{with } i = k + 1, \dots, g \quad \dots(2.1.3)$$

and $p_e < q_i < 1$

for which:

q_i the true probability of not exceedance of Y_0 ,

s the number of systematically recorded flood peaks,

g the number of systematically recorded flood peaks, plus documented peaks from historical events

n the length of the composite series in years

As $p_e \approx k/n$, we finally get the estimator:

$$p_i = \{i/(k+1)\} \cdot k/n \quad \text{for the probability of exceedance of the discharge threshold, where } i = 1, \dots, k \quad \dots(2.1.4)$$

$$q_i = k/n + (n-k)/n \cdot (i-k)/(s-e+1) \quad \text{for the probability of not exceedance of the discharge threshold, where } i = k+1, \dots, g \quad \dots(2.1.5)$$

Applying the equations (2.1.4) and (2.1.5) leads to Figs.2.1.3 through 2.1.5, for the variable chosen discharge thresholds of 2750, 2550 and 2100 m^3s^{-1} respectively.

It is clear, that discontinuity in the connection between the probabilities above and below the threshold is negligible in Fig.2.1.3, whereas it is present in Fig.2.1.4 and clearly in Fig.2.1.5. The Appendices 2.1.2 through 2.1.4 show more details and also the position of the measured peaks.

It is remarkable that the six largest floods above the preferred discharge threshold at 2750 m^3s^{-1} , viz. the documented four historical floods in the period November 1571-1910 and the two recorded floods in the period 1911-2000, have rather close peak values (2850-3175 m^3s^{-1}). Does that point to a physical maximum?

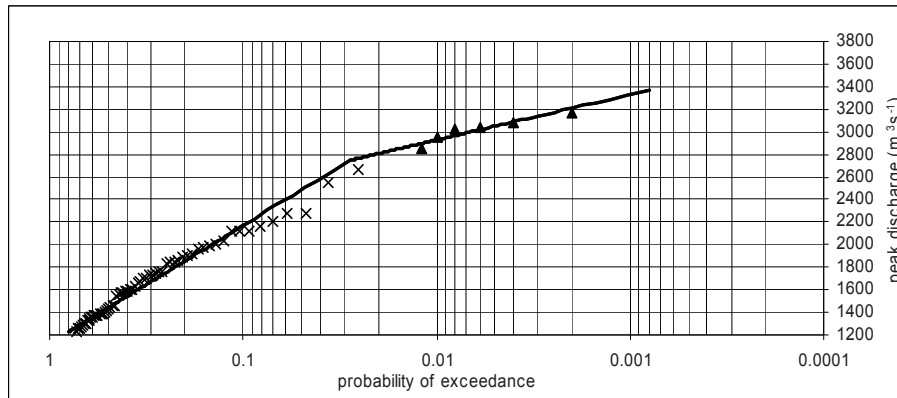


Fig.2.1.3 Probability of exceedance of the peak discharge at Borgharen (1571-2000)*, regression lines in accordance with the E formulae above (▲) and below (×) the threshold discharge at $2750 \text{ m}^3\text{s}^{-1}$

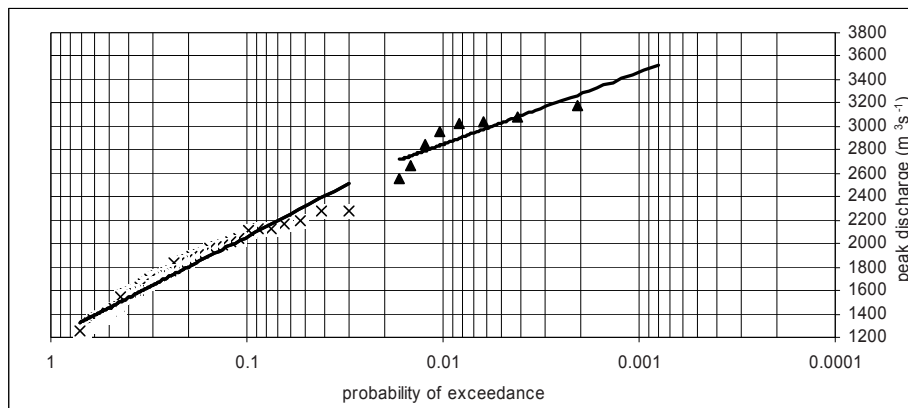


Fig.2.1.4 Probability of exceedance of the peak discharge at Borgharen (1571-2000), regression lines in accordance with the E formulae above (▲) and below (×) the threshold discharge at $2550 \text{ m}^3\text{s}^{-1}$

* Flow year 1571 -or hydrological year 1571- starts from 1 November 1571. The important large flood occurred at 7 February 1571. It is assumed that from this flow year the extreme floods are documented well (RIZA Report 2002.013).

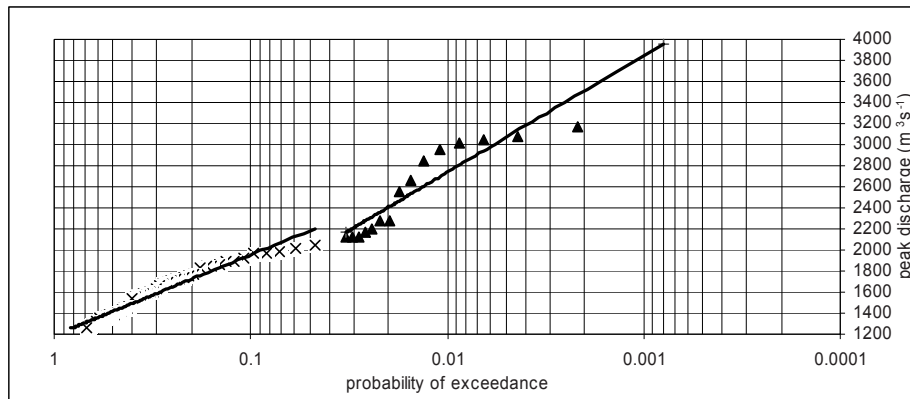


Fig.2.1.5 Probability of exceedance of the peak discharge at Borgharen (1571-2000), regression lines in accordance with the E formulae above (▲) and below (×) the threshold discharge at $2100 \text{ m}^3\text{s}^{-1}$

Apparently, there is a preference for the threshold at $2750 \text{ m}^3\text{s}^{-1}$ when applying the E-formulae. In Fig.2.1.3 the relationship between the probability of exceedance and the peak discharge is split into:

(1) The part above the threshold at $2750 \text{ m}^3\text{s}^{-1}$, for which

$$Q_{\text{peak}} = -174.75 \text{ LN}(x) + 2124 \quad \dots(2.1.6)$$

where x is the probability of exceedance of Q_{peak} , and $x \leq 0.02781$

(2) The part below the threshold at $2750 \text{ m}^3\text{s}^{-1}$, for which

$$Q_{\text{peak}} = -453.75 \text{ LN}(x) + 1125, \text{ and } x > 0.02781 \quad \dots(2.1.7)$$

For the equations of the 2550 and $2100 \text{ m}^3\text{s}^{-1}$ threshold values and methods, also see Appendix 2.1.10.

For the preferred threshold value, the 95% error band of the regression line of the peak discharges is given in Appendix 2.1.5. It is determined with the formula (van der Grinten & Lenoir, 1973):

$$(S_{\text{res.}})^2 = [1/m-2] \sum (Y_i - a \text{ LN}[X_i] - b)^2 \quad \dots(2.1.8)$$

where,

$(S_{\text{res.}})^2$ the residual variance of the discharge peaks Y_i , related to the regression line $Y_i^* = a \text{ LN}[X_i] + b$

m the number of observations of the subset

- Y_i the peak discharges
 X_i the probabilities of exceedance
a the regression coefficient
b the zero intercept of the regression line for which $X_i = 1$.

The Dalrymple method:

Remember that the series of discharges consists of 93 (i.e. 89 recorded and 4 documented) observed annual peak discharges in a period of 429 years, of which four peaks above the threshold of $2750 \text{ m}^3\text{s}^{-1}$ are only documented and two have been systematically recorded, so six above the threshold in 429 years.

A transformed ranking number (i_{trans}) is assigned to each of the floods (Appendix 2.1.11) via the following procedure:

Taking the discharge threshold at $2750 \text{ m}^3\text{s}^{-1}$, then $429 - 6$ is 423 annual discharge peaks are below that threshold. Assuming that the non-registered discharge peaks below the threshold belong to the same distribution as the 87 recorded peaks below the threshold, the transformed ranking numbers (i_{trans}) are given by:

$$i_{\text{trans}} = 6 + (423 / 87) (i - 6), \quad \dots(2.1.9)$$

where i is the ranking number 7...93 of the observed annual peak discharges.

Fig.2.1.6 shows the result for the probability of exceedance of the peak discharges (also see Appendix 2.1.6 for details).

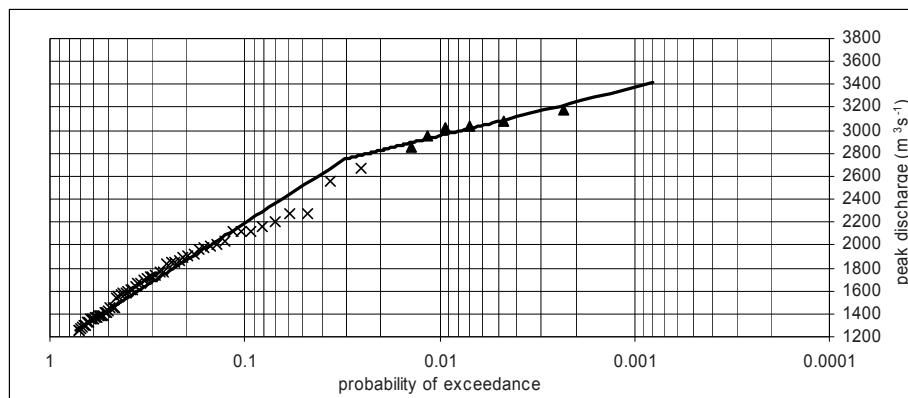


Fig.2.1.6 Probability of exceedance of the peak discharge at Borgharen (1571-2000), regression lines in accordance with the Dalrymple method above (▲) and below (×) the threshold discharge at $2750 \text{ m}^3\text{s}^{-1}$

For the discharge thresholds at 2550 and $2100 \text{ m}^3\text{s}^{-1}$ it is shown in Figs.2.1.7 and 2.1.8, respectively, that the plotting-positions are less consistent than for the threshold at $2750 \text{ m}^3\text{s}^{-1}$ (see Appendix 2.1.10 for the equations).

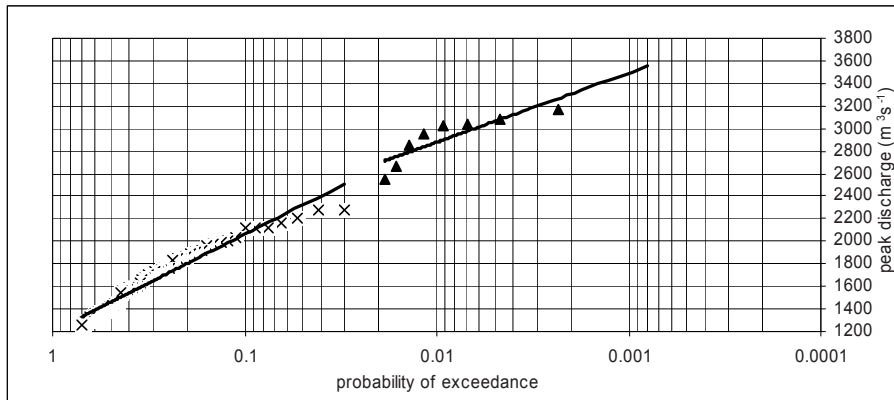


Fig.2.1.7 Probability of exceedance of the peak discharge at Borgharen (1571-2000), regression lines in accordance with the Dalrymple method above (▲) and below (×) the threshold discharge at $2550 \text{ m}^3\text{s}^{-1}$

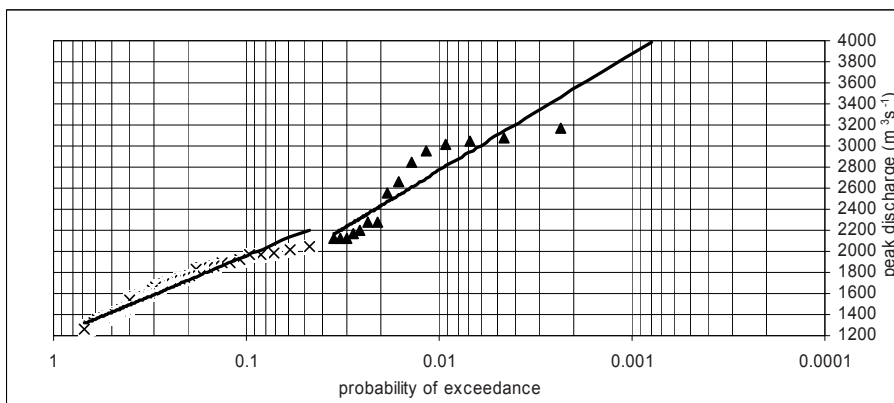


Fig.2.1.8 Probability of exceedance of the peak discharge at Borgharen (1571-2000), regression lines in accordance with the Dalrymple method above (▲) and below (×) the threshold discharge at $2100 \text{ m}^3\text{s}^{-1}$

The results of both methods (E formulae and the Dalrymple method) for the preferred threshold discharge at $2750 \text{ m}^3\text{s}^{-1}$ are summarized in Table 2.1.1.

probability of exceedance yr^{-1}	Exceedance method		Dalrymple method	
	discharge m^3s^{-1}	95%confidence band of the regression line m^3s^{-1}	discharge m^3s^{-1}	95%confidence band of the regression line m^3s^{-1}
0.02	2808	± 85	2827	± 90
0.004	3089	”	3120	”
0.0008	3370	”	3412	”

Table 2.1.1 p.o.e. 1/50, 1/250 and 1/1250 per annum of the discharge at Borgharen, according to either method with threshold discharge at $2750 \text{ m}^3\text{s}^{-1}$

The discharge values for the next best threshold ($2550 \text{ m}^3\text{s}^{-1}$) are given in Table 2.1.2.

probability of exceedance yr^{-1}	Exceedance	Dalrymple
	discharge m^3s^{-1}	discharge m^3s^{-1}
0.02	2666	2695
0.004	3093	3123
0.0008	3520	3550

Table 2.1.2 p.o.e. 1/50, 1/250 and 1/1250 per annum of the discharges at Borgharen, according to either method with threshold discharge at $2550 \text{ m}^3\text{s}^{-1}$

The discharge difference for the same p.o.e. between the two methods for threshold $2750 \text{ m}^3\text{s}^{-1}$ is 0.7 to 1.2%, and for the threshold $2550 \text{ m}^3\text{s}^{-1}$ 0.9 to 1.1%. The discharge difference for the same p.o.e. according to the same method, but with different threshold values, namely 2750 and $2550 \text{ m}^3\text{s}^{-1}$, is from 4.5 % (0.0008), via 0.1% (0.004), to 5.1% (0.02) for the two thresholds.

2.2 Hydrological background

In the sixteenth, seventeenth and eighteenth century, one flood in each century exceeded $2750 \text{ m}^3\text{s}^{-1}$ at Borgharen, whereas in each of the nineteenth and twentieth century two peaks exceeded this value. Deforestation in the Meuse basin cannot be the reason of this increase, as the forested area in the Ardennes has increased by 8% since 1835 (WL | Delft Hydraulics, 1994, Report 4, page 10.1). Changes in land use however, have cancelled out the increased sponge function of forest areas. During the last 40 years the construction of buildings and pavements has increased and now covers approximately 5% of the basin area in Belgium (WL | Delft Hydraulics, 1994, Report 4, page 9.10). It seems plausible that moderate floods between 1600 and 2000 m^3s^{-1} have 5% higher peak discharges at Borgharen since 1960. For very extreme floods the influence of paving on the peak discharge is negligible, since such floods happen in the case of long-lasting rainfall, due to which the basin is already completely saturated with water before the top of the flood has arrived. Although the amount of rainfall on the basin may have changed through the centuries, there are no reliable data to confirm this: the measuring instruments before the twentieth century were too inaccurate to be able to indicate a significant trend. Even in the twentieth

century the positions of the rain-gauges have been changed so many times, that the basin rainfall data are sometimes dubious because of non-homogeneity. Furthermore, the variation in the amounts of rainfall is so large -in a wet year there may be more than two times as much as in a dry year- that it is not possible to identify a significant trend.

As far as the climate change is concerned, we can conclude that its influence is not significant. For the larger return periods of the floods the influence is even considered to be negligible (WL | Delft Hydraulics, 1994 , Report 4, page 9.11). Also the double mass curve for the period 1933-1992 (WL | Delft Hydraulics, 1994 , Report 4, page 7.10 – 7.12) applied to the rainfall sum in the Ardennes is consistent with the discharge sum at Borgharen.

For the future the possible climate change is still to uncertain to speculate on its influence on the small-scale Meuse River basin.

2.3 Sensitivity of the probability of exceedance at Borgharen to variable historical peak discharges

It is advised to use the estimated extreme values of the historical peak discharges as an additional source of reliable discharge values (Investigation of the Royal Dutch Meteorological Institute, 1994). However, suppose the hypothetical case that in historical times, without systematic recordings, there have been one or more extreme floods which have not been documented, got lost or underestimated. Suppose for the highest documented flood of $3075 \text{ m}^3\text{s}^{-1}$, the real discharge had been $3275 \text{ m}^3\text{s}^{-1}$. In that case, the peak discharge for a probability of exceedance of 0.0008 per annum is $135 \text{ m}^3\text{s}^{-1}$ higher than the estimated values on the basis of the Exceedance formula 2.1.6 (see Fig.2.3.1 and Table 2.3.1). This corresponds with 0.1 m increase of water level. For a p.o.e. at 0.004 per annum the peak discharge is $55 \text{ m}^3\text{s}^{-1}$ higher in that case. In other words: the above mentioned p.o.e. 0.0008 and 0.004 of the discharge, changes into 0.0015 and 0.0051, respectively.

If the highest historical peak discharge has been $500 \text{ m}^3\text{s}^{-1}$ higher ($3575 \text{ m}^3\text{s}^{-1}$) than documented, the line (5) in Fig.2.3.1 (also see Table 2.3.1) results. This corresponds with 0.3 m increase of water level. Such an extreme event is not very likely to have escaped notice. In this case the p.o.e. of the discharge changes into 0.0029 and 0.0062 instead of 0.0008 and 0.004, respectively.

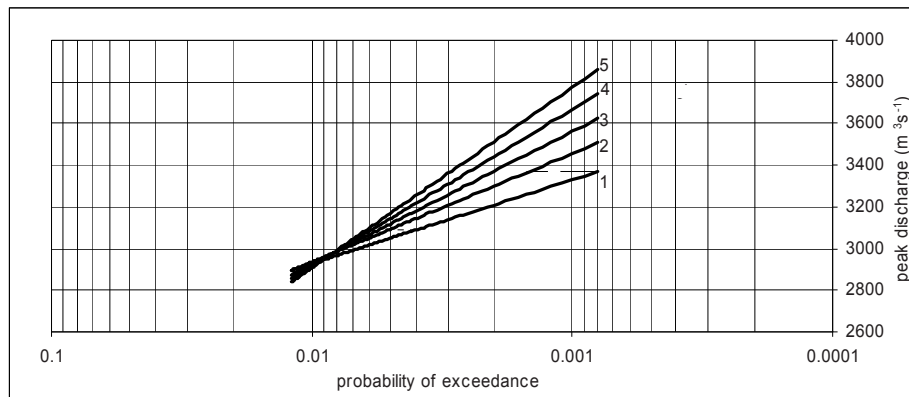


Fig.2.3.1 Consequences for the relation between p.o.e. and discharge, if the highest historical flood peak has been higher than estimated

- (1) estimated floods, according to the preferred p.o.e. for floods above the threshold at $2750 \text{ m}^3\text{s}^{-1}$
- (2) $200 \text{ m}^3\text{s}^{-1}$ added to the highest historical flood of $3075 \text{ m}^3\text{s}^{-1}$
- (3) $300 \text{ m}^3\text{s}^{-1}$ added to the highest historical flood
- (4) $400 \text{ m}^3\text{s}^{-1}$ added to the highest historical flood
- (5) $500 \text{ m}^3\text{s}^{-1}$ added to the highest historical flood

Instead of the preferred $3370 \text{ m}^3\text{s}^{-1}$ at p.o.e. 0.0008 per annum (Table 2.1.1), the discharges considered in the hypothetical cases, viz. $3505 \text{ m}^3\text{s}^{-1}$ (line 2) and higher (see Fig.2.3.1) are outside the 95% confidence band of the preferred regression line 1 of the peak discharge at Borgharen, viz. $3455 \text{ m}^3\text{s}^{-1}$, as is shown in Appendix 2.1.5. It is shown in this Appendix that the confidence band above the threshold discharge at $2750 \text{ m}^3\text{s}^{-1}$ has a width of plus or minus 2.5 to 3% related to the regression line.

Table 2.3.1 gives the raising of the discharge at p.o.e. 0.0008 and 0.004 in relation to the preferred regression line 1 of Fig.2.3.1, as a consequence of adding the given discharges (column 2) to the highest documented historical flood peak.

(1)	(2)	(3)	(4)
regression line number	added... m^3s^{-1} to the highest historical flood	p.o.e. 0.0008 diff with regression line 1 in m^3s^{-1}	p.o.e. 0.004 diff with regression line 1 in m^3s^{-1}
1	0	0	0
2	200	135	55
3	300	255	90
4	400	370	125
5	500	490	165

Table 2.3.1 Increase of discharge at p.o.e. 0.0008 and 0.004, if the highest historical flood peak would be higher (column 2) than estimated

Suppose that one or more peak discharges near the threshold of $2750 \text{ m}^3\text{s}^{-1}$, e.g. $2800 \text{ m}^3\text{s}^{-1}$, have not been documented. For these extreme discharge peaks the sensitivity at the same p.o.e. of the discharge is negligible, as is shown in Fig.2.3.2. There is no difference from the preferred reference line.

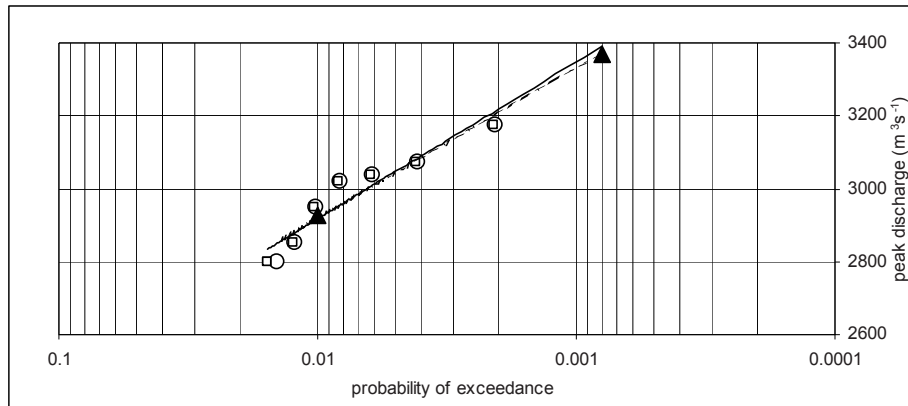


Fig.2.3.2 Effect of adding one (o, broken regression line) and two (□, thin regression line) peak discharges of $2800 \text{ m}^3\text{s}^{-1}$ to the series above $2750 \text{ m}^3\text{s}^{-1}$. Points ▲ of the line representing the reference case (no discharges added)

Suppose there has been another historical peak discharge of $3075 \text{ m}^3\text{s}^{-1}$ that got lost. Then the discharge corresponding with p.o.e. at 0.0008 per annum corresponds with p.o.e. at 0.0006 in that case, while the discharge corresponding with p.o.e. at 0.004 per annum corresponds with p.o.e. at 0.0045.

2.4 Comparison of the results of the DWL 2001 principle with those of the present study

The result of the method generally used to determine the probability of exceedance of the peak discharge at Borgharen (DWL 2001) is shown in Fig.2.4.1. This relation is based on the recorded peak discharge data from the period 1911-2000 and in accordance with the 'werklijn' for the relationship between discharges and their return periods for the Hydraulic Conditions 2001 (RIZA Report 2002.013). The same RIZA Report considers the historical floods from 1572. On basis of the investigation into the statistical distribution of the annual discharge peaks and their return periods, derived from the series of measurements in the period 1911-1997, and the historical analysis of flood events in former centuries, it turns out that the very extreme peak discharges of the series 1572-1997 lie within the 95% confidence band of the first series. In other words, the historical analysis supports the results of the statistical analysis of the series 1911-1997. So, the assumption that the series 1911-1997 is representative for the long series can not be rejected.

At p.o.e. 0.004 and 0.0008 the 95% confidence band has a width of plus or minus 15 to 20% related to the expected line, according to Report 4, page 8.6 of WL| Delft Hydraulics (1994), from which it turned out that the 'werklijn' for the period 1911-1994 equals that for the period 1911-2000.

Fig.2.4.1 also shows the relation between the probability of exceedance and the peak discharge resulting from the present study. More details are given in Appendix 2.4.1.

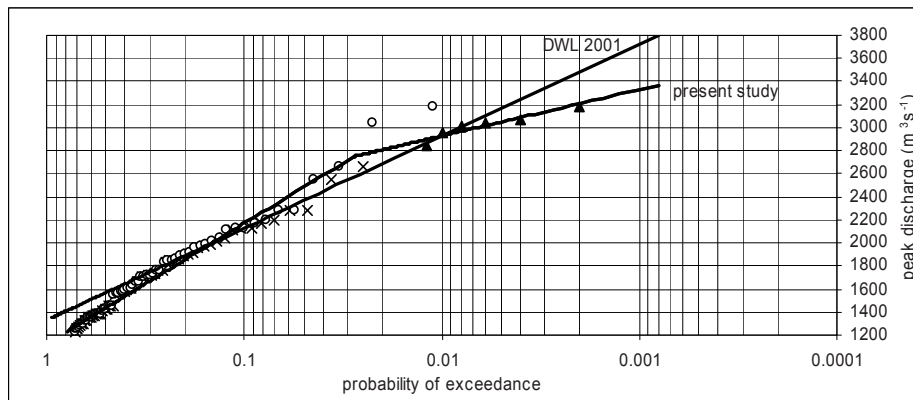


Fig.2.4.1 Comparison of the generally used probability of exceedance of the peak discharge at Borgharen with that resulting from the present study (o symbols from the generally used series 1911-2000, and x, ▲ symbols from the series 1571-2000)

The discharge differences at measuring-station Borgharen village (km16), due to the 'DWL 2001' and the results of the present study are given in Table 2.4.1.

probability of exceedance yr^{-1}	DWL 2001 principle $\text{m}^3 \text{s}^{-1} \text{ } ^2$	present study $\text{m}^3 \text{s}^{-1}$	difference $\text{m}^3 \text{s}^{-1}$
0.1	2142	2170	-28
0.05	2387	2484	-97
0.02	2710	2808	-98
0.01	2955	2929	+26
0.004	3278	3089	+189
0.0008	3800	3370	+430

Table 2.4.1 Discharge differences at Borgharen as a result of the DWL 2001 principle and the present study

For the water level differences this means:

probability of exceedance yr^{-1}	DWL 2001 principle m^2	present study m^3	difference m
0.1	45.15	45.20	-0.05
0.05	45.43	45.50	-0.07
0.02	45.70	45.77	-0.07
0.01	45.89	45.86	+0.03
0.004	46.12	45.98	+0.14
0.0008	46.43	46.17	+0.26

Table 2.4.2 Water level differences at Borgharen as a result of the DWL 2001 principle and the present study

² also see Appendix 4.9.1

³ also see Appendix 4.4.3

One may simply apply the E-formulae for the series 1571-2000 and 1911-2000 for the p.o.e.-plot above the peak discharge of $1200 \text{ m}^3\text{s}^{-1}$ (the beginning of the free flow situation downstream of Borgharen). Fig.2.4.2 shows, that (1) for p.o.e. 0.0008 the difference between the two series is $506 \text{ m}^3\text{s}^{-1}$ (0.28 m), that (2) for p.o.e. 0.004 it is $371 \text{ m}^3\text{s}^{-1}$ (0.24 m), and that (3) the long-term series regression line (Δ) practically coincides with the generally used thin line.

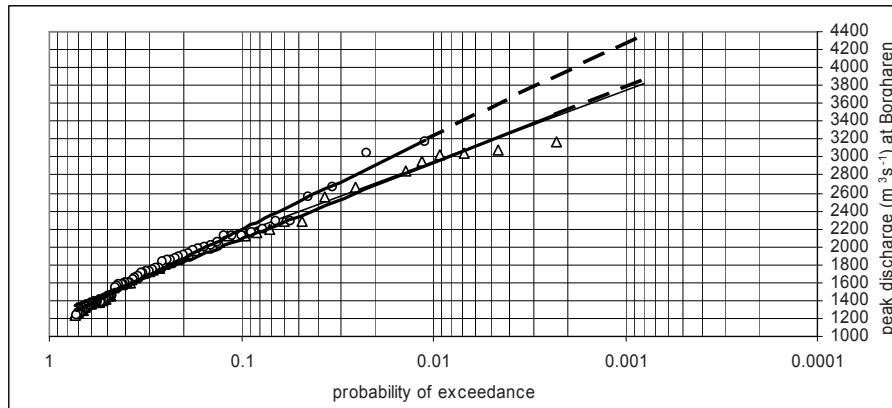


Fig.2.4.2 The long-term series 1571-2000 (Δ) compared with the short-term series 1911-2000 (o), both series with discharge threshold at $1200 \text{ m}^3\text{s}^{-1}$; generally used thin line

If, instead of the $1200 \text{ m}^3\text{s}^{-1}$ the discharge threshold at $2750 \text{ m}^3\text{s}^{-1}$ is introduced into both series and the E- equations are used, Fig.2.4.3 shows the resulting short-term and long-term regression lines, as well as the generally used thin line.

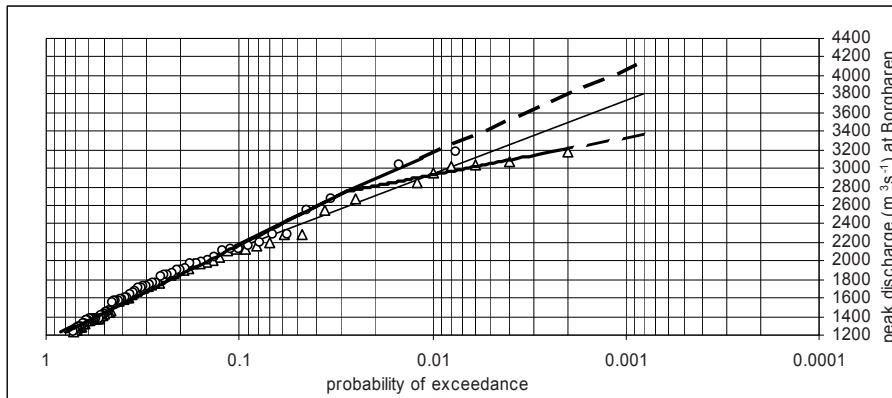


Fig.2.4.3 Series 1571-2000 (Δ) compared with the short-term series 1911-2000 (o), both series with discharge threshold at $2750 \text{ m}^3\text{s}^{-1}$; generally used thin line

The water level differences between both series of Fig.2.4.3 correspond to 0.47 m (p.o.e. 0.0008) and 0.29 m (p.o.e. 0.004). However, the part of the short-term regression line above the threshold is based on two measuring-points only, and therefore its existence is uncertain, as also follows from the large extrapolation

interval to p.o.e. 0.0008, contrary to that of the long-term series (Δ) above the threshold.

2.5 Generalization of the findings for the Dutch Meuse River to other rivers

From the case study of the Dutch Meuse River we can derive for similar rivers how to deal with the problem of determination of p.o.e.-plots from available, possibly interrupted, annual peak discharge series.

Suppose the available discharge series consists of a set of systematic recordings and some documented historic peaks, for which the time and approximate magnitude are known. Then the E-formulae 2.1.4 and 2.1.5 can be used, assuming that certain river perceptions are known, so that discharge thresholds can be introduced.

Attention has to be paid to (1) the effects of misspecification of the length of the observed period, in the case of an interrupted series of historic peak discharge data (2) the sensitivity of the p.o.e. to variable (historic) peak discharges (3) the uncertainty in the discharge threshold(s) and (4) the homogeneity of the data series.

CHAPTER 3

FLOOD WAVE CHARACTERISTICS AT BORGHAREN DETERMINING THE RIVER STAGES

3.1 Introduction

River flood waves with the same peak discharge may produce different water levels at the same location further downstream. This is due to the shape of the flood wave, which in a rain-fed river depends on various conditions, such as the rainfall history, the duration of the rain period in its basin, the rain intensity, etc. Wave volume, centre of gravity and its variance, skewness and crest curvature of the wave are parameters to describe flood waves. Different base discharges, prior to a rain period, may cause different maximum water levels along the river for the same precipitation volume, as the water storage capacity in the river differs depending on the base discharge. During its passage through the river the flood wave attenuates, and the stronger the peakedness the more attenuation. The relation between the upstream peak discharge and the downstream water level is not necessarily monotonous, may be even non-unique. This property is illustrated in Fig. 3.1.1 for the peak discharge measurements in the Meuse River at Borgharen and the Sobek computations for the corresponding water levels at Venlo, about 100 km downstream of Borgharen.

As there is a unique monotonous ‘stage–discharge’ relationship between the water level and the discharge at Borgharen (Appendix 4.4.3), the probability of exceedance of the discharge at Borgharen is the same as that of the corresponding water level, contrary to the relation in Fig.3.1.1. By lack of a reasonable number of local discharge measurements downstream of Borgharen, local probabilities of exceedance of discharges and corresponding water levels could not be determined directly. This why, so far, the p.o.e. of the water levels downstream of Borgharen has been taken equal to that of the discharges at Borgharen. This casts doubt on the present used Design Water Levels 2001 for river dikes and levees, which have been derived under this assumption. Therefore a new approximation is applied in the present study.

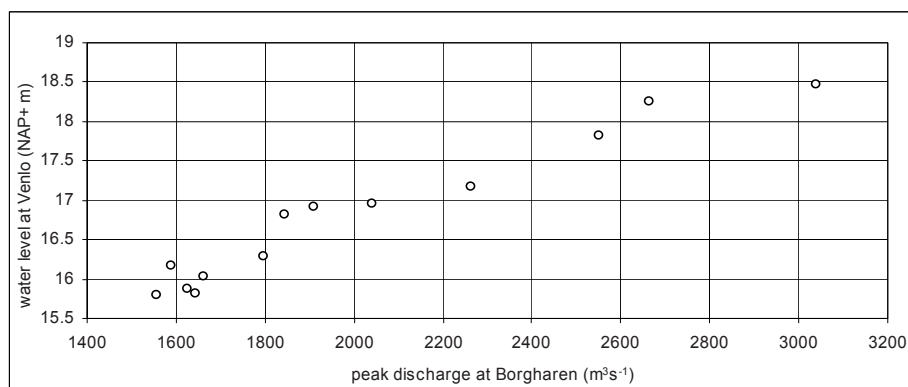


Fig.3.1.1 Computed water levels at Venlo related to the measured peak discharges at Borgharen

To offer more reliable estimates of local flood levels with p.o.e. 0.02, 0.004 and 0.0008 per annum, which are the bases of the design criteria for structures on the Dutch Meuse River, the aforementioned characteristics of the Borgharen discharge flood waves that determine the downstream water levels need to be identified. After identifying the significant flood wave parameters in this chapter, the synthesization of flood waves at Borgharen will be described in Chapter 4.

3.2 Observed flood waves at Borgharen

Daily 08:00 a.m. observations of the discharge at Borgharen between 1931 and 2000 are available (Delden 1999). Values of flood wave characteristics have been derived from these data. To exclude the effects of artificial interventions, such as weir operations, while keeping a statistically sound number of data to study, floods are used with a peak discharge over $1850 \text{ m}^3\text{s}^{-1}$ at Borgharen. This set consists of 16 floods, characterised by the discharge peaks and other characteristic parameters. They are relevant to this part of the study, and are classified in Appendix 3.2.1.

The daily observations during a flood show that single-peaked waves at Borgharen generally have a steep slope in the rising stage, and the peak is reached after three to six days. The falling stage is about half as steep and consists of direct runoff until the deflection point, followed by a slow runoff until all water from the flood event has been depleted.

As there are no physical criteria to discriminate between a single-peaked flood wave and a complex flood wave, the following assumptions are made :

- (1) If a wave has two peaks with an interval of eight days or more, it is assumed to consist of two single waves (Dixhoorn 1978, Gerretsen 1999, Made 1968).
- (2) If two peaks occur less than eight days apart, they are considered as one single-peaked wave, with the lower peak as a part of the wave.

As stated before, upstream weir operations may be a source of discharge fluctuations. Calculations, made within the framework of Investigation Flooding Meuse River (WL | Delft Hydraulics, 1994, Report 4, page 9.19) for the Belgian river section, show that these weir operations may result in fluctuations at Borgharen between $30 \text{ m}^3\text{s}^{-1}$ and $800 \text{ m}^3\text{s}^{-1}$ (worst-case approach). In the author's view, discharge fluctuation rates up to $200 \text{ m}^3\text{s}^{-1}$ per hour are still realistic in practice. If there is evidence of such fluctuations within one flood wave period, they are corrected, while preserving the wave volume and the peak discharge. This is the case for two floods over $1850 \text{ m}^3\text{s}^{-1}$ after 1931.

3.3 Flood wave parameters at Borgharen

A flood wave is defined on the time interval between the beginning of the rising stage at a certain base discharge level, and the end of the falling stage when the same base discharge is (roughly) reached again. On this interval the discharge hydrograph $Q'(t) = Q(t) - Q_{\text{base}}$ at Borgharen is defined (Fig.3.3.1). The base discharge, Q_{base} , still decreases at the beginning of the flood and increases after the peak of the flood (retardation effect). The rate of change will be small and in the case of floods unimportant. Therefore the base flow is assumed to be constant from the beginning till the end of the flood wave.

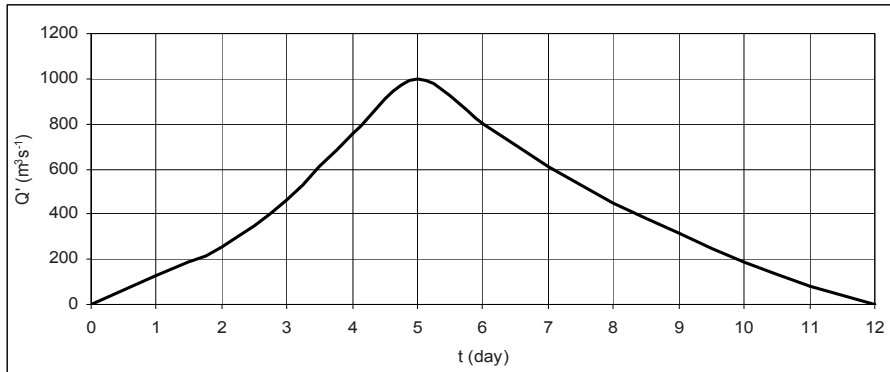


Fig.3.3.1 Example of a flood wave hydrograph $Q'(t)$ at Borgharen

The phenomena that may cause the differences in the downstream water levels, as mentioned in section 3.1, will be identified, using the moments X_0 through X_4 of the discharge hydrograph in Fig.3.3.1. They are expressed by the Equations 3.3.1 through 3.3.5 and computed for a flood wave at Borgharen in Table 3.3.1.

$$X_0 = \Sigma Q' dt \quad \text{wave volume} \quad \dots(3.3.1)$$

$$X_1 = \Sigma Q' t / \Sigma Q' \quad t_{mean}, \text{ centre of gravity} \quad \dots(3.3.2)$$

$$X_2 = [\Sigma \{Q' (t - t_{mean})^2\} / \Sigma Q']^{1/2} \quad \text{stdev. of } t_{mean} \quad \dots(3.3.3)$$

$$X_3 = \Sigma [Q' (t - t_{mean} / X_2)^3] / \Sigma Q' \quad \text{skewness} \quad \dots(3.3.4)$$

$$X_4 = - (Q'_{peak-1day} + Q'_{peak+1day} - 2 Q'_{peak}) / \{(dt)^2 Q'_{peak}\} \quad \dots(3.3.5)$$

in which $(dt)^2 = (24 \cdot 3600)^2$ (Made 1966) *crest curvature*

X_4 is a discrete approximation of the curvature of the top part of the discharge hydrograph $Q'(t)$ from one day before till one day after the peak. This crest curvature can be approximated by the second derivative of Q' with respect to t . If X_4 is taken positive for the top part of the wave and defined relative to the peak discharge Q'_{peak} it can be calculated from Equation 3.3.5.

t(day)	Q'	Eq.3.3.1	Eq.3.3.2	Eq.3.3.3	Eq.3.3.4	Eq.3.3.5
0	0	0x86400	0	0	0	
1	129	129x86400	129	2730	-1179	
2	258	258x86400	516	3344	-1130	
3	460	460x86400	1380	3110	-759	
4	755	755x86400	3020	1933	-290	
5	1000	1000x86400	5000	360	-20	
6	800	800x86400	4800	128	5	
7	612	612x86400	4284	1200	158	
8	450	450x86400	3600	2592	584	
9	315	315x86400	2835	3641	1163	
10	190	190x86400	1900	3678	1520	
11	80	80x86400	880	2333	1183	
12	0	0x86400	0	0	0	
Σ	5049	436 10 ⁶	28344	25048	1233	
variance				4.96		
parameter	Q'	X ₀	X ₁	X ₂	X ₃	X ₄
value		436 10 ⁶	5.6	2.2	0.2	60 10 ⁻¹²
dimension	L ³ T ⁻¹	L ³	T	T	-	T ⁻²
	relative discharge	volume	t _{mean}	stdev.of t _{mean}	skewness	crest curvature

Table 3.3.1 Calculation of the flood wave parameter values for the flood at Borgharen, shown in Fig.3.3.1

At the end of the nineteenth century large river works started, which continued with interruptions till 1980, when the old weir at Visé was removed after a modern new weir had been put into operation at Lixhe, downstream of Visé close to the Dutch border.

To be aware of a possible trend breach in the series of parameter values (X₀...X₄, Q'_{max} and Q_{base}) because of these river works, the floods on record are split into two sets, namely before and after 1980. Trends are tested by Spearman's Rank Correlation Coefficient (r_s) for the differences Σd^2 in the ranks of times and observations (Appendix 3.3.1)

The test statistic:

$$r_s = 1 - 6\Sigma d^2 / (n^3 - n) \quad \dots(3.3.6)$$

is compared with the critical value r_{s, 0.025, n} (one-tailed) from the appropriate Spearman Table XIV (McClave 1997).

The one-tailed rejection region is:

$$r_s > r_{s, 0.025, n} \quad \dots(3.3.7)$$

with n pairs of observations

It turned out that there is no trend breach in the series Q'_{max}, X₀ through X₄ and Q_{base} before and after 1980, as from the original parameter values (Appendix 3.2.1) it is found (Appendix 3.3.1) that for the series 1930-1980 and 1980-2000 the respective standard deviations (F-test) and their averages (t-test) do not differ significantly. So,

each of the flood wave parameter value series 1930-1980 (10 events) as well as 1980-2000 (6 events) can be considered as belonging to the same homogeneous data set.

3.4 Which flood wave parameters at Borgharen are important for the downstream water levels

To synthesize flood waves $Q'(t)$, given Q'_{\max} , by random sampling of combinations of flood wave parameter values ($X_{0..4}$), it is needed that these are mutually independent. For mutual comparison we made the original parameter values non-dimensional and standardized.

The flood wave parameters with their dimensions are given in Table 3.3.1.

The original values in Appendix 3.2.1 are made non-dimensional as follows:

$$X_0 \text{ (non dim.)} = X_0 \text{ (orig.)} / \{\text{mean } Q'_{\max} \text{ (orig.)} \cdot \text{mean } X_1 \text{ (orig.)}\}$$

$$X_1 \text{ (non dim.)} = X_1 \text{ (orig.)} / \text{mean } X_1 \text{ (orig.)}$$

$$X_2 \text{ (non dim.)} = X_2 \text{ (orig.)} / \text{mean } X_2 \text{ (orig.)}$$

$$X_3 \text{ (non dim.)} = X_3 \text{ (orig.)}$$

$$X_4 \text{ (non dim.)} = X_4 \text{ (orig.)} \cdot \{\text{mean } X_1 \text{ (orig.)}\}^2$$

$$Q'_{\max} \text{ (non dim.)} = Q'_{\max} \text{ (orig.)} / \text{mean } Q'_{\max} \text{ (orig.)}$$

The degree of influence of X_i ($i = 0..4$) on each other also depends on their scattering. To make them standardized, we have to multiply the non-dimensional parameters by the factor

$$F_i = \sigma_{Q'_{\max}} / \sigma_{X_i} \quad \dots(3.4.1)$$

in which $\sigma_{Q'_{\max}}$ the standard deviation of the non-dimensional Q'_{\max} .
 σ_{X_i} is the standard deviation of the corresponding non-dimensional X_i values.

The non-dimensional and standardized flood wave parameters are given in Appendix 3.4.1.

These data are used to estimate the mutual linear dependence of the parameters and the results are summarized in Table 3.4.1. Note that this goes for the non-linear relations, too, as is clear in the pictures of Appendix 3.4.2 (a,b,c). Table 3.4.1 shows that X_0 , X_3 and X_4 can be considered mutually independent, whilst X_0 , X_2 and X_1 , X_2 turn out to be inter-dependent, as their R^2 (the square of the coefficient of correlation) values are 0.69 and 0.77. For X_0 , X_1 the independency is doubtful.

So, for further investigation into the influence on the water levels downstream of Borgharen, the flood wave parameters volume (X_0), skewness (X_3) and crest curvature (X_4) are used initially to synthesize $Q'(t)$, given Q'_{\max} .

R^2 ⁴	X_0	X_1	X_2	X_3	X_4
X_0	1	0.57	0.69	0.08	0.10
X_1		1	0.77	0.03	0.02
X_2			1	0.05	0.06
X_3				1	0.00
X_4					1

Table 3.4.1 Mutual linear dependency of characteristic flood wave parameters from the 16 floods over $1850 \text{ m}^3\text{s}^{-1}$ at Borgharen in the period 1930-2000

To estimate the influence of the skewness X_3 of the flood wave at Borgharen on the downstream water levels, some floods have been analysed.

(1) The floods derived from that of January 1993 with similar Q'_{\max} , Q_{base} and X_0 , and furthermore also a constant X_4 , but a variable X_3 are compared in Fig.3.4.1.

(2) The synthetic floods with the mentioned constants in Fig.3.4.2 and variable X_3 are compared.

It turned out that the influence on the downstream water levels of variations of X_3 is small to negligible. In our case the realistic interval of the skewness goes from -0.2 to 1, according to Appendix 3.3.1. Note that the extent of skewness depends on the difference from 0. The given variable X_3 in Fig.3.4.1 varies from 0.1 to 1, roughly, nevertheless the downstream water levels differ very poorly.

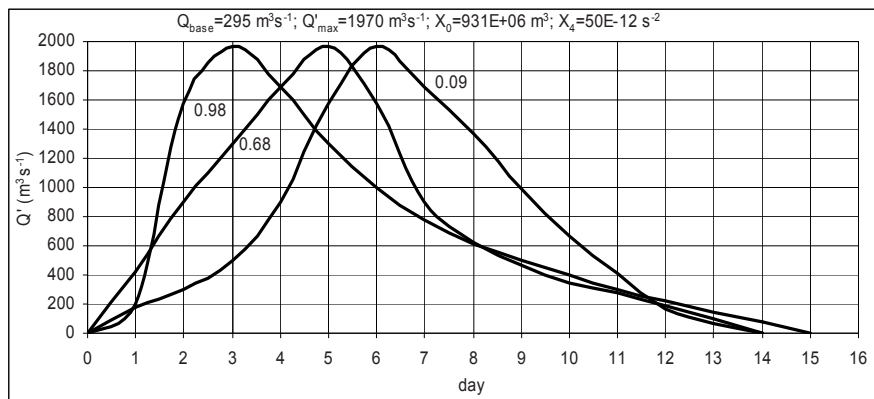


Fig.3.4.1 Adaptations of the flood derived from that of January 1993 at Borgharen to different skewness coefficients X_3 , namely 0.98, 0.68 and 0.09, and other parameters constant.

Taking into account the base discharge, the water levels at Venlo and Mook are 0.01 m and 0.04 m higher, respectively, if the floods with $X_3 = 0.68$ as well as 0.09 are compared with that for which $X_3 = 0.98$

⁴ square of the correlation coefficient

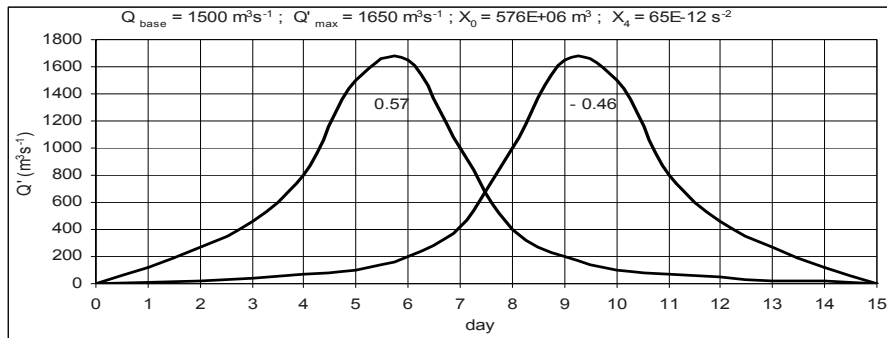


Fig.3.4.2 Synthetic floods at Borgharen with rightward and leftward skewness (coefficients 0.57 and -0.46 , respectively), other parameters constant.

Taking into account the base discharge, the water levels at Venlo as well as at Mook are 0.01 m lower for $X_3 = -0.46$

In Section 3.5 the influence of the other parameters, viz. X_0 and X_4 , is examined.

In order to assess to what extent the results for unsteady flow (Q) deviate from those for quasi-steady flow (Q_s), the formula of Jones for the hysteresis effect (Jansen et al. 1979) is applied:

$$Q - Q_s = [Q_s / 2 I_b c] dh / dt \quad \dots(3.4.2)$$

in which I_b is the bottom slope of the river and c is the flood wave celerity. Gerretsen (2002) considered the application to the Meuse River at Venlo:

$$I_b = 0.1 \cdot 10^{-3} \text{ and } c \approx 1.5 \text{ times the mean flow velocity (m s}^{-1}\text{)}$$

dh = daily water-level difference (m) and $dt = 86400$ (sec.)

Q_s is derived from the provisional 'stage-discharge curve at Venlo' (Appendix 3.4.3).

For the flood of February 1984, with peak discharge $2550 \text{ m}^3\text{s}^{-1}$ at Borgharen, a more or less average volume and a strongly curved crest, the Sobek model shows that the deviation from quasi-steady flow at Venlo is $80 \text{ m}^3\text{s}^{-1}$, corresponding with a 0.12 m lower water level than the 'stage-discharge curve' indicates.

For the flood of December 1993, with a peak discharge of $3039 \text{ m}^3\text{s}^{-1}$ at Borgharen, a more or less average volume and an average crest curvature, the maximum deviation from the quasi-steady flow at Venlo is $9 \text{ m}^3\text{s}^{-1}$, corresponding with 0.01 m water level difference from the 'stage-discharge curve'.

For the synthetic flood waves, with $Q_{\text{peak}} 3150 \text{ m}^3\text{s}^{-1}$ at Borgharen, with either a peaked or a flat crest curvature and with a constant average volume, the deviation from the steady flow at Venlo is $70 \text{ m}^3\text{s}^{-1}$, corresponding with 0.1 m water level difference at both sides of the 'stage-discharge curve'.

The hysteresis at Borgharen is negligible because of the much larger bottom slope and flood wave celerity than at Venlo.

3.5 A first-order estimate of the influence of significant flood wave properties on the downstream water levels

A first-order approximation of the influence of the properties X_0 and X_4 of the Borgharen flood waves on the downstream water levels at Venlo and Mook, for instance, has been made by synthesizing flood waves with prescribed realistic values of these parameters. With the input of these flood waves $Q(t)$ at Borgharen, the Sobek computational model⁵ calculates the water levels at Venlo and Mook. The Sobek model was based on the Dutch Meuse River schematisation 1995, including the levees constructed in that year according to the Dutch Deltaplan for Large Rivers.

The synthetic floods have been derived from the highest floods $Q(t)$ of the period 1980-2000, namely those of 1984, 1993 and 1995, with peak discharges 2550, 3039 and 2664 m^3s^{-1} , respectively (Fig.3.5.1), and with relative peak discharges $Q'(t)$ 1571, 2009 and 1073 m^3s^{-1} , respectively (Fig.3.5.2).

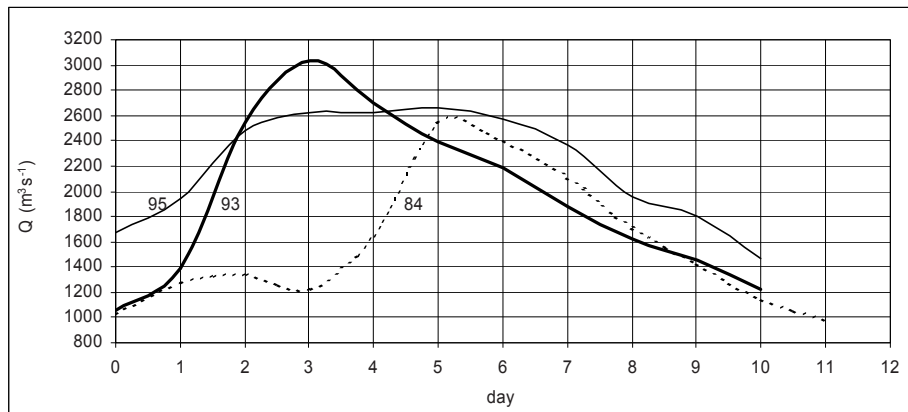


Fig.3.5.1 Floods $Q(t)$ at Borgharen in 1984, 1993 and 1995

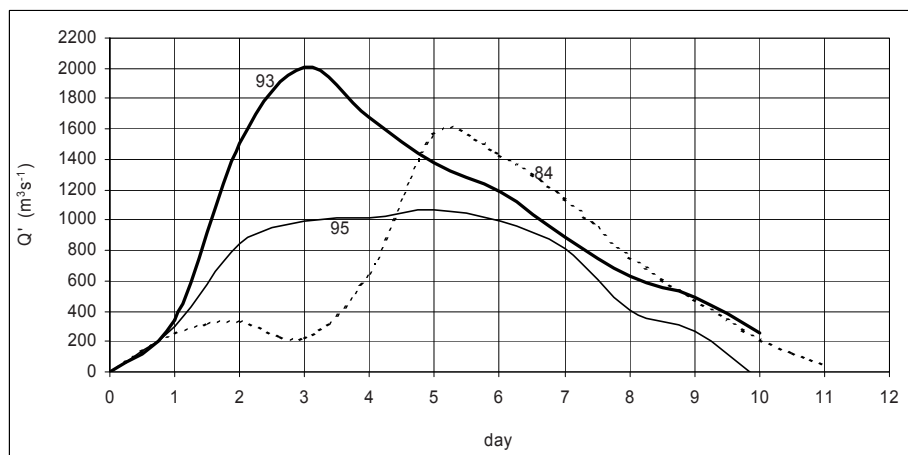


Fig.3.5.2 Relative floods $Q'(t)$ at Borgharen in 1984, 1993 and 1995

⁵ More about the Sobek model in Section 4.4

In order to compare the water levels at Venlo and Mook, the Q'_{\max} values of the 1984 and 1995 floods at Borgharen have been made equal to that of the reference flood 1993. From the variables X_0 and X_4 , one value has been made the same as that of the 1993 flood and, alternately, the other has the original value of the 1984 or 1995 flood. The resulting flood wave shapes (Q') are shown in Figs.3.5.3 and 3.5.4

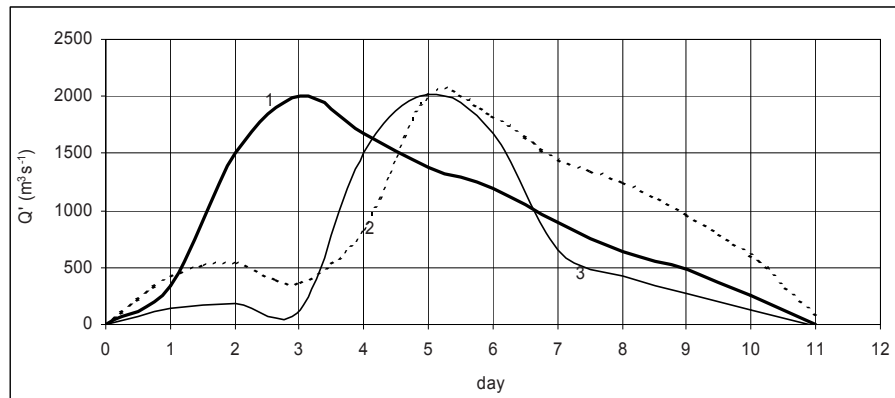


Fig.3.5.3 Flood wave shapes at Borgharen, also see Table 3.5.1

1: the reference flood Q' 1993

2: X_0 and Q'_{\max} of flood 1993 and X_4 of flood 1984 (896, 2009, 90)

3: X_4 and Q'_{\max} of flood 1993 and X_0 of flood 1984 (56, 2009, 615)

By adding the Q_{base} value of $1030 \text{ m}^3 \text{ s}^{-1}$ (i.e. the base discharge of the 1993 flood) to the Q' values of Fig.3.5.3 and 3.5.4, we get the comparable total daily Q values of the three above mentioned floods. The elaborations for the adapted Q' flood waves are shown in the Appendices 3.5.1 and 3.5.2, whilst Appendices 3.5.3 and 3.5.4 give the elaborations for the adapted Q floods.

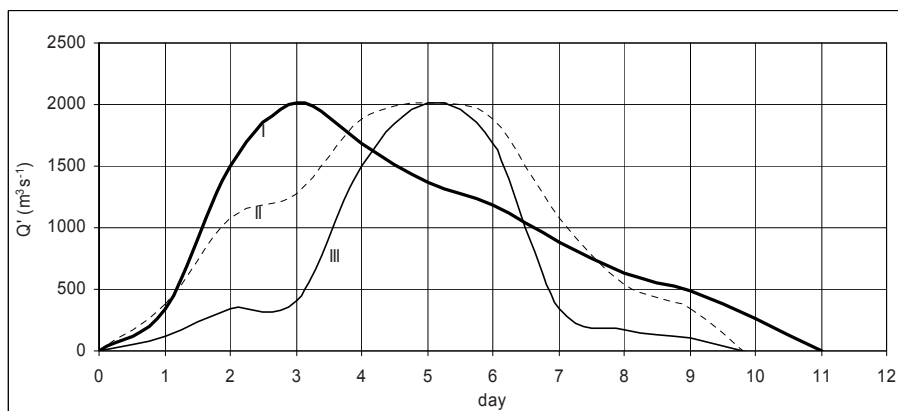


Fig.3.5.4 Flood wave shapes at Borgharen, also see Table 3.5.1

I: the reference flood Q' 1993

II: X_0 and Q'_{\max} of flood 1993 and X_4 of flood 1995 (896, 2009, 17)

III: X_4 and Q'_{\max} of flood 1993 and X_0 of flood 1995 (56, 2009, 575)

The computed differences in the water levels at the same locations further downstream, caused by the different flood wave shapes at Borgharen and taking the base discharge into consideration, are shown in Table 3.5.1. For the shape parameter qualifications, also see Appendix 4.3.1 and the footnotes to the Table.

Q _{peak} : 3039 m ³ s ⁻¹ Q' _{max} : 2009 m ³ s ⁻¹	wave number, also see App.3.5.1 through 3.5.4	X ₀ m ³ * 10 ⁶	X ₄ s ⁻² * 10 ⁻¹²	Δ Venlo from reference m	Δ Mook from reference m
reference	1	896 ⁶	56 ⁷	0.00	0.00
1984	2	896	90 ⁸	-0.05	-0.09
Flood	3	615 ⁹	56	-0.04	-0.11
reference	I	896	56	0.00	0.00
1995	II	896	17 ¹⁰	+0.22	+0.23
Flood	III	575 ¹¹	56	0.00	-0.06

Table 3.5.1 Influence on the water levels at Venlo and Mook due to different flood wave properties X₀ and X₄ of the adapted extreme floods of 1984 and 1995 to the extreme flood of 1993 (Q_{peak} 3039 m³ s⁻¹), which latter is used as reference.

Concerning the crest curvature we conclude:

If a peaked flood wave (90) at Borgharen is compared with one that has a medium crested curvature (Table 3.5.1) and both have the same volume, Q_{peak} and Q_{base}, the water level differences are twice as much at Mook (-0.09 m) as at Venlo.

If a flat flood wave (17) at Borgharen is compared with one that has a medium crested curvature and both have the same volume, Q_{peak} and Q_{base}, the water level differences are the same at Venlo and Mook (+0.23 m).

Concerning the volume we conclude:

If a flood wave with a large volume (896) at Borgharen is compared with one that has a medium volume and both have the same crest curvature, Q_{peak} and Q_{base}, the water level differences are at Mook (0.11 m) three times as much as at Venlo.

3.6 Generalization of the findings for the Dutch Meuse River to other rivers

Local probabilities of exceedance of water levels are needed to design river-engineering works to attain a desired safety against inundation. However usually the number of gauged river locations is too small, or even limited to only one measuring-station per river, to draw firm conclusions on the p.o.e. of water levels along the river.

6 large
7 medium
8 peaked
9 medium
10 flat
11 medium

It is obvious that in a rain-fed river the shape of a flood wave depends on the rainfall history, the length of the rain period and the rain intensity. Furthermore, the flood wave undergoes various deformations during its passage through the river due to wave dynamics, irregular lateral inflow and water storage. So the unique relationship that exists between discharge and water level at a gauged river-point cannot be taken for granted if it comes to the relationship between the discharge at that river-point and the water level further downstream.

Therefore the p.o.e. of the water level at a certain un-gauged river location needs further investigation to find the cause of non-monotonous, even non-unique relations between the upstream measured peak discharges and the downstream water levels (see example in Fig.3.1.1).

From the discharge hydrograph $Q'(t)$ at a gauged river location it is possible to estimate the water level at any downstream un-gauged location by considering the flood wave characteristics. Besides the initial discharge Q_{base} and the maximum discharge Q_{peak} it is important to know the shape of the discharge hydrograph $Q'(t)$ (i.e. $Q_{peak} - Q_{base}$), characterized by the moments X_0 through X_4 (Table 3.3.1¹²).

The data base, consisting of the parameter values X_0 through X_4 and Q'_{max} , Q_{base} , Q_{peak} , has to be tested on trend breaches and possibly corrected to the present-day situation.

To obtain the p.o.e. of un-gauged water levels, we non-dimensionalised and standardized the aforementioned parameters to investigate their mutual dependence, (Section 3.4). The result can be that some parameters drop out because of their mutual dependency, as mutual independency is required for randomly sampling combinations of them, needed to synthesize floods at a gauged river-point. The synthesization of flood waves $Q(t)$ will be treated in Chapter 4 and from that the computation of the water levels at any location can be performed with a hydrodynamic model.

As a first-order approximation it is useful to compare a flood that has occurred at an upstream gauged river-point with synthetic floods having the same parameters except one. On the basis of the result of these comparisons one can estimate the influence of that parameter on the downstream water levels, and still decide to neglect one or more parameters for which the water levels at a downstream river-point do not differ significantly.

Even though it may be important to examine the influence of all parameters X_0 through X_4 , investigating that of the crest curvature (X_4) is of prime importance. It refers to the types of rivers for which the phenomenon of attenuation of flood waves plays an important role.

For the crest attenuation Forchheimer's formula (Made, 1968) reads as follows:

$$dQ_{peak} / dx = \{ [B_b^2 Q_{peak}] / [2S_b (dQ_{peak} / dy)^3] \} [d^2 Q_{peak} / dt^2] \quad \dots(3.6.1)$$

in which:

dQ_{peak} / dx the rate of change of the peak runoff along the river

¹² the crest curvature (X_4) deviates from the fourth moment (curtosis) as it is a discrete approximation of the curvature of the top part of the hydrograph $Q'(t)$ from one day before till one day after the peak (also see Eq. 3.3.5)

B_b storage width at the water surface
 S_b bottom slope
 dQ_{peak} / dy the slope of the tangent to the 'stage – discharge' relationship

If $\partial^2 Q_{\text{peak}} / \partial t^2 = R Q_{\text{peak}}$, i.e. the crest curvature equals R times Q_{peak} ,

with R is a constant, then the crest attenuation is:

$$dQ_{\text{peak}} / dx = [B_b^2 Q_{\text{peak}}^2] R / [2S_b (dQ_{\text{peak}} / dy)^3] \quad \dots(3.6.2)$$

According to Manning for a rectangular discharge profile, we get:

$$Q_{\text{peak}} = B_s K S_b^{1/2} y^{5/3} \quad \dots(3.6.3)$$

where:

B_s stream carrying width
 K Manning coefficient
 y the water depth

Because of Eq.3.6.2 and 3.6.3 we find:

$$dQ_{\text{peak}} / dx = -27/250 [B_b^2 R Q_{\text{peak}}^{4/5}] / [S_b (B_s K S_b^{1/2})^{9/5}] \quad \dots(3.6.4)$$

For the Unit profile of Fig.3.6.1, $B_b = B_s$, the water depth is h, and the Unit runoff Q_u is the bank-full discharge for which:

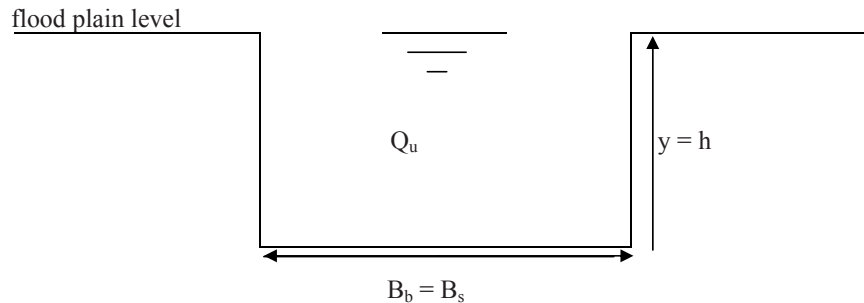


Fig.3.6.1 Unit rectangular discharge profile

$$Q_u = B_s K S_b^{1/2} h^{5/3} \quad \dots(3.6.5)$$

From Eqs.3.6.4 and 3.6.5 we find:

$$(dQ_{\text{peak}} / dx)_u = -27/250 [B_s^2 R Q_u^{4/5}] / [S_b (B_s K S_b^{1/2})^{9/5}] \quad \dots(3.6.6)$$

Definitions:

$$dq = [dQ_{\text{peak}} / dx] / [(dQ_{\text{peak}} / dx)_u], \text{ and } q = Q_{\text{peak}} / Q_u$$

In an arbitrary rectangular profile the ratio between Eq. 3.6.4 and 3.6.6 then becomes:

$$dq = (B_b^2 / B_s^2) (Q_{\text{peak}}^{4/5} / Q_u^{4/5}) \text{ and}$$

according to Fig. 3.6.2 and aforementioned definition we get:

$$dq = (1+p)^2 q^{4/5} \quad \dots(3.6.7)$$

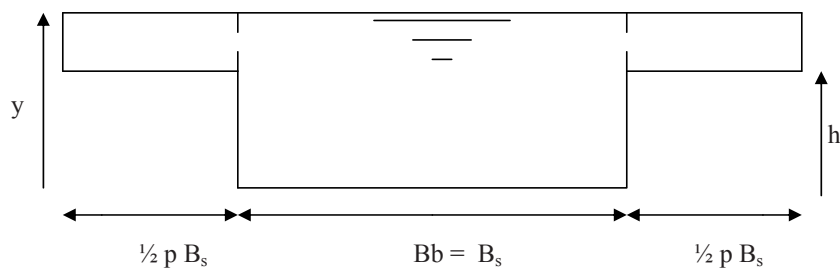


Fig.3.6.2 Rectangular discharge profile and the width $p B_s$ without flow
 $B_b = (1 + p) B_s$

A similar derivation can be made for the profile with longitudinal flow over the flood plains, and partly storage capacity without flow (Fig.3.6.3).

Then $Q_{\text{peak}} = Q_u + Q(\text{stream carrying floodplains})$ and so:

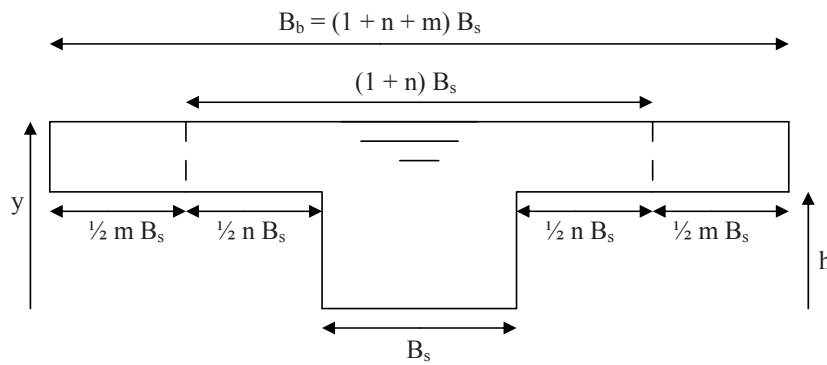


Fig.3.6.3 Profile with longitudinal flow over the flood plains; $n B_s$ is the width of the floodplains with longitudinal flow, whereas $m B_s$ is the width without flow

$$Q_{\text{peak}} = B_s K S_b^{1/2} y^{5/3} + n B_s K S_b^{1/2} (y - h)^{5/3} \quad \dots(3.6.8)$$

$$Q_{\text{peak}} = h^{5/3} B_s K S_b^{1/2} (y/h)^{5/3} + h^{5/3} n B_s K S_b^{1/2} (y/h - 1)^{5/3}$$

With respect to equation 3.6.5 we get:

$$Q_{\text{peak}} = Q_u \{(y/h)^{5/3} + n(y/h - 1)^{5/3}\} \text{ or:}$$

$$q = (y/h)^{5/3} + n (y/h - 1)^{5/3} \quad \dots(3.6.9)$$

The crest attenuation follows from substitution of Eq.3.6.8 into Eq.3.6.2.

$$\frac{dQ_{\text{peak}}}{dx} = -27/250 [B_b^2 R h^{4/3} / S_b (B_s K S_b^{1/2})] * [\{(y/h)^{5/3} + n (y/h - 1)^{5/3}\}^2 / \{(y/h)^{2/3} + n (y/h - 1)^{2/3}\}^3] \quad \dots(3.6.10)$$

From Eq.3.6.5 follows that:

$$h^{4/3} = (Q_u / B_s K S_b^{1/2})^{4/5} \quad \dots(3.6.11)$$

Substitution into Eq.3.6.10 leads to:

$$\left(\frac{dQ_{\text{peak}}}{dx}\right) = -27/250 [B_b^2 R Q_u^{4/5} / S_b (B_s K S_b^{1/2})^{9/5}] * sf \quad \dots(3.6.12)$$

in which the factor sf is the ratio of the last two terms in Eq. 3.6.10, viz.:

$$\{(y/h)^{5/3} + n (y/h - 1)^{5/3}\}^2 / \{(y/h)^{2/3} + n (y/h - 1)^{2/3}\}^3$$

Furthermore, dividing Eq.3.6.12 by Eq.3.6.6 we get:

$$\frac{dQ_{\text{peak}}}{dx} = \left[\left(\frac{dQ_{\text{peak}}}{dx}\right)_u (B_b / B_s)^2\right] * sf \quad \dots(3.6.13)$$

Given Eq.3.6.13 and the definition of dq (mentioned above), and Fig. 3.6.3, we find:

$$dq = (B_b / B_s)^2 sf \text{ or:}$$

$$dq = (1 + n + m)^2 sf \quad \dots(3.6.14)$$

In summary, given:

B_s stream carrying width of the unit profile (Fig.3.6.1),

Q_u bank-full discharge,

h unit water depth (Fig.3.6.1),

y water depth (Fig.3.6.2),

S_b bottom slope,

K Manning coefficient,

R a constant,

$n B_s$ width of the stream carrying floodplain (Fig.3.6.3),

$m B_s$ width without flow, only water storage (Fig.3.6.3),

the computation procedure becomes:

- (i) Determine Q_u from Eq.3.6.5
- (ii) Determine $(dQ_{\text{peak}} / dx)_u$ from Eq.3.6.6
- (iii) Determine sf from the ratio of the last two terms in Eq. 3.6.10
- (iv) Determine dq from Eq.3.6.14
- (v) Determine (dQ_{peak} / dx) from Eq.3.6.13

Depending on the river length Δx , for which we want to know the attenuation, we obtain dQ_{peak} .

We learn from this, that:

- (1) For rivers with a steep bottom slope, the attenuation will be small, or even negligible (Eq.3.6.12).
- (2) Changes in the ratio y / h may influence the attenuation factor sf (Eq.3.6.12).
- (3) The storage width $B_b = B_s(1 + n + m)$ at the water surface has much influence on the attenuation rate (Eq.3.6.14).

3.7 Discussion and conclusions

Q_{base} at Borgharen affects the downstream water levels, such as mentioned in the introduction of this chapter. Furthermore the influence of Q_{peak} is taken for granted. In the relationship $Q_{\text{peak}} - Q_{\text{base}}$, the variability around the mean of Q_{base} can not be explained by the regression function between Q_{base} and Q_{peak} . Therefore, Q_{base} and Q_{peak} can be considered independent.

The moments X_0 , X_3 and X_4 of the discharge hydrograph $Q'(t)$ are considered mutually independent for the same reason (Table 3.4.1). Therefore, random combinations of those parameter values for synthesizing flood waves $Q'(t)$, given Q_{peak} and Q_{base} , is conceivable. The analysis of the influence of these parameters leads to the following conclusions.

- Concerning the skewness (X_3):

In the case of the Meuse River, different skewness values (X_3) of the flood wave at Borgharen -other parameters constant- did hardly yield any difference in the water levels at Venlo and Mook. For that reason X_3 is ignored in our case.

- Concerning the crest curvature:

For a peaked flood at Borgharen the water level difference with a medium crested flood, and for the rest the same parameter values, is twice as much at Mook (0.09 m) as at Venlo, however they are moderate.

The effects on the downstream water level of a flat flood wave at Borgharen compared with a medium crested flood wave, and for the rest the same parameter values, is the same at Venlo and Mook. The influence is considerable (0.23 m).

- Concerning the volume:

If a flood wave with a medium volume at Borgharen is compared with one with a large volume, and for the rest the same parameter values, the water level difference at Mook (0.11 m) is moderate and about three times as much as at Venlo.

For the previous three cases it concerns flood waves with peaks of about $3000 \text{ m}^3\text{s}^{-1}$.

•Concerning the summer floods:

The preceding conclusions are not valid for summer flood waves, in which the influence of vegetation resistance on the water levels is considerable. For instance, the summer flood of 1980 caused a water level at Borgharen about 1 m above that of a comparable winter flood, whereas further downstream the water levels were much lower than for that winter flood.

Generalization to similar rivers:

In general, we have to investigate the mutual independency of the non-dimensional and standardized parameter values that characterise the flood wave and may determine the downstream water levels. These parameter values are derived from measured discharge hydrographs $Q'(t)$. Independency is required, as random samples of combinations of them have to be taken to synthesize floods, as the number of measured flood hydrographs is inadequate usually to determine the desired p.o.e. of local water levels. Some parameters may drop out because of mutual dependency.

For a number of flood wave parameters (e.g. Q_{peak} , Q_{base} , volume) it is obvious that they play a role in the radiation of downstream water levels, but the influence of the crest curvature (X_4) requires thorough analysis. Also other parameters, such as the first, second and third moment of the discharge hydrograph $Q'(t)$ may play a role.

Concerning X_4 , we can conclude from the analysis in Section 3.6 that (1) for river sections with a steep bottom slope, flood wave attenuation is negligible and (2) the ratio between the total water depth and that of the bank-full discharge bed (y / h) influences the attenuation rate, and (3) the storage width at the water surface influences the flood wave attenuation considerably.

In the case of a steeper rising than falling stage of the flood wave hydrograph there may be a reason for flood wave attenuation, as the supply of water can not be discharged in its entirety directly after the peak and flows out into the storage. The skewness (X_3) of the flood wave indicates this phenomenon, but in our case the crest curvature dominates by far the skewness.

Flood wave attenuation on the Rhine branches:

The land use in the large floodplains of the Dutch Meuse River, without primary dikes, differs from that of the relatively small floodplains of the Dutch Rhine River, with primary dikes. Comparatively, wooded areas and nature, agriculture, industry and home-building are three to five times as much for the Meuse River as for the Rhine River. Moreover, there is, comparatively, three to four times more grassland, so relatively less roughness at the floodplains of the Rhine River. This means that the large non-flowing pure storage width mBs (Section 3.6) of the Meuse River floodplains plays an important role for the flood wave attenuation, whereas the factor mBs hardly plays a role for the Rhine River. All this considered, it means that the flood wave attenuation will count for little for the Rhine River.

An exceptional case are the more nature-friendly floodplains of the Yssel River, a branch of the Rhine River, with relatively large stream carrying and storage widths, because of former river-bend cut-offs. Just there, a flood wave attenuation appears.

CHAPTER 4

DOWNSTREAM WATER LEVELS VERSUS CHARACTERISTIC FLOOD WAVE PROPERTIES AT BORGHAREN

4.1 Introduction

The fact that also other flood wave properties than the peak discharge at Borgharen influence the downstream river stages significantly requires their inclusion in the translation algorithm to local water levels. Deformation of the flood wave during its course through the river, mainly due to bottom slope, water depth and storage in the flood plains, complicates this translation and makes it vary from location to location. In this study water levels are considered at Venlo (km 107.5) and at the beginning of the embanked part (primary dikes) of the Dutch Meuse River at Mook (km 165.8). These local water levels are determined by a procedure consisting of the following steps:

- (1) Take the records of the 50 measured floods over $1350 \text{ m}^3\text{s}^{-1}$ at Borgharen in the period 1930-2000 and determine the mutual relations between the characteristic flood wave parameters, namely Q_{peak} , Q_{base} , volume X_0 and crest curvature X_4 (Section 4.2).
- (2) Randomly sample combinations of these parameters. Here we have taken 1000 samples of those combinations from the distributions of the parameters.
- (3) Synthesize for each sample a flood wave at Borgharen with the given parameter values (Section 4.3).
- (4) Use the 1-D flow model Sobek to compute the local water levels for each of these 1000 flood waves. The backgrounds of Sobek are described in Section 4.4.
- (5) Statistical analysis of the resulting water levels at Venlo and Mook yields relative frequency distributions (Section 4.5).
- (6) Adapt the probability of exceedance functions to the relative cumulative frequency distribution of the computed local water levels. Check the goodness of fit of these functions. Especially the agreed design probabilities of exceedance for the Dutch Meuse River of 0.02, 0.004 and 0.0008 per annum are important (Section 4.6).
- (7) Determine the difference between the computed water levels and the preferred probability of exceedance function (Section 4.7).
- (8) Check the reliability of the computed water levels in relation to the measured peak discharge at Borgharen (Section 4.8)

(9) Finally compare the computed water levels at Venlo and Mook and their related probability of exceedance function, with those of the DWL 2001¹³ (Section 4.9).

4.2 Mutual correlation between the relevant flood wave variables

In Section 3.3 parameters of the flood waves at Borgharen are defined and their values are determined. Analogously to Table 3.4.1 for the floods over $1850 \text{ m}^3\text{s}^{-1}$, in Table 4.2.1 the mutual relations of the significant parameters are shown for the floods over $1350 \text{ m}^3\text{s}^{-1}$. Their values are mentioned in Appendix 4.2.1. The square of the coefficient of correlation R^2 , gives the proportion of the total variability around y_{mean} that is explained by the linear relationship between y and x , e.g. 19% of the variability around the mean of X_0 is explained by the linear relationship between X_0 and Q_{base} .

R^2	X_0	X_4	Q_{peak}	Q_{base}
X_0	1	0.04	0.17	0.19
X_4		1	0.01	0.00
Q_{peak}			1	0.20
Q_{base}				1

Table 4.2.1 Results of mutual linear dependency of characteristic flood wave parameters from the 50 floods over $1350 \text{ m}^3\text{s}^{-1}$ at Borgharen in the period 1930-2000

Table 4.2.1 shows the degree of mutual linear dependency of the characteristic flood wave parameters. They can be considered to be independent.

4.3 Synthesization of a flood wave with given relevant parameters

The flood wave at Borgharen can be synthesized on the basis of (1) peak discharge (Q_{peak}), (2) base discharge at the beginning of the flood wave (Q_{base}), (3) volume of the flood wave (X_0) and (4) crest curvature of the flood wave (X_4). In Appendix 4.3.1 more insight is given into the variability of the parameters (2), (3) and (4).

On the basis of the last two decades of the twentieth century the time lapse between the beginning of the flood wave to the peak is three to six days and four days on average at Borgharen (Appendix 4.3.2).

The crest curvature X_4 can be categorized as flat for $X_4 < 50$; medium for $50 \leq X_4 \leq 76$ and peaked for $X_4 > 76$. These categories follow from Fig.4.3.1, where 50 and 76 are the partitions between one third and two thirds of the area under the Normal probability distribution.

For the above estimated class-limits for X_4 , viz. flat, medium and peaked crest curvatures, the values Q'_{-1} / Q'_{+1} are 1.05, 0.9, and 0.65 respectively (Fig.4.3.2). From Appendix 4.3.3 it turns out that the trend in X_4 has not changed significantly since 1930.

¹³ also see Appendix 4.9.1

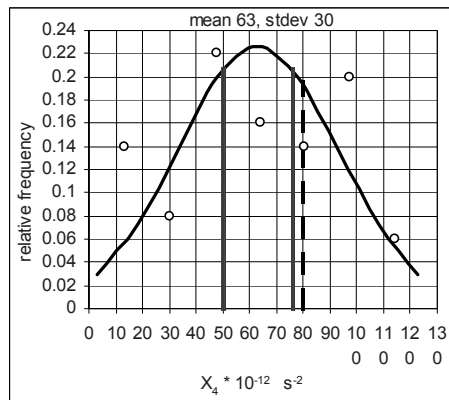


Fig.4.3.1 Open symbols of the class-mid of the measured crest curvatures from the period 1930-2000 and Normal distribution flat(<50), medium(50-76), peaked(>76), dashed line: medium upper limit on floods > 1850 m³s⁻¹

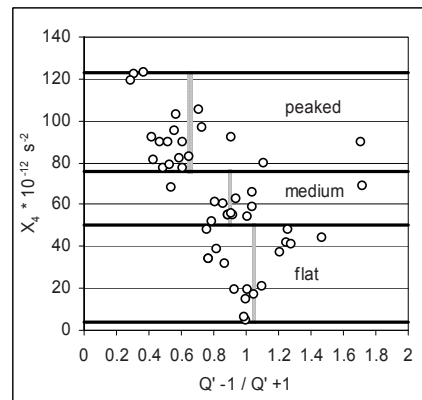


Fig.4.3.2 Mean ratio values Q'_{-1} / Q'_{+1} around Q'_{peak} discharge, for flat (ratio 1.05), medium (ratio 0.90) and peaked (ratio 0.65) crest curvature

The measured flood data in the period 1980-2000 (Appendix 4.3.2) show, that second-degree polynomials give a reasonable approximation of the discharge-time relation $Q'(t)$, for the rising as well as the falling stage of the flood waves. According to the results of the average duration to the peak (Appendix 4.3.2), we define that the peak at Borgharen occurs 4 days after the beginning of the rising stage. For the rising stage it is the polynomial through the beginning of the rising at a certain base discharge level $(0;0)$, through $(3;Q'_{-1})$ and through $(4;Q'_{peak})$. For the falling stage it is the polynomial through $(4;Q'_{peak})$, through $(5;Q'_{+1})$ and through $(n;0)$, where n is the number of the last day of the flood period. This n can be estimated from Fig.4.3.3.

As an example of the synthesization of a flood wave, the measured flood wave at the end of December 1999, is chosen.

Measured data analysis (see Appendix 4.2.1) :

- $Q_{peak} = 2042 \quad L^3 T^{-1}$
- $Q_{base} = 751 \quad L^3 T^{-1}$
- $X_0 = 459 \times 10^6 \quad L^3$
- $X_4 = 77 \times 10^{-12} \quad T^{-2}$
- flood period 10d T
- peak on day 4 T

Calculations:

$$\circ Q'_{\text{peak}} = Q_{\text{peak}} - Q_{\text{base}} = 1291 \text{ m}^3\text{s}^{-1}$$

$$\circ \Sigma Q'_{\text{measured (0...n)}} = X_0 / 86400 = 5318 \text{ m}^3\text{s}^{-1}$$

\circ From Fig.4.3.3 the flood period is estimated at 10 days

\circ Given that $X_4 = 77 \times 10^{12}$, we take for the ratio Q'_{-1} / Q'_{+1} the value 0.9 (Fig.4.3.2).

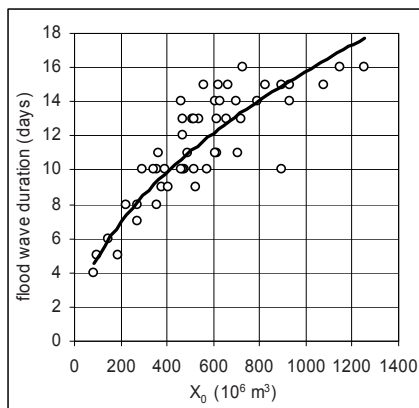


Fig.4.3.3 Relation between the wave volume and the flood period; $R^2=0.76$

Using equation 3.3.5:

$$77 \times 10^{12} = - (Q'_{-1} + Q'_{+1} - 2 Q'_{\text{peak}}) / (86400^2 \times Q'_{\text{peak}}), \text{ and given}$$

$$Q'_{\text{peak}} = 1291 \text{ m}^3\text{s}^{-1} \text{ and } Q'_{-1} = 0.9 Q'_{+1}$$

we find:

$$Q'_{+1} = 968 \text{ m}^3\text{s}^{-1} \text{ and } Q'_{-1} = 871 \text{ m}^3\text{s}^{-1}$$

For the rising stage of the synthesized flood wave through (0;0), (3;871), (4;1291):

$$Q' = 32.4 t^2 + 193.1 t \quad (t=0...4)$$

For the falling stage through (4;1291), (5;968), (10;0):

$$Q' = 21.57 t^2 - 517.1 t + 3014 \quad (t=4...10)$$

This synthesized flood wave is compared with the measured flood wave at Borgharen in Table 4.3.1 and in Fig.4.3.8. Table 4.3.2 shows that the resulting difference in the computed maximum water levels at Venlo and Mook is 0.03 m in either case. In practice this is well within the accuracy band of water level observations, formerly at best 0.1 m for visual observations, at present 0.05 m for electronic devices. Moreover,

the DWL 2001 have been rounded off to 0.1 m (also see Design Hydraulic Conditions, 2001). The accuracy of the Sobek computations of the water levels is also estimated at 0.1 m at main observation points (RIZA 2002).

day	measured Q'	synthesized Q'	measured Q	synthesized Q
0	0	0	751	751
1	152	225	903	976
2	689	516	1440	1267
3	1291	871	2042	1622
4	1155	1291	1906	2042
5	813	968	1554	1719
6	530	688	1281	1439
7	315	451	1066	1202
8	173	257	924	1008
9	109	107	860	858
10	91	0	842	751

Table 4.3.1 Measured and synthesized Q' and Q (m^3s^{-1}) at Borgharen; Flood at the end of December 1999, also see Fig.4.3.8

Figs.4.3.4 through 4.3.8 and Table 4.3.2 compare synthesized and measured peaks for each flood above $2000 \text{ m}^3\text{s}^{-1}$ in the period 1980-2000 (see Appendix 4.2.1 for the characteristic flood wave parameter values). The corresponding water levels at Venlo and Mook, as computed with the Sobek model, are mentioned in the figure captions. We conclude from these figures and Table 4.3.2 that the synthesized maximum water levels do not differ significantly from the measured ones.

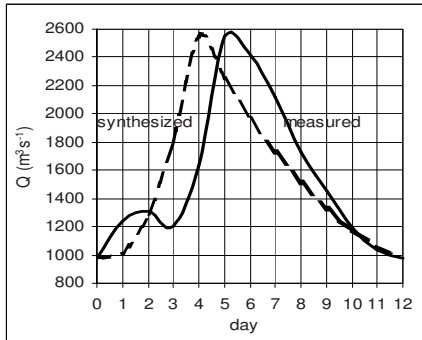


Fig.4.3.4 Measured and synthesized flood wave at Borgharen in February 1984
 measured: $H_V=17.97$; $H_M=11.26$
 synthesized: $H_V=17.90$; $H_M=11.16$

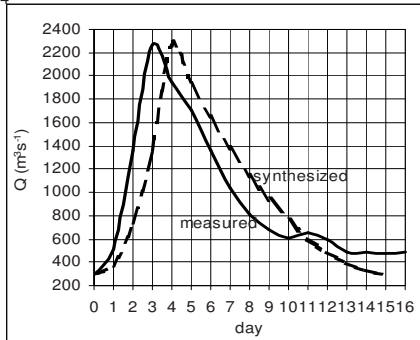


Fig.4.3.5 Measured and synthesized flood wave at Borgharen in January 1993
 measured: $H_V=17.22$; $H_M=10.54$
 synthesized: $H_V=17.21$; $H_M=10.53$

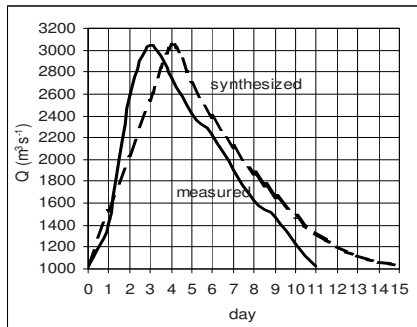


Fig.4.3.6 Measured and synthesized flood wave at Borgharen in December 1993
 measured: $H_V=18.52$; $H_M=11.81$
 synthesized: $H_V=18.54$; $H_M=11.85$

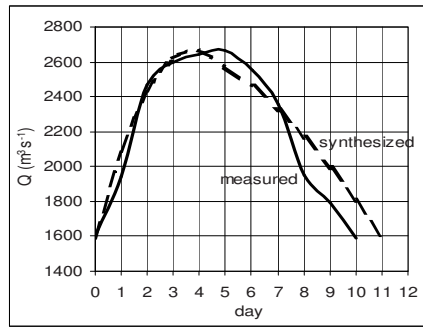


Fig.4.3.7 Measured and synthesized flood wave at Borgharen in January 1995
 measured: $H_V=18.42$; $H_M=11.80$
 synthesized: $H_V=18.39$; $H_M=11.75$

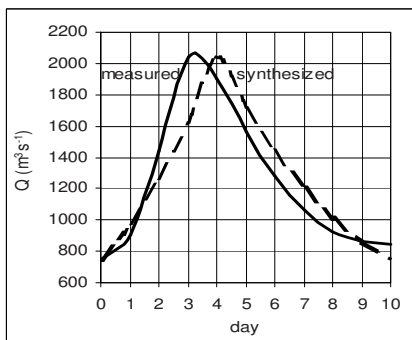


Fig.4.3.8 Measured and synthesized flood wave at Borgharen in December 1999
 measured: $H_V=17.11$; $H_M=10.44$
 synthesized: $H_V=17.08$; $H_M=10.41$

H from measured flood wave Borgharen		H from synthesized flood wave Borgharen		differ. max. water level	differ. max. water level	year of the flood event	meas. peak Borgh.
H _{Venlo} NAP+...m (1)	H _{Mook} NAP+...m (2)	H _{Venlo} NAP+...m (3)	H _{Mook} NAP+...m (4)	(1-3) m	(2-4) m		m ³ s ⁻¹
17.97	11.26	17.90	11.16	0.07	0.10	Feb.'84	2550
17.22	10.54	17.21	10.53	0.01	0.01	Jan. '93	2265
18.52	11.81	18.54	11.85	-0.02	-0.04	Dec.'93	3039
18.42	11.80	18.39	11.75	0.03	0.05	Jan. '95	2664
17.11	10.44	17.08	10.41	0.03	0.03	Dec.'99	2042

Table 4.3.2 Summarized results of the water levels at Venlo and Mook, computed from the measured and synthesized flood waves at Borgharen

4.4 Background of the Sobek water motion model

A thousand samples of random combinations of Q_{peak} , Q_{base} , X_0 and X_4 determine a thousand synthetic flood waves at Borgharen.

Sobek, a one-dimensional model system for 1-D flow problems, allows for a quick computation of the water levels further downstream. The model was developed by Delft Hydraulics and RIZA and has been applied to the Dutch Meuse River, in our case based upon the daily 08 o'clock discharges at Borgharen. Structure, calibration and verification are described in RIZA Report (2002).

In the case of the structure of the Sobek model, special importance is given to reproduce schematisations on basis of the river data sets (by Baseline), 2-D computation results (by Waqua) and applications for the translation of 2-D flow systems into a 1-D model (by Gis).

The goal of the hydraulic calibration of the Sobek Meuse model is to attain a fair specification of the water motion in the river in terms of water levels, discharges and discharge divisions between summer bed, bank sides and winter bed, within the limitations of a 1-D model.

The 2-D Waqua results, available in May 2000 for the Dutch Meuse River for a permanency of $3800 \text{ m}^3\text{s}^{-1}$, are the basis of the hydraulic calibration of Sobek, assumed that these results are well.

The translation of the 2-D hydraulic properties in Waqua into a 1-D reproduction in Sobek was studied by RIZA. For this the important steps are: (1) the spatial integration of the flow pattern -because of the symplification Chezy's formula is often used- and (2) identity conditions, such as similar water levels and discharge divisions in the cross sections of the river for the two models.

At the upstream boundary (i.e. water level measuring-station Eysden, km 2.560) the discharge series has been calculated on basis of the measured historic discharges at

Borgharen, taking into account the travel time between the two, and the lateral discharges. In the calibration the difference between the discharge at Borgharen according to the 'stage – discharge relationship' and according to the model was minimized by adjusting the summer bed roughness between Eysden and Borgharen.

The water levels from the automatic measuring-station Keizersveer (km 247.1) also see Appendix 4.4.1, are used as downstream boundary condition. However, Lith village (km 202.370) is the final measuring-station for which the Sobek calibration has been performed, as it concerns the free flow discharges and not the reproduction of tidal movement. The river stretch between Keizersveer and Lith is calibrated such that at Lith the water level is presented well.

For the estimation of the lateral inflow under various hydrological conditions, mainly caused by the tributaries of the Meuse River, the regression functions between the mean weekly river discharges at Borgharen and Lith are used.

The spatial geometry of the river is reproduced by representative cross-sections, at a distance of about 500 m from each other. They are characterised by the bottom level, the total width and the wetted perimeter. The summer bed, the bank sides and the winter bed have their own formulation of the hydraulic roughness. Obstacles, such as structures, are represented by extra resistance, with the head loss adapted to that in the 2-D Waqua model. The winter bed and bank roughness are determined by the ecological diversity and also by the model roughness caused by the simplification to a 1-D model. They are projected onto the Nikuradse roughness lengths, k_N . The summer bed roughness is expressed by the Chézy factor¹⁴, chosen such that it corresponds with the results of the 2-D Waqua-model. In the 1-D Sobek model, the head loss per unit river length in the summer bed has to be equal to that in the winter bed. For this, the lines of equal water levels from the Waqua-model are used. An arbitrary example of the river stretch (Appendix 4.4.2) downstream of the sluices at Belfeld (km101 – km106), with summer bed, winter bed, lakes within and outside the wetted area, contours of the stream carrying and only storage area, and lines of equal water levels across both areas, gives a rough outline of the flow pattern according to 2-D Waqua.

As is shown in Appendix 4.4.1, the Sobek model consists of branches B, and nodes O connecting the branches. In each branch there is a number of grid points. Furthermore nodes are situated at the model boundaries, at the bifurcation points, at the links with detention areas and at measuring-stations.

The Sobek model is widely used in flood prediction and river basin management. For the Dutch Meuse River it is used for the Integral Reconnaissance Meuse River (IVM), for the 'Maaswerken' project, for morphological studies, for water quality studies and for the design of river interventions. This usually requires model support at short notice, which so far, rules out using 2-D models such as the existing Waqua model.

The accuracy of the results of the Sobek computations depends, to a significant extent, on the reliability and accuracy of the available data.

¹⁴ $C = 18 \log(12h/k_N)$ Nikuradse-Colebrook
 $C = v / (h i_{bo})^{1/2}$ Chézy

The 1-D Sobek model for the Dutch Meuse River arising from the aforementioned specification has been calibrated on the basis of the flat-crested flood of January 1995 (version 2000.1) and verified by the medium-crested floods of December 1993 (version 2000.2) and December 1999 (version 2000.3). It turned out that the downstream peak water-levels, especially for the more extreme floods, are reproduced with an accuracy of 0.1 m at the automatic measuring-stations (MSW) along the river for the flood of 1995 and 0.15 m for the flood of 1993. For the flood of 1999, with the most recent data, the occurrence is consistent with the others. Unforeseen emergency measures, in the case of an extreme flood that tends to overflow the levees, make an estimation of this effect precarious. Stream carrying areas behind the levees are not considered, so far.

4.5 Relative frequency distribution of the water levels

Water levels at Venlo:

The water levels at Venlo, derived from the synthesized floods at Borgharen and the Sobek computations, are divided into classes of 0.1 m each. The water level data and corresponding flood wave number can be found in Appendix 4.5.1. They are divided into three parts, namely those from the flood wave numbers 1 through 335, from 1 through 671 (the extension to nrs. 1...335), and from 1 through one thousand (the extension to nrs. 1...671). In Figs.4.5.1 through 4.5.3 the histograms are shown.

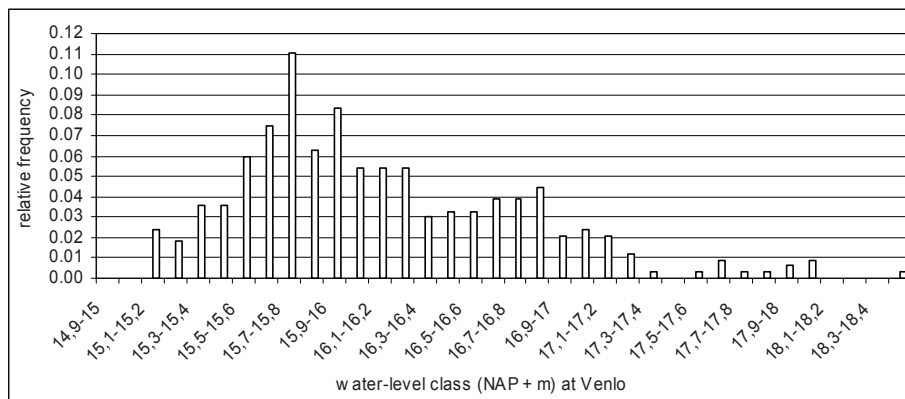


Fig.4.5.1 Relative frequency histogram for flood levels at Venlo derived from 335 synthetic flood waves at Borgharen (nrs.1...335)

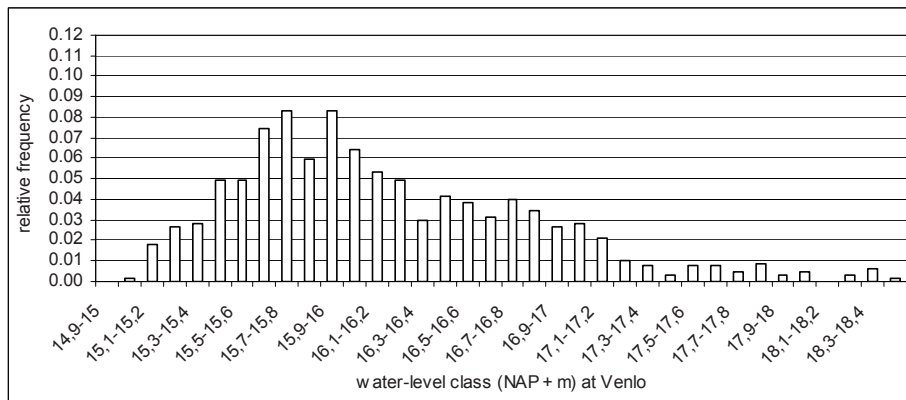


Fig.4.5.2 Relative frequency histogram for flood levels at Venlo derived from 671 synthetic flood waves at Borgharen (nrs.1...671)

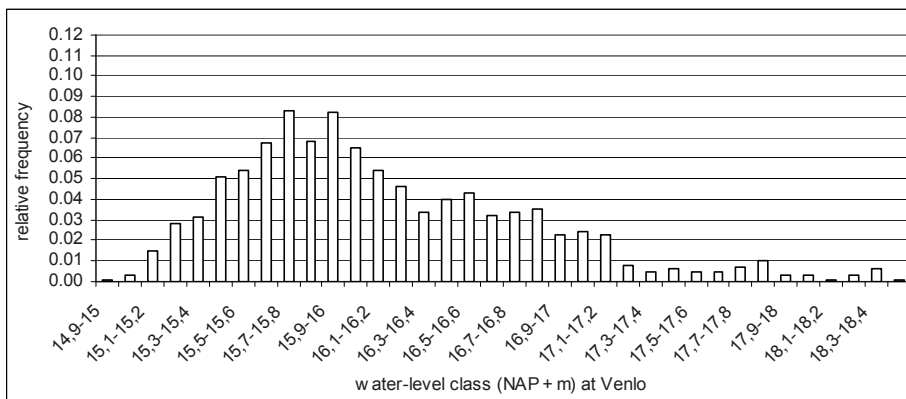


Fig.4.5.3 Relative frequency histogram for flood levels at Venlo derived from one thousand synthetic flood waves at Borgharen (nrs.1...1000)

From these figures it is clear, that the difference between the distribution of the series of 671 and one thousand random samples is very small and that the series of 335 random samples differs somewhat more from the other two. Fig.4.5.4 shows the differences by the three flowing lines through the class-mid of the relative frequency.

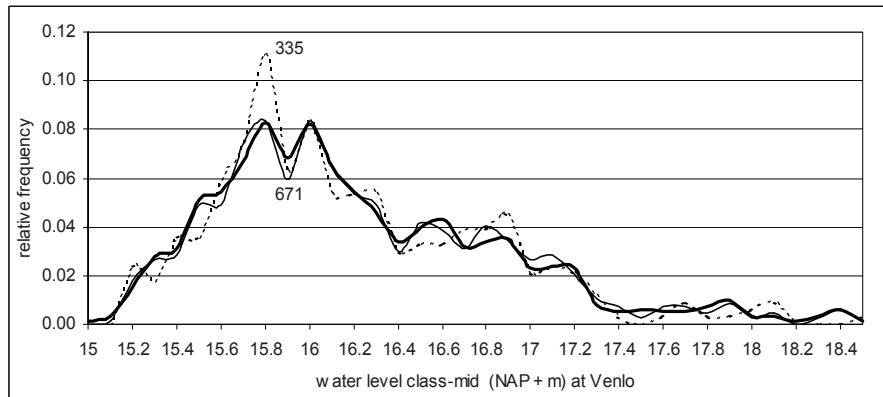


Fig.4.5.4 Relative frequency of computed water levels at Venlo from three flood wave series of different length at Borgharen (also see Figures 4.5.1 through 4.5.3)

Water levels at Mook:

Analogous to the investigation into the water levels at Venlo, the water level histograms at Mook are determined. The basic data also can be found in Appendix 4.5.1. Figs.4.5.5 through.4.5.7 show the results.

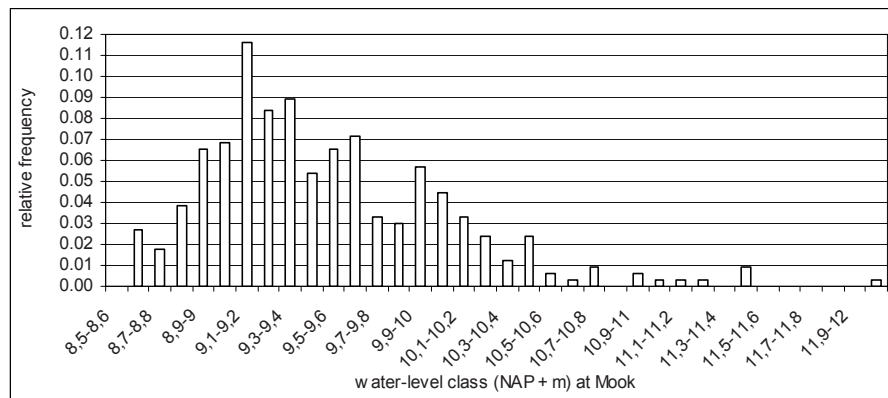


Fig.4.5.5 Relative frequency histogram for flood levels at Mook derived from 335 synthetic flood waves at Borgharen (nrs.1...335)

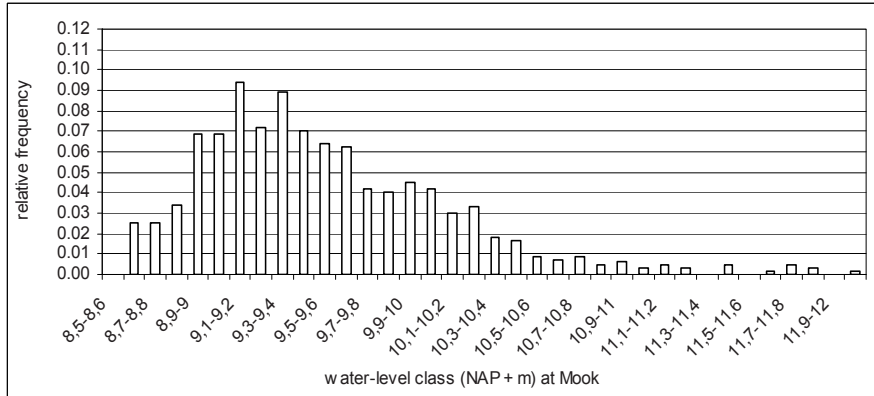


Fig.4.5.6 Relative frequency histogram for flood levels at Mook derived from 671 synthetic flood waves at Borgharen (nrs.1...671)

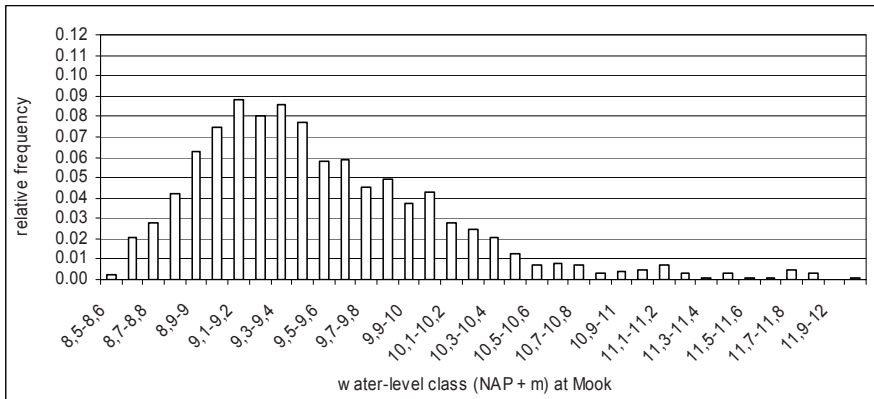


Fig.4.5.7 Relative frequency histogram for flood levels at Mook derived from one thousand synthetic flood waves at Borgharen (nrs.1...1000)

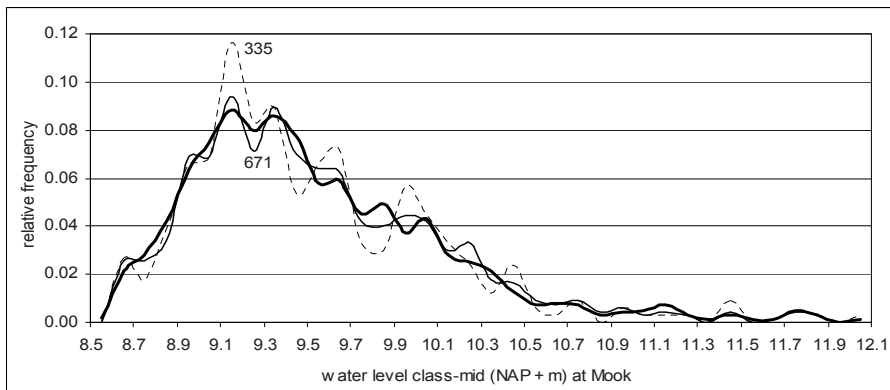


Fig.4.5.8 Relative frequency of computed water levels at Mook from three flood wave series of different length at Borgharen (also see Figures 4.5.5 through 4.5.7)

We conclude that, by random sampling of one thousand combinations of significant flood wave characteristics at Borgharen resulting in just as much computed water levels at Venlo and Mook, we are able to determine enough stable pdf 's for these two locations to adapt appropriate analytical curves to these of Figures 4.5.4 and 4.5.8.

4.6 Adaptation of probability distribution functions to the relative frequency distributions

Adapted probability distribution functions for the water level measuring-station at Venlo (km.107.470)

A number of often used distribution functions in hydrology are fitted to the one thousand water levels at Venlo as derived from the synthetic flood waves at Borgharen. These functions (F) are tested for their similarity to the cumulative frequency distribution (P) of the computed water levels by the Kolmogorov-Smirnov test (Yevjevich, 1972, page 224, Table 10.3). In the case of similarity, the probability of exceedance function of the water levels can be extrapolated to values beyond the reach of the computed water levels. The formulae of the functions (F) are given in Appendix 4.6.1.

To determine the adapted function, the parameter values as mentioned in Table 4.6.1 are needed.

distribution	mean (m)	stdev. (m)	α (shape)	β (scale) (m)	Γ (α)	γ (lower limit) (m)
Normal	16.17	0.65				
Lognormal	2.78	0.04				
Pearson III	1.22	0.65	3.531 (-)	0.346	3.4395	14.95
Gumbel	16.17	0.65	1.97 (m ⁻¹)	15.88		

Table 4.6.1 Parameter values for adaptation of a distribution function to the computed water levels at Venlo

The histograms of the computed water levels are shown in Figs.4.6.1 through 4.6.4, together with the adapted probability distribution functions. The cumulative probability distribution functions are compared with the 95% confidence band of the cumulative frequency distribution of the computed water levels, to test the goodness of fit. The critical value Δ_0 of the K-S test statistic Δ depends on α (i.e. the chosen probability of exceedance Δ_0) and on the number N of computed water levels from the synthetic floods and can be found in the K-S Table (Yevjevich, 1972, Table 10.3). This Table is shown in Appendix 4.6.2. In our case α equals 0.05, two-tailed, and \sqrt{N} equals 31.62 for one thousand computations. Δ_0 equals $1.36 / 31.62 = 0.043$, and both confidence limits around the cumulative frequency distribution (P) of the computed water levels are drawn at a distance of 0.043 above and below (Fig.4.6.1b). The maximum of $|F-P|$, i.e. the maximum difference between the cumulative probability distribution function (F) and the computed cumulative frequency distribution (P) or Δ (the test statistic), equals to 0.12 for the water level NAP + 16.05, so $\Delta > \Delta_0$ and so the null hypothesis is rejected. This is confirmed by the fact that the function (F) exceeds the 95% confidence band of the cumulative frequency distribution (P) of the computed water level class-mid (x x x) of Fig.4.6.1b.

The K-S test is an objective test without conditions as sorting of data in class intervals and a minimal number of observations in the class intervals, such as for the χ^2 test.

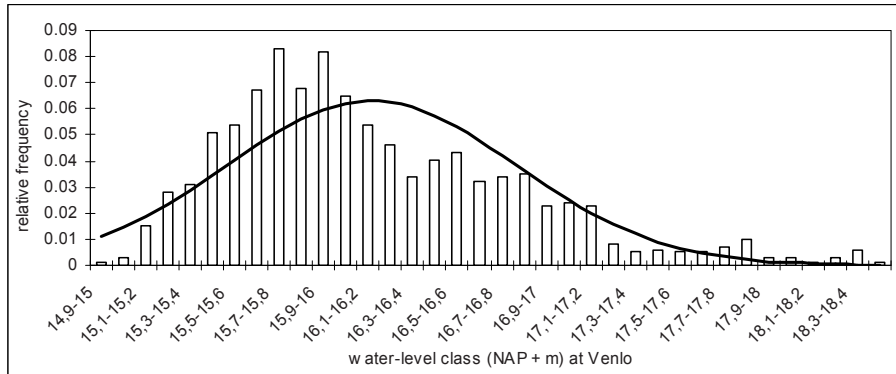


Fig.4.6.1a Fit of the Normal Distribution function to the relative frequency histogram of the water levels at Venlo computed from one thousand synthetic floods at Borgharen

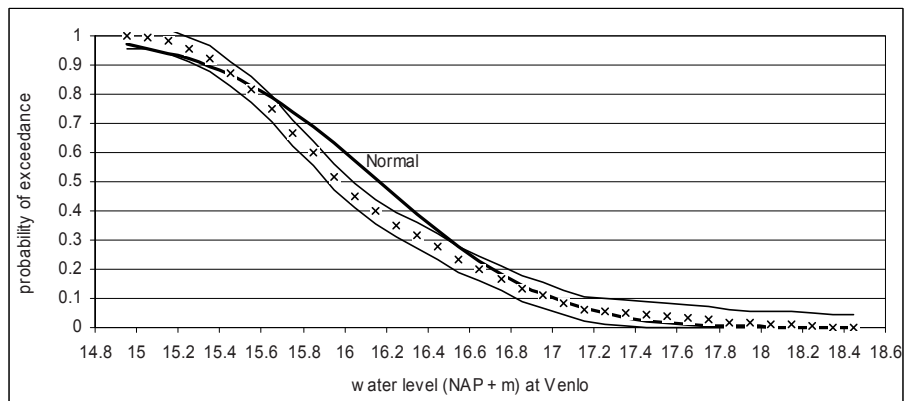


Fig.4.6.1b Kolmogorov-Smirnov test ($\Delta_0 = 0.043$) for agreement between the 95% confidence band of the cumulative frequency distribution of the computed water levels at Venlo and the Normal cumulative distribution function

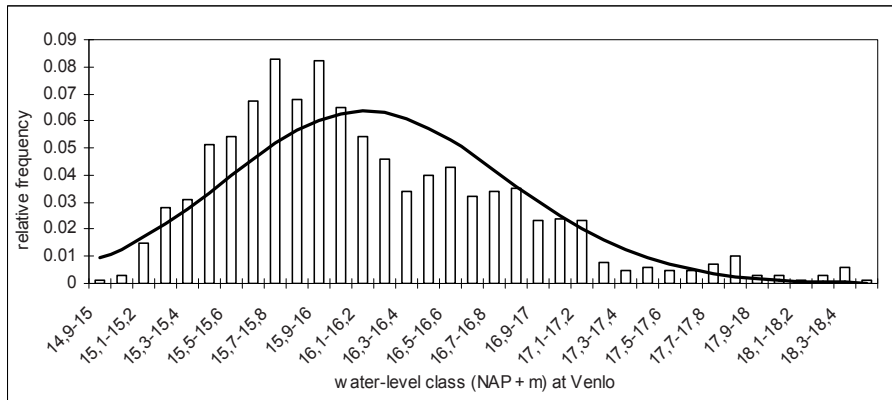


Fig.4.6.2a Fit of the Lognormal Distribution function to the relative frequency histogram of the water levels at Venlo computed from one thousand synthetic floods at Borgharen

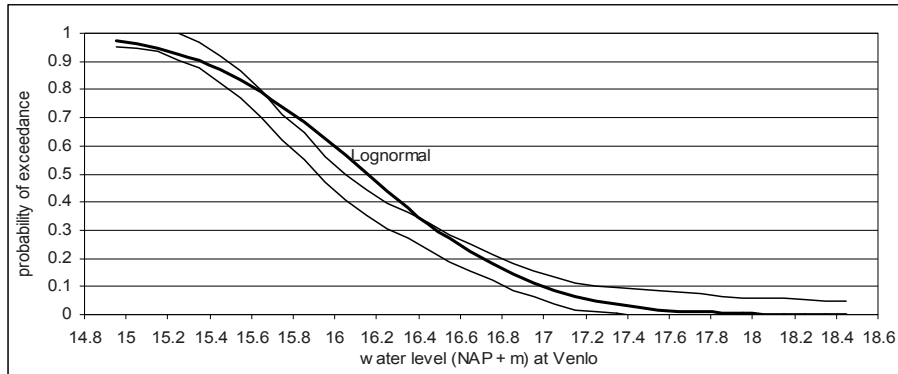


Fig.4.6.2b Kolmogorov-Smirnov test ($\Delta_0 = 0.043$) for agreement between the 95% confidence band of the cumulative frequency distribution of the computed water levels at Venlo and the Lognormal cumulative distribution function

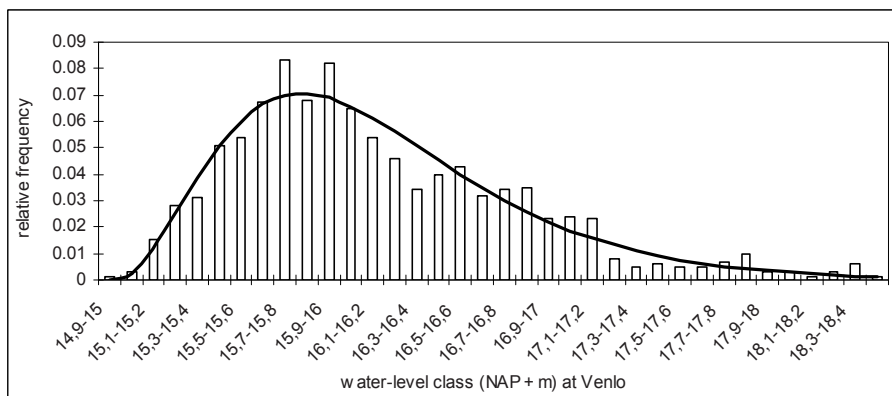


Fig.4.6.3a Fit of the Pearson type III Distribution function to the relative frequency histogram of the water levels at Venlo computed from one thousand synthetic floods at Borgharen

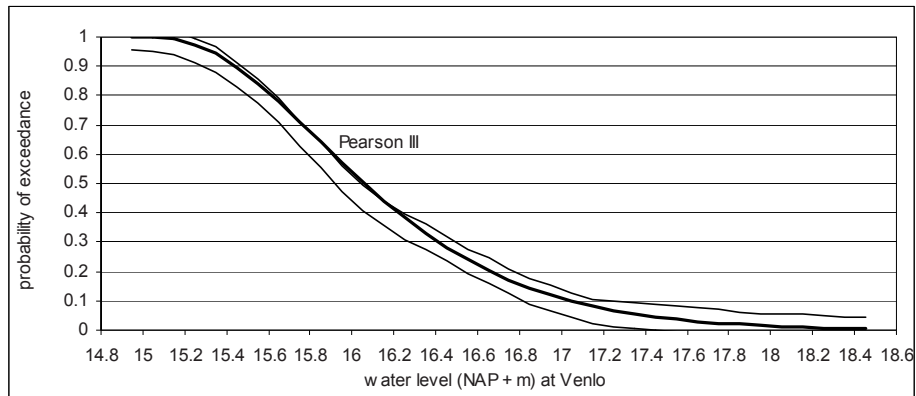


Fig.4.6.3b Kolmogorov-Smirnov test ($\Delta_0 = 0.043$) for agreement between the 95% confidence band of the cumulative frequency distribution of the computed water levels at Venlo and the Pearson type III cumulative distribution function

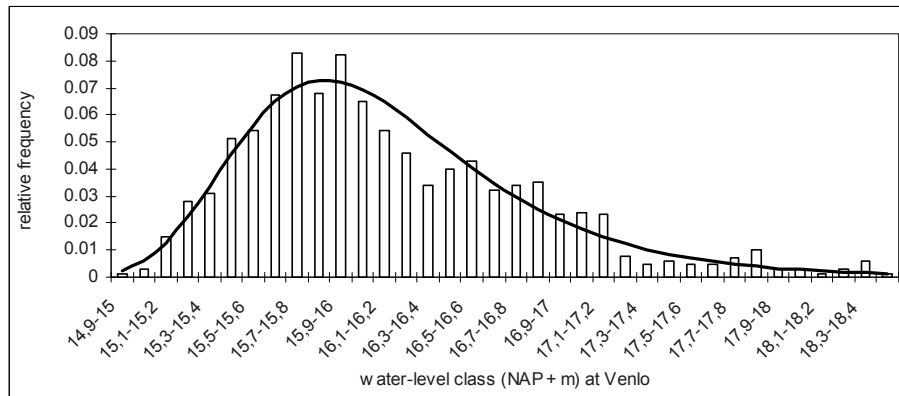


Fig.4.6.4a Fit of the Gumbel Distribution function to the relative frequency histogram of the water levels at Venlo computed from one thousand synthetic floods at Borgharen

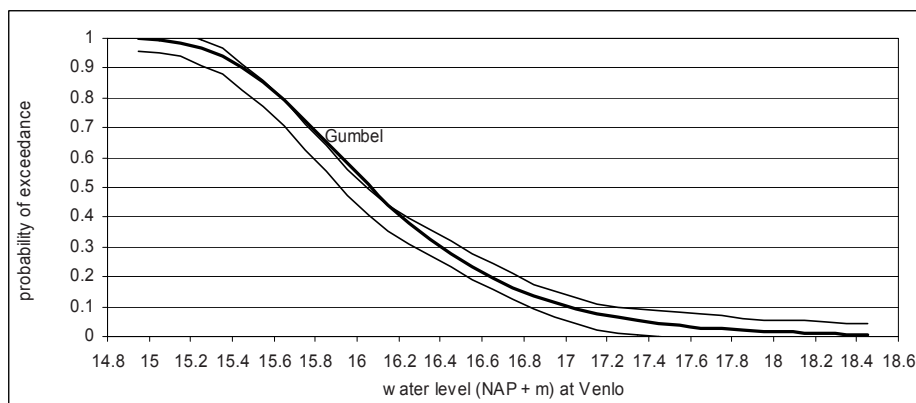


Fig.4.6.4b Kolmogorov-Smirnov test ($\Delta_0 = 0.043$) for agreement between the 95% confidence band of the cumulative frequency distribution of the computed water levels at Venlo and the Gumbel cumulative distribution function

The Kolmogorov-Smirnov test indicates that the Pearson type III cumulative distribution function is the best adaptation to the cumulative frequency distribution of the computed water levels. The Gumbel distribution gets the benefit of the doubt. This is confirmed by Figs. 4.6.3b and 4.6.4b where the functions lie inside the 95% confidence band of the computed water levels. In Table 4.6.2 the implication is shown for the probability of exceedance of the water levels at Venlo (km 107.470) for the situation at the end of the twentieth century.

probability of exceedance yr^{-1}	Pearson type III $H_{\text{Venlo}} (\text{NAP} + m)$ (1)	Gumbel $H_{\text{Venlo}} (\text{NAP} + m)$ (2)	average H_{Venlo} from (1) and (2)
0.1	17.05	17.00	17.05
0.04	17.50	17.50	17.50
0.02	17.85	17.85	17.85
0.01	18.15	18.20	18.15
0.004	18.55	18.65	18.60
0.002	18.90	19.00	18.95
0.0008	19.25	19.50	19.35

Table 4.6.2 Probability of exceedance of the water levels at Venlo

For the preferred Pearson type III and also for the Gumbel function, the results for the water levels at Venlo, as mentioned in Table 4.6.2, are shown in Fig.4.6.5.

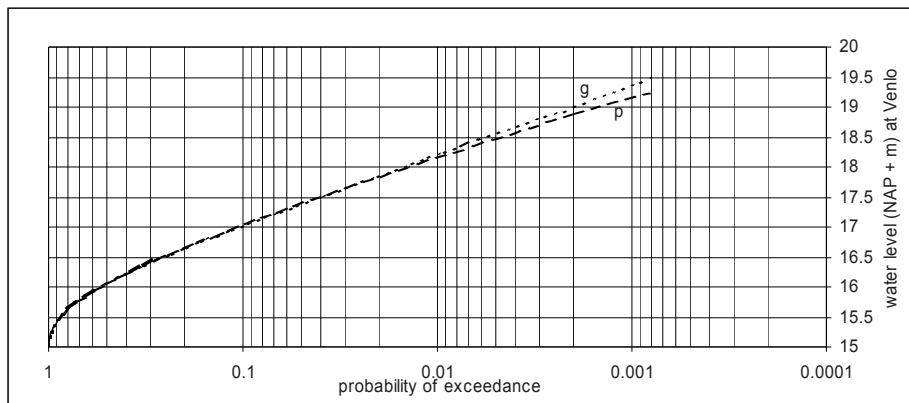


Fig.4.6.5 Probability of exceedance of the water levels at Venlo, according to the Pearson type III function (p), and the Gumbel function (g)

Adapted probability distribution functions for the water level measuring-station at Mook (km.165.800)

The functions are derived in the same way as those for Venlo.

Table 4.6.3 gives the parameters, needed to determine a function adapted to the computed water levels at Mook.

distribution	mean (m)	stdev. (m)	α (shape)	β (scale) (m)	Γ (α)	γ (lower limit) (m)
Normal	9.54	0.58				
Lognormal	2.25	0.06				
Pearson III	0.99	0.58	2.854 (-)	0.346	1.7554	8.55
Gumbel	9.54	0.58	2.20 (m^{-1})	9.27		

Table 4.6.3 Parameter values for adaptation of a probability distribution function to the computed water levels at Mook (also see Appendix 4.6.1)

The histograms of the computed water levels are shown in Figs.4.6.6 through 4.6.9, together with the adapted probability distribution functions. The cumulative probability distribution functions are compared with the 95% confidence band of the cumulative frequency distribution of the computed water levels, to test the goodness of fit, according to the Kolmogorov-Smirnov test.

The conditions for acceptance of the null hypothesis are the same as for the measuring-point Venlo (Δ_0 equals 0.043). In Fig.4.6.6b, for instance, the test statistic Δ equals 0.12, for which the water level is NAP + 9.45 m. The null hypothesis is rejected for the Normal distribution as $\Delta > \Delta_0$. This is in accordance with the fact that a part of the Normal function lies outside the 95% confidence band of the computed cumulative frequency distribution.

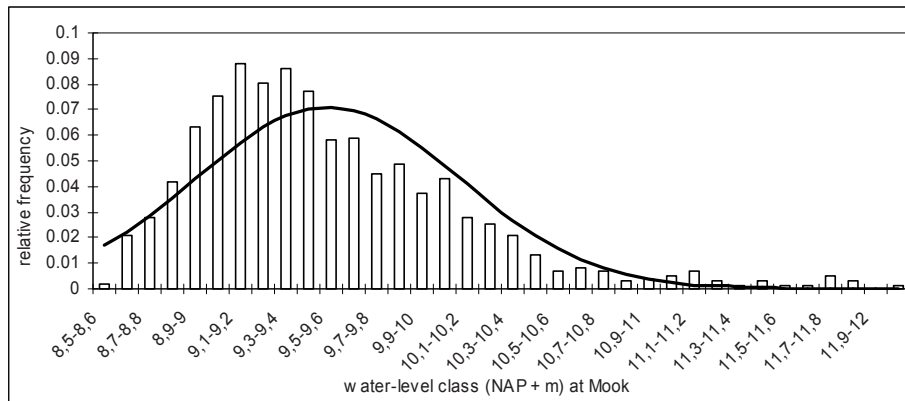


Fig.4.6.6a Fit of the Normal Distribution function to the relative frequency histogram of the water levels at Mook computed from one thousand synthetic floods at Borgharen

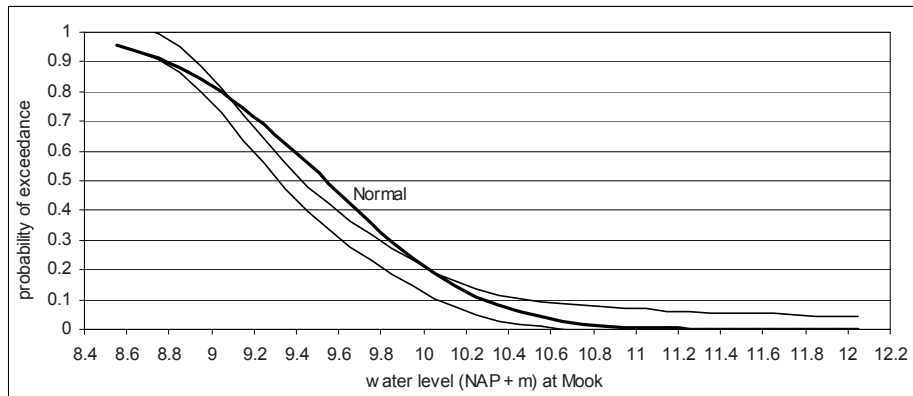


Fig.4.6.6b Kolmogorov-Smirnov test ($\Delta_0 = 0.043$) for agreement between the 95% confidence band of the cumulative frequency distribution of the computed water levels at Mook and the Normal cumulative distribution function

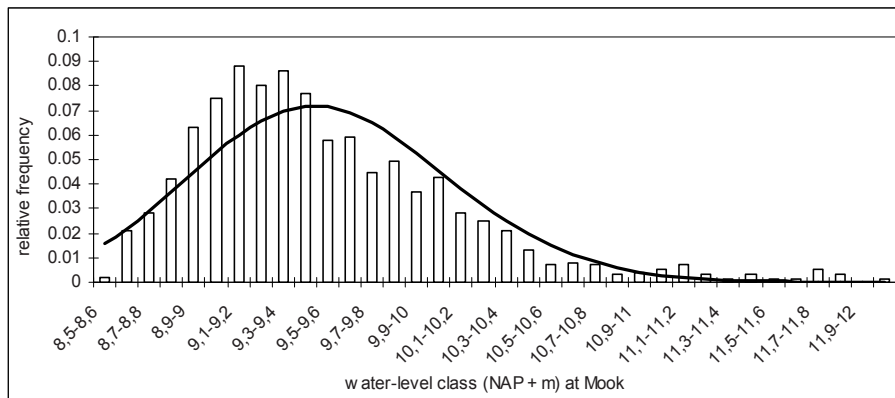


Fig.4.6.7a Fit of the Lognormal Distribution function to the relative frequency histogram of the water levels at Mook computed from one thousand synthetic floods at Borgharen

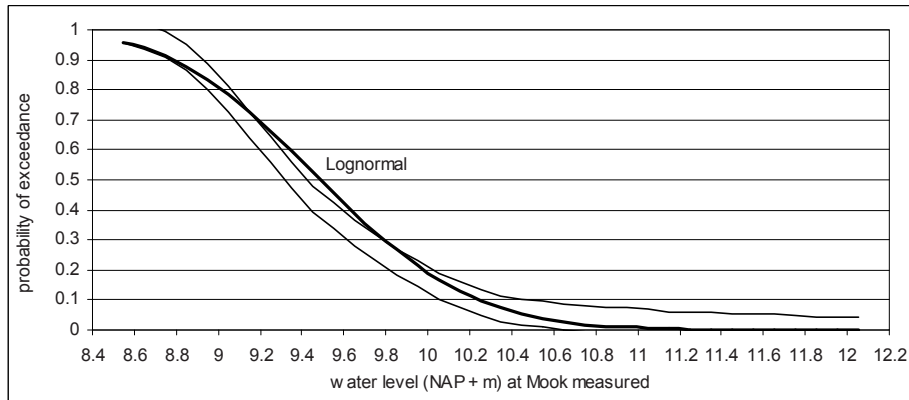


Fig.4.6.7b Kolmogorov-Smirnov test ($\Delta_0=0.043$) for agreement between the 95% confidence band of the cumulative frequency distribution of the computed water levels at Mook and the Lognormal cumulative distribution function

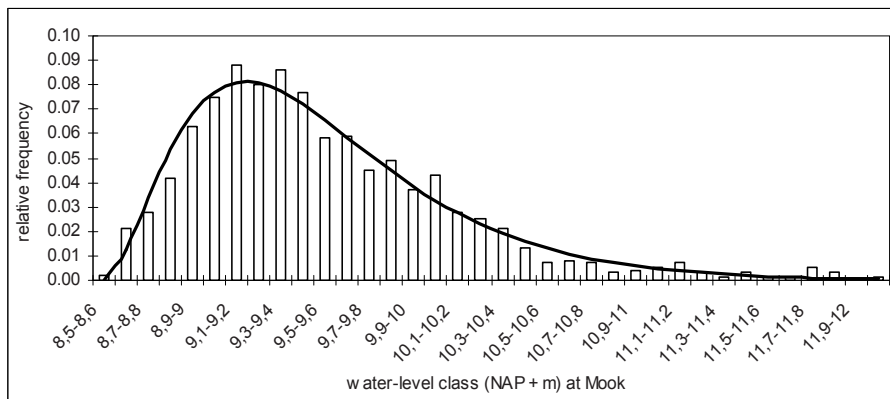


Fig.4.6.8a Fit of the Pearson typeIII Distribution function to the relative frequency histogram of the water levels at Mook computed from one thousand synthetic floods at Borgharen

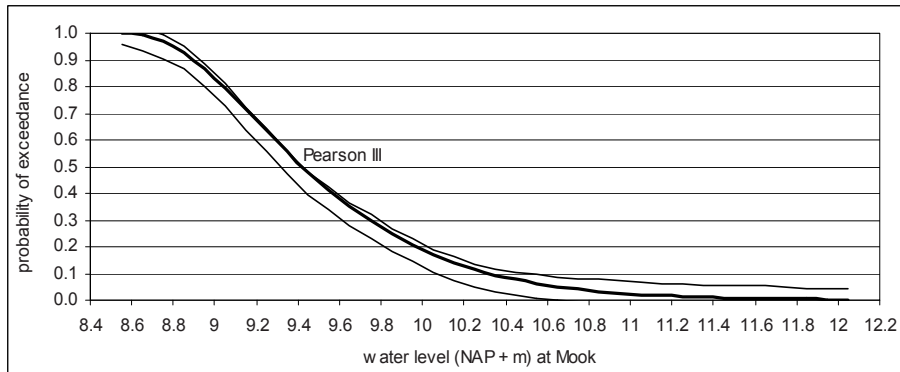


Fig.4.6.8b Kolmogorov-Smirnov test ($\Delta_0 = 0.043$) for agreement between the 95% confidence band of the cumulative frequency distribution of the calculated water levels at Mook and the Pearson type III cumulative distribution function

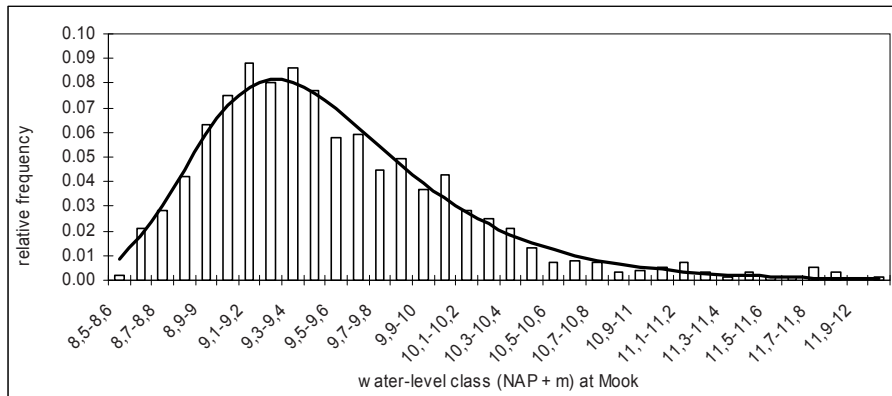


Fig.4.6.9a Fit of the Gumbel Distribution function to the relative frequency histogram of the water levels at Mook computed from one thousand synthetic floods at Borgharen

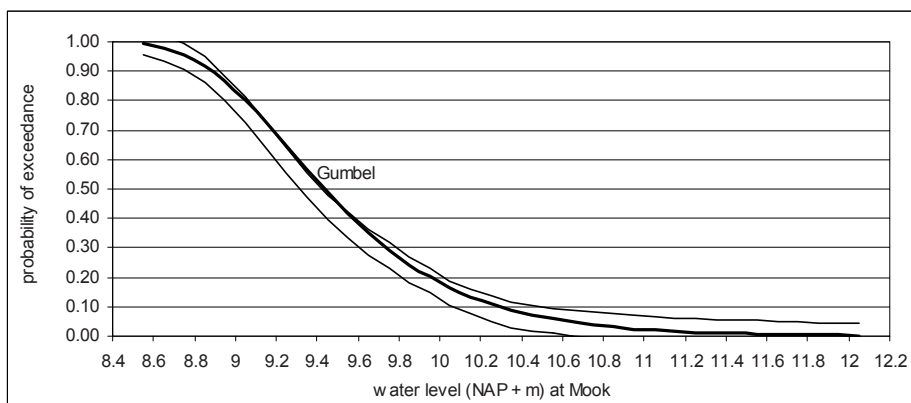


Fig.4.6.9b Kolmogorov-Smirnov test ($\Delta_0 = 0.043$) for agreement between the 95% confidence band of the cumulative frequency distribution of the computed water levels at Mook and the Gumbel cumulative distribution function

Figs. 4.6.6 through 4.6.9 show that the Pearson type III cumulative distribution function and the Gumbel cumulative distribution function do not exceed the 95% confidence band of the computed water levels. So, for the location Mook the same conclusions can be drawn as for the location Venlo. Table 4.6.4 gives the probability of exceedance of the water level at Mook (km.165.800) for the situation at the end of the twentieth century.

probability of exceedance yr^{-1}	Pearson type III $H_{\text{Mook}} (\text{NAP} + m)$ (1)	Gumbel $H_{\text{Mook}} (\text{NAP} + m)$ (2)	average H_{Mook} from (1) and (2)
0.1	10.30	10.30	10.30
0.04	10.75	10.75	10.75
0.02	11.05	11.05	11.05
0.01	11.35	11.35	11.35
0.004	11.75	11.80	11.75
0.002	12.05	12.10	12.05
0.0008	12.45	12.50	12.45

Table 4.6.4 Probability of exceedance of the water levels at Mook

For the preferred Pearson type III and also for the Gumbel function, the results for the water levels at Mook, as mentioned in Table 4.6.4, are shown in Fig.4.6.10.

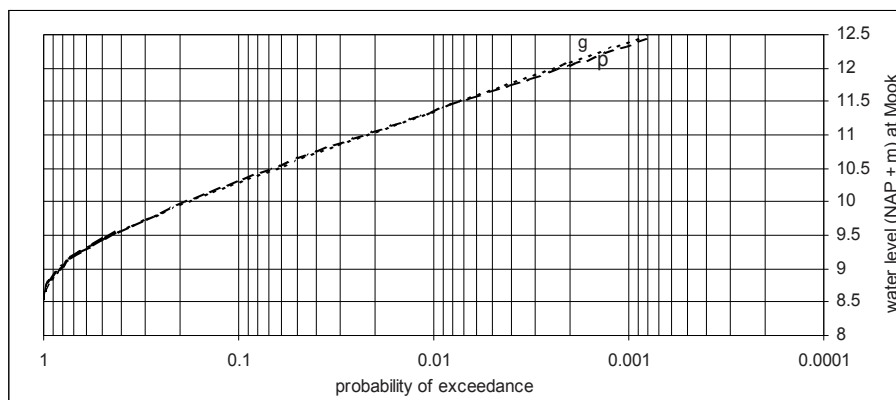


Fig.4.6.10 Probability of exceedance of the water levels at Mook, according to the Pearson type III function (p), and the Gumbel function (g)

4.7 Water level differences between the computations and the adapted probability distribution functions

Figs.4.7.1 and 4.7.2 compare the computed values of the water levels at Venlo and Mook with the preferred adapted Pearson and Gumbel functions.

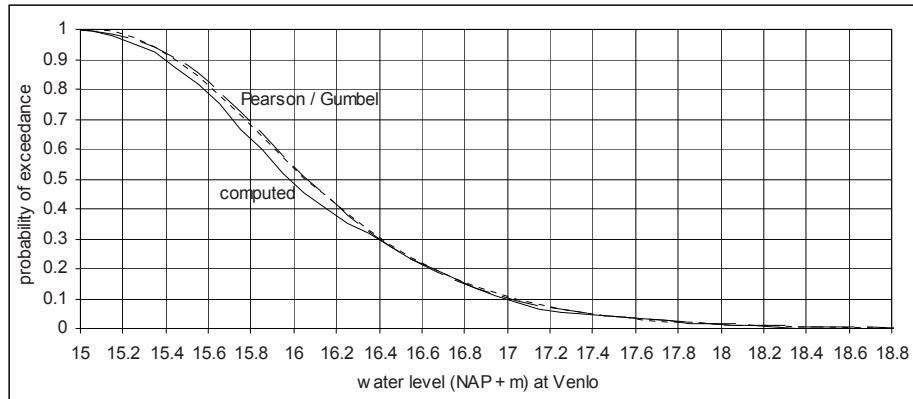


Fig.4.7.1 Comparison of the p.o.e. of the computed water levels at Venlo with that of the adapted functions

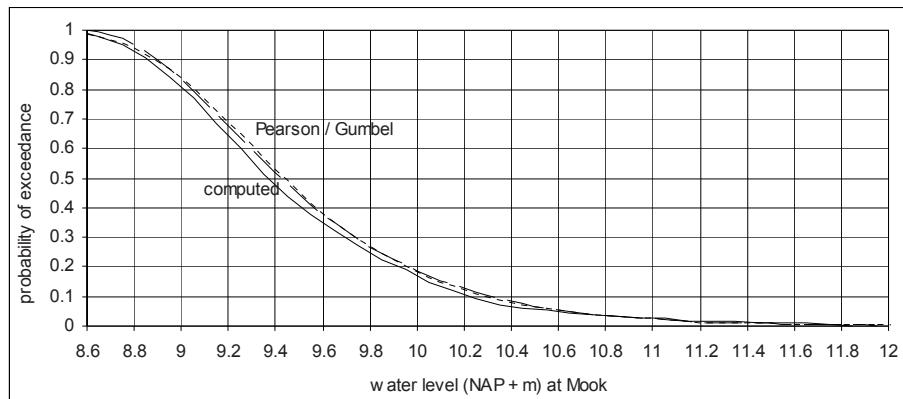


Fig.4.7.2 Comparison of the p.o.e. of the computed water levels at Mook with that of the adapted functions

It is shown that for smaller p.o.e. the water level differences are negligible and for the rest they are less than 0.1 m. So, the Pearson type III and Gumbel functions for exceeding probabilities are satisfactory approximations to the computed water levels, in view of practice as mentioned in the text above Table 4.3.1.

4.8 The reliability of the local water levels related to the peak discharges at Borgharen

Venlo

This section examines the spreading of downstream water levels at Venlo and Mook, computed from synthetic floods with varying wave shapes at Borgharen (Appendix 4.2.1), brought together in series with the same peak discharge at Borgharen. Appendix 4.8.1 gives these series of computed water levels at Venlo, ordered according to the peak discharges of the floods that have occurred at Borgharen in the

period 1980-2000. The means and standard deviations of the series are given in Table 4.8.1.

Q_{peak} m^3s^{-1}	Borgh.	mean NAP+... m	stdev. m	number of synthetic floods
2060		17.10	0.05	8
2165		17.21	0.09	8
2265		17.33	0.12	10
2550		17.64	0.13	13
2664		17.77	0.16	18
3039		18.19	0.22	15

Table 4.8.1 Means and standard deviations of the water levels at Venlo for various series of synthetic floods, ordered according to the measured peak discharge at Borgharen

Fig. 4.8.1 shows the water levels at Venlo, and the 98% and 80% confidence bands of the regression line, extrapolated to the ruling discharge ($3370 \text{ m}^3\text{s}^{-1}$) at Borgharen, derived from the means and standard deviations of Table 4.8.1, assuming a normal distribution of the water level variations.

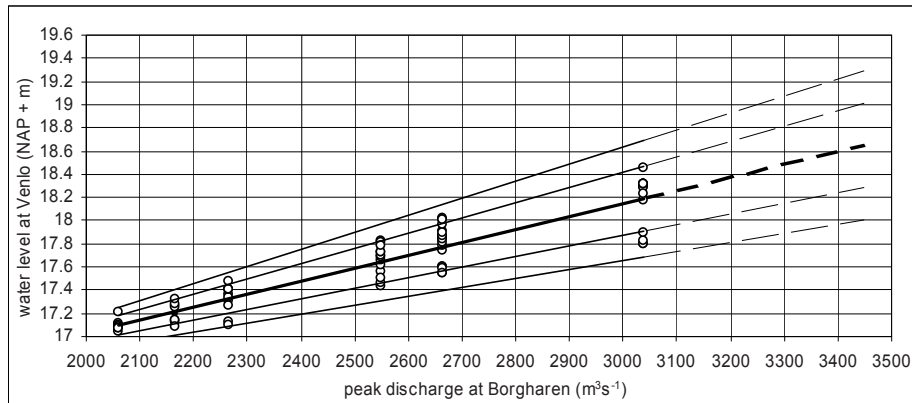


Fig.4.8.1 Water level series at Venlo related to peak discharges at Borgharen and 98% and 80% confidence bands of the water levels; the regression line (thick) refers to the mean of each series

Mook

Appendix 4.8.2 gives series of computed water levels at Mook, ordered according to the peak discharges of the floods that have occurred at Borgharen in the period 1980-2000. The means and standard deviations of the series are given in Table 4.8.2.

Analogous to the Venlo case, the results at Mook are shown in Fig.4.8.2.

Q_{peak} Borgh.	mean	stdev	number of synthetic floods
m^3s^{-1}	NAP+...m	m	
2060	10.34	0.07	8
2165	10.47	0.12	8
2265	10.59	0.15	10
2550	10.94	0.20	13
2664	11.08	0.27	18
3039	11.53	0.41	15

Table 4.8.2 Means and standard deviations of the water levels at Mook for various series of synthetic floods, ordered according to the peak discharge at Borgharen

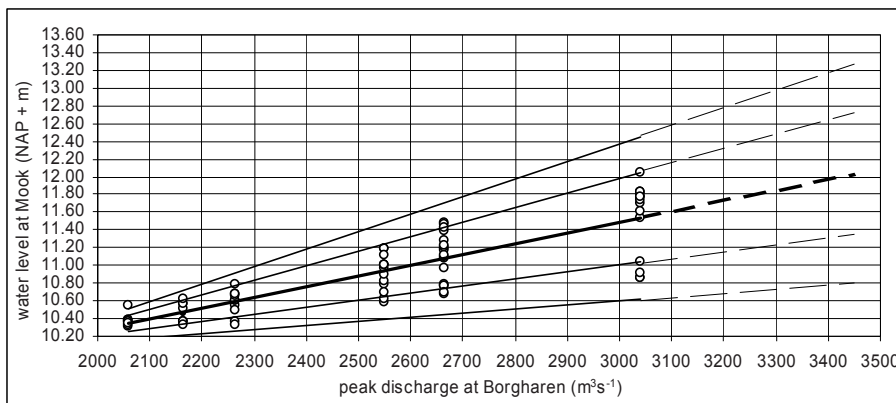


Fig.4.8.2 Water level series at Mook related to peak discharges at Borgharen and 98% and 80% confidence bands of the water levels; the regression line (thick) refers to the mean of each series

Five water levels that were computed at Venlo and Mook for the floods above $2000 \text{ m}^3\text{s}^{-1}$ at Borgharen in the period 1980-2000, are plotted in Figs.4.8.3 and 4.8.4, respectively, together with the confidence bands from Figs.4.8.1 and 4.8.2. Clearly, the flood of 1995 is very exceptional for Venlo and rather exceptional for Mook. This exceptional event is caused by the measured extreme flood wave parameter values at Borgharen, namely the very extreme base discharge of $1591 \text{ m}^3\text{s}^{-1}$ (then the winter bed was already amply inundated) and the very flat crest curvature of $17 \cdot 10^{-12} \text{ s}^{-2}$ (also see Appendix 4.3.1 and Table 4.8.3). The probability that a flood with this peak discharge results in a still higher water level at Venlo is much less than 1%. As was mentioned in Section 4.4, the calibration of the Sobek-Maas model is based on this flood of January 1995 and verified against the floods of December 1993 and December 1999, when the floodplains were not inundated at the beginning of the flood and the crest curvature was medium. In spite of that, the results of the verification were considered to be satisfactory (RIZA, 2002, page 92)

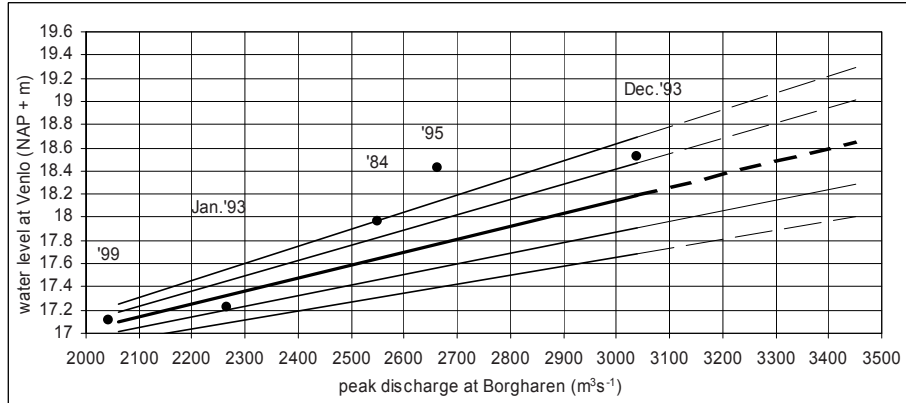


Fig.4.8.3 Real flood waves in the period 1980-2000 at Borgharen and corresponding computed water levels at Venlo (solid symbols); underlying pattern taken from Fig.4.8.1

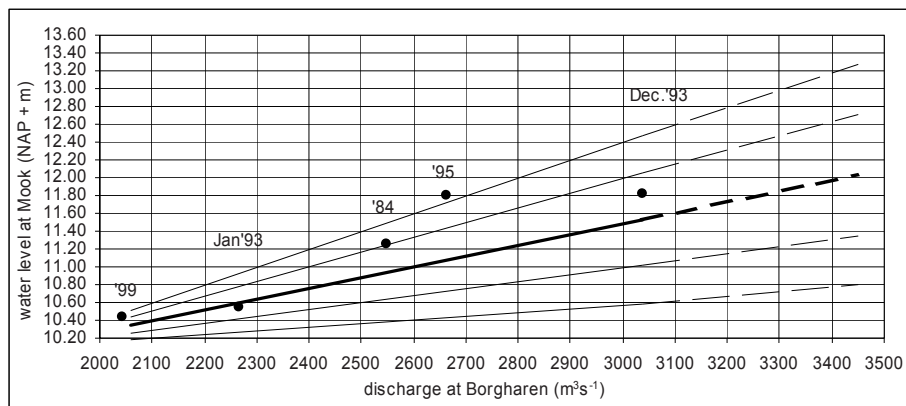


Fig.4.8.4 Real flood waves in the period 1980-2000 at Borgharen and corresponding computed water levels at Mook (solid symbols); underlying pattern taken from Fig.4.8.2

Table 4.8.3 shows the parameter values of the five aforementioned flood waves (1980-2000) underlying Figs.4.8.3 and 4.8.4 (solid symbols)

date of the flood	Q_{peak} m^3s^{-1}	Q_{base} m^3s^{-1}	X_0 10^6 m^3	X_4 10^{-12} s^{-2}	H_{Venlo} NAP + m	H_{Mook} NAP + m
Dec.1999	2042	751	459	77	17.11	10.44
Jan.1993	2265	293	931	83	17.22	10.54
Febr.1984	2550	979	615	90	17.97	11.26
Jan.1995	2664	1591	575	17	18.42	11.80
Dec.1993	3039	1030	896	56	18.52	11.81

Table 4.8.3 Measured flood wave parameter values 1980-2000 at Borgharen and results of Sobek water level computations, from measured flood waves at Borgharen, for Venlo and Mook

The flood wave parameter values corresponding with the maximum and minimum computed water levels at Venlo and Mook of each Q_{peak} series at Borgharen are shown in Table 4.8.4. For a given Q_{peak} series the differences between the maximum and minimum water levels at Venlo and Mook are due to the characteristic parameters Q_{base} , X_0 and X_4 .

Q_{peak} series Borgharen m^3s^{-1}	synthetic flood wave number	Q_{base} m^3s^{-1}	X_0 10^6 m^3	X_4 10^{-12} s^{-2}	H_{Venlo} NAP + m	H_{Mook} NAP + m
2060						
Maximum computed	912	899	727	6	17.21	10.55
Minimum computed	401	1030	512	55	17.04	10.31
differences					0.17	0.24
2165						
Maximum computed	285	751	810	19	17.32	10.62
Minimum computed	745	895	561	82	17.08	10.33
differences					0.24	0.29
2265						
Maximum computed	793	766	1011	19	17.48	10.79
Minimum computed	831	540	810	81	17.10	10.32
differences					0.38	0.47
2550						
Maximum computed	46	494	1407	21	17.82	11.18
Minimum computed	594	604	724	92	17.43	10.59
differences					0.39	0.59
2664						
Maximum computed	52	1030	1051	19	18.02	11.48
Minimum computed	514	583	676	97	17.54	10.68
differences					0.48	0.80
3039						
Maximum computed	139	1199	1185	20	18.45	12.05
Minimum computed	666	405	728	114	17.79	10.85
differences					0.66	1.20

Table 4.8.4 Maximum and minimum values of the computed water levels at Venlo and Mook, caused by the synthetic flood waves with given parameter values at Borgharen, shown in Appendix 4.8.1 and 4.8.2, and related to the peak discharges

From Table 4.8.4 and Appendix 4.3.1 it turns out that:

(1) For $Q_{\text{peak}} \geq 2165 \text{ m}^3\text{s}^{-1}$ the maximum values of the water levels at Venlo and Mook are from floods at Borgharen that have flat crest curvatures, large volumes and medium to large base discharges.

(2) The corresponding minimum values of the water levels at Venlo and Mook are from floods at Borgharen that have peaked crests, medium volumes and mainly medium base discharges.

From Tables 4.8.1 and 4.8.2 we conclude, that for a constant peak discharge at Borgharen, the spreading in the local water levels increases in downstream direction. Moreover, the larger the discharge peak the larger the spreading.

4.9 Water levels at Venlo and Mook: the results of the present study compared with the Design Water Levels 2001

Fig.4.9.1 shows the best fitting probability functions according to the present study, taken from Fig.4.6.5, together with the Design¹⁵ Water Levels 2001 (open symbols) at Venlo. The DWL 2001 for river parts embanked by primary dikes have been published by the Dutch Government in ‘Design Hydraulic Conditions 2001’. The DWL 2001 for various p.o.e.’s are listed in Appendix 4.9.1. In close consultation with RIZA, they are determined via additional 2-D Waqua computations, made by Rijkswaterstaat Directorate Limburg. This is the so-called continuation of Waqua computations for the Dutch Meuse River upstream of Mook (also see Section 2.4).

Fig.4.9.1 shows that, for p.o.e. 0.004 per annum, the expected water level, according to the present study, is 0.3 m lower than the DWL 2001 (for data: compare Table 4.6.2 with Appendix 4.9.1). For shorter return periods the water level differences are larger, the maximum is 0.5 m for p.o.e. 0.02 and 0.05 per annum. The difference is due to the fact (1) that the DWL 2001 at Venlo have (by definition) the p.o.e.’s from those at Borgharen, whereas the present study presents the local p.o.e.’s at Venlo, and moreover (2) the ruling synthetic flood waves of the two methods are different, such as turns out from Figs. 6.3.1 and 6.3.2.

¹⁵ The *design* water level, according to the publication ‘Design Hydraulic Conditions 2001’ is defined in river areas which are embanked by dikes, in this case only relevant to the Meuse River part downstream of Mook at the right bank and to the river part downstream of Boxmeer at the left bank, in the strict sense. However, for the Dutch Meuse River upstream of these locations, other probabilities of exceedance are used for the design water levels (also see footnote 1 in Section 1.2).

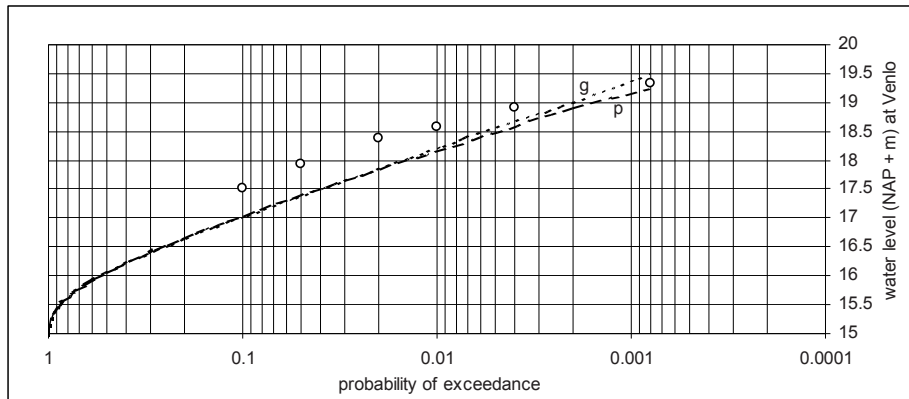


Fig.4.9.1 2-D Waqua computations for the DWL 2001 at Venlo (open circles), compared with the preferred probability distribution functions (p) and (g) of the expected water levels according to the present study

Fig.4.9.2 shows that the floods that have occurred at Borgharen in the period 1980-2000 have led to water levels below the DWL 2001 (thick line) at Venlo, except an insignificant deviation in 1995 with $Q_{\text{peak}} = 2664 \text{ m}^3\text{s}^{-1}$, because of an extreme flat crest curvature just as an extreme high base discharge. It turns out that for discharge peaks at Borgharen up to $3100 \text{ m}^3\text{s}^{-1}$ the DWL 2001 at Venlo (thick curve through open symbols) fall outside the 98% confidence band of the mean water levels in accordance with the present study.

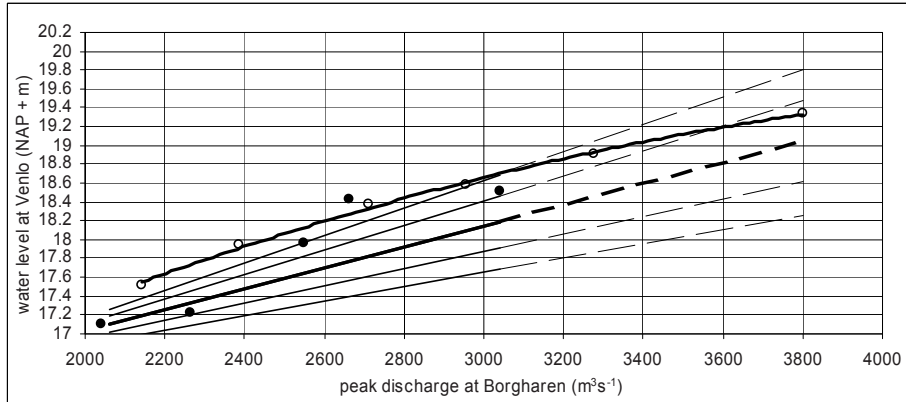


Fig.4.9.2 2-D Waqua computations for the DWL 2001 at Venlo (open circles), compared with the values (solid symbols) computed by Sobek for the floods that have occurred in the period 1980-2000; the regression curve of the DWL 2001 is shown (thick curve); underlying pattern taken from Fig.4.8.1

In Fig.4.9.3 the DWL 2001 at Mook is compared with the preferred probability functions of the present study, taken from Fig.4.6.10. For p.o.e. 0.0008 the DWL 2001 is 0.4 m higher than our present results (for data: compare Table 4.6.4 with Appendix 4.9.1). For p.o.e. 0.004 it is 0.6 m and for larger p.o.e. the difference even rises to 0.8 m. The reason is the same as that at Venlo.

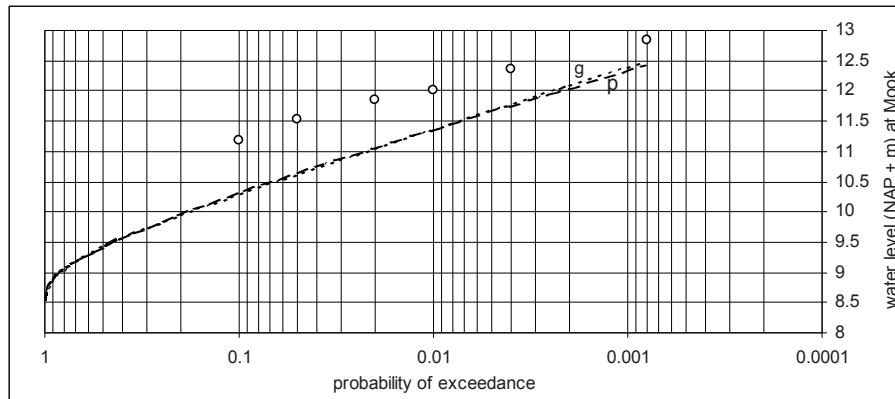


Fig.4.9.3 2-D Waqua computations for the DWL 2001 at Mook (open circles), compared with the preferred probability distribution functions (p) and (g) of the expected water levels according to the present study

Fig.4.9.4 shows that the floods that have occurred at Borgharen in the period 1980-2000 have given rise to water levels at Mook lower than or equal to the DWL 2001. It turns out that for discharge peaks at Borgharen up to $2700 \text{ m}^3\text{s}^{-1}$ the DWL 2001 at Mook (thick curve through open symbols) fall outside the 98% confidence band of the mean water levels in accordance with the present study.

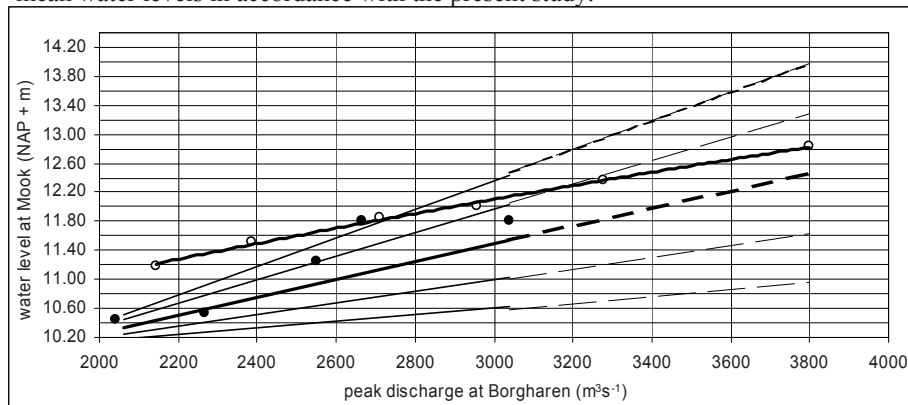


Fig.4.9.4 2-D Waqua computations for the DWL 2001 at Mook (open circles), compared with the values (solid symbols) computed for the floods that have occurred in the period 1980-2000; the regression curve of the DWL 2001 is shown (thick curve); underlying pattern taken from Fig.4.8.2

4.10 Generalization of the findings for the Dutch Meuse River to other rivers

The synthesization of flood waves at a measuring-station, given the data base of characteristic flood wave values at that station, leads via hydrodynamic model computations to water levels at un-gauged locations further downstream. Statistical data processing yields p.o.e.'s at those locations.

(1) The synthesization of a flood wave is performed as follows:

(i) Determine the average time lapse between the beginning of the flood waves and the peaks of the discharge hydrographs $Q'(t)$ at the measuring-station. We define that the peaks of all synthetic floods occur at the average time lapse after the beginning of the rising stage. Not exactly coinciding peaks with corresponding measured ones did not differ in peak-value, in our case.

(ii) The relationship between flood period (duration) and flood wave volume is needed to estimate the last day of the flood period (e.g. see Fig.4.3.3).

(iii) It turns out from the measurements that for the rising stage as well as for the falling stage of the discharge hydrograph $Q'(t)$ we can use polynomial functions power 2, in our case.

(iv) From the relative frequency distribution of X_4 we classify the flat, medium and peaked crest curvature (e.g. see Fig.4.3.1) and for these specifications we estimate the average ratio Q'_{-1} / Q'_{+1} around the crest of the flood (e.g. see Fig.4.3.2). The values of Q'_{-1} and Q'_{+1} are found by Eq.3.3.5, given X_4 and Q'_{peak} .

(v) The rising stage of the synthesized hydrograph $Q'(t)$ goes through the points $(0;0)$, $(3;Q'_{-1})$ and $(4;Q'_{\text{peak}})$ as our definition for the peak reads $t = 4$, and the falling stage through $(4;Q'_{\text{peak}})$, $(5;Q'_{+1})$ and $(n;0)$, where n is the last day of the flood period.

(vi) If more characteristic flood wave properties are important (e.g. X_3), they can be used for synthesizing a still more accurate hydrograph $Q'(t)$.

(vii) The synthesized flood wave $Q(t)$ can be derived from $Q'(t)$ by adding the given base discharge.

(viii) An elaborate example is given in Section 4.3

(2) Use a flow model starting at the measuring-station to compute the downstream water levels for each of these synthesized flood waves. It is recommended to compare a number of computed water levels of the synthesized flood waves with those of the measured ones, to assess whether the differences in peak water levels are acceptable (e.g. see Figs.4.3.4 through 4.3.8).

(3) The statistical data processing of downstream water levels should yield a stable relative frequency distribution if enough random samples are taken. A goodness of fit test can be used to determine the adapted preferred probability distribution function.

(4) Determine the variability of the computed water levels at a downstream location, for each value of the discharge peak at the measuring-station.

4.11 Discussion and conclusions

After determining the relevant characteristic parameters (peak discharge, base discharge, wave volume and wave crest curvature) and their values derived from the flood waves that have occurred at Borgharen in the period 1930-2000, it is shown that these parameters can be considered as mutually independent. The highest degree of

linear dependency, in this case between Q_{peak} and Q_{base} , indicates that only 20% of the variability around the mean of Q_{peak} can be explained by the linear regression between that parameter and the other (Q_{base}). For the used method of synthesizing flood waves by randomly sampling combinations of parameter values, mutual independency of the parameters is required.

One thousand floods have been synthesized according to the procedure of Sections 4.1 and 4.3. For the five measured large flood peaks at Borgharen ($Q_{\text{peak}} > 2000 \text{ m}^3\text{s}^{-1}$) of the last twenty years of the twentieth century, the results of the synthesization, in combination with water level computations with the 1-D Sobek flow model, have been compared with those of the actual floods. It turns out that the synthesized flood hydrographs at Borgharen yield fairly good estimates of the water levels at Venlo and Mook. Fixing the peaks at the average time lapse between start and top (in our case 4 days) creates discrepancies in the peak moment, but turns out to be irrelevant to the water levels downstream.

From the one thousand computed water levels at Venlo as well as at Mook it turned out that the frequency distributions of the water levels can safely be assumed stable. Subsequently, water levels statistics can be applied to determine the p.o.e.'s.

The Kolmogorov-Smirnov test for goodness of fit shows that the Pearson type III and the Gumbel probability distribution functions give the best approximation to the computed water levels at Venlo and Mook.

The influence of the aforementioned flood wave characteristics at Borgharen on the downstream water levels varies for each location and is larger at Mook than at Venlo. For more extreme floods at Borgharen this influence is larger than for less extreme ones.

If the floods with $Q_{\text{peak}} > 2000 \text{ m}^3\text{s}^{-1}$ at Borgharen that have occurred in the period 1980-2000 are compared with the results of all the synthetic ones, it turns out that especially the flood of January 1995 has caused much higher water levels at Venlo and Mook than expected on the basis of the peak discharge at Borgharen. This is attributed to the extremely high Q_{base} going together with a very flat crest curvature of that flood.

For reasons of different basic assumptions (ruling flood waves, local water levels statistics) the DWL 2001 at Venlo and Mook exceed the expected water levels following from the present study. The differences are substantial, up to 0.5 (0.3-0.5 m Venlo) and 0.8 m (0.6-0.8 m Mook), respectively, and the most for the lower floods.

The DWL 2001 at Venlo and Mook do not only exceed the expected water levels of the present study, but also those of the water levels of the floods that have occurred in the period 1980-2000, except the striking flood ($2664 \text{ m}^3\text{s}^{-1}$) of January 1995 and that is remarkable, although the difference is not significant.

Generalization to similar rivers:

We have learned that combinations of random sampled values of independent flood wave characteristics are a tool to synthesize floods. With a 1-D flow model, we can translate these into computed water levels downstream of the measuring-station.

The number of samples that have to be taken depends on the extent to which a stable probability density distribution of the computed water levels is obtained. A good adapted probability distribution function properly fitted to the computed water levels, checked for its goodness of fit by e.g. the Kolmogorov-Smirnov test, yields the relation between the water levels and their p.o.e.'s.

The range of variation of the computed peak water levels at the downstream locations, for a given peak discharge at the measuring-station, may be considerable because of the various possible compositions of the synthesized floods.

CHAPTER 5

FLOOD PREDICTION

5.1 Introduction

In operational flood management there is an urgent need for a facility that, in the case of an approaching flood, quickly yields a first estimate of the peak discharge at Borgharen. The corresponding water level is found by the current stage–discharge curve at Borgharen. The water levels along the Dutch Meuse River can be determined by estimating the discharge hydrograph at Borgharen and putting that into a flow model. A first-order check on the results is provided by the current ‘stage–relation curves’ (Rijkswaterstaat, 1998), which relate the water levels at Borgharen to those of the downstream water level measuring-stations. With the proceedings of the ‘Maaswerken’ this relationship will change.

As the Dutch Meuse River responds very quickly to the rainfall in the sub-catchments abroad, especially to the rainfall in the steep Ardennes basin, it is of essential importance to be able to take timely protective measures, especially in the most endangered part, namely the upper course of the Dutch Meuse River.

Because of this quick response to rainfall in the neighbouring countries, it is necessary to estimate the peak discharge at Borgharen on beforehand, largely on the basis of the expected rainfall in Northeast France and the Belgian Ardennes.

An algorithm will be developed, relating the measured river discharges at Borgharen to effective rainfall data in the upstream basin from the period 1980-2000. The reliability of the algorithm will be assessed.

In a later stage of a flood event more accurate estimates can be produced with an advanced forecasting model (Berger 1992), once more the cooperating Hydrological Services in North-East France and Walloon can give more insight into the actual development of the rainfall and the discharges of the upstream tributaries. This later stage is outside the scope of this study.

5.2 Development of an algorithm for provisional discharge-peak predictions at Borgharen

Because of the extensive Meuse River basin upstream of Borgharen ($2.1 \cdot 10^4 \text{ km}^2$), with its variety of soil properties, topographies and rainfall intensities, the direct relationship between effective rainfall and runoff is complicated and non-unique. The sub-catchments react differently, particularly in periods of flood. To estimate the average daily rainfall in the operational situation, the basin has been divided into the French part (48%), the Belgian Ardennes part (38%) and the Sambre part (14%) of the catchment area. As the floods are considered to occur in winter, evaporation is neglected. Also groundwater flow is neglected in the light of the flood events. The proportion of rainfall related to direct runoff will be determined on the basis of the river discharge measurements at Borgharen. In the literature various methods are used to relate rainfall to runoff (Shaw, 1994). In this investigation the ‘1-day Unit Hydrograph’ method will be considered.

5.3 The 1-day Unit Hydrograph method

For the period 1980-2000 the daily operational rainfall data available during flood events are known (Appendix 5.3.1).

From the daily measured river discharges ($Q(t)$) at 08:00 a.m. and the base discharge (Q_{base}) at Borgharen, the relative discharge hydrograph $Q'(t)$ is known (Fig.5.3.1a and Table 5.3.1). For this first flood in the period 1980-2000, the surface runoff (the direct runoff into the river) starts from the base discharge level of $980 \text{ m}^3\text{s}^{-1}$, i.e. the zero level in Fig.5.3.1a. The effective rainfall follows from the volume of the relative discharge hydrograph $Q'(t)$. In this case (Table 5.3.1): $7120 \times 864 \times 10^2 = 615 \times 10^6 \text{ m}^3$ effective rainfall during the flood period of 11 days. For the basin upstream of Borgharen of $21 \times 10^9 \text{ m}^2$, this is 29.29 mm. Consequently the 1-day Unit Hydrograph for each day is $Q'(t) / 29.29$, as shown in Fig.5.3.1b and Table 5.3.1.

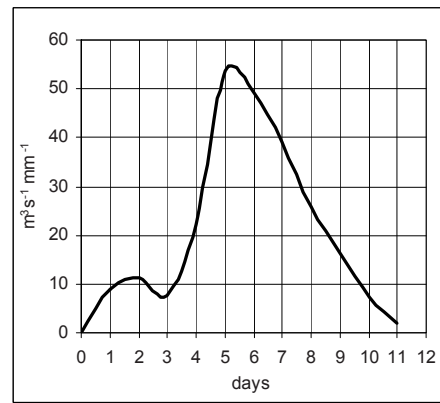
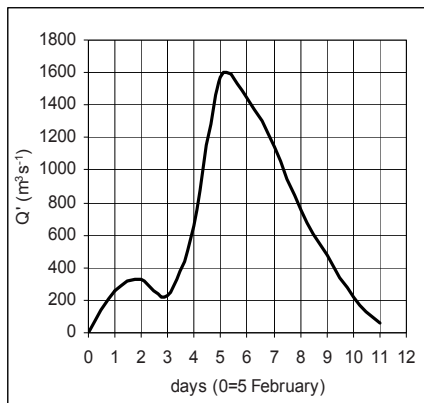


Fig.5.3.1a Measured $Q'_{\text{Borgharen}}$ (Febr.1984) Fig.5.3.1b 1-day Unit Hydrograph at Borgharen

day $t_{(0...11)}$	Q'_{measured} (river survey) m^3s^{-1}	1-day UH $\text{m}^3\text{s}^{-1}\text{mm}^{-1}$
0	0	0
1	258	8.81
2	327	11.16
3	225	7.68
4	654	22.33
5	1571	53.64
6	1436	49.03
7	1144	39.06
8	754	25.74
9	480	16.39
10	214	7.31
11	57	1.95
Sum	7120	243

Table 5.3.1 Daily measured Q' at Borgharen and derived 1-day Unit Hydrograph (Febr.1984)

For the eight highest flood events in the period considered, the eight 1-day Unit Hydrographs have been determined (Fig.5.3.2), to yield an average 1-day UH. This will be used as a tool to calculate the relative river discharge (Q'_{calc}) at Borgharen in connection with the effective rainfall.

The average 1-day UH has been determined (1) by the arithmetic means of the individual peaks Q' and times (t) to the peaks. Further (2) by the points

$U_t = \Sigma Q'_t / 8$ where $t = 0 \dots 15$ and (3) a smoothed line through the points of (1) and (2) so that the result is adapted to the volume of the individual shapes, which has to be $243 \times 86400 = 21 \cdot 10^6 \text{ m}^3$ per mm effective rainfall in the catchment upstream of Borgharen. This average 1-day Unit Hydrograph is indicated by U .

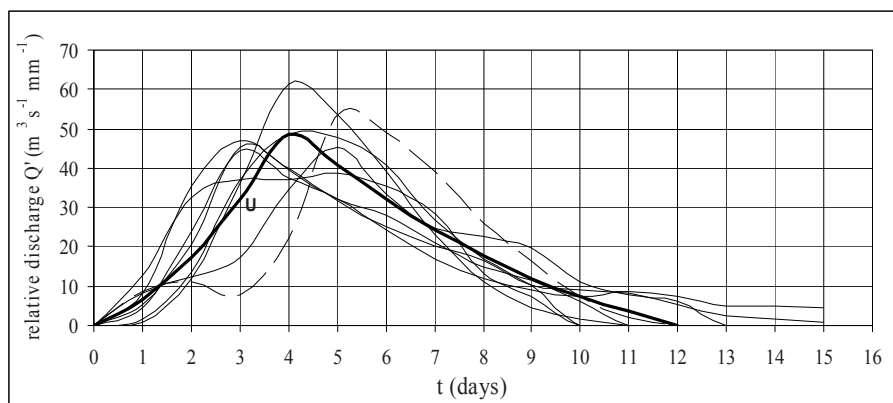


Fig.5.3.2 Average 1-day Unit Hydrograph (thick line) from eight 1-day Unit Hydrographs of the highest flood events in the period 1980-2000 at Borgharen, of which the dashed line is the February 1984 storm from Table 5.3.1.

Each effective daily rainfall R_i produces a component part of the surface runoff Q'_{calc} at a later time jT , viz. $R_i \times U_{j-i}$.

Q'_{calc} therefore follows from summation of all the components for all the effective daily rainfall:

$$Q'_j = \sum R_i U_{j-i} \quad \dots(5.3.1)$$

$$j = 1, 2, 3, \dots, n \text{ and } i = 0, 1, 2, \dots, m-1$$

in which U is the ordinate value of the average 1-day UH

The calculations for the surface runoff are:

$$Q'_1 = R_0 U_1$$

$$Q'_2 = R_1 U_1 + R_0 U_2$$

$$Q'_3 = R_2 U_1 + R_1 U_2 + R_0 U_3$$

$$Q'_m = R_{m-1} U_1 + R_{m-2} U_2 + \dots R_0 U_m$$

$$Q'_{m+n-1} = R_{m-1} U_n$$

By using the average 1-day Unit Hydrograph (Fig.5.3.3a) we can calculate from day to day the relative discharge and peak ($Q'_{\text{cal. peak}}$) from the effective rainfall. The peak (Q) can be compared with the measured one at Borgharen.

As an illustration, the result of the first flood event (Febr.1984) at Borgharen is shown in Fig.5.3.3b. Appendix 5.3.2 gives the calculation.

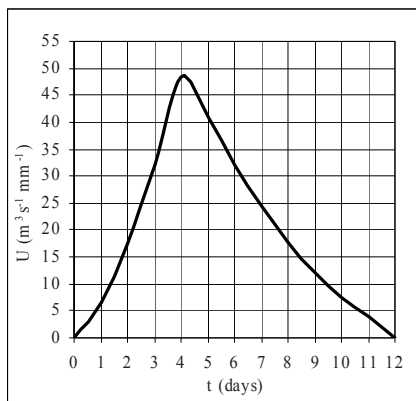


Fig.5.3.3a Average 1-day Unit Hydrograph

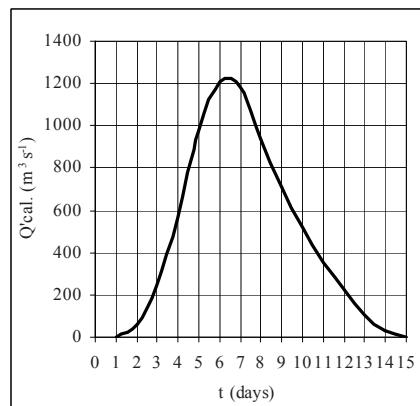


Fig.5.3.3b Calculated Q' (Febr. 1984), based on equation 5.3.1, average 1-day Unit Hydrograph (U) and effective rainfall (R)

The results of the calculations are shown in Table 5.3.2

date	rain days	operational rainfall	effective rainfall	Q' peak calculated Eq.5.3.1	Q' peak from river survey	Q _{base}
		mm	mm	m ³ s ⁻¹	m ³ s ⁻¹	m ³ s ⁻¹
Feb. 1984	3	41.6	29.3	1212	1571	979
Nov.1984	4	57.2	31.8	1365	1426	199
April 1986	3	34.5	17.3	814	1060	604
Jan. 1987	4	38.3	22.5	915	992	563
Jan. 1991	3	50	17.8	796	867	976
Jan. 1993	2	63	44.3	2061	1972	293
Dec. 1993	3	61	42.7	1893	2009	1030
Jan. 1995	3	66.1	27.4	1111	1073	1591

Table 5.3.2 Q' peak calculated from the average 1-day UH (Fig.5.3.3a) and the effective rainfall, compared with Q' peak at Borgharen from river survey

Taking into account that $Q_{\text{peak}} = Q'_{\text{peak}} + Q_{\text{base}}$, the predicted Q_{peak} for the above mentioned set of floods is calculated in Table 5.3.3. The peak discharges at Borgharen by river survey and those from the calculations, correspond with the water level differences (via Appendix 4.4.3) such as summarized in Table 5.3.3.

date	Q _{peak} measured (river survey at Borgharen)	Q _{peak} calculated Eq.5.3.1 + Q _{base}	water level diff. at Borgharen
	m ³ s ⁻¹	m ³ s ⁻¹	m
Feb. 1984	2550	2191	-0.34
Nov.1984	1625	1564	-0.12
April 1986	1664	1418	-0.51
Jan. 1987	1555	1478	-0.16
Jan. 1991	1842	1772	-0.14
Jan. 1993	2267	2354	+0.08
Dec. 1993	3039	2923	-0.08
Jan. 1995	2664	2702	+0.03

Table5.3.3 Measured and calculated Q_{peak} at Borgharen and their difference expressed in water level terms

5.4 The forecasting-algorithm for future use

The effective rainfall has been found via its relation with the operational rainfall. For the mentioned eight floods in the period 1980-2000 this relation is shown in Fig.5.4.1, also see Table 5.3.2 for the individual events.

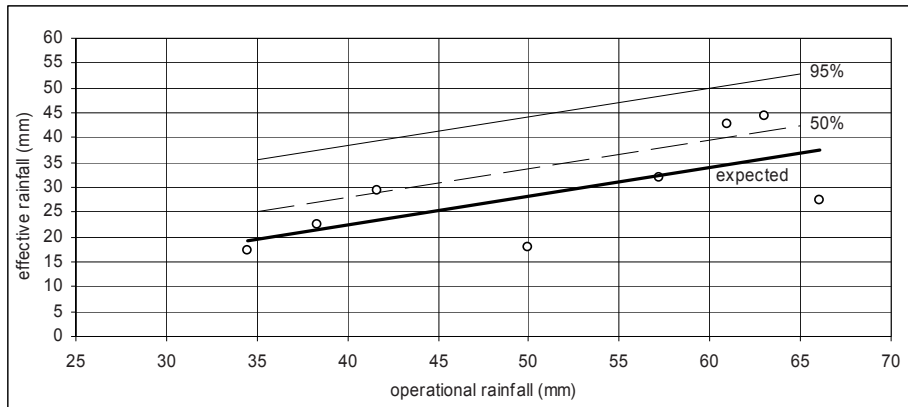


Fig.5.4.1 Relation between the operational rainfall on the catchment upstream of Borgharen and the effective rainfall from surveyed flood wave volume (open symbols); expectation (thick line) and upper limit of the 95% and 50% of its confidence band

47% of the variability (spread) around the mean effective rainfall is explained by the linear regression between effective rainfall and operational rainfall, a poor result but significantly. To distinguish the effective rainfall of each of the eight individual floods from that of the regression curve, we call the latter the *adjusted* effective rainfall. This quantity is found by the equation:

$$R_E = 0.58 R_O - 0.66 \quad \dots(5.4.1)$$

for which R_E is the adjusted effective rainfall (mm) and R_O the operational rainfall (mm).

From the average 1-day Unit Hydrograph and the adjusted effective rainfall derived from Eq.5.4.1 we find the expected Q_{peak} . An example is shown in Appendix 5.5.1. The corresponding water levels and their deviation from the measured data are given in Table 5.4.1. Step 1 in Section 5.5 goes into this table in more detail.

date	Q_{peak} , measured river survey at Borgharen $\text{m}^3 \text{s}^{-1}$	measured water level at Borgharen NAP + m	operat. rainfall mm	adjusted effective rainfall mm	Q_{peak} calc. predict. at Borgh. $\text{m}^3 \text{s}^{-1}$	predict. water level at Borgh. NAP + m	water level diff. at Borgh. m
Feb. 1984	2550	45.56	41.6	23.5	1956	44.97	-0.59
Nov. 1984	1625	44.27	57.2	32.5	1591	44.20	-0.07
April 1986	1664	44.34	34.5	19.4	1512	44.04	-0.30
Jan. 1987	1555	44.13	38.3	21.6	1424	43.85	-0.28
Jan. 1991	1842	44.69	50.0	28.3	2208	45.24	+0.55
Jan. 1993	2267	45.30	63.0	35.9	1978	45.00	-0.30
Dec. 1993	3039	45.94	61.0	34.7	2599	45.60	-0.34
Jan. 1995	2664	45.65	66.1	37.7	3119	46.00	+0.35

Table 5.4.1 Prediction of Q_{peak} and corresponding water levels calculated from adjusted effective rainfall (Eq. 5.4.1) and average 1-day Unit Hydrograph; water level differences from measurements

Analogously to Table 5.4.1, in Table 5.4.2 is shown the predicted Q_{peak} and corresponding water level, if we use the upper limit of the 95% confidence band of the adjusted effective rainfall (Fig. 5.4.1):

$$R_E^* = 0.58R_O + 15.10 \quad \dots(5.4.2)$$

where R_E^* the effective rainfall (mm) and R_O the operational rainfall (mm)

date	Q _{peak} , measured river survey at Borgharen m ³ s ⁻¹ (1)	measured water level at Borgharen NAP + m (2)	operat. rainfall mm (3)	effective rainfall upper limit 95%conf. band mm (4)	Q _{95%} upper limit m ³ s ⁻¹ (5)	water level 95% upper limit NAP+m (6)	water level difference m (7)
Feb. 1984	2550	45.56	41.6	39.2	2608	45.61	0.05
Nov. 1984	1625	44.27	57.2	48.3	2268	45.30	1.03
April 1986	1664	44.34	34.5	35.1	2247	45.28	0.94
Jan. 1987	1555	44.13	38.3	37.3	2050	45.08	0.95
Jan. 1991	1842	44.69	50.0	44.1	2896	45.84	1.15
Jan. 1993	2267	45.30	63.0	51.6	2715	45.69	0.39
Dec. 1993	3039	45.94	61.0	50.5	3313	46.14	0.20
Jan. 1995	2664	45.65	66.1	53.4	3755	46.42	0.77

Table 5.4.2 Prediction of Q_{peak} and corresponding water levels calculated from the 95% upper limit of the adjusted effective rainfall (Eq.5.4.2) and average 1-day Unit Hydrograph; water level differences from measurements

The water levels corresponding with the upper limit of the 95% confidence band of the adjusted effective rainfall (column 6) are compared with the measured ones (column 2) and the differences are given in column 7. Step 2 in Section 5.5 goes into Table 5.4.2 in more detail.

Table 5.4.3 shows the predicted Q_{peak} and corresponding water level, if we use the upper limit of the 50% confidence band of the adjusted effective rainfall (Fig.5.4.1):

$$R_{E^{**}} = 0.58R_O + 4.70 \quad \dots(5.4.3)$$

where R_{E^{**}} the effective rainfall (mm) and R_O the operational rainfall (mm)

date	Q_{peak} , measured river survey at Borgharen m^3s^{-1} (1)	measured water level at Borgharen NAP + m (2)	operat. rainfall mm (3)	effective rainfall upper limit 50%conf. band mm (4)	$Q_{50\%}$ upper limit m^3s^{-1} (5)	water level 50% upper limit NAP+m (6)	water level difference m (7)
Feb. 1984	2550	45.56	41.6	28.8	2176	45.21	-0.35
Nov. 1984	1625	44.27	57.2	37.9	1822	44.65	0.38
April 1986	1664	44.34	34.5	24.7	1760	44.53	0.19
Jan. 1987	1555	44.13	38.3	26.9	1635	44.29	0.16
Jan. 1991	1842	44.69	50.0	33.7	2443	45.46	0.77
Jan. 1993	2267	45.30	63.0	41.2	2227	45.26	-0.04
Dec. 1993	3039	45.94	61.0	40.1	2843	45.80	-0.14
Jan. 1995	2664	45.65	66.1	43.0	3334	46.15	0.50

Table 5.4.3 Prediction of Q_{peak} and corresponding water levels calculated from the 50% upper limit of the adjusted effective rainfall (Eq.5.4.3) and average 1-day Unit Hydrograph; water level differences from measurements

The water levels corresponding with the upper limit of the 50% confidence band of the adjusted effective rainfall (column 6) are compared with the measured ones (column 2) and the differences are given in column 7. Step 3 in Section 5.5 goes into Table 5.4.3 in more detail.

5.5 Application of the forecasting–algorithm

To predict the expected peak discharge at Borgharen, we have to take into account that many relevant facts become available rather late. Therefore this algorithm has to be considered as a first aid. The following data are required:

(1) The operational rainfall and rainfall forecast.

As the aim is to predict the peak-stage at Borgharen with a lead time of two days at least, the weather forecast at least two days ahead is needed.

(2) The base discharge Q_{base} .

Estimates from the daily measured discharges at Borgharen in a quasi stationary runoff situation, shortly before and close to the flood period.

(3) The expectation of the wind-force and wind direction.

The wind direction is important, as Meuse River floods at Borgharen tend to arise from south westerly to southerly winds only, moving the depression more or less in longitudinal direction over the river basin. In the case of a strong wind, the water level will be over-predicted, as in reality the depression will blow over the river basin without having the chance to release all of its water.

(4) The snow depths.

In the case of snowmelt, the snow depth is translated into rainfall depths by experience: 10% of the snow depth for newly fallen snow and 15% for compact snow is considered to be the equivalent rainfall depth. Then the local air temperature is important, as well as the variability of the snow depth over the hilly basin.

As an illustration, the flood of February 1984 is considered. For this flood we know from survey that the measured peak discharge at Borgharen equals $2550 \text{ m}^3\text{s}^{-1}$ and the corresponding water level is NAP + 45.56 m (Table 5.4.1). The daily operational rainfall of the Meuse River basin upstream of Borgharen is shown in Table 5.5.1. The adjusted effective rainfall calculated from Eq. 5.4.1 amounts 23.5 mm. The daily operational rainfall is reduced by a constant to get this adjusted effective rainfall.

day	operational rainfall (mm)	adjusted effective rainfall (mm)
0	0	0
1	13.8	7.76
2	15.4	9.36
3	12.4	6.36
4	0	0
Sum	41.6	23.5

Table 5.5.1 Calculated adjusted effective rainfall for the flood event of February 1984

Step 1

We predict the peak discharge at Borgharen by means of the average 1-day Unit Hydrograph (Fig.5.3.3a) and the adjusted effective rainfall 23.5 mm (Eq.5.4.1). Also see Eq.5.3.1.

According to Appendix 5.5.1, the predicted (expected) peak discharge at Borgharen is $976 \text{ m}^3\text{s}^{-1}$ (relative peak discharge Q') plus $980 \text{ m}^3\text{s}^{-1}$ (base discharge), so $1956 \text{ m}^3\text{s}^{-1}$ and the corresponding water level, according to the current stage-discharge curve, is NAP + 44.97 m (see Table 5.4.1 for judging). The measured water level is 0.59 m higher.

Step 2

If we take, by definition, the upper limit of the 95% confidence band in Fig.5.4.1 as 'maximum' for the predicted water level, then the maximum water level for 41.6 mm operational rainfall (i.e. 39.2 mm effective rainfall according to Eq.5.4.2), is estimated at NAP + 45.61 m, analogously to step 1. The measured water level is 0.05 m lower.

Also see Table 5.4.2 column 3, 4, 6, 2 and 7, for judging. Initially, one will prefer this definition, for safety.

Step 3

We use Eq.5.4.3 to translate the operational rainfall into effective rainfall for the upper limit of the 50% confidence band in Fig.5.4.1 and find 28.8 mm. It turns out that the measured water level is 0.35 m higher, analogously to step 1. Also see Table 5.4.3 column 3, 4, 6, 2 and 7, for judging.

For verifying this ‘forecasting-algorithm for future use’, the prediction will be made for the flood peaks of the latest serious flood events of 2002 and 2003, so beyond the period of study.

From both floods the operational rainfall, Q_{peak} and Q_{base} are known. There has been neither snow nor particularly strong south westerly wind-force.

In this case, each six hours the operational rainfall depths are provided by KNMI, via RIZA, (1) from seven measuring stations in the French sub-basin, (2) from five stations in the Ardennes sub-basin and (3) from three stations in the Sambre sub-basin.

For each day the rainfall sum of the six hourly observations at each measuring station is determined as a proxy of the daily rainfall per sub-basin (France, Ardennes, Sambre). The total rainfall upstream of Borgharen is determined, using the assigned weights (section 5.2) for the sub-basins.

Flood event of February 2002¹⁶ :

Date	operational rainfall (mm)
09-02-2002	4.5
10-02-2002	9.1
11-02-2002	2.3
12-02-2002	7.9
13-02-2002	19.8
14-02-2002	7.8
15-02-2002	0.0
Sum	51.4

Table 5.5.2 Measured operational rainfall (mm) for calculations of the water levels, according to Eqs. 5.4.1 and 5.4.2, for the flood event of February 2002

Given:

The measured base discharge is $850 \text{ m}^3\text{s}^{-1}$ and the measured Q_{peak} equals $2441 \text{ m}^3\text{s}^{-1}$, corresponding with NAP + 45.46 m.

It is a complex flood, existing of four peaks of 2020, 2441, 1792 and 2113 within one month.

Later, from Section 5.7 it will be clear that using Eq.5.4.3, to find the peak discharge that results from the 50% upper limit of the confidence band of the expected effective rainfall, is not advisable for floods over $2000 \text{ m}^3\text{s}^{-1}$.

¹⁶ Groenenberg, M. (2002) *Flood report 2002*. Rijkswaterstaat, Directorate Limburg, ANWR, Maastricht, NL.

Solution:

For the rainfall sum, or operational rainfall, of 51.4 mm (Table 5.5.2) during the flood period 09/02-14/02, the expected peak discharge for 29.1 mm adjusted effective rainfall (Eq.5.4.1) and using the average UH, equals $2031 \text{ m}^3\text{s}^{-1}$ corresponding with NAP + 45.06 m (Appendix 5.5.2). The maximum predicted peak discharge, according to Eq.5.4.2 (44.9 mm effective rainfall) and using the average UH, equals $2548 \text{ m}^3\text{s}^{-1}$ corresponding with NAP + 45.55 m (Appendix 5.5.2).

Resuming:

The expected water level NAP + 45.06 m is 0.40 m lower than the measured NAP + 45.46 m, and the 95% upper limit NAP + 45.55 m is 0.09 m higher.

Flood event of January 2003¹⁷ :

date	operational rainfall (mm)
28-12-2002	3.1
29-12-2002	15.9
30-12-2002	12.1
31-12-2002	4.0
01-01-2003	14.4
02-01-2003	28.1
03-01-2003	7.1
04-01-2003	7.9
Sum	57.5

Table 5.5.3 Measured operational rainfall (mm) for calculations of the water levels, according to Eqs. 5.4.1 and 5.4.2, for the flood event of January 2003

Given:

The measured base discharge is $880 \text{ m}^3\text{s}^{-1}$, because of the river situation before 01-01-2003, and Q_{peak} equals $2661 \text{ m}^3\text{s}^{-1}$, corresponding with NAP + 45.65 m.

Solution:

For the rainfall sum of 57.5 mm (Table 5.5.3) during the flood period 01/01/-04/01, the expected peak discharge according to Eq.5.4.1 (effective rainfall 32.7 mm) and using the average UH, equals $2337 \text{ m}^3\text{s}^{-1}$ corresponding with NAP + 45.36 m water level (Appendix 5.5.3). The maximum predicted peak discharge according to Eq.5.4.2 (effective rainfall 48.5 mm) and using the average UH, equals $2886 \text{ m}^3\text{s}^{-1}$ corresponding with NAP + 45.83 m water level (Appendix 5.5.3).

Resuming:

The expected water level NAP + 45.36 m is 0.29 m lower than the measured NAP + 45.65 m, and the upper limit NAP + 45.83 m is 0.18 m higher.

¹⁷ Rijkswaterstaat (2003). *Daily discharges at Borgharen village, method v.10*. Directorate Limburg, ANWR, Maastricht, NL.

Conclusion:

Verifying the predicted water levels by the two available floods, it turns out that the measured water levels lie between the expected and maximum predicted values and as such they are satisfactory, however the margins between expected and maximum are 0.47 to 0.49 m for both floods. The measured values are rather close to their maximum – derived from the 95% upper limit of the confidence band of the expected effective rainfall–, viz. 0.09 and 0.18 m lower, so the use of the 95% level is preferred for the prediction of water levels at Borgharen in the case of floods over $2000 \text{ m}^3\text{s}^{-1}$.

Operational versus validated rainfall data

The Meteorological Services operate with different meteorological observation networks, namely for synoptic and for climatic purposes.

The synoptic measuring-network, subject of this study, is especially used for a short clear view of the weather situation over large areas.

The climatic measuring-network is in service to build up reliable long-term data series. Several checks are applied to the observations and missing values are filled up by neighbouring stations.

The validated data have been derived from this climatic measuring-network by the Meteorological Services of France (North-East), Belgium (Walloon) and the Netherlands, after deciding in consultation. These data are not available in the short term, so they are not suitable for predictions.

It is shown that the totals of the *validated* data differ substantially from those of the used *operational* rainfall (Fig.5.5.1). If they would have been used for the prediction of peak water levels, these would not have been better than those derived from the operational rainfall.

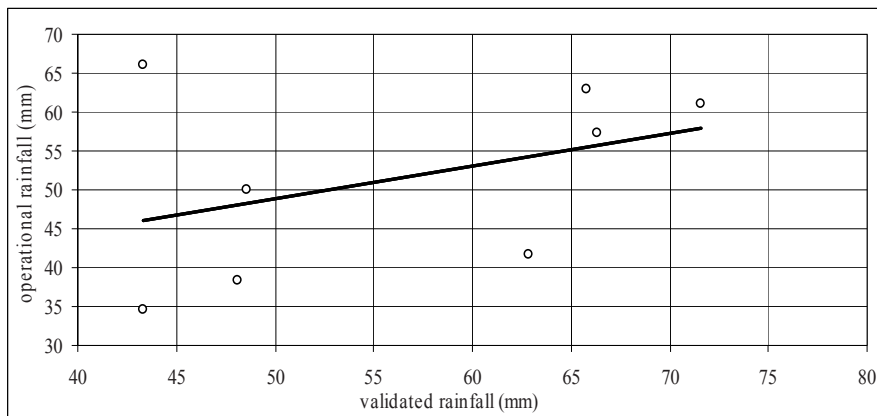


Fig.5.5.1 Total operational and validated rainfall of the Meuse River basin upstream of Borgharen during each of the floods in the period 1980-2000

5.6 Generalization to other rivers

To develop a simple model for peak water level predictions, preferably some days ahead, at a certain point along the river, we need operational rainfall data in the river catchment upstream of that point. Determining the effective rainfall from operational rainfall depths requires appropriate records of former flood events.

The effective rainfall (mm) follows from the volume (m^3) of the measured Q' -hydrograph (e.g. Fig.5.3.1a) divided by the catchment area (m^2) upstream of the measuring-point.

For a number of measured former floods the Time Unit Hydrographs (e.g. Fig.5.3.1b) can be determined and from these the average TUH (e.g. Fig.5.3.2).

The effective rainfall during the flood period depends on the operational rainfall, but their relation may be rather scattered. For optimal use of the forecasting algorithm it is necessary to adjust the effective rainfall on the basis of a stable regression function between these parameters.

The prediction of Q' can be calculated from the average TUH and the adjusted effective rainfall at each T , using Eq.5.3.1. The predicted Q_{peak} is found from

$$Q_{peak} = Q'_{peak} + Q_{base}$$

for which Q_{base} is the discharge just before the beginning of the water level rise.

Then, from the current 'discharge – water level' relationship at the measuring point, the predicted water level is known and has to be checked with the measured value from river survey, as (predicted) rainfall, effective rainfall, catchment management and the use of an average TUH make the results uncertain. Also, attention has to be paid to the extent to which the rainfall runoffs of the various sub-catchments may be added, depending on the movement of the rain depression. A downstream tributary may flow out earlier than an upstream tributary. Also the accuracy of the catchment area is a point of attention.

All these conditions may necessitate the introduction of a margin to the initial predictions. In our case study the upper limits of the 95% and 50% confidence band of the expected effective rainfall were applied (Fig.5.4.1).

Careful maintenance of a forecasting-model is necessary but difficult, as on the one hand it is necessary to choose an observation period for which the 'discharge–stage' curve at the measuring point is fairly stable and long enough to have sufficient flood and rainfall data, and on the other, one has a reasonable chance that the 'discharge–stage' curve at that point has changed meanwhile, by autonomous development or artificial interventions in the river.

To improve the predictions for rivers rapidly responding to rainfall, it is advisable to pay much attention to the reliability of the weather forecast with respect to the actual rainfall depths.

A timely first-order prediction algorithm of the water level peaks at a measuring-point along the river, some days ahead, can be developed if reliable river survey data and rainfall depths from former flood periods are available for testing and verification.

In the event of non-gauged rivers, a crude estimation with wide margins of error is given by Shaw (2002):

$$Q_{peak} (m^3s^{-1}) = 0.278 C i A \quad \dots(5.6.1)$$

where

- C runoff coefficients which vary from 0.05 for flat sandy areas to 0.95 for impervious surfaces
 i intensity of rainfall in mm h^{-1}
 A catchment area in km^2

5.7 Discussion and conclusions

Outsiders sometimes suggest that, since we live in the computer era, we should be able to deliver better flood-peak water level predictions. However, rainfall predictions have a certain confidence band and so do even the best models we have. Hence one may not expect exact river discharge or water level predictions. Nevertheless, a timely first-order prediction of the water level peaks at Borgharen, some days ahead, turns out to be feasible with the aid of the average 1-day Unit Hydrograph and the adjusted effective rainfall, derived from the floods of the period 1980-2000 (Appendix 5.7.1). However, it appears that:

- (1) the expected water levels can deviate from the measured ones to 0.6 m (flood numbers 1 and 5 of Appendix 5.7.1),
- (2) most of the measured water levels are lower than the results obtained by using the 50% upper limit of the confidence band of the expected effective rainfall,
- (3) the most safe estimate is obtained by using the 95% upper limit,
- (4) in the latter case much predictions are overestimated strongly, generally the lower discharge peaks, that means for $Q_{\text{peak}} < 2000 \text{ m}^3\text{s}^{-1}$, corresponding to water levels at Borgharen lower than NAP + 45 m. In those cases the 50% upper limit yields a better approximation to the measured water levels.

The measured water levels of the higher floods of February 2002 and January 2003, used for verification, are 0.09 m and 0.18 m below the results obtained by using the upper limit of the 95% confidence band of the expected effective rainfall, respectively, but 0.40 m and 0.29 m above the expected water level, respectively.

In this study the operational rainfall data from Flood Reports (Rijkswaterstaat, RIZA and Directorate Limburg) are based on rainfall in the three parts of the Meuse river basin upstream of Borgharen, namely in the northeast French part, in the Ardennes part and in the Sambre part.¹⁸ The daily rainfall is averaged over the total catchment upstream of Borgharen by assigning weights, proportional to the size of the relevant sub-catchments. Daily renewal of the prediction on the basis of the renewed predicted rainfall throughout the flood period is highly recommendable.

In view of all sorts of uncertainties in rainfall depths and weather forecasts, one may wonder whether a sophisticated model is able to yield better predictions with a lead time of some days, at all.

Generalization to similar rivers:

In general terms, the procedure to predict water levels from rainfall is like that of our case study.

¹⁸ The operational rainfall depths are from the rain gauges of the measuring-stations at Nancy, St.Dizier, Reims, Charleroi, Florennes, Luxembourg, St.Hubert, Spa, and occasionally also data gained from isohyets.

Because of autonomous development or artificial interventions, the forecasting model needs regular updating. It is advisable to pay much attention to the stability of the relationship between the operational rainfall during a flood period and the effective rainfall. It is also advisable to investigate the influence of the variability of the TUH on the predictions as well as the reliability of the rainfall forecast.

If the prediction of the peak discharge (Q_{peak}) at a river measuring-station has been performed, it is possible to predict the water levels for other local un-gauged river-points (1) by estimating the flood wave shape at the runoff measuring-station and (2) by using that flood wave in a flow model that translates flood waves into downstream river water levels.

CHAPTER 6

DISCUSSION WITH REGARD TO THE RESEARCH QUESTIONS

6.1 Summary of the research questions

The following main questions were addressed in this dissertation:

- Do the results of the first part of the study give cause for changing the design discharges? In other words, does the probability of exceedance of the peak discharges at Borgharen change in such a way, that the corresponding water levels differ significantly?
- Are the water levels downstream of Borgharen, e.g. at Venlo and Mook, resulting from the present study significantly different from those according to the Design Water Levels 2001?
- To what extent can the discharge peaks and corresponding water levels at Borgharen and the uncertainties therein be estimated with an easy-to-use early warning algorithm? How do the results comply with recent measured flood peaks?
- What can we learn from the Dutch Meuse River case for other rivers of a similar type?

6.2 Change of the design discharges at Borgharen

If the level of significance for the discharge and corresponding water level difference between the DWL 2001 and the present study is reasonable taken on 0.1 m, then for the probability of exceedance less than 0.006 per annum the water level differences turn out to be significant. They vary from 0.14 to 0.26 m for p.o.e. 0.004 to 0.0008, respectively. This can be explained from the following 4 points:

(i) In the present study a much higher discharge threshold has been considered because of the river dynamics in the river reach upstream of Borgharen. The DWL 2001 principle starts from a lower discharge threshold. Consequently, the DWL 2001 exhibits a strong influence of minor floods on the major ones in the 'probability of exceedance – discharge' relation, resulting into a wide 95% confidence interval and a considerable uncertainty in the discharge prediction, varying from 15% to 20% in relation to the average.

(ii) In the present study, four extreme floods from former centuries are added to the subset above the high discharge threshold. They fit in well with more recent peak discharges.

(iii) For equal p.o.e., the difference between the discharges and corresponding water levels of either method is caused by the introduction of a separation-point between set-up and free-flow river situations abroad. This yields a significantly narrower confidence interval and a greater accuracy than in the DWL 2001

(iv) Discharge observations of several hundred years are needed to accurately estimate river design levels for which the risk of flooding does not exceed a few percents in a

human lifetime. Therefore, the present observations consisting of a limited series of systematically recorded annual peak discharges from recent data are extended with some documented serious floods from former centuries on which the 'E formulae for exceedance' have been applied.

6.3 Significant local water level differences between the results of the present study and the DWL 2001

6.3.1 Approach underlying the DWL 2001

In 2001, the design discharge (p.o.e. 0.0008 per annum) of the Dutch Meuse River at Borgharen has been determined at $3800 \text{ m}^3\text{s}^{-1}$. The ruling synthetic flood wave shapes for the different p.o.e.'s at Borgharen (Fig.6.3.1) are obtained by an investigation of Vrisou van Eck & Klopstra (1998). The authors used two approaches to determine the design flood properties.

Starting points of their first approach ('regression method') are the duration of the rise of the flood wave, the total duration and the flood wave volume measured from a number of different discharge levels of 22 selected flood hydrographs in the period 1911-1997. The relationship between the discharge levels and durations and flood wave volume has been determined by linear regression.

In their second approach ('enlargement method') the measured floods are enlarged from the actual discharge to the design discharge¹⁹. Subsequently, the treatment is the same as for the 'regression method'. The results of either method were similar up to a discharge of $2000 \text{ m}^3\text{s}^{-1}$. In the higher discharge range the methods could not be compared, as the 'regression method' could not be applied by lack of sufficient data from such extreme floods.

In conclusion, the 'enlargement method' was chosen, as this poses no problem to estimate flood waves above the discharge level of $2000 \text{ m}^3\text{s}^{-1}$.

In Fig.6.3.1 these DWL 2001 discharge flood waves with p.o.e. 0.0008, 0.004, 0.02 and 0.1 are shown. They are the basic assumption of the computations for the 'Maaswerken'. We remark that the crest curvature of the discharge flood wave is the same for all return periods. The wave volumes are between 700 and $1100 \cdot 10^6 \text{ m}^3$, the crest curvatures are $43 \cdot 10^{-12} \text{ s}^{-2}$ and the base discharges are between 850 and $1700 \text{ m}^3\text{s}^{-1}$.

The design water levels further downstream have been determined for these flood waves with the 2-D Waqua flow model (Appendix 4.9.1).

¹⁹ for the enlargement, the ratio between the design discharge and the measured peak discharge of the flood wave was used as multiplication factor.

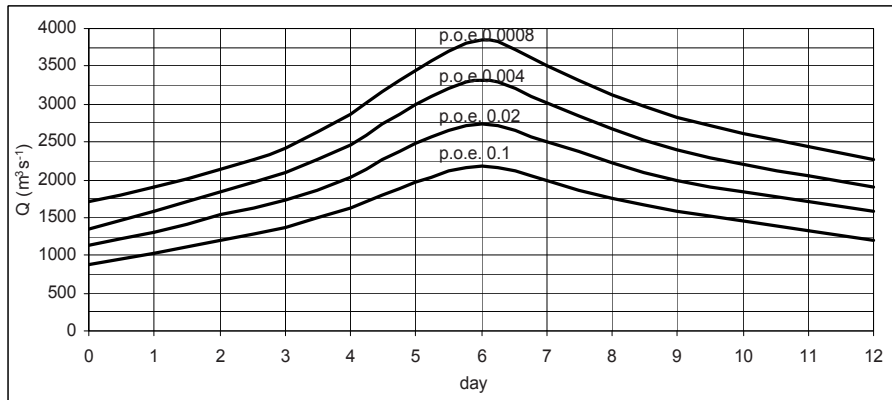


Fig.6.3.1 Synthesized flood waves at Borgharen underlying the DWL 2001

6.3.2 Approach to the present study

In the present study, one thousand flood waves at Borgharen were synthesized on the basis of combinations of a number of characteristic flood wave parameters, which are to a large extent mutually independent. These parameter ranges were derived from measured discharge hydrographs. For the design discharge flood waves with p.o.e. 0.0008, 0.004 and 0.02 per annum, according to the present study 3370, 3089 and 2808 m^3s^{-1} at Borgharen, respectively, we used the mean flood wave characteristics of the series synthetic floods with measured peaks 3039 and 2664 m^3s^{-1} (Appendix 4.8.1) adapted by a multiplication factor depending on the ratio between the design discharge and the measured peak discharge (Fig.6.3.2). With the flow model Sobek (Section 4.4) the water levels further downstream were computed for the relevant flood waves of Fig.6.3.2 (results in Table 6.3.1).

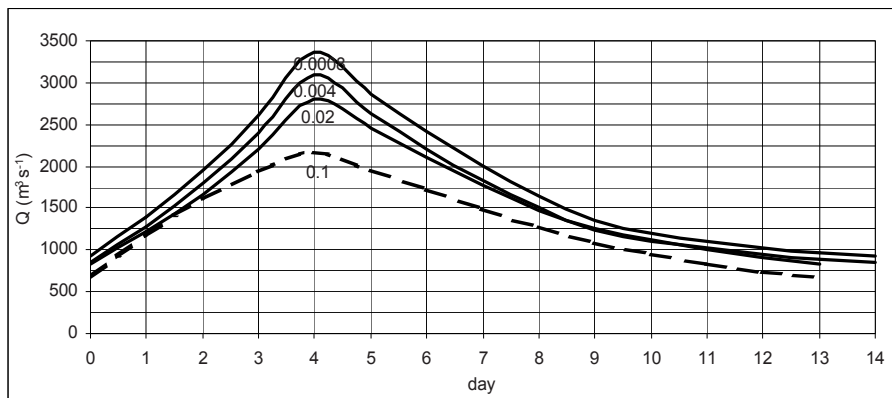


Fig. 6.3.2 Synthesized flood waves at Borgharen according to the present study

6.3.3 Consideration

(i) In the DWL 2001, the difference between measured and design discharges is such (e.g. measured discharge 3000 m^3s^{-1} , design discharge 3800 m^3s^{-1}) that amplification of the mean highest flood hydrograph measured is a too uncertain procedure to determine the design discharge. In the present study the amplification is less uncertain (measured discharge 3000 m^3s^{-1} , design discharge 3370 m^3s^{-1}).

(ii) As a consequence of the amplification procedure all crest curvatures of the design flood waves are equal, viz. $43 \cdot 10^{-12} \text{ s}^{-2}$. This means a rather flat crest curvature. In the present study, the crest curvatures vary from 40 to $70 \cdot 10^{-12} \text{ s}^{-2}$, i.e. from rather flat via medium to almost peaked.

(iii) For the major floods (peaks $> 1850 \text{ m}^3 \text{ s}^{-1}$) in the period 1980-2000, the measured rise of the flood waves from the base discharge to the peak takes four days, on average (Appendix 4.3.2). According to the DWL 2001 flood wave hydrograph it is six days, derived from floods in the period 1911-1997.

(iv) If we compare the ranges of values of wave volume ($\text{m}^3 \cdot 10^6$), crest curvature (10^{-12} s^{-2}) and base discharge ($\text{m}^3 \text{ s}^{-1}$) according to the present study and the DWL 2001, we obtain the following summary:

	measured medium Appendix 4.3.1	present study Fig.6.3.2	DWL 2001 Fig.6.3.1
volume	600 – 850	760 – 1025	700 – 1100
crest curvature	50 – 80	40 – 70	43
base discharge	600 – 900	675 – 930	850 – 1700

This shows that, apart from the peak discharges, the differences between the present study and the DWL 2001 concern mainly the crest curvature and the base discharge, and that the values of the present study agree better with the measured values than those for the DWL 2001. As a consequence, the results of the two approaches to the downstream water levels must be different.

Different water motion models have been used, indeed, viz. 2-D Waqua for DWL 2001 and 1-D Sobek for the present study, but the latter has been checked against Waqua (Section 4.4).

(v) The present study yields significantly different water levels at Venlo and Mook (Table 6.3.1) for the flood series of Figs. 6.3.1 and 6.3.2.

p.o.e. yr ⁻¹	Venlo			Mook		
	DWL 2001 flood wave NAP+ m	present study flood wave NAP+ m	difference m	DWL 2001 flood wave NAP+ m	present study flood wave NAP+ m	difference m
0.02	18.37	18.22	0.15	11.86	11.49	0.37
0.004	18.91	18.45	0.46	12.36	11.71	0.65
0.0008	-	-	-	12.83	11.98	0.85

Table 6.3.1 Results of the downstream water levels caused by different approaches, viz. the flood waves at Borgharen according to DWL2001 and those according to the present study

6.4 The reliability of water level predictions with an easy-to-use warning algorithm

Starting from discharge hydrographs at Borgharen and operational rainfall depths on the river basin from previous floods, we determined (1) the effective rainfall of each single flood and furthermore (2) the average 1-day Unit Hydrograph of all floods considered at Borgharen. These two components, as well as the base discharge, enable peak discharge and corresponding water level prediction, but it turned out that they often disagreed with the measured peaks. Therefore, we investigated the relationship between operational and effective rainfall and observed a rather scattered but significant coherence. Their confidence bands allow only first-order estimates of water levels.

For the future, we take this relationship (Fig.5.4.1) as basis and, given the operational rainfall, we translate the effective rainfall into expected discharges and corresponding water levels with the help of the 1-day UH and base discharge. From the upper limits of the 50% and 95% confidence band of the mentioned relationship we also calculate the water level predictions.

Although the expected water levels agree with the surveyed values, on average, it turned out that in individual cases they may differ to 0.6 m from the measured ones. The margin from the expected water levels to their maximum possibility -by definition 95% upper limit of the confidence band of the relationship in Fig.5.4.1- is large for lower measured floods ($<2000 \text{ m}^3\text{s}^{-1}$) and small for higher measured floods, hence for the first category the 50% upper limit is introduced as a fair maximum measure (Appendix 5.7.1).

Recently serious flood peaks beyond the period of study have occurred (1) in February 2002 with a peak water level at Borgharen of NAP + 45.46 m and corresponding discharge of $2441 \text{ m}^3\text{s}^{-1}$, and (2) in January 2003 with a peak water level of NAP + 45.65 m and corresponding discharge of $2661 \text{ m}^3\text{s}^{-1}$. They provide for an independent test opportunity.

For the first flood, the expected water level was 0.40 m lower than the actually measured value of NAP + 45.46 m and the measured value was 0.09 m lower than that predicted by means of the 95% upper limit of the effective rainfall.

For the second flood, the expected water level was 0.29 m lower than the actually measured value of NAP + 45.65 m and the measured value was 0.18 m lower than that predicted by means of the 95% upper limit of the effective rainfall. This verification is in fair accordance with the conclusions of the investigated series of the period 1980-2000.

6.5 Learning from the Dutch Meuse River case for other rivers of this type

6.5.1 The probability analysis of floods at a measuring-station

Generally speaking, too few annual peak discharges are available to reliably predict the properties of very rare floods .

To improve the reliability of the prediction (1) we used some extreme floods from former centuries and used the E-formulae, derived by Hirsch and Stedinger (1987) and (2) we distinguished between different types of river behaviour, in this case the transition from set-up to free flow. These two additions to the recorded series of annual peak discharges may introduce uncertainty, via the historic water level

estimates and corresponding discharges, and via the transition point in the river behaviour. The accuracy of the former discharge peaks has been investigated by the Royal Dutch Meteorological Institute (1994) and by Lorenz (1997). By trial and error, the inaccuracy in the choice of the discharge threshold between the set-up and free flow regime was minimized.

Adding some historic very high flood peaks to the recorded series of annual peak discharges and introducing the discharge threshold have enabled us to produce reasonable estimates of the probability of occurrence of discharge peaks with long return periods.

6.5.2 Downstream water levels versus characteristic flood wave properties

By random sampling the characteristic flood wave parameter values which determine the downstream water levels, a set of combinations is taken to synthesize a number of flood waves. The water level at any downstream location is computed with a flow model. The number of combinations is chosen such that a stable probability distribution of the computed set of local water levels is obtained.

In view of the reliability of protective measures it is important to determine the margin into the computed local water levels, for given discharges at an upstream measuring-station, in this way.

The values of the adapted fourth moment (Eq.3.3.5) of the relative discharge hydrograph are divided into three categories, each with an average value, viz. flat, medium and peaked crest curvature. This division may be too crude and a further investigation into the relation between crest curvature and Q'_{-1} / Q'_{+1} would be useful.

6.5.3 Flood prediction

To develop a simple first-order model for the prediction of peak discharge levels we need (1) operational rainfall depths in the river catchments during preceding flood events and (2) the corresponding discharge measurements. From these we derive the effective rainfall and the average Time Unit Hydrograph. From the latter we know the discharge caused by one mm rainfall on the catchment per unit time.

We found a scattered but significantly linear relationship between operational rainfall during flood events and corresponding effective rainfall. After comparing, we concluded that the expectations often deviate from the measured water levels, whence the upper limits of the 95% and 50% confidence band of the effective rainfall could be used best to indicate the maximum possibly water level of the large floods and the smaller floods, respectively. First aid prediction of water levels requires rainfall forecast, which may have consequences for the reliability of the prediction.

In un-gauged rivers and without rain-gauging stations a crude prediction can be made, using Eq.5.6.1

In rivers in which drastic (artificial) interventions are under discussion, it may take many decades after the completion of the works before a reasonably stable relation between discharge and water level is realized again. This depends on the morphological response and the time needed to reach a new equilibrium state, hence on the sediment-transporting capacity of the river and the available bed load. As long as this state has not been reached, only rainfall data are available to produce predictions about the peak discharge of an imminent flood. To estimate the needed base discharge may be a problem, but possibly this could be derived from a river-point out of the influence of the river interventions. Predicting the peak water levels, however, will be a problem for influenced locations.

CHAPTER 7

CONCLUSIONS

- When comparing the results of the present study with the DWL 2001, there is a significant difference in the probabilities of exceedance of discharges and corresponding water levels at the measuring-point Borgharen.

The difference is due to the fact that in the present study a discharge threshold to distinguish between the set-up and free flow river situation upstream of the measuring-station at Borgharen was introduced, and historical extreme floods were added.

- Also the water level statistics downstream of Borgharen differ significantly. These differences are (1) the result of the differences in the assumed ruling flood wave shapes for the same p.o.e. at Borgharen and (2) the use of local water levels statistics (present study) instead of assuming so far the local water levels to have the same p.o.e. as those at Borgharen (DWL 2001).

- If we distinguish between large and smaller floods, a first-order prediction of maximum possible peak water levels at Borgharen some days ahead is possible by means of an easy-to-use algorithm. A reliable weather forecast is a necessary condition.

We verified the developed forecasting-algorithm against two recently large floods (about $2550 \text{ m}^3\text{s}^{-1}$) and found differences from the measured peak water levels well within a narrow range of 0.2 m below the predicted maximum. Both floods are in fair accordance with the results of the investigated series of floods in the period 1980-2000.

- Generalizing which we have learned from the Dutch Meuse River case for other similar rivers, we conclude that:

(i) The confidence band of the estimated frequency of occurrence of floods can be narrowed by (1) adding some extreme historic floods to the recorded series of annual peak discharges, and (2) by considering one or more points of distinction between different types of river behaviour (from set-up to free flow, flooding of a levee, etc.).

(ii) Flood wave shape characteristics that may be important to flood stages along the river are in principle all moments 0 through 4 of the time-discharge hydrograph. These moments need to be mutually independent. These characteristics enable synthesizing flood waves that can be translated with a flow model into local water level distributions along the river. Statistical analysis leads to frequency distributions of these water levels.

(iii) Flood wave attenuation, this depends on the value of the fourth moment of the 'time – discharge hydrograph', is generally negligible in rivers with a steep bottom slope (0.5 m km^{-1} or more). The ratio between the depth at bank-full discharge and the total water depth during a flood has a moderate influence, whereas the total storage

width has a strong influence on flood wave attenuation in rivers with small hydraulic gradients.

(iv) A provisional flood peak prediction some days ahead requires the effective rainfall and the time unit hydrograph (TUH). For that an algorithm could be developed derived from (1) operational rainfall depths and (2) corresponding measured flood wave discharges from a preceding period of sufficient length and river stability.

CHAPTER 8

RECOMMENDATIONS

As the phenomenon of flood wave attenuation is, besides the crest curvature, also related to the difference in steepness between the rising and falling stage of the discharge hydrograph of the flood wave, it is conceivable that for certain rivers this phenomenon, expressed by the skewness (third moment) of the discharge hydrograph, plays a role in the determination of the local water levels. Further investigation is advisable. For the Dutch Meuse River this phenomenon turned out to be of minor importance.

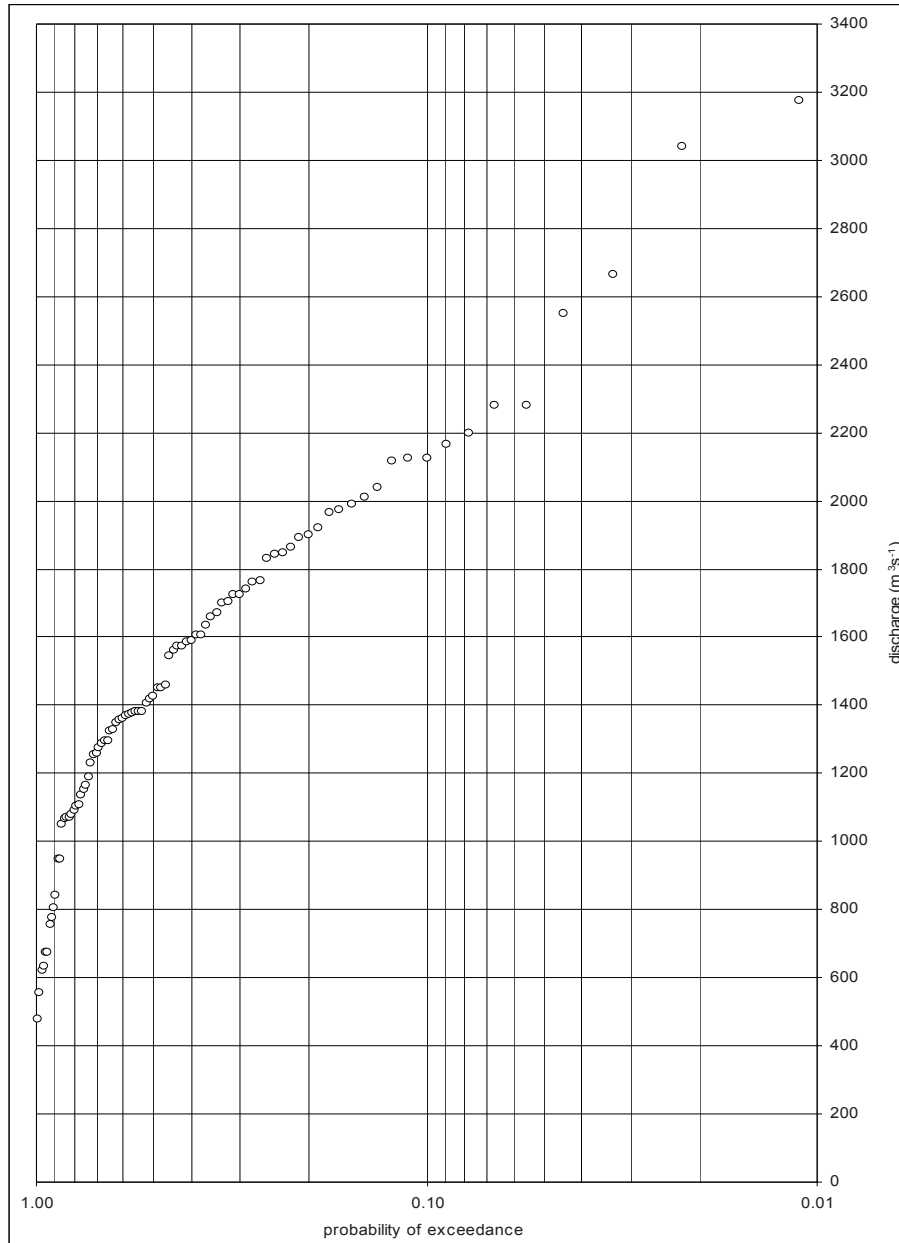
In rivers with a large storage width and a small hydraulic gradient, flood wave attenuation is a function of the crest curvature. A more detailed gradation than the categories flat, medium and peaked floods may describe the effects on the local water levels more accurately. Investigation into this gradation will give a definite answer.

It is recommended to show that the provisional water level predictions with an easy-to-use algorithm may be improved by (1) considering the soundness of the relation between weather forecast and realistic rainfall in the river catchments and (2) reinforcing the stability of the relationship between operational rainfall and effective rainfall. For instance, it is possible that the stability increases by omitting one or more rain-gauging stations in France. Furthermore, one should investigate whether the 'average' Time Unit Hydrograph, derived from a number of occurred floods, is the best representation to use for the algorithm.

In the present study attention has been given to the water level distribution of two arbitrary locations, to get an impression of the differences between the water levels according to the DWL 2001 and those according to the present study. It is advised to work out the probabilities of exceedance of the water levels for more locations along the river to obtain water level lines of equal p.o.e. In the author's view, such an approach is more realistic than linking the local water levels to the p.o.e. of the discharges at an upstream measuring-station (Borgharen). This especially concerns rivers in which flood waves undergo large shape alterations while propagating through the river.

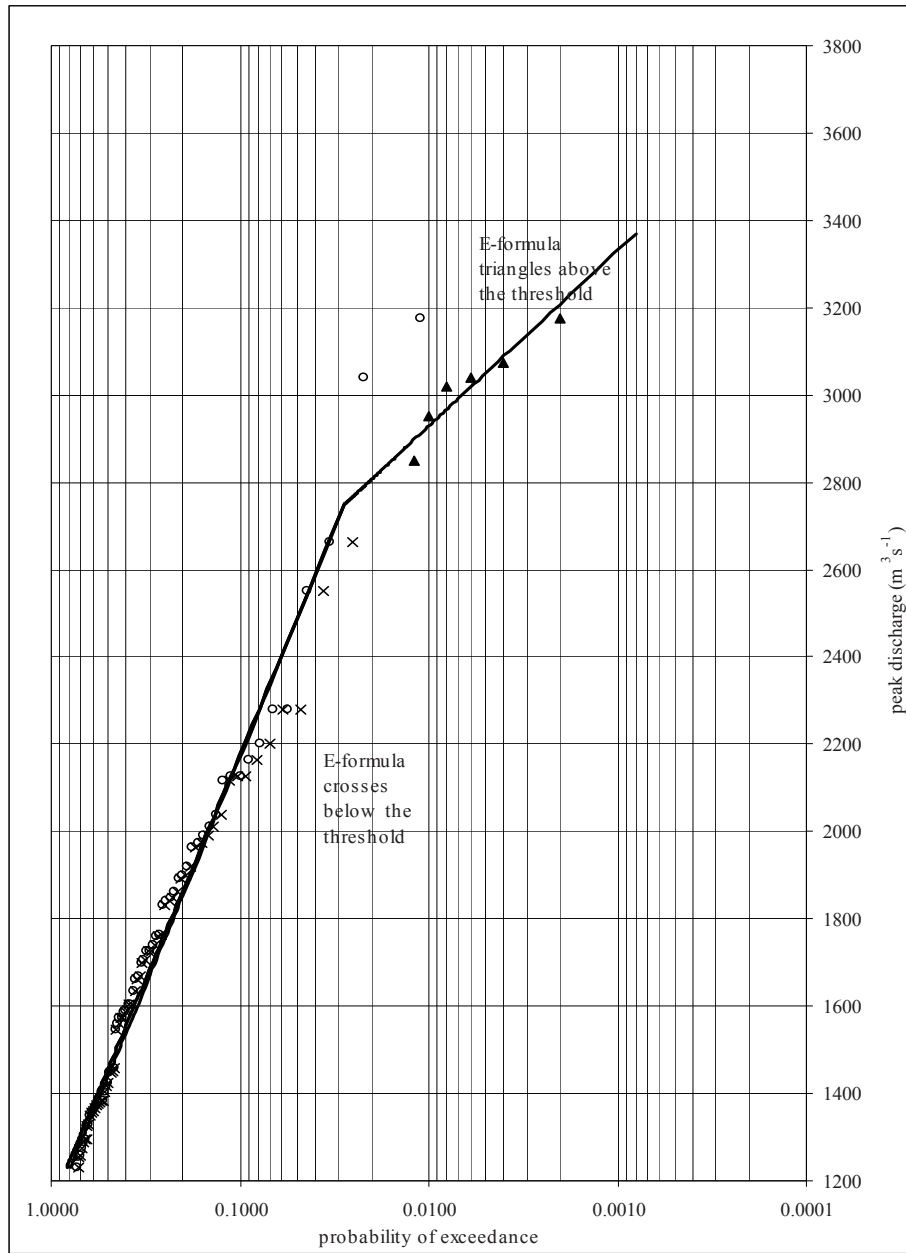
For the Rhine River the statistical characteristics of flood waves may be a valuable input into models which describe the influence of soaking of dikes.

APPENDICES

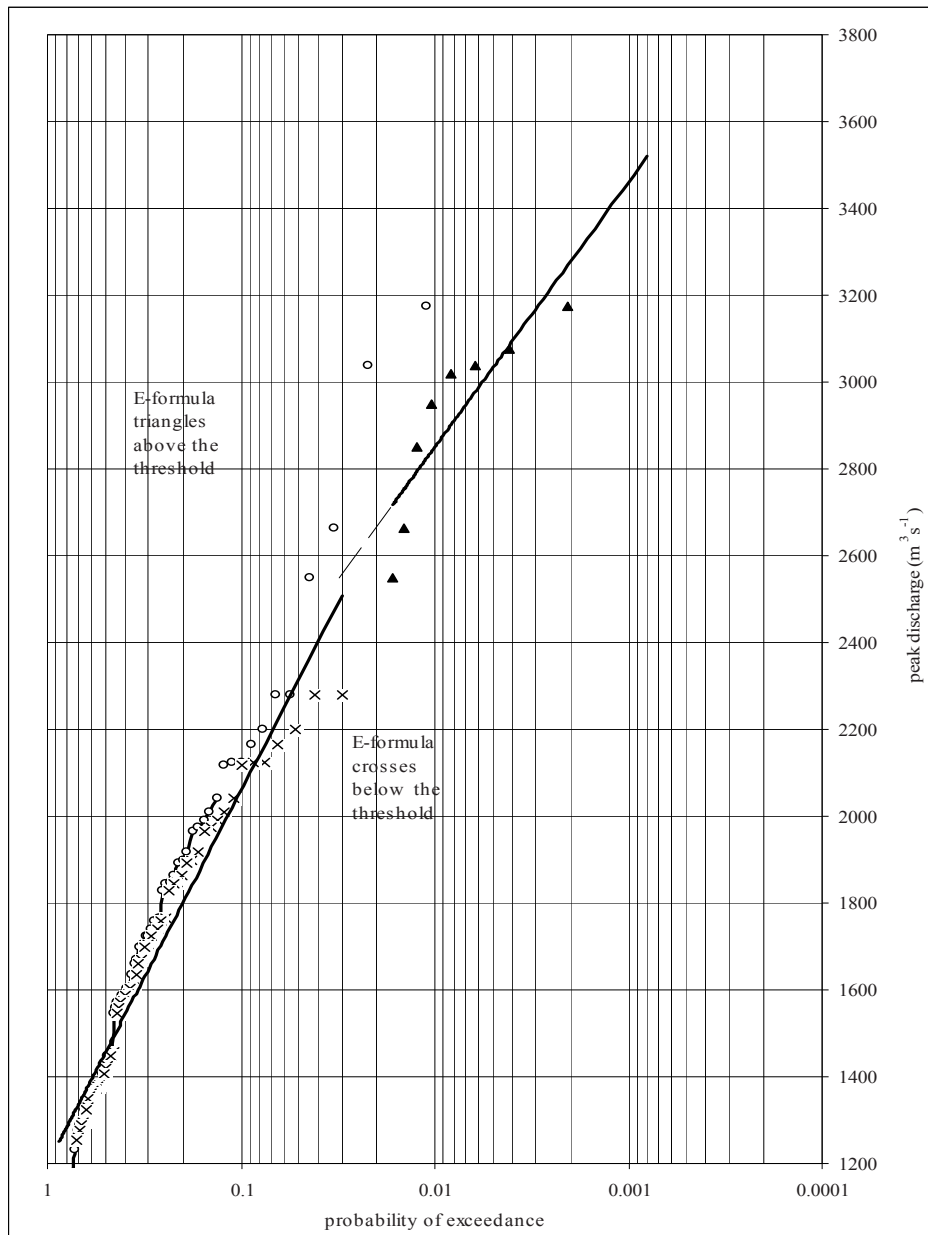


**Probability of exceedance of the annual peak discharges at Borgharen
1911-2000, according to Weibull**

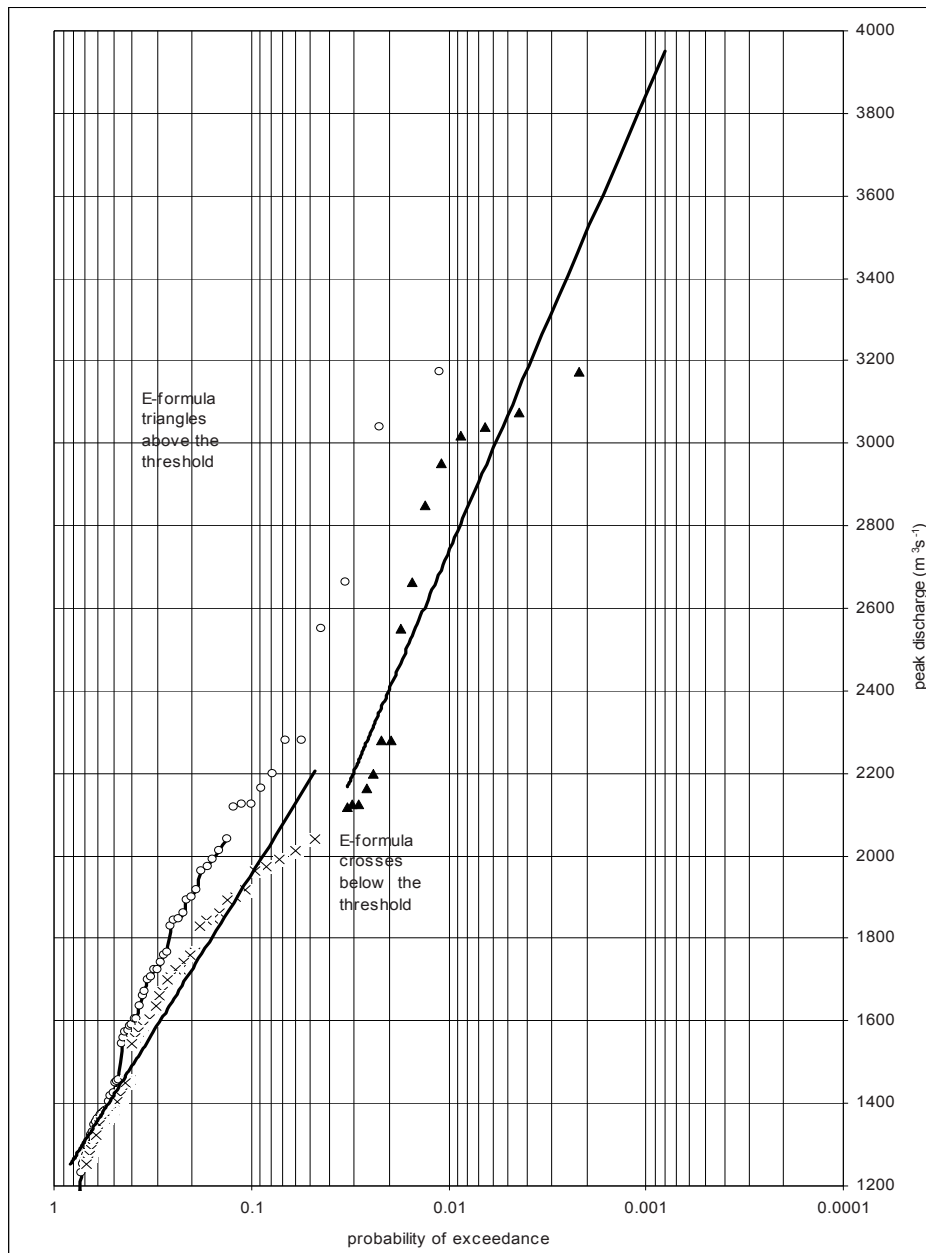
Appendix 2.1.1



Probability of exceedance of the peak discharge at Borgharen, regression lines in accordance with the E formulae (1571-2000) above and below the threshold discharge at 2750 m³s⁻¹ ; open symbols of the measured annual peaks 1911-2000
Appendix 2.1.2

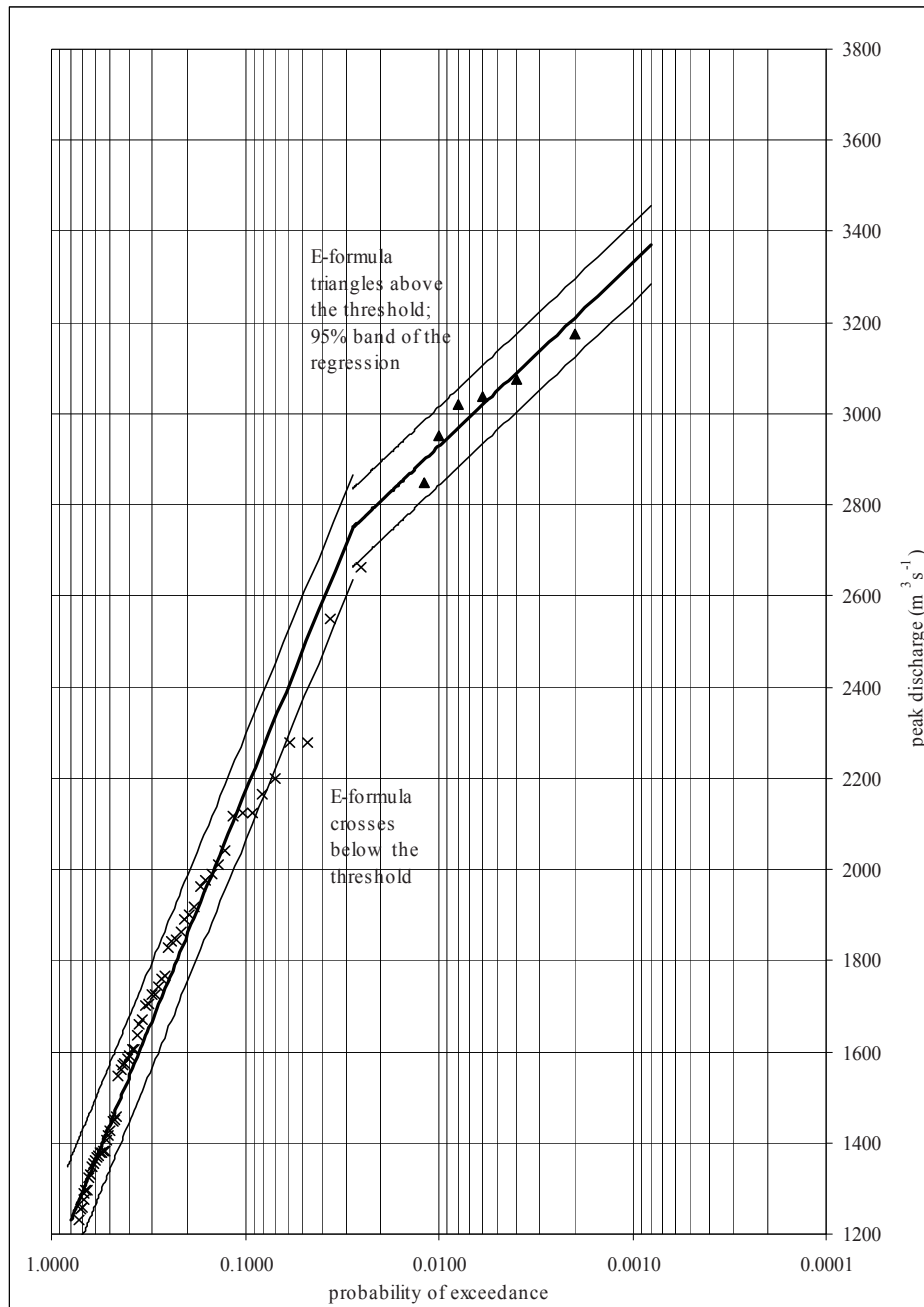


Probability of exceedance of the peak discharge at Borgharen, regression lines in accordance with the E formulae (1571-2000) above and below the threshold discharge at 2550 m³ s⁻¹; open symbols of the measured annual peaks 1911-2000



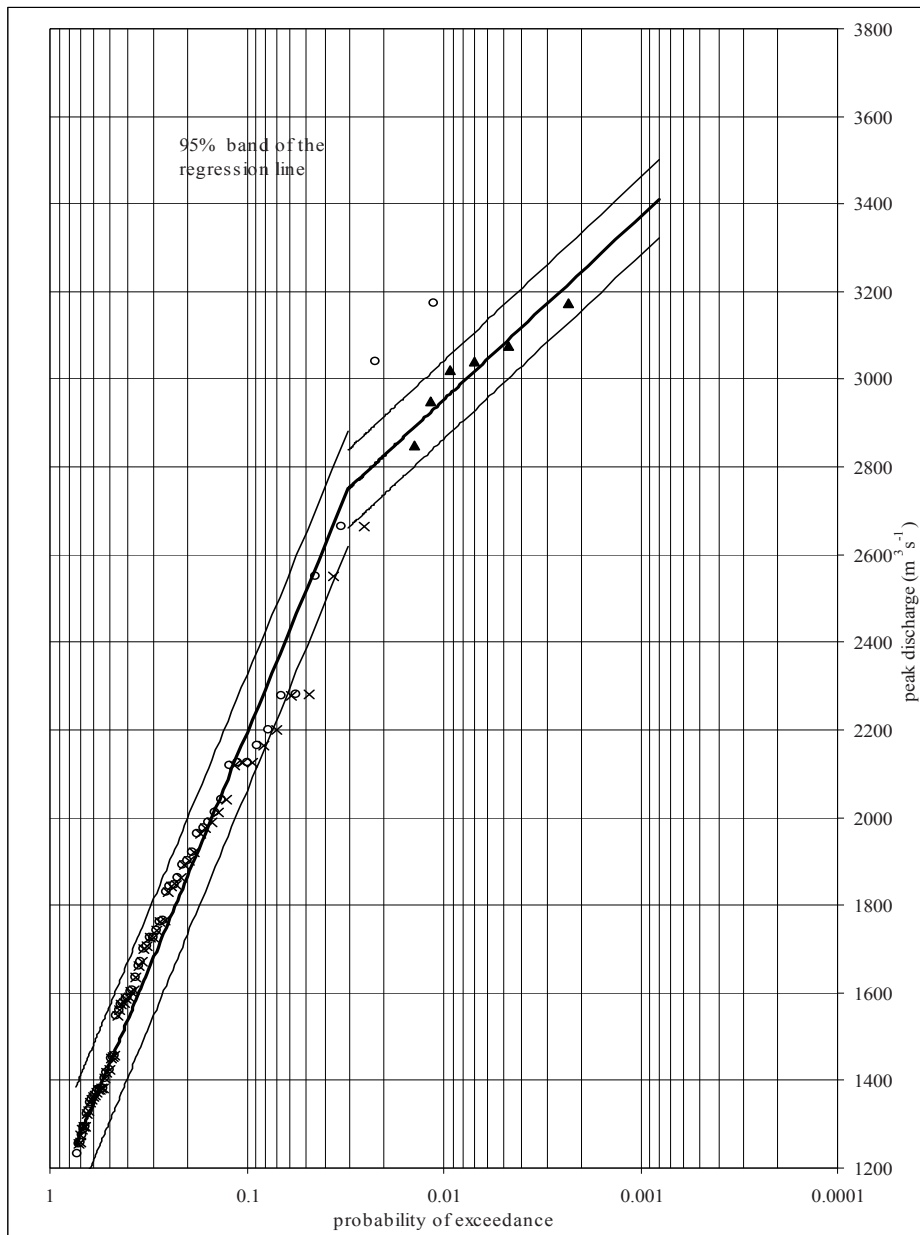
Probability of exceedance of the peak discharge at Borgharen, regression lines in accordance with the E formula (1571-2000) above and below the threshold discharge at 2100 m³s⁻¹ ; open symbols of the measured annual peaks 1911-2000

Appendix 2.1.4



Probability of exceedance of the peak discharge at Borgharen, regression lines in accordance with the E formulae (1571-2000) above and below the threshold discharge at 2750 m³ s⁻¹; 95% confidence band of the regression lines

Appendix 2.1.5



Probability of exceedance of the peak discharge at Borgharen, regression lines in accordance with the Dalrymple method (1571-2000) above and below the threshold discharge of 2750 m³s⁻¹; open symbols of the measured annual peaks 1911-2000; 95% confidence band of the regression lines

Appendix 2.1.6

Flow year	measured daily top	flow year	measured daily top
1911	1377	1961	1705
1912	1295	1962	1077
1913	1741	1963	1670
1914	1405	1964	1373
1915	1990	1965	1892
1916	1725	1966	1964
1917	1847	1967	1586
1918	1295	1968	777
1919	2279 * adjusted	1969	2165
1920	673	1970	950
1921	843	1971	477
1922	1383	1972	1071
1923	1135	1973	1071
1924	2040	1974	1259
1925	3175 * adjusted	1975	635
1926	1604	1976	1231
1927	1355	1977	1102
1928	1361	1978	1367
1929	1107	1979	2200
1930	1725	1980	1349
1931	1289	1981	1418
1932	1383	1982	1165
1933	557	1983	2550
1934	1065	1984	1635
1935	1190	1985	1760
1936	1457	1986	1575
1937	1590	1987	1919
1938	1546	1988	1275
1939	2125	1989	1449
1940	1425	1990	1843
1941	1151	1991	1660
1942	1330	1992	2280
1943	950	1993	3039
1944	2011	1994	2664
1945	1765	1995	754
1946	1560	1996	1093
1947	1605	1997	1051
1948	622	1998	1863
1949	1324	1999	2118
1950	1572		
1951	1700		
1952	1900		
1953	673		
1954	1380		
1955	1830		
1956	1452		
1957	1975		
1958	1254		
1959	804		
1960	2125		

Annual peak discharges at Borgharen (m³s⁻¹)
Appendix 2.1.7

flow year	measured daily top	flow year	measured daily top	flow year	measured daily top
1643	*3075	1941	1151	1975	635
1740	*3020	1942	1330	1976	1231
1850	*2850	1943	950	1977	1102
1880	*2950	1944	2011	1978	1367
1911	1377	1945	1765	1979	2200
1912	1295	1946	1560	1980	1349
1913	1741	1947	1605	1981	1418
1914	1405	1948	622	1982	1165
1915	1990	1949	1324	1983	2550
1916	1725	1950	1572	1984	1635
1917	1847	1951	1700	1985	1760
1918	1295	1952	1900	1986	1575
1919	*2279	1953	673	1987	1919
1920	673	1954	1380	1988	1275
1921	843	1955	1830	1989	1449
1922	1383	1956	1452	1990	1843
1923	1135	1957	1975	1991	1660
1924	2040	1958	1254	1992	2280
1925	*3175	1959	804	1993	3039
1926	1604	1960	2125	1994	2664
1927	1355	1961	1705	1995	754
1928	1361	1962	1077	1996	1093
1929	1107	1963	1670	1997	1051
1930	1725	1964	1373	1998	1863
1931	1289	1965	1892	1999	2118
1932	1383	1966	1964		
1933	557	1967	1586		
1934	1065	1968	777		
1935	1190	1969	2165		
1936	1457	1970	950		
1937	1590	1971	477		
1938	1546	1972	1071		
1939	2125	1973	1071		
1940	1425	1974	1259		

* adjusted to present day situation, because of river-works
flow year from 1 November to 1 November (def. Rijkswaterstaat)
e.g. flow year 1925 starts from 1 November 1925

Annual peak discharges at Borgharen (m^3s^{-1})
Period 1571-2000

Appendix 2.1.8

measured	ranknr.i	E-formula	measured	ranknr.	E-formula	measured	ranknr.i	E-formula
3175	1	0.002	1705	33	0.3165	1295	63	0.6527
his.doc. 3075	2	0.004	1700	34	0.3277	1295	64	0.6639
3039	3	0.006	1670	35	0.3389	1289	65	0.6751
his.doc. 3020	4	0.008	1660	36	0.3501	1275	66	0.6863
his.doc. 2950	5	0.01	1635	37	0.3613	1259	67	0.6975
his.doc. 2850	6	0.012	1605	38	0.3725	1254	68	0.7087
2664	7	0.0252	1604	39	0.3837	1231	69	0.7199
2550	8	0.0364	1590	40	0.3949	1190	70	0.7311
2280	9	0.0476	1586	41	0.4062	1165	71	0.7423
2279	10	0.0588	1575	42	0.4174	1151	72	0.7535
2200	11	0.07	1572	43	0.4286	1135	73	0.7647
2165	12	0.0812	1560	44	0.4398	1107	74	0.7759
2125	13	0.0924	1546	45	0.451	1102	75	0.7871
2125	14	0.1036	1457	46	0.4622	1093	76	0.7983
2118	15	0.1148	1452	47	0.4734	1077	77	0.8095
2040	16	0.126	1449	48	0.4846	1071	78	0.8207
2011	17	0.1372	1425	49	0.4958	1071	79	0.8319
1990	18	0.1484	1418	50	0.507	1065	80	0.8431
1975	19	0.1596	1405	51	0.5182	1051	81	0.8543
1964	20	0.1709	1383	52	0.5294	950	82	0.8655
1919	21	0.1821	1383	53	0.5406	950	83	0.8767
1900	22	0.1933	1380	54	0.5518	843	84	0.888
1892	23	0.2045	1377	55	0.563	804	85	0.8992
1863	24	0.2157	1373	56	0.5742	777	86	0.9104
1847	25	0.2269	1367	57	0.5854	754	87	0.9216
1843	26	0.2381	1361	58	0.5966	673	88	0.9328
1830	27	0.2493	1355	59	0.6078	673	89	0.944
1765	28	0.2605	1349	60	0.619	635	90	0.9552
1760	29	0.2717	1330	61	0.6302	622	91	0.9664
1741	30	0.2829	1324	62	0.6414	557	92	0.9776
1725	31	0.2941				477	93	0.9888
1725	32	0.3053						

n=429 length of the observed period in years
 s=89 systematically recorded flood peaks
 g=93 systematically recorded flood peaks,
 plus documented peaks from previous
 centuries, together called
 "the observed floods"
 k=6 number of floods in the subset above
 the
 discharge threshold
 e=2 systematically recorded floods of the subset

Registered peak discharges at Borgharen
(m^3s^{-1}),
related to the p.o.e. according to the E-
formulae

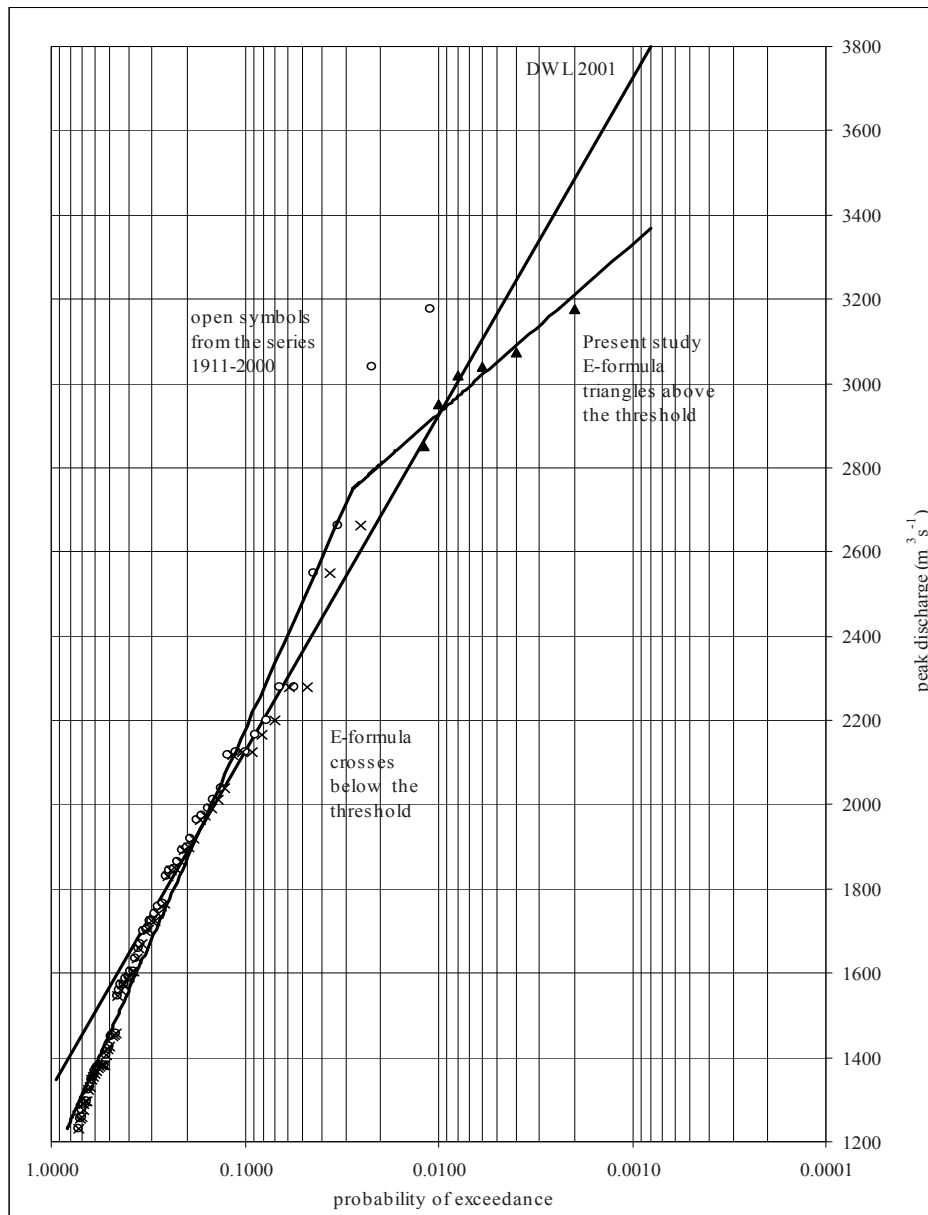
Appendix 2.1.9

Exceedance method	threshold 2750 m³s⁻¹	threshold 2550 m³s⁻¹	threshold 2100 m³s⁻¹
above the threshold	y = -174.8 LN(x) + 2124 x ≤ 0.02781 <i>(3370)</i>	y = -265.3 LN(x) + 1628 x ≤ 0.0166 <i>(3520)</i>	y = -481 LN(x) + 522 x ≤ 0.0328 <i>(3952)</i>
below the threshold	y = -453.8 LN(x) + 1125 x > 0.02781	y = -374.3 LN(x) + 1198 x > 0.0301	y = -332.6 LN(x) + 1189 x > 0.0472
Dalrymple method	threshold 2750 m³s⁻¹	threshold 2550 m³s⁻¹	threshold 2100 m³s⁻¹
above the threshold	y = -181.8 LN(x) + 2116 x ≤ 0.03049 <i>(3412)</i>	y = -265.3 LN(x) + 1658 x ≤ 0.0186 <i>(3550)</i>	y = -481 LN(x) + 552 x ≤ 0.0349 <i>(3982)</i>
below the threshold	y = -469.7 LN(x) + 1110 x > 0.03049	y = -373.7 LN(x) + 1201 x > 0.0301	y = -331.7 LN(x) + 1193 x > 0.0472

p.o.e (x) and peak discharge (y) ;between brackets in italics: p.o.e. 0.0008; **App.2.1.10**

3175	1	1	0.0023	1383	53	235	0.5454
his.doc.3075	2	2	0.0047	1380	54	239	0.5567
3039	3	3	0.007	1377	55	244	0.568
his.doc.3020	4	4	0.0093	1373	56	249	0.5793
his.doc.2950	5	5	0.0116	1367	57	254	0.5906
his.doc.2850	6	6	0.014	1361	58	259	0.6019
2664	7	11	0.0253	1355	59	264	0.6132
2550	8	16	0.0366	1349	60	269	0.6245
2280	9	21	0.0479	1330	61	273	0.6358
2279	10	25	0.0592	1324	62	278	0.6472
2200	11	30	0.0705	1295	63	283	0.6585
2165	12	35	0.0818	1295	64	288	0.6698
2125	13	40	0.0931	1289	65	293	0.6811
2125	14	45	0.1044	1275	66	298	0.6924
2118	15	50	0.1157	1259	67	303	0.7037
2040	16	55	0.127	1254	68	307	0.715
2011	17	59	0.1383	1231	69	312	0.7263
1990	18	64	0.1496	1190	70	317	0.7376
1975	19	69	0.1609	1165	71	322	0.7489
1964	20	74	0.1723	1151	72	327	0.7602
1919	21	79	0.1836	1135	73	332	0.7715
1900	22	84	0.1949	1107	74	337	0.7828
1892	23	89	0.2062	1102	75	341	0.7941
1863	24	94	0.2175	1093	76	346	0.8055
1847	25	98	0.2288	1077	77	351	0.8168
1843	26	103	0.2401	1071	78	356	0.8281
1830	27	108	0.2514	1071	79	361	0.8394
1765	28	113	0.2627	1065	80	366	0.8507
1760	29	118	0.274	1051	81	371	0.862
1741	30	123	0.2853	950	82	376	0.8733
1725	31	128	0.2966	950	83	380	0.8846
1725	32	132	0.3079	843	84	385	0.8959
1705	33	137	0.3192	804	85	390	0.9072
1700	34	142	0.3306	777	86	395	0.9185
1670	35	147	0.3419	754	87	400	0.9298
1660	36	152	0.3532	673	88	405	0.9411
1635	37	157	0.3645	673	89	410	0.9524
1605	38	162	0.3758	635	90	414	0.9638
1604	39	166	0.3871	622	91	419	0.9751
1590	40	171	0.3984	557	92	424	0.9864
1586	41	176	0.4097	477	93	429	0.9977
1575	42	181	0.421				
1572	43	186	0.4323				
1560	44	191	0.4436				
1546	45	196	0.4549				
1457	46	200	0.4662				
1452	47	205	0.4775				
1449	48	210	0.4889				
1425	49	215	0.5002				
1418	50	220	0.5115				
1405	51	225	0.5228				
1383	52	230	0.5341				

Peak discharges at Borgharen (m^3s^{-1}) and transformed ranking numbers (i), according to the Dalrymple method Appendix 2.1.11



Comparison of the presently used DWL 2001 principle, derived from the measured flood series 1911-2000 at Borgharen, with those of the present study on the basis of the Borgharen series 1571-2000, the preferred E-formulae and threshold at 2750 m³s⁻¹ Appendix 2.4.1

Original values

date	Q' max	X0	X1	X2	X3	X4	Q base	Q peak
29-11-1939	1463	793	5.2	3.1	0.8	63	597	2060
26-11-1944	1348	933	7.5	3.4	0.2	34	492	1850
13-02-1945	716	187	2.9	1.1	0.2	123	1229	1945
22-12-1952	881	468	4.7	2.5	0.4	77	974	1855
27-02-1958	1270	697	6.7	3	0.3	55	680	1950
01-02-1961	1875	1254	8.4	3.9	0.4	103	250	2125
11-12-1965	1061	656	6.8	3.2	-0.1	82	786	1847
21-12-1965	997	627	7	3.4	0.2	79	895	1892
13-12-1966	1368	1078	7	3.9	0.5	6	482	1858
23-02-1970	1582	828	6.1	3.4	0.7	90	583	2165
08-02-1984	1571	615	5.9	2.1	-0.2	90	979	2550
17-03-1988	1297	704	4.8	2.6	0.6	41	613	1910
13-01-1993	1972	931	5.8	3.4	1	83	293	2265
22-12-1993	2009	896	4.7	2.3	0.5	56	1030	3039
30-01-1995	1073	575	4.7	2	0.1	17	1591	2664
27-12-1999	1291	459	4.3	1.9	0.8	77	751	2042
sum:	21774	11701	92.3	45.2	6.4	1076	12225	34017
mean:	1361	731	5.8	2.8	0.4	67	764	2126

non-dimensional
values:

	Q' max	X0	X1	X2	X3	X4	Q base	Q peak
29-11-1939	1.0749	0.1005	0.8966	0.5345	0.8	2119	0.781414	0.968955
26-11-1944	0.9904	0.1182	1.2931	0.5862	0.2	1144	0.643979	0.870178
13-02-1945	0.5261	0.0237	0.5	0.1897	0.2	4138	1.608639	0.914863
22-12-1952	0.6473	0.0593	0.8103	0.431	0.4	2590	1.274869	0.872530
27-02-1958	0.9331	0.0883	1.1552	0.5172	0.3	1850	0.890052	0.917215
01-02-1961	1.3777	0.1589	1.4483	0.6724	0.4	3465	0.327225	0.999529
11-12-1965	0.7796	0.0831	1.1724	0.5517	-0.1	2758	1.028796	0.868767
21-12-1965	0.7325	0.0794	1.2069	0.5862	0.2	2658	1.171466	0.889934
13-12-1966	1.0051	0.1366	1.2069	0.6724	0.5	202	0.63089	0.873941
23-02-1970	1.1624	0.1049	1.0517	0.5862	0.7	3028	0.763089	1.018344
08-02-1984	1.1543	0.0779	1.0172	0.3621	-0.2	3028	1.281414	1.199435
17-03-1988	0.953	0.0892	0.8276	0.4483	0.6	1379	0.802356	0.898400
13-01-1993	1.4489	0.1179	1	0.5862	1	2792	0.383508	1.065381
22-12-1993	1.4761	0.1135	0.8103	0.3966	0.5	1884	1.348168	1.429445
30-01-1995	0.7884	0.0728	0.8103	0.3448	0.1	572	2.082461	1.253057
27-12-1999	0.9486	0.0581	0.7414	0.3276	0.8	2590	0.982984	0.960489
sum:	15.9985	1.4823	15.9483	7.7931	6.4	36197	16.00131	16.00047
mean:	0.9999	0.0926	0.9968	0.4871	0.4	2262	1.000082	1.000029
stdev:	0.2769	0.0329	0.2442	0.1361	0.3327	1049	0.4546	0.1629

Original and non-dimensional values of flood
wave parameters

Appendix 3.2.1

Spearman's Rank Correlation Coefficients (r_s):

Q'	X 0	X 1	X 2	X 3	X 4	Qbase	Period
0.22	0.22	0.3	0.55	0.07	0.13	-0.22	1930 - 1980
-0.43	-0.49	-0.89	-0.6	0.31	-0.43	0.31	1980 - 2000

crit.value:

 r_s 0.025; 10: 0.65 From Table XIV, McClave 1997 r_s 0.025; 6: 0.89Rejection region: $r_s > r_s$ 0.025; n

n pairs of observations

Equivalence of averages of the sets before and after 1980

date	Q'	duration	X 0	X 1	X 2	X 3	X 4
29-11-1939	1463	14	793	5.2	3.1	0.8	63
26-11-1944	1348	14	933	7.5	3.4	0.2	34
13-2-1945	716	5	187	2.9	1.1	0.2	123
22-12-1952	881	10	468	4.7	2.5	0.4	77
27-2-1958	1270	14	697	6.7	3	0.3	55
01-2-1961	1875	16	1254	8.4	3.9	0.4	103
11-12-1965	1061	13	656	6.8	3.2	-0.1	82
21-12-1965	997	14	627	7	3.4	0.2	79
13-12-1966	1368	15	1078	7	3.9	0.5	6
23-2-1970	1582	15	828	6.1	3.4	0.7	90
mean	1256	13	752	6.2	3.1	0.4	71
stdev	348	3.23	303	1.6	0.8	0.3	32
08-2-1984	1571	11	615	5.9	2.1	-0.2	90
17-3-1988	1297	11	704	4.8	2.6	0.6	41
13-1-1993	1972	15	931	5.8	3.4	1	83
22-12-1993	2009	10	896	4.7	2.3	0.5	56
30-1-1995	1073	10	575	4.7	2	0.1	17
27-12-1999	1291	10	459	4.3	1.9	0.8	77
mean	1536	11	697	5	2.4	0.5	61
stdev	386	2	186	0.7	0.5	0.5	28
medium	1200-1500		600-850				50-80

values of 16 observations

Calculation:

F	1.23	2.77	2.65	5.83	2.19	3.39	1.3
S'	362	3	267	1.32	0.72	0.34	31
T	0.4	0.33	0.11	-0.75	0.51	0.17	0.18

crit.value:

F = 6.68

t 0.025; 14

= 2.15

F = (stdev I / stdev II)², in which I the series 1930-1980 and in which II the series 1980-2000

$$s^2 = [9/14(\text{std I})^2 + 5/14(\text{std II})^2]^{0.5}$$

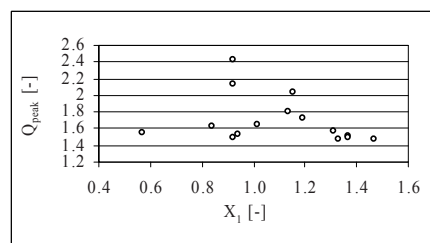
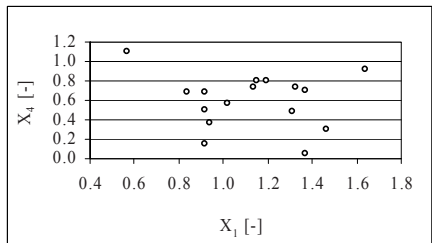
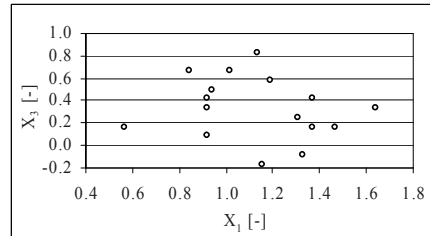
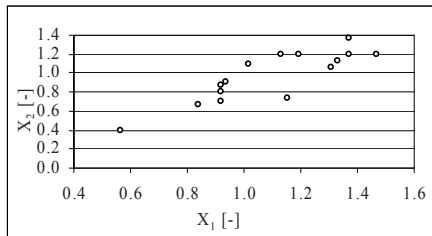
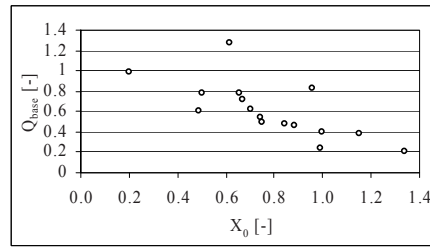
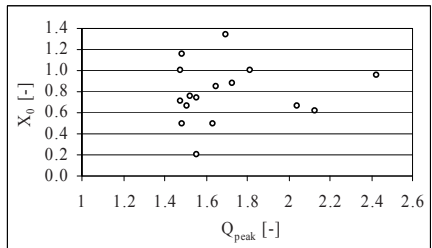
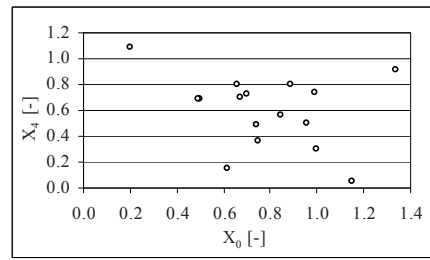
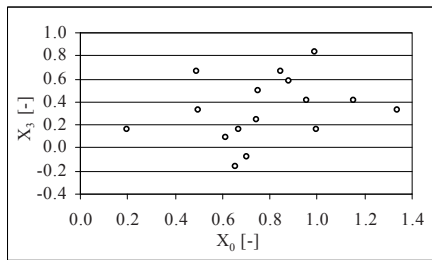
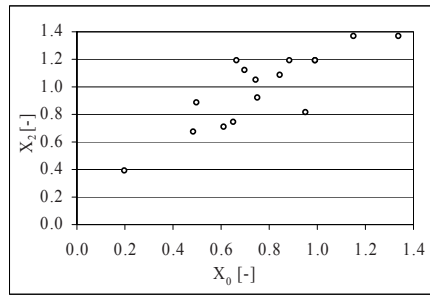
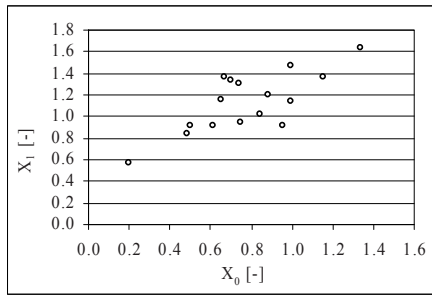
Study of trend breach in the series of flood wave properties ($Q_{\text{peak}} > 1850 \text{ m}^3 \text{ s}^{-1}$) at Borgharen;

Statistical equivalence of the standard deviations and the averages of the sets before and after 1980

Appendix 3.3.1

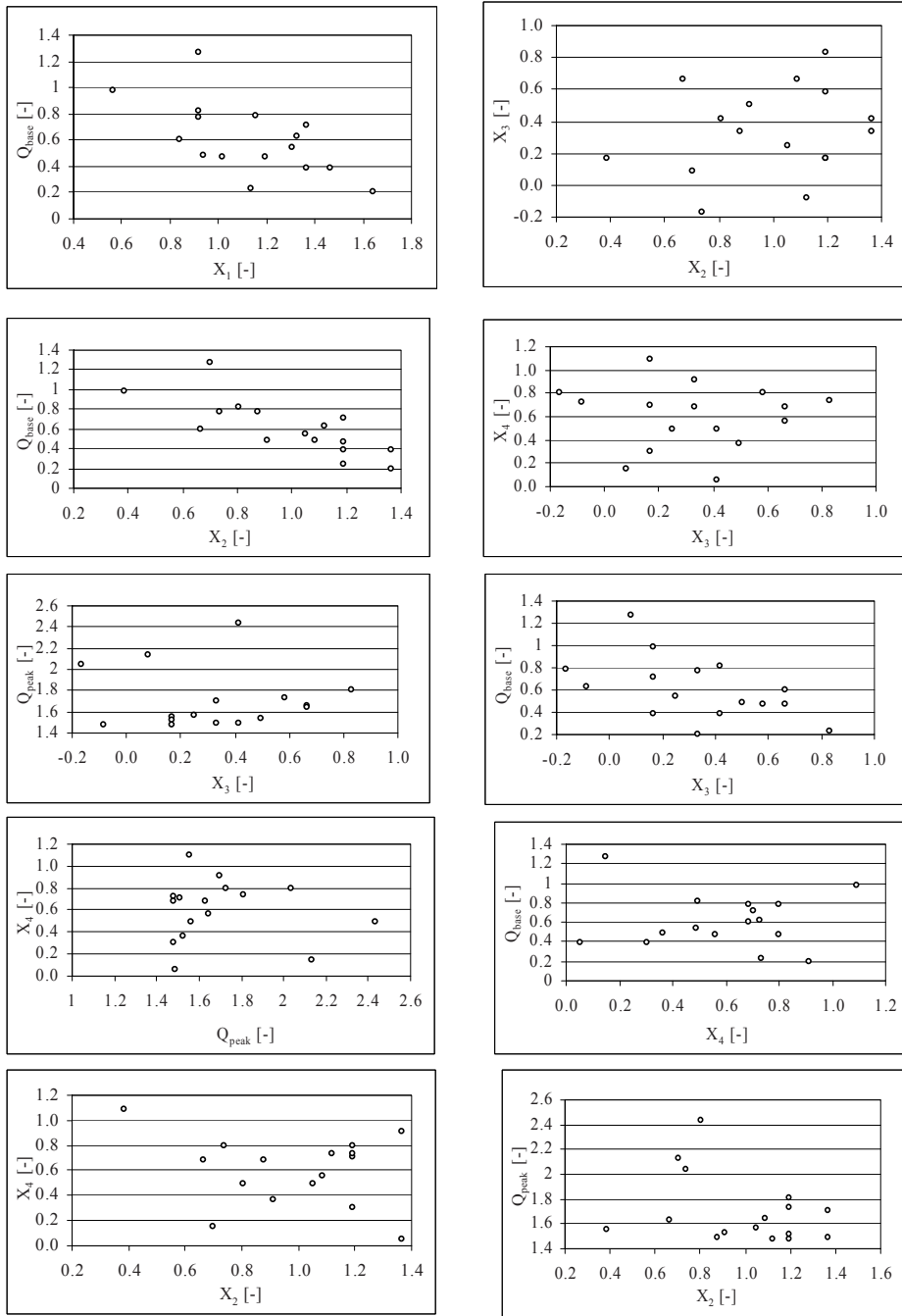
Q' max	X0	X1	X2	X3	X4	Qbase	Qpeak
1.0749	0.8468	1.0167	1.0872	0.6658	0.5595	0.4758	1.648
0.9904	0.9959	1.4664	1.1924	0.1665	0.302	0.3921	1.480
0.5261	0.1997	0.567	0.3858	0.1665	1.0924	0.9795	1.556
0.6473	0.4996	0.9189	0.8768	0.3329	0.6838	0.7763	1.484
0.9331	0.744	1.31	1.0521	0.2497	0.4885	0.542	1.560
1.3777	1.3388	1.6423	1.3678	0.3329	0.9147	0.1993	1.700
0.7796	0.7002	1.3295	1.1223	-0.0832	0.7282	0.6264	1.478
0.7325	0.669	1.3686	1.1924	0.1665	0.7016	0.7133	1.514
1.0051	1.1509	1.3686	1.3678	0.4162	0.0533	0.3842	1.486
1.1624	0.8838	1.1927	1.1924	0.5826	0.7993	0.4647	1.732
1.1543	0.6563	1.1536	0.7365	-0.1665	0.7993	0.7803	2.040
0.9530	0.7515	0.9385	0.9118	0.4994	0.3641	0.4886	1.528
1.4489	0.9934	1.134	1.1924	0.8323	0.7371	0.2335	1.812
1.4761	0.9563	0.9189	0.8066	0.4162	0.4973	0.8209	2.431
0.7884	0.6134	0.9189	0.7014	0.0832	0.151	1.268	2.131
0.9486	0.4895	0.8407	0.6663	0.6658	0.6838	0.5985	1.634
0.9999	0.7806	1.1303	0.9908	0.3329	0.5972	0.6090	1.701 mean
0.2769	0.2771	0.2769	0.2769	0.2769	0.2769	0.2768	0.2769 stdev.

Non-dimensional and standardized flood wave parameter values
Appendix 3.4.1



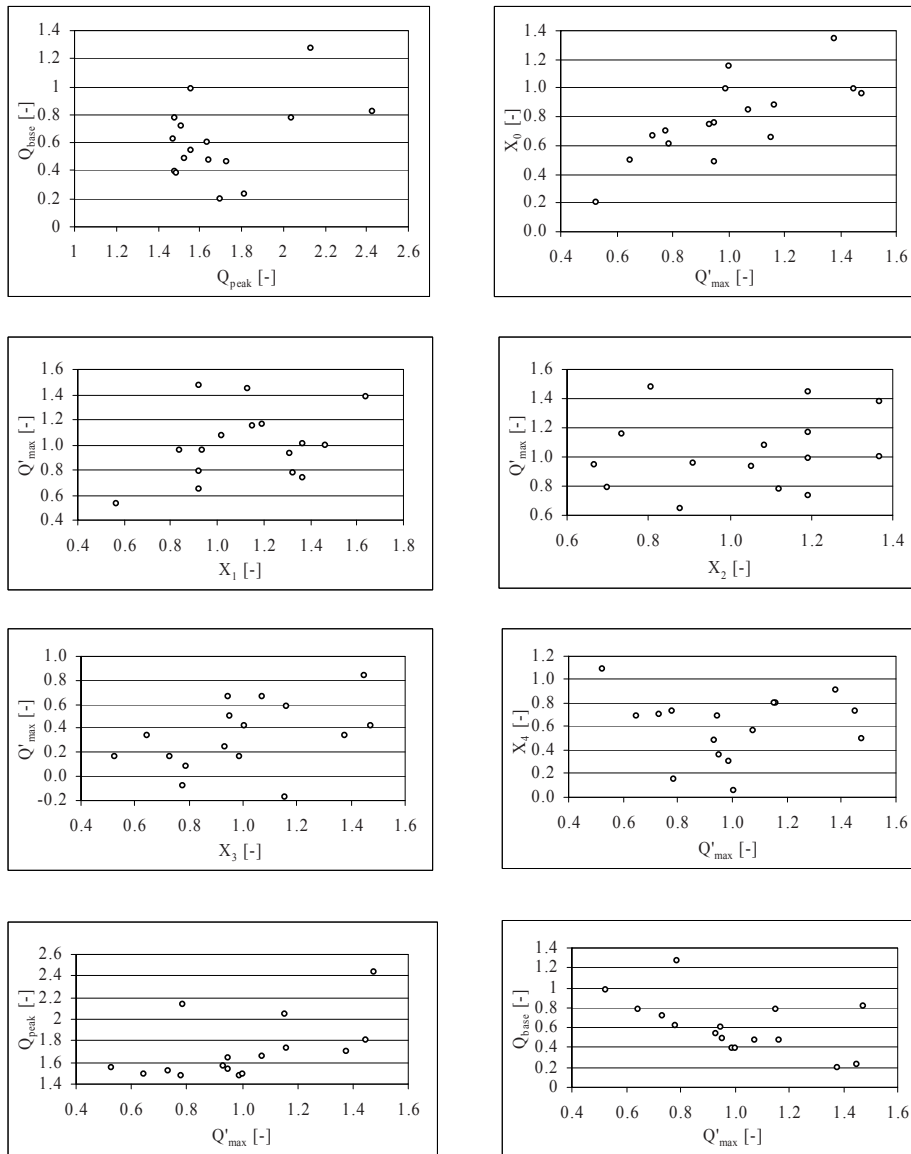
Relations between flood wave properties

Appendix 3.4.2a



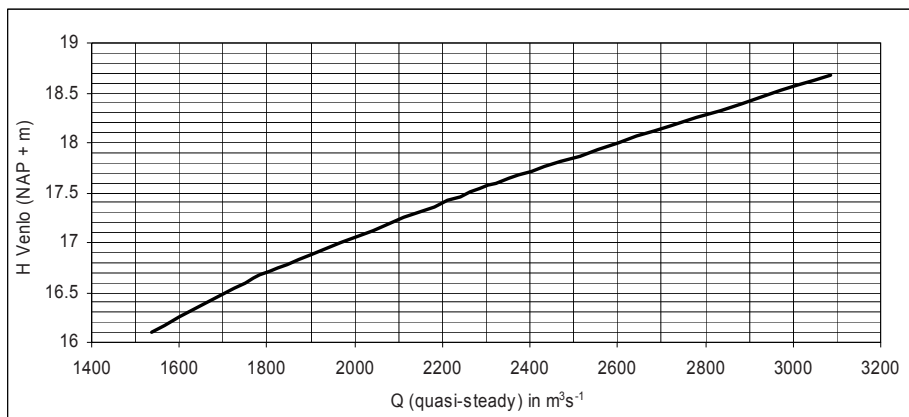
Relations between flood wave properties

Appendix 3.4.2b



Relations between flood wave properties

Q_{Venlo}	H_{Venlo}
1538	16.10
1770	16.65
1805	16.72
2285	17.55
2404	17.72
2719	18.17
2926	18.46
3085	18.68



**Quasi-steady discharge curve at Venlo
(km. 107.470), January 1996**

t	Q'		
0	0	0	0
1	345	424	147
2	1505	537	187
3	2009	369	128
4	1680	837	1505
5	1375	2011	2011
6	1189	1838	1680
7	888	1450	653
8	633	1250	430
9	487	960	274
10	258	610	122
11	0	80	-20
	10369	10366	7117
X ₀	8.96E+08	8.96E+08	6.15E+08
X ₄	5.55E-11	8.97E-11	5.58E-11
Q _{base}	1030	1030	1030
	1	2	3

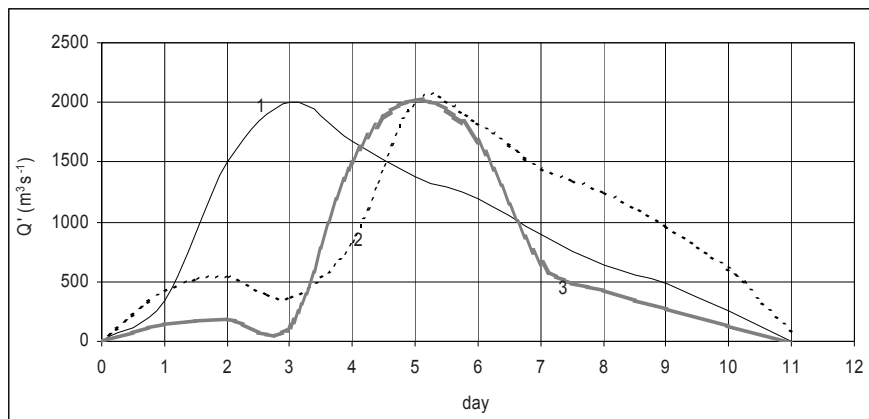


Fig.3.5.3 Flood wave shapes at Borgharen

1 reference relative flood of 1993

2 original X₄ of 1984 and adapted X₀ and Q'_{max} to that of 1993 (90, 896, 2009, respectively)

3 original X₀ of 1984 and adapted X₄ and Q'_{max} to that of 1993 (615, 56, 2009, respectively)

X₀ in 10⁶ m³

X₄ in 10⁻¹² s⁻²

Q'_{max} in m³ s⁻¹

Influence on the flood wave shape of each of the variables X₀ and X₄, because of alternately adaptation of the variables X₀ and X₄ of 1984 to those of 1993

Appendix 3.5.1

0	0	0	0
1	345	383	121
2	1505	1077	341
3	2009	1270	402
4	1680	1879	1505
5	1375	2009	2009
6	1189	1878	1680
7	888	1081	342
8	633	539	171
9	487	341	108
10	258	-84	-26
11	0		
	10369	10373	6653
X_0	8.96E+08	8.96E+08	5.75E+8
X_4	5.55E-11	1.74E-11	5.55E-11
Q_{base}	1030	1030	1030
	I	II	III

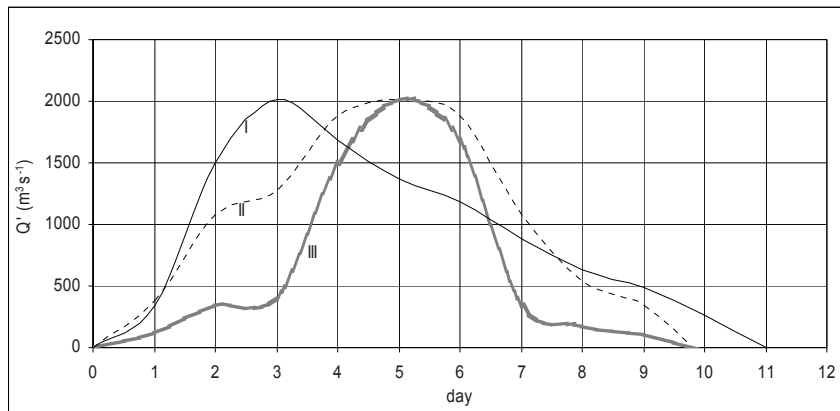


Fig.3.5.4 Flood wave shapes at Borgharen

I reference relative flood of 1993

II original X_4 of 1995 and adapted X_0 and Q'_{max} to that of 1993 (17,896,2009, respectively)

III original X_0 of 1995 and adapted X_4 and Q'_{max} to that of 1993 (575,56, 2009, respectively)

X_0 in 10^6 m^3

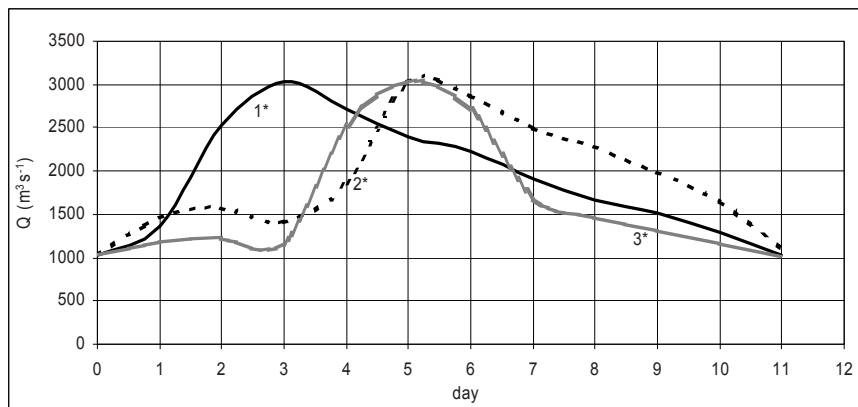
X_4 in 10^{-12} s^{-2}

Q'_{max} in $\text{m}^3 \text{ s}^{-1}$

Influence on the flood wave shape of each of the variables X_0 and X_4 , because of alternately adaptation of the variables X_0 and X_4 of 1995 to those of 1993

t	Q	Q	Q
0	1030	1030	1030
1	1375	1454	1177
2	2535	1567	1217
3	3039	1399	1158
4	2710	1867	2535
5	2405	3041	3041
6	2219	2868	2710
7	1918	2480	1683
8	1663	2280	1460
9	1517	1990	1304
10	1288	1640	1152
11	1030	1110	1010

X_0	8.96E+08	8.96E+08	6.15E+8
X_4	5.55E-11	8.97E-11	5.58E-11
	1*	2*	3*



Flood wave shapes at Borgharen. Discharges of Fig.3.5.3 increased by the base discharge of the 1993 flood

1* reference flood of 1993

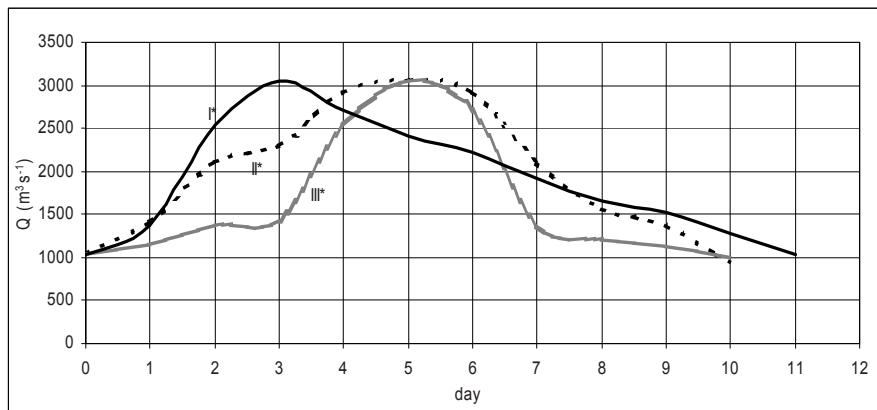
2* original X_4 of 1984 and adapted X_0 and Q_{\max} to that of 1993

3* original X_0 of 1984 and adapted X_4 and Q_{\max} to that of 1993

Comparable flood waves in 1984, 1993 and 1995 with variable X_0 and X_4 for the 1984 flood

Appendix 3.5.3

t	Q	Q	Q
0	1030	1030	1030
1	1375	1413	1151
2	2535	2107	1371
3	3039	2300	1432
4	2710	2909	2535
5	2405	3039	3039
6	2219	2908	2710
7	1918	2111	1372
8	1663	1569	1201
9	1517	1371	1138
10	1288	946	1004
11	1030		
	I*	II*	III*
X ₀	8.96E+08	8.96E+08	5.75E+08
X ₄	5.55E-11	1.74E-11	5.55E-11



Flood wave shapes at Borgharen. Discharges of Fig.3.5.4 increased by the base discharge of the 1993 flood

I* reference flood of 1993

II* original X₄ of 1995 and adapted X₀ and Q_{max} to that of 1993

III* original X₀ of 1995 and adapted X₄ and Q_{max} to that of 1993

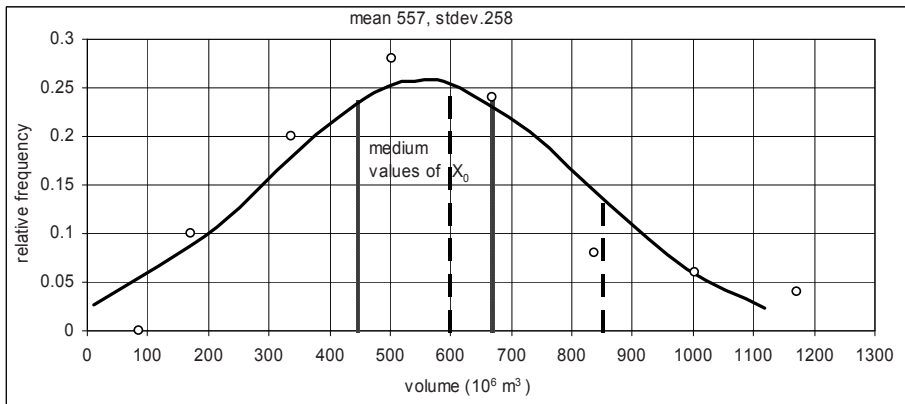
Comparable flood waves of 1984, 1993 and 1995 with variable X₀ and X₄ of the 1995 flood

Appendix 3.5.4

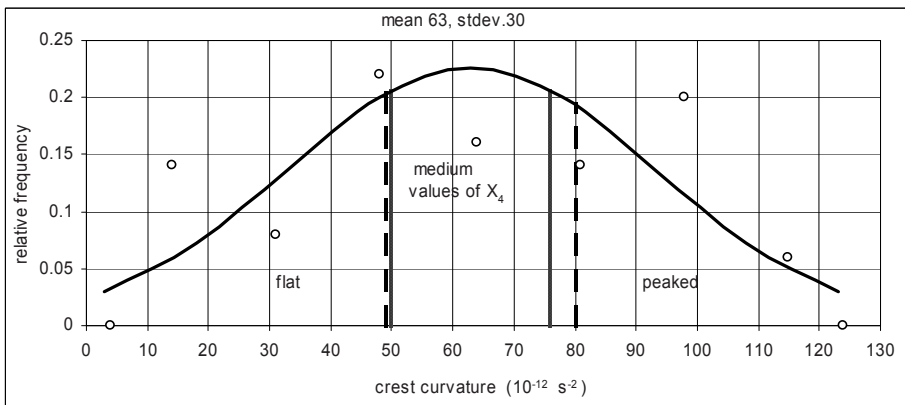
Date	Q _{peak}	Q _{base}	X ₀	Q' ₋₁	Q' ₊₁	X ₄	Q' _{max}	duration
05-1-1931	1425	318	731	911	1042	32	1107	16
15-1-1938	1525	583	514	670	877	48	942	13
25-1-1939	1481	899	149	312	429	97	582	6
29-11-1939	2060	597	793	1085	1157	63	1463	14
06-11-1940	1360	96	526	909	1051	60	1264	9
26-11-1944	1840	492	933	1025	1329	34	1348	14
13-2-1945	1945	1229	187	210	563	123	716	5
08-2-1946	1640	579	899	1041	1041	5	1061	15
09-4-1947	1495	389	473	1071	971	21	1106	10
04-1-1948	1495	746	297	390	728	68	749	10
16-1-1948	1540	699	355	667	642	59	841	10
21-1-1951	1485	766	227	279	664	92	719	8
04-1-1952	1413	442	376	728	818	55	971	9
13-1-1952	1630	543	557	1082	735	44	1087	15
13-2-1952	1440	553	273	822	620	50	887	7
22-12-1952	1855	974	468	412	846	77	881	10
19-1-1955	1360	494	607	772	834	19	866	14
05-3-1956	1830	366	516	1079	972	80	1464	10
16-2-1957	1422	633	358	737	727	19	789	8
27-2-1957	1360	947	86	347	203	90	413	4
27-2-1958	1950	680	697	965	1050	55	1270	14
06-12-1960	1600	540	404	850	845	54	1060	9
01-2-1961	2125	250	1254	838	1470	103	1875	16
14-2-1962	1645	464	613	307	981	122	1181	13
22-11-1963	1530	462	472	1008	831	37	1068	12
11-12-1965	1847	786	656	546	923	82	1061	13
21-12-1965	1892	895	627	488	916	79	997	14
04-1-1966	1690	926	273	716	574	42	764	8
13-12-1966	1850	482	1078	1330	1340	6	1368	15
25-12-1967	1586	309	722	881	1091	61	1277	13
16-1-1968	1370	558	491	344	792	81	812	11
23-2-1970	2165	583	828	797	1310	90	1582	15
12-12-1979	1456	100	1151	967	1223	52	1356	16
06-2-1980	1413	559	539	808	804	15	854	13
08-2-1984	2550	979	615	664	1427	90	1571	11
24-11-1984	1625	201	668	644	1249	90	1424	15
01-4-1986	1664	604	363	261	914	119	1060	11
03-1-1987	1555	563	472	760	732	66	992	13
17-3-1988	1910	613	704	1230	964	41	1297	11
16-2-1990	1440	256	622	551	978	95	1184	15
05-1-1991	1843	976	516	659	853	34	867	13
23-12-1991	1645	345	394	816	892	92	1300	10
13-1-1993	2265	293	931	1067	1652	83	1972	15
22-12-1993	3039	1030	896	1515	1670	56	2009	10
08-1-1994	1588	1199	99	366	213	69	389	5
30-1-1995	2664	1591	575	1027	981	17	1073	10
02-11-1998	1798	658	461	573	810	105	1140	14
04-3-1999	1492	685	341	739	585	48	807	10
14-12-1999	1447	433	606	783	953	39	1014	11
27-12-1999	2042	751	459	696	1148	77	1291	10

Parameter values of the floods at Borgharen

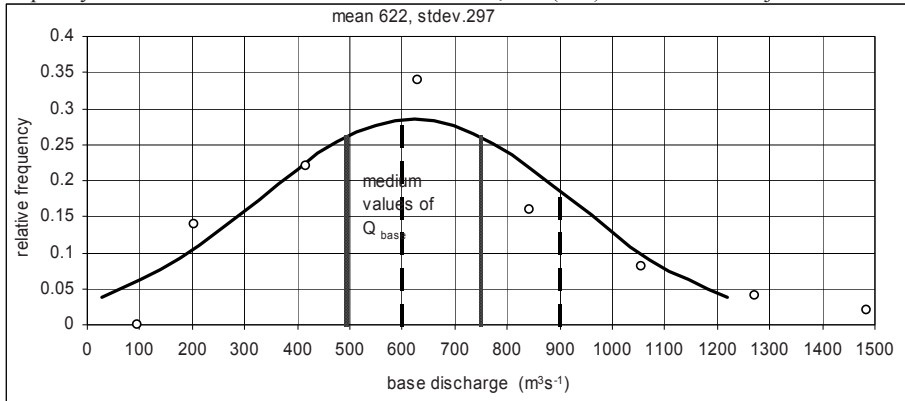
Appendix 4.2.1



Open symbols: class-mid measured from all floods, and (- - -) derived from major floods



Open symbols: class-mid measured from all floods, and (- - -) derived from major floods



Open symbols: class-mid measured from all floods, and (- - -) derived from major floods

Normal frequency distributions of the significant flood wave parameter values in the period 1930-2000. Floods over $1350 \text{ m}^3 \text{ s}^{-1}$ with medium interval (—) and Floods over $1850 \text{ m}^3 \text{ s}^{-1}$ with medium interval (- - -) Appendix 4.3.1

Date	Q peak	Q' peak	wave period	duration to the top	equations to the measured Q' top	R ²
08-2-1984	2550	1571	11	5	$Q' = 84.55t^2 - 167.3t + 149$	0.89
24-11-1984	1625	1424	15	3	$Q' = 154t^2 + 12.8t$	1
01-4-1986	1664	1060	11	5	$Q' = 56.84t^2 - 114.91t + 71$	0.84
03-1-1987	1555	992	13	5	$Q' = 28.14t^2 + 57.77t + 14$	0.99
17-3-1988	1910	1297	11	5	$Q' = -70.8t^2 + 585.3t + 78$	0.96
16-2-1990	1440	1184	15	5	$Q' = 61.07t^2 - 97.87t + 69$	0.95
05-1-1991	1843	867	13	3	$Q' = -1.25t^2 + 306.65t - 21$	0.98
23-12-1991	1645	1300	10	3	$Q' = 89.25t^2 + 190.55t - 37$	0.97
13-1-1993	2265	1972	15	3	$Q' = 176.25t^2 + 149.15t - 31$	0.99
22-12-1993	3039	2009	10	3	$Q' = 39.75t^2 + 599.45t - 74$	0.96
08-1-1994	1588	389	5	3	$Q' = -25.75t^2 + 215.55t - 13$	0.97
30-1-1995	2664	1073	10	5	$Q' = -59.21t^2 + 515.04t - 41$	0.97
02-11-1998	1798	1140	14	6	$Q' = 28.60t^2 - 16.43t + 88$	0.91
04-3-1999	1492	807	10	3	$Q' = -71.5t^2 + 493.7t - 15$	0.99
14-12-1999	1447	1014	11	2	$Q' = -272t^2 + 1051t$	1
27-12-1999	2042	1291	10	3	$Q' = 112.5t^2 + 103.5t - 16$	1

average 12 average 4

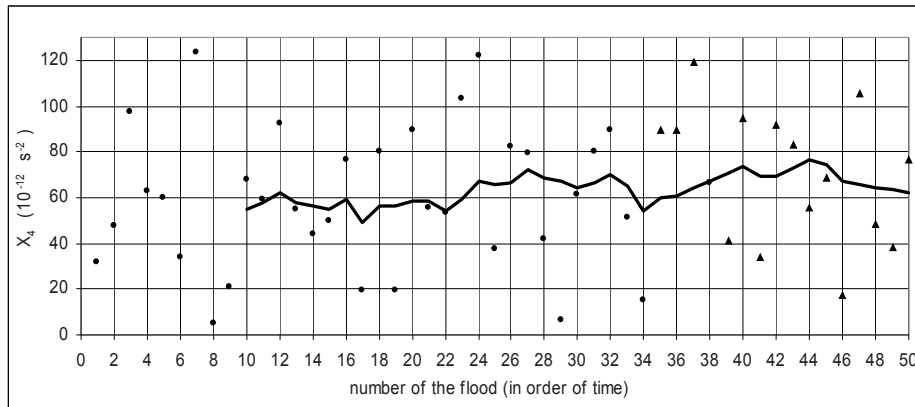
equations after

the measured Q' top

Equation	R ²
$Q' = 3t^2 - 321.2t + 3174$	0.99
$Q' = 9.92t^2 - 291.13t + 2211$	0.99
$Q' = 17.77t^2 - 461.7t + 2975$	0.99
$Q' = 6.996t^2 - 234.2t + 1931$	0.98
$Q' = 42.19t^2 - 844.4t + 4472$	0.98
$Q' = 7.88t^2 - 248.37t + 2169$	0.95
$Q' = 2.95t^2 - 120.23t + 1199$	0.78
$Q' = 27.62t^2 - 534.37t + 2605$	0.98
$Q' = 14.88t^2 - 416.8t + 3054$	0.97
$Q' = 6.697t^2 - 337.66t + 2937.4$	1
$Q' = 30t^2 - 404.6t + 1340$	0.99
$Q' = -13.89t^2 - 19.18t + 1558$	0.98
$Q' = 18.90t^2 - 517.14t + 3551$	0.98
$Q' = 9.53t^2 - 226.38t + 1372$	0.98
$Q' = -1.82t^2 - 46.26t + 998$	0.72
$Q' = 20.83t^2 - 460.24t + 2560$	0.99

All flood events (t; Q') 1980-2000 at Borgharen described with second degree polynomials

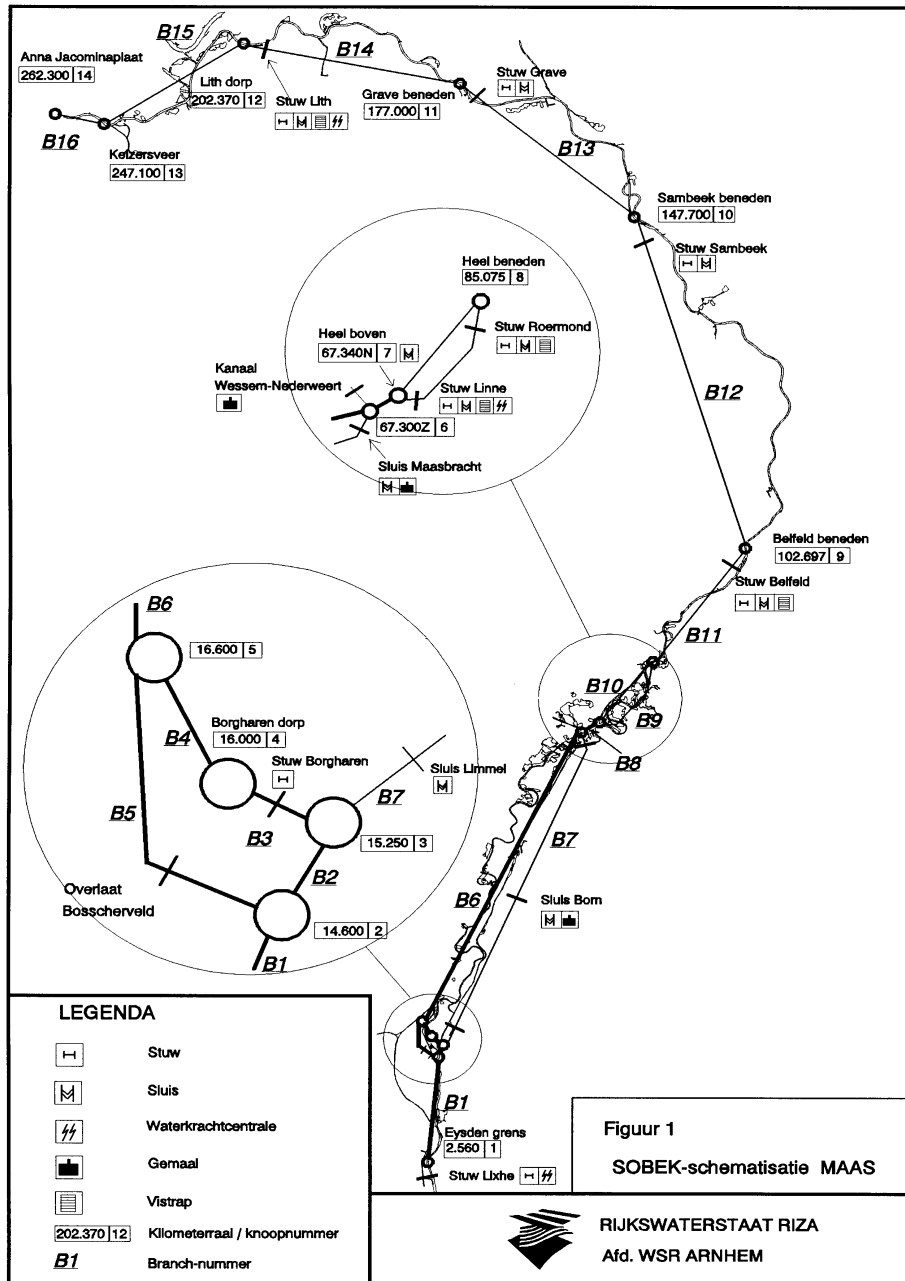
Appendix 4.3.2



The period 1980-2000 starts at flood number 35

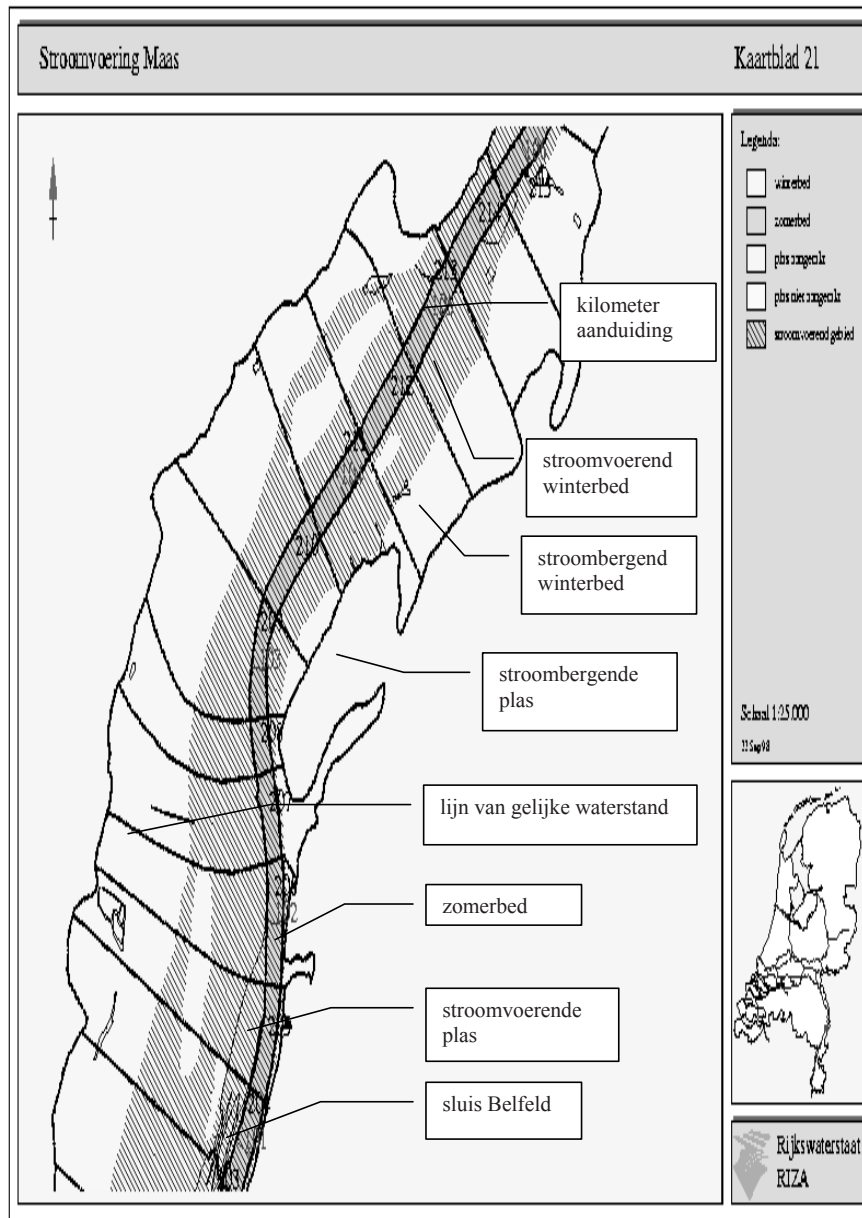
**Progressive mean of each 10 consecutive flood wave crest curvatures (X_4)
at Borgharen in the period 1931-2000**

Appendix 4.3.3

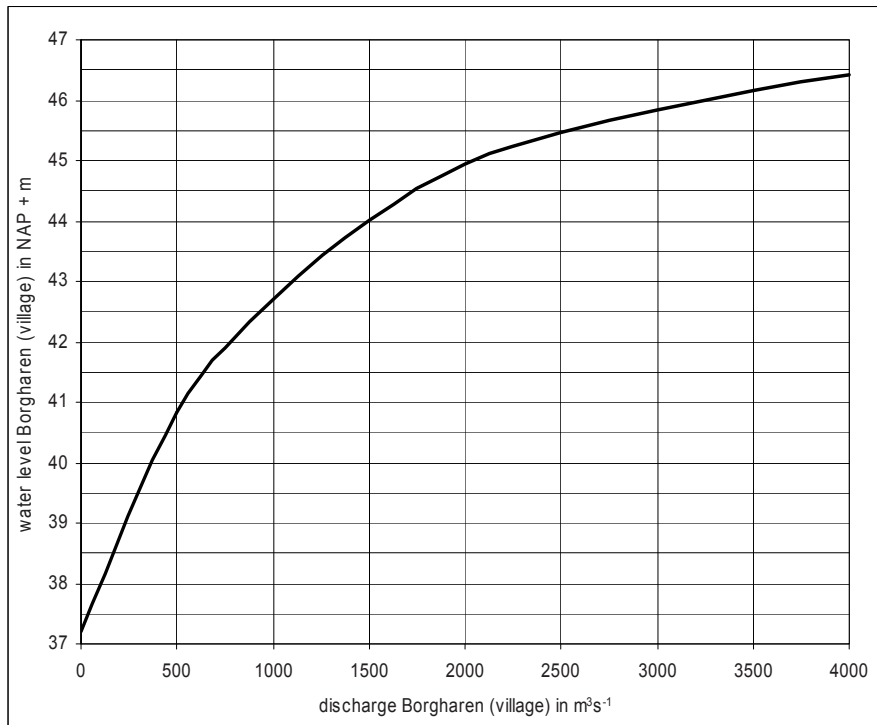


Appendix 4.4.1

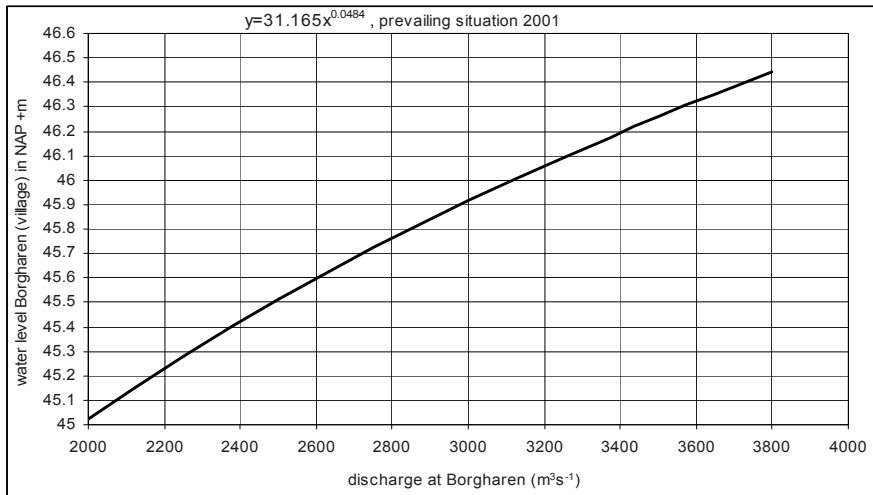
1



Appendix 4.4.2



H.Barneveld & A. Bastings (1998). Stage-discharge curve Borgharen village (km 16) Directorate Limburg, valid from 20-12-1995



Stage-discharge curve 2001 at Borgharen

wave number	H Venlo	H Mook	wave number	H Venlo	H Mook	wave number	H Venlo	H Mook
1	15.72	9.15	51	15.46	8.92	101	15.39	8.87
2	16.73	9.98	52	18.02	11.48	102	16.83	10.11
3	15.18	8.69	53	15.98	9.4	103	16.31	9.69
4	16.97	10.24	54	16.44	9.79	104	15.38	8.87
5	15.39	8.85	55	17.2	10.47	105	16.41	9.72
6	15.82	9.23	56	16.14	9.52	106	15.69	9.14
7	15.34	8.82	57	15.99	9.38	107	15.54	8.99
8	16.52	9.81	58	16.25	9.62	108	16.26	9.58
9	15.76	9.15	59	16.75	10.02	109	16.81	10.03
10	16.38	9.69	60	15.7	9.09	110	16.41	9.71
11	15.64	9.06	61	15.79	9.23	111	16.26	9.62
12	17.66	10.9	62	16.53	9.81	112	16.14	9.51
13	15.97	9.39	63	16.13	9.51	113	15.56	8.98
14	15.49	8.95	64	17.91	11.27	114	15.83	9.24
15	16.19	9.57	65	16.28	9.64	115	16.31	9.68
16	16	9.39	66	15.37	8.85	116	15.78	9.18
17	15.75	9.18	67	16.46	9.77	117	15.71	9.14
18	15.71	9.14	68	16.73	10.01	118	15.91	9.33
19	16.52	9.78	69	15.65	9.1	119	15.78	9.19
20	15.66	9.1	70	15.53	8.97	120	15.66	9.06
21	15.94	9.34	71	18.01	11.46	121	15.94	9.34
22	15.78	9.2	72	15.68	9.1	122	16.18	9.55
23	15.7	9.12	73	16.31	9.64	123	16.65	9.94
24	16.08	9.42	74	15.25	8.73	124	15.66	9.09
25	16.87	10.12	75	15.76	9.18	125	16.81	10.03
26	15.59	9.04	76	17.13	10.36	126	17.25	10.45
27	16.07	9.48	77	15.71	9.13	127	16.23	9.6
28	16.82	10.05	78	16.96	10.22	128	15.83	9.28
29	17.56	10.78	79	15.39	8.87	129	15.51	8.96
30	15.77	9.18	80	15.66	9.09	130	16.25	9.62
31	17.15	10.41	81	15.77	9.2	131	16.37	9.67
32	15.1	8.62	82	15.77	9.2	132	15.37	8.83
33	15.48	8.95	83	16.21	9.57	133	16.59	9.88
34	15.78	9.2	84	17.09	10.37	134	15.45	8.9
35	15.11	8.63	85	16.02	9.4	135	15.53	8.95
36	15.19	8.68	86	16.13	9.47	136	16.51	9.82
37	16.34	9.64	87	15.73	9.17	137	15.94	9.33
38	15.44	8.91	88	16.04	9.41	138	15.9	9.28
39	15.41	8.87	89	15.97	9.39	139	18.45	12.05
40	15.91	9.34	90	15.49	8.93	140	16.79	10.07
41	16.18	9.57	91	15.67	9.1	141	16.19	9.53
42	15.98	9.37	92	16.49	9.79	142	16.25	9.62
43	16.65	9.94	93	15.66	9.08	143	16.68	9.96
44	15.84	9.27	94	16.7	9.97	144	17.74	10.97
45	16.87	10.12	95	15.9	9.32	145	16.59	9.9
46	17.82	11.18	96	16.76	10.04	146	15.83	9.27
47	15.75	9.16	97	15.91	9.3	147	15.75	9.19
48	17.03	10.25	98	16.72	9.93	148	17.6	10.78
49	15.69	9.13	99	17.03	10.28	149	16.65	9.92
50	16.31	9.66	100	15.97	9.39	150	16.12	9.5

File with maximum water levels at Venlo and Mook, as a result of one thousand samples of combinations of four significant flood wave parameter values at Borgharen and Sobek water level computations for the synthesized flood waves at Borgharen out of the samples
Appendix 4.5.1 (7 pages)

wave number	H Venlo	H Mook	wave number	H Venlo	H Mook	wave number	H Venlo	H Mook
151	15.69	9.12	204	16.06	9.43	257	15.54	8.99
152	16.28	9.6	205	15.76	9.19	258	15.96	9.36
153	15.58	9.02	206	16.09	9.5	259	16.08	9.46
154	16.97	10.18	207	15.41	8.89	260	17.12	10.42
155	15.82	9.26	208	17.01	10.24	261	15.75	9.17
156	15.68	9.11	209	16.01	9.39	262	15.57	9.03
157	16.74	10.01	210	15.51	8.97	263	16.81	10.01
158	16.2	9.55	211	15.6	9.04	264	16.64	9.91
159	16.39	9.68	212	16.09	9.5	265	16.65	9.94
160	15.64	9.08	213	16.69	9.95	266	15.38	8.83
161	15.16	8.65	214	16.28	9.61	267	15.74	9.16
162	15.15	8.65	215	16.11	9.51	268	16.08	9.46
163	15.89	9.29	216	15.43	8.9	269	15.39	8.85
164	16.66	9.94	217	15.11	8.63	270	16.67	9.93
165	15.98	9.4	218	15.62	9.07	271	15.99	9.39
166	16.69	9.95	219	15.49	8.95	272	15.88	9.28
167	16.14	9.51	220	16.42	9.76	273	15.46	8.92
168	16.44	9.76	221	16.03	9.41	274	16.21	9.6
169	15.65	9.07	222	16.81	10.07	275	16.58	9.83
170	16.04	9.37	223	15.76	9.18	276	15.55	9
171	17.07	10.35	224	15.75	9.25	277	16.46	9.77
172	15.24	8.73	225	15.66	9.08	278	15.59	9.06
173	15.51	8.96	226	15.71	9.15	279	15.64	9.11
174	15.82	9.22	227	15.94	9.27	280	16.23	9.62
175	15.63	9.07	228	15.8	9.25	281	15.77	9.2
176	15.93	9.33	229	16.03	9.36	282	15.72	9.15
177	15.22	8.68	230	15.9	9.32	283	16.92	10.2
178	15.91	9.31	231	15.87	9.27	284	15.7	9.15
179	15.3	8.79	232	17.27	10.56	285	17.32	10.62
180	16.26	9.63	233	15.6	9.04	286	16.83	10.12
181	15.74	9.15	234	16.74	9.97	287	16.93	10.11
182	16.54	9.81	235	16.87	10.12	288	17.6	10.76
183	16.28	9.58	236	16.86	10.04	289	16.86	10.05
184	15.53	8.99	237	15.97	9.41	290	15.96	9.38
185	15.55	8.99	238	15.98	9.4	291	15.92	9.32
186	15.61	9.04	239	15.71	9.13	292	15.86	9.3
187	18	11.43	240	16.77	10.02	293	15.82	9.24
188	16.14	9.53	241	17.02	10.25	294	16.42	9.73
189	15.88	9.33	242	15.87	9.31	295	16.09	9.48
190	15.74	9.18	243	16	9.33	296	16.07	9.46
191	16.31	9.68	244	15.97	9.35	297	15.23	8.73
192	17.19	10.43	245	15.36	8.82	298	15.98	9.37
193	15.37	8.84	246	15.81	9.23	299	15.74	9.2
194	15.51	8.96	247	15.68	9.11	300	15.91	9.31
195	15.55	9	248	17.07	10.33	301	15.88	9.29
196	15.86	9.29	249	17.02	10.27	302	16.32	9.69
197	15.17	8.68	250	16.88	10.14	303	16.04	9.44
198	16.75	10.02	251	16.66	9.96	304	17.18	10.44
199	16.21	9.58	252	16.28	9.65	305	16.46	9.76
200	15.61	9.02	253	16.82	10.05	306	16.15	9.55
201	16.11	9.49	254	16.59	9.86	307	17.19	10.46
202	15.57	9.03	255	16.79	9.97	308	16.56	9.87
203	16.29	9.62	256	15.57	9.04	309	16.91	10.11

wave number	H Venlo	H Mook	wave number	H Venlo	H Mook	wave number	H Venlo	H Mook
310	16.71	9.97	363	16	9.39	416	15.7	9.09
311	15.5	8.94	364	16.44	9.76	417	15.69	9.12
312	15.2	8.7	365	16.32	9.69	418	15.74	9.16
313	15.68	9.12	366	16.88	10.08	419	17	10.24
314	16.14	9.47	367	16.34	9.66	420	15.33	8.82
315	17.25	10.51	368	17.36	10.6	421	15.83	9.27
316	16.66	9.89	369	15.54	8.99	422	16.27	9.64
317	16.16	9.54	370	16.09	9.46	423	17.87	11.19
318	16.44	9.68	371	16.61	9.89	424	15.48	8.93
319	16.98	10.18	372	15.62	9.07	425	16.02	9.43
320	16.19	9.56	373	15.84	9.23	426	16.4	9.77
321	17.9	11.04	374	15.88	9.22	427	15.77	9.2
322	17.17	10.41	375	15.84	9.26	428	16.43	9.75
323	15.86	9.26	376	16.06	9.46	429	15.27	8.75
324	15.73	9.14	377	17.14	10.43	430	15.87	9.27
325	16.86	10.13	378	15.24	8.71	431	16.73	9.97
326	15.47	8.93	379	15.49	8.93	432	16.64	9.91
327	16.12	9.5	380	15.84	9.23	433	15.69	9.1
328	15.8	9.21	381	15.45	8.91	434	15.99	9.38
329	15.72	9.15	382	16.54	9.83	435	15.69	9.13
330	15.79	9.17	383	15.46	8.93	436	15.74	9.12
331	15.8	9.22	384	17.13	10.36	437	17.83	10.92
332	16.68	9.96	385	16.51	9.86	438	16.11	9.45
333	16.58	9.87	386	18.28	11.7	439	15.98	9.37
334	15.72	9.15	387	15.98	9.39	440	16.01	9.4
335	15.28	8.77	388	15.89	9.28	441	16.25	9.58
336	16.56	9.85	389	16.77	10.05	442	16.45	9.69
337	16.81	10.04	390	15.69	9.13	443	15.56	9
338	16.8	10.07	391	16.84	10.04	444	16.53	9.82
339	17.31	10.55	392	16.19	9.54	445	16.2	9.58
340	15.73	9.16	393	15.98	9.39	446	15.79	9.19
341	17.5	10.7	394	16.86	10.12	447	16.13	9.51
342	15.54	9	395	15.68	9.07	448	15.53	8.96
343	16.71	9.92	396	16.44	9.74	449	15.46	8.93
344	15.4	8.87	397	15.99	9.38	450	16.52	9.86
345	16.11	9.49	398	15.77	9.19	451	16.92	10.21
346	16.96	10.25	399	18.31	11.8	452	15.9	9.33
347	15.15	8.63	400	16.5	9.8	453	15.41	8.89
348	16.2	9.57	401	17.04	10.31	454	16.02	9.4
349	17.7	11	402	17.41	10.68	455	16.68	9.95
350	15.45	8.91	403	15.55	8.98	456	15.46	8.92
351	17	10.23	404	16	9.42	457	16.27	9.59
352	16.45	9.75	405	17.59	10.77	458	15.49	8.97
353	15.41	8.89	406	15.66	9.09	459	17.86	11.2
354	16.02	9.43	407	16.86	10.1	460	15.61	9.04
355	16.78	10.03	408	16.06	9.46	461	16.56	9.86
356	16.94	10.17	409	16.5	9.8	462	16.02	9.4
357	15.17	8.66	410	15.31	8.79	463	15.99	9.42
358	15.84	9.25	411	15.86	9.29	464	15.68	9.07
359	16.54	9.84	412	15.56	8.99	465	16.59	9.84
360	15.61	9.08	413	15.49	8.95	466	15.21	8.68
361	15.37	8.85	414	17.34	10.6	467	15.53	8.97
362	16.03	9.42	415	15.73	9.25	468	16.97	10.23

wave number	H Venlo	H Mook	wave number	H Venlo	H Mook	wave number	H Venlo	H Mook
469	15.98	9.39	522	16.05	9.47	575	15.84	9.23
470	16.74	9.97	523	15.25	8.76	576	16.4	9.7
471	16.12	9.53	524	16.26	9.62	577	17.55	10.7
472	16.77	10.05	525	16.2	9.57	578	17.28	10.56
473	15.6	8.98	526	17.26	10.5	579	15.95	9.38
474	16.47	9.71	527	17.14	10.37	580	16.21	9.57
475	16.41	9.72	528	18.31	11.77	581	15.89	9.32
476	15.92	9.31	529	17.14	10.36	582	16	9.43
477	16.74	10.01	530	16.4	9.72	583	15.59	9.06
478	15.72	9.16	531	17.69	10.97	584	16.38	9.65
479	15.86	9.26	532	15.7	9.11	585	15.28	8.74
480	15.57	9.02	533	16.27	9.57	586	17	10.18
481	16	9.38	534	15.59	9.04	587	15.96	9.36
482	17.02	10.23	535	16.5	9.78	588	15.72	9.12
483	15.11	8.62	536	15.65	9.05	589	16.46	9.77
484	15.41	8.89	537	16.37	9.66	590	15.57	9.01
485	16.78	10.01	538	16.6	9.88	591	15.78	9.21
486	15.43	8.9	539	16.15	9.55	592	16	9.4
487	15.92	9.33	540	15.25	8.75	593	16.32	9.68
488	15.95	9.38	541	16.94	10.25	594	17.43	10.59
489	16.04	9.46	542	16.19	9.57	595	16.78	9.98
490	15.2	8.69	543	16.18	9.52	596	17.8	10.86
491	17.32	10.44	544	15.94	9.32	597	15.94	9.34
492	17.07	10.28	545	15.83	9.17	598	15.63	9.05
493	15.65	9.09	546	15.22	8.7	599	15.22	8.71
494	16.14	9.48	547	15.47	8.94	600	15.72	9.17
495	15.55	8.95	548	16.83	10.06	601	15.34	8.83
496	15.68	9.1	549	15.95	9.37	602	15.24	8.74
497	17.04	10.24	550	15.68	9.14	603	16.18	9.55
498	16.26	9.59	551	16.76	10.02	604	17.03	10.24
499	15.69	9.12	552	18.23	11.6	605	16.28	9.65
500	16.09	9.47	553	15.42	8.89	606	15.31	8.79
501	16.75	10.03	554	16.14	9.51	607	15.63	9.06
502	17.11	10.29	555	15.65	9.08	608	15.99	9.42
503	15.63	9.07	556	16.68	9.96	609	16.04	9.45
504	15.57	9.03	557	16.71	9.96	610	15.73	9.16
505	16.18	9.57	558	15.92	9.3	611	17.06	10.3
506	15.94	9.35	559	15.93	9.33	612	15.48	8.95
507	15.65	9.08	560	16.1	9.44	613	15.71	9.1
508	16.57	9.85	561	16.28	9.65	614	16.14	9.51
509	15.07	8.6	562	16.99	10.28	615	15.88	9.27
510	16.26	9.63	563	16.11	9.51	616	15.76	9.16
511	15.83	9.25	564	15.99	9.39	617	16.93	10.1
512	15.31	8.81	565	15.67	9.09	618	17.14	10.39
513	16.02	9.43	566	17.22	10.31	619	15.8	9.22
514	17.54	10.68	567	16.41	9.78	620	15.7	9.13
515	15.79	9.18	568	15.93	9.35	621	16.68	9.96
516	15.86	9.24	569	18.31	11.78	622	15.64	9.09
517	15.36	8.82	570	15.83	9.22	623	16.3	9.66
518	16.04	9.45	571	17.18	10.44	624	16.43	9.78
519	16.32	9.63	572	16.49	9.79	625	16.49	9.79
520	15.18	8.69	573	16	9.39	626	16.19	9.53
521	17.03	10.26	574	16.26	9.63	627	15.2	8.68

wave number	H Venlo	H Mook	wave number	H Venlo	H Mook	wave number	H Venlo	H Mook
628	15.93	9.31	681	16.05	9.47	734	15.89	9.28
629	15.23	8.71	682	16.62	9.89	735	15.92	9.28
630	16.46	9.77	683	15.4	8.88	736	16.05	9.45
631	16.92	10.16	684	16.87	10.05	737	16.41	9.74
632	16.53	9.81	685	15.82	9.26	738	16.13	9.51
633	15.91	9.35	686	16.14	9.45	739	16.41	9.76
634	16.3	9.67	687	17.84	11.16	740	15.94	9.34
635	15.97	9.37	688	15.23	8.74	741	16.9	10.11
636	15.81	9.23	689	15.74	9.19	742	16.17	9.55
637	15.75	9.16	690	15.48	8.95	743	16.46	9.75
638	16.45	9.76	691	15.47	8.95	744	15.96	9.36
639	15.96	9.35	692	15.35	8.82	745	17.08	10.33
640	16.08	9.46	693	15.88	9.28	746	15.94	9.35
641	15.43	8.9	694	17.4	10.66	747	16.34	9.65
642	16.6	9.85	695	16.55	9.83	748	16.11	9.49
643	16.01	9.39	696	15.16	8.65	749	15.84	9.26
644	16.35	9.66	697	16.33	9.63	750	16.37	9.72
645	16.57	9.84	698	15.3	8.79	751	17.46	10.62
646	15.43	8.9	699	16.24	9.61	752	15.56	9.02
647	17.81	11.18	700	16.1	9.5	753	15.78	9.22
648	16.7	9.98	701	16.57	9.85	754	15.34	8.82
649	16.84	10.15	702	15.71	9.11	755	15.92	9.31
650	16.66	9.92	703	16.55	9.85	756	16.07	9.46
651	16.95	10.14	704	16.81	10.01	757	17.15	10.42
652	16	9.41	705	15.88	9.32	758	15.63	9.08
653	15.94	9.33	706	17.04	10.3	759	16.35	9.72
654	16.98	10.15	707	16.35	9.65	760	16.17	9.54
655	17.62	10.83	708	15.73	9.15	761	16.11	9.44
656	16.27	9.6	709	15.79	9.2	762	15.8	9.23
657	18.3	11.83	710	15.58	9.02	763	18.29	11.74
658	15.99	9.4	711	15.38	8.86	764	15.49	8.96
659	16.12	9.53	712	16.49	9.79	765	15.49	8.95
660	15.6	8.98	713	15.9	9.3	766	15.59	9.04
661	15.43	8.9	714	15.9	9.34	767	16.02	9.4
662	16.59	9.87	715	16.02	9.45	768	16.14	9.49
663	15.69	9.12	716	15.76	9.19	769	16.87	10.01
664	16.32	9.63	717	15.58	9.01	770	15.56	8.99
665	16.99	10.29	718	15.7	9.12	771	15.95	9.33
666	17.79	10.85	719	15.87	9.27	772	15.35	8.83
667	16.01	9.44	720	16.89	10.16	773	16.43	9.75
668	17.1	10.34	721	15.24	8.72	774	15.76	9.18
669	15.48	8.94	722	16.42	9.71	775	16.58	9.85
670	16.12	9.46	723	15.86	9.27	776	16.1	9.49
671	16.76	10.04	724	15.58	9.05	777	15.41	8.89
672	17.09	10.36	725	15.82	9.27	778	16.63	9.93
673	16.03	9.45	726	15.66	9.09	779	15.87	9.28
674	15.53	9	727	16.6	9.87	780	16.59	9.89
675	15.56	9.02	728	16.89	10.16	781	15.79	9.17
676	15.44	8.91	729	16.08	9.48	782	15.73	9.14
677	15.85	9.24	730	17.73	11.01	783	16.1	9.48
678	15.75	9.17	731	15.97	9.37	784	16.79	10.03
679	15.66	9.09	732	15.83	9.15	785	15.94	9.34
680	16.77	10.04	733	17.15	10.22	786	16.09	9.47

wave number	H Venlo	H Mook	wave number	H Venlo	H Mook	wave number	H Venlo	H Mook
787	15.36	8.84	840	16.12	9.51	893	15.89	9.3
788	17.72	11	841	15.61	9.01	894	16.25	9.55
789	15.89	9.27	842	15.47	8.92	895	16.35	9.72
790	15.23	8.71	843	15.92	9.31	896	16.56	9.86
791	15.7	9.1	844	15.95	9.38	897	17.81	11.1
792	15.65	9.08	845	15.28	8.77	898	16.24	9.62
793	17.48	10.79	846	16.56	9.85	899	16.09	9.46
794	16.61	9.89	847	16.82	10.03	900	16.87	10.01
795	15.38	8.85	848	15.57	9	901	16.37	9.68
796	14.97	8.54	849	16.65	9.91	902	15.41	8.89
797	15.66	9.09	850	16.42	9.74	903	15.89	9.27
798	17.03	10.29	851	16.05	9.43	904	15.81	9.21
799	16.18	9.55	852	16.91	10.19	905	16.3	9.59
800	15.83	9.2	853	15.46	8.92	906	15.51	8.91
801	15.79	9.19	854	15.64	9.07	907	16.66	9.92
802	16.61	9.89	855	16.65	9.93	908	16.8	10.04
803	17.11	10.34	856	15.41	8.88	909	16.56	9.82
804	15.96	9.37	857	16.59	9.89	910	15.94	9.37
805	15.79	9.2	858	15.62	9.01	911	16.53	9.82
806	15.56	9.01	859	15.4	8.88	912	17.21	10.55
807	17.12	10.38	860	15.77	9.21	913	15.72	9.14
808	16.23	9.58	861	15.73	9.16	914	16.18	9.51
809	15.69	9.13	862	16.06	9.43	915	15.27	8.77
810	16.47	9.77	863	16.03	9.45	916	16.26	9.63
811	15.74	9.17	864	15.62	9.09	917	15.9	9.3
812	15.09	8.61	865	15.33	8.81	918	16.45	9.76
813	15.37	8.81	866	16.07	9.45	919	15.36	8.84
814	15.91	9.34	867	15.17	8.68	920	18.31	11.77
815	16.5	9.78	868	15.82	9.26	921	16.02	9.4
816	16.21	9.6	869	18.32	11.83	922	15.52	8.96
817	17.1	10.39	870	15.95	9.37	923	16.06	9.47
818	16.34	9.66	871	15.51	8.92	924	15.94	9.36
819	16.31	9.7	872	15.9	9.3	925	16.52	9.8
820	15.65	9.07	873	16.72	10	926	16.32	9.64
821	17.05	10.3	874	15.57	9.01	927	15.56	9
822	15.98	9.36	875	15.52	8.99	928	16.39	9.7
823	16.45	9.73	876	16.16	9.54	929	15.98	9.38
824	16.34	9.65	877	16.1	9.48	930	16.73	10.01
825	15.03	8.57	878	16.59	9.88	931	15.23	8.72
826	15.64	9.08	879	16.04	9.43	932	16.21	9.6
827	16.08	9.47	880	15.79	9.19	933	16.7	9.98
828	17.4	10.67	881	15.99	9.39	934	15.96	9.29
829	15.81	9.24	882	15.69	9.13	935	17.11	10.38
830	15.12	8.64	883	16.9	10.14	936	16.02	9.42
831	17.1	10.32	884	15.81	9.21	937	16.65	9.93
832	15.71	9.11	885	16.81	10.04	938	16.37	9.69
833	17.78	11.08	886	16.18	9.57	939	15.22	8.72
834	16.06	9.45	887	15.78	9.23	940	15.46	8.92
835	15.85	9.29	888	15.7	9.13	941	16.93	10.14
836	16.59	9.86	889	15.27	8.77	942	16.11	9.49
837	16.51	9.81	890	16.78	10.06	943	15.81	9.23
838	16.27	9.63	891	15.62	9.07	944	15.45	8.93
839	15.63	9.05	892	16.56	9.85	945	16.81	10.09

wave number	H Venlo	H Mook	wave number	H Venlo	H Mook
946	16.23	9.56	991	15.64	9.08
947	15.56	9	992	17.84	11.12
948	16.4	9.76	993	16.27	9.64
949	15.75	9.16	994	15.51	8.97
950	15.49	8.93	995	17.97	11.38
951	16.79	10.05	996	15.97	9.35
952	16.23	9.62	997	16.95	10.13
953	15.85	9.27	998	15.51	8.97
954	15.32	8.82	999	15.77	9.19
955	15.41	8.89			
956	17.19	10.27			
957	16	9.42			
958	16.87	10.07			
959	16.56	9.84			
960	16.13	9.52			
961	16.61	9.85			
962	16.64	9.9			
963	15.83	9.21			
964	18.17	11.54			
965	16.85	10.15			
966	16.08	9.46			
967	15.87	9.28			
968	15.43	8.89			
969	16.27	9.6			
970	15.97	9.36			
971	16.09	9.47			
972	15.65	9.09			
973	15.58	9.03			
974	15.21	8.71			
975	15.36	8.83			
976	15.72	9.16			
977	15.87	9.29			
978	15.76	9.17			
979	16.24	9.57			
980	17.89	11.23			
981	15.57	9			
982	17.19	10.45			
983	15.24	8.74			
984	15.8	9.21			
985	15.86	9.25			
986	16.44	9.82			
987	15.98	9.36			
988	15.43	8.89			
989	17.78	11.11			
990	15.71	9.1			

Appendix 4.5.1 (page 7, last one)

1. Normal distribution

$$f(x) = [1 / \sigma\sqrt{2\pi}] \exp [-(x-\mu)^2 / 2\sigma^2]$$

μ , the mean of the discharges x
 σ , the standard deviation of the discharges

$$F(x) = [1 / \sigma\sqrt{2\pi}] \int \exp [-(x-\mu)^2 / 2\sigma^2] dx$$

2. Lognormal distribution

$$f(x) = [1 / x\sigma_{\ln}\sqrt{2\pi}] \exp [-\frac{1}{2}\{(\ln x - \mu_{\ln}) / \sigma_{\ln}\}^2]$$

μ_{\ln} , the mean of the $\ln x$ values
 σ_{\ln} , the standard deviation of the $\ln x$ values

$$F(x) = [1 / \sigma_{\ln}\sqrt{2\pi}] \int (1/x) \exp [-\frac{1}{2}\{(\ln x - \mu_{\ln}) / \sigma_{\ln}\}^2] dx, \text{ whilst}$$

$$\mu_{\ln} = \frac{1}{2} \ln[\mu^2 / (\mu^2 + \sigma^2)]$$

$$\sigma_{\ln}^2 = \ln [(\mu^2 + \sigma^2) / \mu^2]$$

3. Gumbel distribution

$$f(x) = \alpha \exp \{-\alpha(x-\beta) - \exp [-\alpha(x-\beta)]\}$$

$$\alpha = \pi / \sigma\sqrt{6}$$

$$\beta = x_{\text{mean}} - \gamma / \alpha$$

$$\gamma = 0,57721 \text{ (Euler's const.)}$$

$$F(x) = \exp \{-\exp [-\alpha(x-\beta)]\}$$

4. Pearson III distribution

$$f(x) = [1 / \beta^\alpha \Gamma(\alpha)] (x-\gamma)^{\alpha-1} \exp [-(x-\gamma) / \beta]$$

$$E(x) = \mu = \alpha\beta$$

$$\text{Var}(x) = \alpha\beta^2$$

x =discharge

γ =lower limit of the discharge

Hydrological probability density, and cumulative probability functions

N	α			
	0.20	0.10	0.05	0.01
5	0.45	0.51	0.56	0.67
10	0.32	0.37	0.41	0.49
15	0.27	0.30	0.34	0.40
20	0.23	0.26	0.29	0.36
25	0.21	0.24	0.27	0.32
30	0.19	0.22	0.24	0.29
35	0.18	0.20	0.23	0.27
40	0.17	0.19	0.21	0.25
45	0.16	0.18	0.20	0.24
50	0.15	0.17	0.19	0.23
N > 50	$1.07 / \sqrt{N}$	$1.22 / \sqrt{N}$	$1.36 / \sqrt{N}$	$1.63 / \sqrt{N}$

Derived from Yevjevich's Table 10.3 of the Water Resources Publication 1972

Δ (test statistic) is the maximum of $|F - P|$,

if F is the cumulative distribution function and P is the cumulative frequency distribution of the computed water levels

α the two-tailed chosen threshold value (probability of exceedance of Δ_0)

N number of computed water levels from the synthetic floods

Reject the null hypothesis H_0 (goodness of fit), for the chosen threshold value α , if $\Delta \geq \Delta_0$

Critical value Δ_0 of the Kolmogorov-Smirnov test statistic Δ , for various values of N and values α , often used in hydrology

wave nr.	Q _{base}	Q _{peak}	X ₀	X ₄	duration	H Venlo
935	899	2060	551	37	10	17.11
817	685	2060	962	21	16	17.1
672	492	2060	702	17	8	17.09
401	1030	2060	512	55	14	17.04
84	464	2060	1037	17	13	17.09
248	974	2060	496	48	12	17.07
171	1229	2060	343	68	12	17.07
912	899	2060	727	6	11	17.21
232	947	2165	676	37	15	17.27
315	685	2165	770	32	11	17.25
578	250	2165	1205	15	12	17.28
285	751	2165	810	19	11	17.32
76	685	2165	559	52	8	17.13
527	604	2165	739	48	13	17.14
529	583	2165	694	48	10	17.14
745	895	2165	561	82	13	17.08
384	613	2265	776	80	14	17.13
831	540	2265	810	81	15	17.1
339	979	2265	455	63	8	17.31
526	540	2265	905	50	13	17.26
368	751	2265	684	43	10	17.36
414	979	2265	644	56	15	17.34
402	786	2265	758	34	11	17.41
694	766	2265	844	37	16	17.4
828	699	2265	770	32	10	17.4
793	766	2265	1011	19	14	17.48
594	604	2550	724	92	12	17.43
751	751	2550	606	97	11	17.46
29	766	2550	668	83	10	17.56
341	583	2550	888	83	15	17.5
655	579	2550	817	61	10	17.62
12	633	2550	936	56	13	17.66
531	895	2550	725	60	11	17.69
514	583	2664	676	97	10	17.54
148	604	2664	797	90	13	17.6
288	613	2664	607	90	8	17.6
405	583	2664	797	90	12	17.59
577	462	2664	810	90	11	17.55
144	543	2664	865	63	10	17.74
596	424	3039	693	114	9	17.8
666	405	3039	728	114	10	17.79
437	533	3039	672	112	9	17.83
349	766	2550	948	52	14	17.7
730	583	2550	1021	42	14	17.73
788	604	2550	975	44	14	17.72
46	494	2550	1407	21	15	17.82
647	1030	2550	676	37	9	17.81
989	751	2550	1001	37	15	17.78
833	1199	2664	513	90	10	17.78
423	583	2664	960	41	10	17.87

Appendix 4.8.1a

Continuation						
wave nr.	Q _{base}	Q _{peak}	X ₀	X ₄	duration	H Venlo
687	947	2664	677	59	9	17.84
897	976	2664	703	68	12	17.81
992	559	2664	995	48	13	17.84
64	926	2664	870	44	14	17.91
459	1229	2664	572	69	11	17.86
980	464	2664	1259	34	14	17.89
995	563	2664	1382	21	14	17.97
52	1030	2664	1051	19	13	18.02
71	926	2664	1117	19	13	18.01
187	1229	2664	812	32	13	18
321	532	3039	736	103	9	17.90
139	1199	3039	1185	20	13	18.45
386	699	3039	1124	50	11	18.28
399	979	3039	1024	44	13	18.31
528	766	3039	980	42	9	18.31
569	751	3039	1199	41	15	18.31
657	1591	3039	639	80	13	18.3
763	947	3039	916	54	10	18.29
869	658	3039	1452	30	17	18.32
920	974	3039	966	48	12	18.31
964	947	3039	930	83	14	18.17
552	604	3039	1050	56	10	18.23

Synthetic flood wave series at Borgharen and computed water levels at Venlo by using the Sobek model

Appendix 4.8.1b

wave nr.	Q _{base}	Q _{peak}	X ₀	X ₄	duration	H Mook
935	899	2060	551	37	10	10.38
817	685	2060	962	21	16	10.39
672	492	2060	702	17	8	10.36
401	1030	2060	512	55	14	10.31
84	464	2060	1037	17	13	10.37
248	974	2060	496	48	12	10.33
171	1229	2060	343	68	12	10.35
912	899	2060	727	6	11	10.55
232	947	2165	676	37	15	10.56
315	685	2165	770	32	11	10.51
578	250	2165	1205	15	12	10.56
285	751	2165	810	19	11	10.62
76	685	2165	559	52	8	10.36
527	604	2165	739	48	13	10.37
529	583	2165	694	48	10	10.36
745	895	2165	561	82	13	10.33
384	613	2265	776	80	14	10.36
831	540	2265	810	81	15	10.32
339	979	2265	455	63	8	10.55
526	540	2265	905	50	13	10.5
368	751	2265	684	43	10	10.6
414	979	2265	644	56	15	10.6
402	786	2265	758	34	11	10.68
694	766	2265	844	37	16	10.66
828	699	2265	770	32	10	10.67
793	766	2265	1011	19	14	10.79
594	604	2550	724	92	12	10.59
751	751	2550	606	97	11	10.62
29	766	2550	668	83	10	10.78
341	583	2550	888	83	15	10.7
655	579	2550	817	61	10	10.83
12	633	2550	936	56	13	10.9
531	895	2550	725	60	11	10.97
514	583	2664	676	97	10	10.68
148	604	2664	797	90	13	10.78
288	613	2664	607	90	8	10.76
405	583	2664	797	90	12	10.77
577	462	2664	810	90	11	10.7
144	543	2664	865	63	10	10.97
596	424	3039	693	114	9	10.86
666	405	3039	728	114	10	10.85
437	533	3039	672	112	9	10.92
349	766	2550	948	52	14	11
730	583	2550	1021	42	14	11.01
788	604	2550	975	44	14	11
46	494	2550	1407	21	15	11.18
647	1030	2550	676	37	9	11.18
989	751	2550	1001	37	15	11.11
833	1199	2664	513	90	10	11.08
423	583	2664	960	41	10	11.19

Appendix 4.8.2a

wave nr.	Q _{base}	Q _{peak}	Continuation		duration	H Mook
			X ₀	X ₁		
687	947	2664	677	59	9	11.16
897	976	2664	703	68	12	11.1
992	559	2664	995	48	13	11.12
64	926	2664	870	44	14	11.27
459	1229	2664	572	69	11	11.2
980	464	2664	1259	34	14	11.23
995	563	2664	1382	21	14	11.38
52	1030	2664	1051	19	13	11.48
71	926	2664	1117	19	13	11.46
187	1229	2664	812	32	13	11.43
321	532	3039	736	103	9	11.04
139	1199	3039	1185	20	13	12.05
386	699	3039	1124	50	11	11.7
399	979	3039	1024	44	13	11.8
528	766	3039	980	42	9	11.77
569	751	3039	1199	41	15	11.78
657	1591	3039	639	80	13	11.83
763	947	3039	916	54	10	11.74
869	658	3039	1452	30	17	11.83
920	974	3039	966	48	12	11.77
964	947	3039	930	83	14	11.54
552	604	3039	1050	56	10	11.6

Synthetic flood wave series at Borgharen and computed water levels at Mook by using the Sobek model

Appendix 4.8.2b

Probability of exceedance yr ⁻¹	water level at Mook NAP + m	water level at Venlo NAP + m	water level at Borgharen NAP + m	discharge at Borgharen m ³ s ⁻¹
0.1	11.18	17.52	45.15	2142
0.05	11.52	17.94	45.43	2387
0.02	11.86	18.37	45.70	2710
0.01	12.01	18.58	45.89	2955
0.004	12.36	18.91	46.12	3278
0.0008	12.83	19.34	46.43	3800

Design Water Levels 2001

Design Water Levels 2001 at Mook, Venlo and Borgharen from Waqua computations, according to schematisation MHW 1998 – 3g and software version 2002 – 01. The water levels are based on ruling synthetic flood waves at Borgharen*, with given p.o.e of the peak discharge values. The computations have been achieved by Rijkswaterstaat Direction Limburg in close consultation with RIZA Arnhem

* also see Fig. 6.3.1

date	operational	validated	date	operational	validated
5-2-'84	0	7.91	21-11-'84	0	13.01
6-2-'84	13.81	32.97	22-11-'84	7.2	32.29
7-2-'84	15.38	9.77	23-11-'84	16.9	13.18
8-2-'84	12.38	12.19	24-11-'84	21.6	5.7
Sum	41.57	62.84	25-11-'84	11.5	2.18
			Sum	57.2	66.36

date	operational	validated	date	operational	validated
29-3-'86	4.5	9.99	29-12-'86	0	6.37
30-3-'86	9.7	23.62	30-12-'86	7.8	5.57
31-3-'86	20.3	9.74	31-12-'86	4.3	9.4
Sum	34.5	43.35	1-1-'87	14.3	23.32
			2-1-'87	11.9	3.48
			Sum	38.3	48.14

date	operational	validated	date	operational	validated
31-12-'90	0	0	9-1-'93	0	6.12
1-1-'91	10	12.96	10-1-'93	21	18.39
2-1-'91	20	17.41	11-1-'93	42	41.28
3-1-'91	20	18.21	Sum	63	65.79
Sum	50	48.58			

date	operational	validated	date	operational	validated
19-12-'93	18	25.12	26-1-'95	29	14.46
20-12-'93	31.5	36.6	27-1-'95	18.3	18.7
21-12-'93	11.5	9.88	28-1-'95	18.8	10.19
Sum	61.5	71.6	Sum	66.1	43.35

**Rainfall depths (mm) from eight rain gauges in the Meuse River basin*,
upstream of the discharge measuring-station at Borgharen**

*

France: Nancy, St.Dizier, Reims
Ardennes: Luxembourg, St.Hubert, Spa
Sambre: Charleroi, Florenne

day	operational rainfall	effective rainfall	average 1-day UH	9.7 UH	11.3 UH	8.3 UH	calculated Sum
0	0	0 R ₀	0				
1	13.8	9.7 R ₁	6.53 U ₁	0			0
2	15.4	11.3 R ₂	17.5 U ₂	63	0		63
3	12.4	8.3 R ₃	32.12 U ₃	170	74	0	244
4	2.2		48.52 U ₄	312	198	54	564
5	0		40.95 U ₅	471	363	145	979
6	43.8	29.3 Sum	32.12 U ₆	397	548	267	1212
7			24.36 U ₇	312	463	403	1177
8			17.66 U ₈	236	363	340	939
9			12 U ₉	171	275	267	713
10			7.4 U ₁₀	116	200	202	518
11		Loss	3.85 U ₁₁	72	136	147	354
12		4.1	0	37	84	100	221
13		m=4	n=11	0	44	61	105
14					0	32	32
15						0	0
							7120

Also see Table 5.3.1, where Sum 7120 m³s⁻¹ equals 615.10⁶ m³ and that equals to 29.3 mm (according to the beginning of Section 5.3)

Q'_{peak} calculated from the effective rainfall and the average 1-day Unit Hydrograph; Flood of February 1984, using Eq.5.3.1

February 1984

adjusted effected rainfall 23.5 mm, according to the regression line of Fig.5.4.1 or Equation 5.4.1

day	rainfall	eff.rainfall	average 1-day UH	7.76 UH	9.36 UH	6.36 UH	Sum
0	0	0	R_0	0			
1	13.8	7.76	R_1	6.53	U_1	0	0
2	15.4	9.36	R_2	17.5	U_2	51	51
3	12.4	6.36	R_3	32.12	U_3	136	61
4				48.52	U_4	249	164
5	41.6	23.5		40.95	U_5	377	301
6	Sum	Sum		32.12	U_6	318	454
7				24.36	U_7	249	383
8		m=4		17.66	U_8	189	301
9				12	U_9	137	228
10				7.4	U_{10}	93	165
11				3.85	U_{11}	57	112
12				0		30	69
13						0	36
14			n=11			0	24
15							0

$$Q_{\text{base}} = 980 \text{ m}^3\text{s}^{-1}$$

$$Q_{\text{peak}} = 1956 \text{ m}^3\text{s}^{-1}$$

Adjusted effective rainfall of 23.5 mm (also see Eq.5.4.1)
Calculation of Q'_{peak} ($976 \text{ m}^3\text{s}^{-1}$) with the help of the average 1-day Unit Hydrograph (also see Fig.5.3.3a) and the adjusted effective rainfall, Eq.5.3.1 has been used

Appendix 5.5.1

Feb.2002

day	rainfall	eff.rainfall	average	1-day UH	0.5UH	5.1UH	3.9UH	15.8UH	3.8UH	Sum
0	4.5	0.5	0							
1	9.1	5.1	6.53	3						3
2	2.3	0	17.5	9	33					42
3	7.9	3.9	32.12	16	89					105
4	19.8	15.8	48.52	24	164	25				214
5	7.8	3.8	40.95	20	247	68	103			439
6	0	29.1	32.12	16	209	125	277	25		651
7	51.4		24.36	12	164	189	507	67		939
8			17.66	9	124	160	767	122		1181
9			12	6	90	125	647	184		1053
10			7.4	4	61	95	507	156		823
11			3.85	2	38	69	385	122		615
12			0	0	20	47	279	93		
13					0	29	190	67		
14			n=11			15	117	46		

peak 2031 **expected** (NAP + 45.06 m) $Q_{base} 850 \text{ m}^3 \text{ s}^{-1}$

Feb.2002

day	rainfall	eff.rainfall	average	1-day UH	3.4UH	8 UH	1.2UH	6.8UH	18.7UH	6.7UH	Sum
0	4.5	3.42	0								
1	9.1	8.02	6.53	22							22
2	2.3	1.22	17.5	60	52						112
3	7.9	6.82	32.12	110	140	8					258
4	19.8	18.72	48.52	166	258	21	45				489
5	7.8	6.72	40.95	140	389	39	119	122			810
6	0	44.92	32.12	110	328	59	219	328	44		1088
7	51.4		24.36	83	258	50	331	601	118		1441
8			17.66	60	195	39	279	908	216		1698
9			12	41	142	30	219	767	326		1524
10			7.4	25	96	22	166	601	275		1186
11			3.85					456	216		
12			0					331	164		
13								225	119		

peak 2548 **maximum** 95% (NAP + 45.55 m) $Q_{base} 850 \text{ m}^3 \text{ s}^{-1}$

Verification

Appendix 5.5.2

January 2003									
day	rainfall	eff.rainfall	average	1-day UH	8.2UH	21.9UH	0.9UH	1.7UH	Sum
0	14.4	8.2	0						
1	28.1	21.9	6.53	54					54
2	7.1	0.9	17.5	144	143				287
3	7.9	1.7	32.12	263	383	6			653
4	57.5	32.7	48.52	398	703	16	11		1128
5			40.95	336	1063	29	30		1457
6			32.12	263	897	44	55		1258
7			24.36	200	703	37	82		1023
8			17.66	145	533	29	70		777
9			12	98	387	22	55		562
10			7.4	61	263	16	41		381
11			3.85	32	162	11	30		234
12			0						

peak 2337 **expected** (NAP + 45.36 m) $Q_{base} 880 \text{ m}^3\text{s}^{-1}$

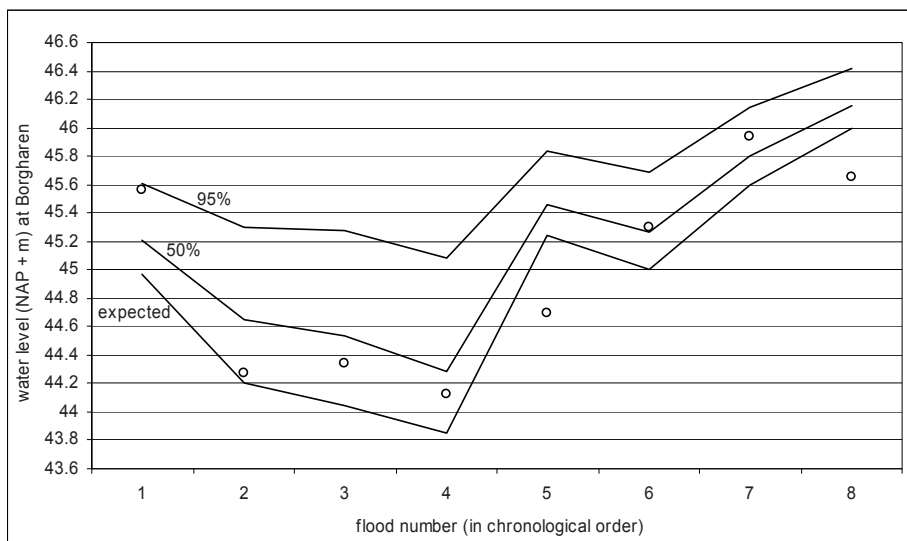
January 2003								
day	rainfall	eff.rainfall	average	12.2UH	25.9UH	4.85UH	5.65UH	Sum
0	14.4	12.15	0					
1	28.1	25.85	6.53	79				79
2	7.1	4.85	17.5	213	169			381
3	7.9	5.65	32.12	390	452	32		874
4	57.5	48.5	48.52	590	830	85	37	1542
5			40.95	498	1254	156	99	2006
6			32.12	390	1059	235	181	1866
7			24.36	296	830	199	274	1599
8			17.66	215	630	156	231	1231
9			12	146	457	118	181	902
10			7.4	90			138	
11			3.85					
12			0					
13			n=11					

peak 2886 **maximum** 95% (NAP + 45.83 m) $Q_{base} 880 \text{ m}^3\text{s}^{-1}$

Verification

Appendix 5.5.3

number		m^3s^{-1}
1	Feb.1984	2550
2	Nov.1984	1625
3	Apr.1986	1664
4	Jan.1987	1555
5	Jan.1991	1843
6	Jan.1993	2265
7	Dec.1993	3039
8	Jan.1995	2664



Prediction of expected water levels of floods 1 through 8; 50% and 95% upper limits of the confidence band of their effective rainfall, translated into water levels; (o) measured water levels

REFERENCES

- Adamowski, K. (2000) *Regional analysis of annual maximum and partial duration flood data by nonparametric and L-moment methods*. University of Ottawa, Ontario, Canada, *Journal of Hydrology* 229.
- Alila, Y. & Mtiraoui, A. (2002) *Implications of heterogeneous flood-frequency distributions on traditional stream-discharge prediction techniques*. University of British Columbia, Faculty of Forestry, Vancouver, Canada, *Hydrological Processes* 16.
- Bakker¹, A. & Luxemburg², W. (2005) *Heterogeneous distributions within flood frequency analysis*. Paper ISSH-Stochastic Hydraulics 2005, (1)Witteveen en Bos, Deventer, NL and (2)Delft University of Technology, Faculty of Civil Engineering, Delft, NL.
- Barneveld, H. & Bastings, A. (1998) *Water level Relation Curves for the Dutch Meuse River, State 1995*. BETRL W3.XLS, HKV lijn in water & Rijkswaterstaat, Directorate Limburg, Department ANWR, Maastricht, NL.
- Benson, M.A. et al. (1950) *Use of historic data in flood-frequency analysis*. Geological Survey, Reston, Virginia, USA.
- Berger, H.E.J. (1992) *Flow forecasting for the River Meuse*. Dissertation, Delft University of Technology, Faculty of Civil Engineering, Delft, NL.
- Chow, K.C.A. & Watt, W.E. (1994) *Practical use of the L-moments*. Stochastic and statistical methods in hydrology and environmental engineering, Volume 1, pp.55-69, Kluwer Academic Publishers Group, Boston, USA.
- Chow, V.T. (1964) *The Weibull formula introduced to frequency analysis*. Handbook of applied Hydrology, Section 8, McGraw-Hill, New York, USA.
- Dalrymple, T. (1960) *Flood frequency analysis*. Manual of Hydrology, part 3 Flood flow techniques, Water supply Paper 1543-A, Geological Survey, Reston, Virginia, USA.
- Delden, van, H. (1999) *Flood wave shapes of historical floods at Borgharen*. Trainee Report, 90 pp., University of Twente, Department CTW, and Rijkswaterstaat, Directorate Limburg, Enschede / Maastricht, NL.
- Directorate Limburg & RIZA. *Reports on remarkable floods in the Dutch Meuse River*. Maastricht / Lelystad, NL.
- Dixhoorn, van, K. (1978) *Investigation discharge hydrograph during floods at Borgharen*. Note 78 J, 16 pp., 3 Appendices and 7 Supplements, Rijkswaterstaat, Directorate Water Management and Water Motion, Arnhem, NL.

- Fiorentino, M. et al. (1985) *Regional flood frequency analysis using the two-component extreme value distribution*. Hydrological Sciences Journal 30, pp.51-64.
- Gabriele, S. & Arnell, N. (1991) *A hierarchical approach to regional flood frequency analysis*. Water resources Research 27, pp.2181- 2189.
- Gerretsen, J.H. (1996) *How to manage flood waves in the Dutch Meuse River*. Proc. Conf. on Destructive Water, IAHS Publication (1997), no. 239 pp. 383-390, Los Angeles, Anaheim, USA, ISBN 1-901502-00-7
- Gerretsen, J.H. (1997) *Operational Water Management in the Dutch Meuse River*. Proceedings of the European Water Resources Association Conference, pp. 341-347, Copenhagen, DK, ISBN 90-5410-897-5
- Gerretsen, J.H. (1999) *Shapes of floods*. 25 pp. and 40 Supplements, University of Twente, Department CTW, Enschede, NL.
- Gerretsen, J.H. (2002) *Some special aspects of the quantitative water management of the Dutch Meuse River*. 37 pp., 3 attachments, 25 Figures and 18 Tables, Rijkswaterstaat, Directorate Limburg, Maastricht, NL.
- Grinten, van der, P. & Lenoir, J. (1973) *Statistical process management*. Prisma – Technica 50, Het Spectrum, Utrecht / Antwerpen, NL / B, ISBN 90-274-7549-0.
- Hirsch, R.M. & Stedinger, J.R. (1987) *Plotting positions for historical floods in addition to systematically recorded annual flood series*. Water Resources Research 23 pp.715-727.
- Hoskin, J.R.M. (1990) *L-moments: analysis and estimation of distributions using linear combinations of order statistics*. J. Royal Statistical Soc., Volume 52, pp.105-124, London, UK.
- Jansen, P. et al. (1979) *Principles of River Engineering*. Delft University of Technology, Delft, NL.
- Keim, B.D. & Faiers, G.E. (1996) *Heavy rainfall distributions by season in Louisiana: synoptic interpretations and quantile estimates*. Water Resources Bulletin, Volume 32, No.1, American Water Resources Association.
- Klemes, V. (2000) *Tall Tales about Tails of Hydrological Distributions*. Fulton Rd., Victoria B.C., Canada, Journal of Hydrologic Engineering, Volume 5, No.3, July2000.
- Klopstra, D. (1998) *Sensitivity analysis for the ruling discharge of the Meuse River at Borgharen*. 7 pp., 2 Tables and 5 Supplements, HKV lijn in water, Rijkswaterstaat, Directorate Limburg, Department ANWR, Maastricht, NL.
- Lorenz, N. (1997) *Historical floods Rhine and Meuse before 1900*. Trainee Report, 66 pp., Delft University of Technology, Faculty of Civil Engineering and Geosciences, Delft, NL.

- Luxemburg, W.M.J. Savenije, H.H.G. Gelder, van, P.H.J.M. Nooyen, R.R.P. Gardsman, B. (2002) *Statistical properties of flood runoff of North Eurasian rivers under conditions of climate change*. Research Program, Delft University of Technology and Russian research institutes at Vladivostok, Irkutsk and St.Petersburg.
- Made, van der, J. (1968) *Meuse River Floods*. Rijkswaterstaat, Directorate Water Management and Water Motion, The Hague, NL.
- Mantje, W. Luxemburg, W. Gelder, van, P. Gartsman, B. Savenije, H. (2007) *Statistical Modelling of Flood Events*. Delft University of Technology, Faculty of Civil Engineering, Delft, NL.
- McClave, J.T. et al. (1997) *Statistics*. Prentice-Hall, London, UK, ISBN 0-13-471542-X.
- Min Tu (2006) *Assessment of the effects of climate variability and land use change on the hydrology of the Meuse River basin*. Dissertation, ISBN 0415 41694 9
- Ministry of Transport, Public Works and Water Management. (1977) *Report Committee River Dikes*. The Hague, NL, 100 pp.
- Ministry of Transport, Public Works and Water Management, Rijkswaterstaat, RIZA. (2002) *Design Hydraulic conditions 2001 to test the primary water-control structures*. Arnhem, NL, ISBN 9036954355
- Rijkswaterstaat. *Monitoring Rijkswateren, Yearbooks of Water levels, Discharges and Temperatures*. RIZA, Lelystad, NL.
- Rijkswaterstaat. (1966) *Flood-peak attenuation of a river, Part A.*, Directorate Water Management and Water Motion, The Hague, NL.
- Rijkswaterstaat (2002) *Analysis of the ruling discharge of the Meuse River at Borgharen*. RIZA Report 2002.013, Lelystad, NL.
- Rossi, F. Fiorentino, M. Versace, P. (1984) *Two-component extreme value distribution for flood frequency analysis*. Water resources research, Volume20, No.7
- Royal Dutch Meteorological Institute (KNMI). (1994) *Historical floods of the Meuse River. AD 858-1880*, De Bilt, NL.
- Shaw, E.M. (2002) *Hydrology in Practice*. Third edition, Nelson Thornes Ltd, Delta Place, Cheltenham, UK, ISBN 0-7487-4448-7.
- Veen, van der, R. et al. (2002) *Structure, calibration and verification Sobek-Meuse*. Rijkswaterstaat, RIZA, Report 2002.031, Arnhem, NL, ISBN 9036954576.
- Vogel, R.M. & Wilson, I. (1996) *Probability distribution of annual maximum, mean, and minimum stream flows in de United States*. Journal of Hydrologic engineering (1996), Volume1, No. 2.

Visou van Eck, N. & Klopstra, D. (1998) *Shape of the design discharge wave of the Meuse River at Borgharen*. Second draft, HKV lijn in water, Lelystad. NL.

WL| Delft Hydraulics. (1994) *Investigation Flooding Meuse River*. Delft, NL, ISBN 90-802314-2-8

Yevjevich V. (1972) *Testing the goodness of fit of probability functions to empirical distributions*. Water Resources Publication, Ford Collins, Colorado, USA.

ACKNOWLEDGEMENTS

I am grateful to my promoter Prof. H.J. de Vriend for his scientific support and willingness to read, improve and brush up the versions of my chapters.

I would like to thank Michiel Knaapen (UT) for applying a model to random sampling combinations of characteristic flood wave properties at Borgharen.

I thank Carla Beaulen and Jan Bremer (RWS, dir. Limburg) for their initial and final computations, respectively, by using a flow model that converts upstream discharge flood waves into downstream water levels in a river.

Great thanks to Anke Wigger (UT) for her secretarial support.

Special thanks to my wife Rie, for her patience, love and all she has done for me. Without her support this thesis should not have been achieved. Our private life often was influenced by my study, but today we can say it is accomplished.

ABOUT THE AUTHOR

The author was born in Elst (Gld), the Netherlands, on 14 November 1933. In 1956 he joined Rijkswaterstaat Directie Bovenrivieren, as investigator in the field of fluvial research on the Rhine River and its branches. In 1965 he joined Rijkswaterstaat Directie Limburg, as head of the department 'Survey and Calculations', that started there to build up knowledge about the Dutch Meuse River. From 1985, after a reorganization as a consequence of the integral thinking about water systems, he was head of the department 'Knowledge and Computations' concerning the Meuse River. In the period 1985-1990 he participated in the Scientific Research Group aimed at the water balance between Liège and Maasbracht, carried out by Belgian and Dutch universities. He was responsible for the determination of the design levels of the Meuse River levees, constructed in 1995 within the framework of the Delta Plan Grote Rivieren. From 1996 to 1999 he was senior advisor Integral Water Policy in the Directie Limburg.

